SOME PHYSICAL AND THERMODYNAMIC PROPERTIES OF ORGANIC MELTS

A thesis submitted to the

University of London

by

J. A. BURGESS, B.Sc., A.R.C.S.

for the

degree of Doctor of Philosophy

Department of Chemical Engineering and Chemical Technology,
Imperial College of Science and Technology,
South Kensington,
London, S.W.7.

April 1968.

ACKNOWLEDGEMENTS

I wish to express my gratitude to Professor A. R. Ubbelohde, C.B.E., F.R.S. for his supervision of this research and for his valuable advice and encouragement throughout.

Thanks are also due to the Science Research Council for the research award.

CONTENTS

CHAPTER 10.

Discussion — Page 299

ABSTRACT

Methods of Synthesis and purification are described for tetraphenyl allene, triphenyl-α-naphthyl allene and triphenyl-4-biphenyl allene. These compounds were selected as representative members of a new class of hydrocarbons, providing rigid non-polar molecules for studying the tendency to interlock in the melt. Chemical stability of the melts was found to be adequate to allow accurate observations of properties such as the molar volume and viscosity as a function of temperature. Measurements were also made on selected binary mixtures. As might be expected from the shapes of their repulsion envelopes, the molecules showed increasing tendency to interlocking in their melts in the sequence:

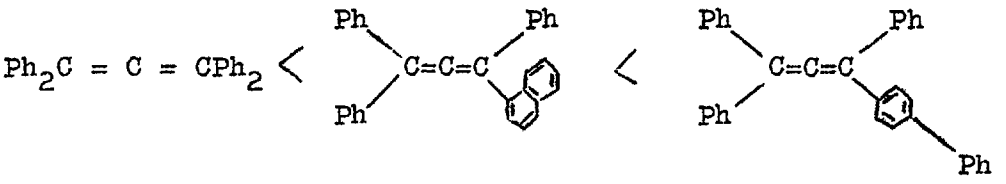

CHAPTER 1.

SOME THEORIES OF THE LIQUID STATE

1.1 Introduction.

There are two factors which combine to determine the specific properties of a particular liquid, viz. the nature of the intermolecular forces, and the shape and size of the constituent molecules or ions. Van de Waals' forces or London dispersion forces are always present, and may be expressed in terms of an attractive force and a repulsive force which, at equilibrium, are balanced. (See this chapter page 21). In the case of simple molten salts such as the alkali halides and nitrates, the dispersion forces are radically modified by the presence of coulombic forces resulting from the interaction of the fully charged species of which the melt is comprised*. Further, in cases in which either the anion or cation is not spherically symmetrical and the charge is localised, and in cases in which the molecules possess permanent dipoles, the orientational effects may exert a marked influence upon the general propertis of the compound. An example of the former may be found in the alkali

---

*This is a rather drastic generalisation since, in some cases, a melt may consist of a strongly polarising cation and a readily polarised anion when the "link" between the anion and cation may possess considerable covalent character, e.g. lithium iodide.

acetates*, and the well known effects of hydrogen bonding in water and the alcohols serve to illustrate the latter. Where intermolecular forces other than dispersion forces are minimised, the influence of molecular shape and size assumes paramount importance, and it is towards a study of these effects that this present work is directed. Hydrocarbons comprising molecules of specific shape and size serve particularly well as "model molecules" for this study, and a discussion of the types selected both for previous work and for the present work, together with the properties particularly sensitive to these effects, is reserved for the following chapters.

This chapter is devoted to a brief review of some of the theories of the liquid state. Owing to the complexities involved with regard to the determination of intermolecular force-fields, these theories obtain, on the whole, to non-polar liquids comprising molecules possessing spherically symmetrical force fields. Since the liquids studied in this present work comprise molecules which are far from spherically symmetrical, direct application of the theories to the molecules studied here would prove unsatisfactory, as any approximation introduced to simplify the influence of shape and size would

---

* Potassium acetate is one of the few materials which contract on melting:- this, together with some other anomalous properties, may be due to the orinetational effects of ionic asymmetry endorsed by charge localisation. See F. J. Hazlewood. Reference 1.

tend to remove the very factors which this work was planned to study. However, some of the principals involved in these theories carry considerable significance in general, and are of value in considering all liquids, at least on a qualitative basis.

A more detailed discussion of the nature and problems attendant upon these complex molecules is reserved for the last section of this chapter.

1.2. The Statistical Mechanics of Normal Liquids[2,3]

The macroscopic thermodynamic properties obtaining to any statistical assembly can be expressed in terms of a complete partition function Z, which is defined by the following expression:

$$Z(V,T) = \sum_{r=1}^{r=\infty} \exp - \epsilon_r/kT \qquad (1.1)$$

In other words, a partition function, relating to any particular degree of freedom, is the sum of all the Boltzmann factors obtaining to each quantum state. When the coefficient of ϵ_r in the exponent is small, i.e. at high temperatures, it is justifiable to replace the summation by an integration:

$$Z(V,T) = \int_{r=1}^{r=\infty} \exp - \epsilon_r/kT \, dr \qquad (1.2)$$

The property most simply expressed in terms of the partition function is the Helmholtz free energy F, given by:

$$F = - kT \ln Z \qquad (1.3)$$

From this expression, employing standard relationships of classical thermodynamics, it is possible to obtain expressions for all the other intensive and extensive properties of the assembly.

A liquid comprises a statistical assembly of non-localised molecules; and provided that the internal degrees of freedom of each molecule remain unaffected by the molecular environment, it is possible to express the total partition function for the assembly as a product of a partition function for the external energy of the molecules, which is a function of volume and temperature, and a partition function for the internal energy of the molecules, which a function of temperature alone.

$$Z_{Total}(T,V) = Z_{Ext.}(T,V).Z_{Int.}(T) \qquad (1.4)$$

The partition function relating to the internal energy of the molecules can, in turn, be expressed as a product of partition functions, each obtaining to an internal degree of freedom, principally intramolecular vibration and rotation of the

molecule about the three perpendicular axes through its centre of gravity. The external energy of an assembly of molecules consists of the kinetic energy arising from molecular motion, i.e. translational energy, and the potential energy of the whole assembly. This external energy can be represented by means of the following Hamiltonian:

$$H(P,r) = \frac{1}{2m} \sum_{i}^{N} (P_x^2 + P_y^2 + P_z^2) + U(r) \qquad (1.5)$$

where P_x, P_y and P_z refer to the momenta of the molecules resolved along the x, y and z axes; m, the molecular mass or reduced mass and $U(r)$, the total potential energy of the assembly of N molecules. Thus, the partition function for the external energy may be written:

$$Z_{Ext.} = \frac{1}{N!} \int \cdots \int \exp H(P,r)/kT \; dr_1 \cdots dr_{3N}, \; dP_1 \cdots dP_{3N} \qquad (1.6)$$

The factor $\frac{1}{N!}$ accounts for the indistinguishability of identical particles in a delocalised system.

If it is further assumed that the translational degrees of freedom of the molecules are classical, an assumption which is not unreasonable in the case of normal liquids at ordinary temperatures, the kinetic and potential energies which comprise the translational partition function may also be separated, allowing the above integration to be performed over all momenta co-ordinates leaving the potential energy part of the

integral untouched:

$$Z_{ext.} = \frac{1}{N!}\left[\frac{(2\pi mkT)^{3/2}}{h^3}\right]^N \int\cdots\int \exp.U(r)/kT\ dr_1 \cdots dr_{3N} \qquad (1.7)$$

The expression contained within the bracket is analogous to the translational partition function for a single molecule of a perfect gas, with the total volume of the system V, omitted. In common with the internal partition functions, this is independent of volume and dependent upon the temperature of the system only. The remaining integral, representing the partition function for the potential energy of the system, is termed the configurational integral β.

$$\beta = \int\cdots\int \exp\ U(r)/kT\ dr_1 \cdots dr_{3N} \qquad (1.8).$$

β is dependent upon both volume and temperature.

Thus, the total partition function for the liquid is given by:

$$Z = Z_{int.}(T)\ Z_{trans.}(T)\ \beta(V,T) \qquad (1.9)$$

In order to describe a liquid completely, and to predict its properties, it is necessary to evaluate the configurational integral, but the lack of knowledge concerning the nature of the potential energy function U(r), coupled with the mathematical difficulties associated with the integration, have so far forbidden a complete solution. Most viable theories of the

liquid state have been based upon assumptions related to a physical model, sufficiently simple to reduce the above difficulties, whilst remaining sufficiently realistic to be of practical use.

1.3. Cell Theories of the Liquid State

The most simple cell theory of the liquid state (Buehler et. al. 1951)[4,5] is based upon the precept that each molecule in a liquid, considered far from its critical point, spends most of its time confined by its neighbours to a comparatively restricted region. The neighbouring molecules form a cage or cell within which the central molecule is free to move. Further, each cell is identical and each contains but one molecule. Whilst this model is more realistic than the earlier lattice models of Frenkel (1935)[6] and Bresler (1939),[7] in which the matrix of the solid lattice is retained and the volume increase on melting is explained by the introduction of a large number of lattice defects, it is subject to the same type of restrictions as the Einstein model for solids in as much as correlations between the motions of neighbouring molecules are neglected. The rather inflexible nature of the model imposes restrictions upon the fluctuations in density and the space available to each molecule. The fact that each molecule is confined to the space contained within its cell results in a

low value for the calculated entropy. The additional entropy which would arise if the molecules were allowed access to the whole space is termed the communal entropy. For rigid non-interacting spherical molecules, the value of the configurational integral corresponding to a model based upon the above assumptions is given by:

$$\beta = \left(\frac{1}{N!}\right)\sum V_f^N \qquad (1.10)$$

The summation is to be taken over all arrangements of the N molecules in N cells; and V_f, termed the free volume, is the volume available to the centre of a molecule in its cell, assuming the neighbours remain fixed at the centres of their cells. Since there are N! different arrangements of N molecules in N cells equation (1.10) gives:

$$\beta = V_f^N \qquad (1.11).$$

Thus, for this simple model, the problems arising in evaluating the configurational integral are incorporated in the free volume V_f.

A rather different approach, developed by Eyring and co-workers[8,9] is based upon a comparison between a liquid and a perfect gas. In a perfect gas the volume occupied by the non-interacting molecules is considered negligible compared with

the volume of the system V, and the total molecular partition function may be written:

$$Z_{Total} = \frac{(2\pi mkT)^{3/2}}{h^3} \; V.Z_{Rot.}.Z_{Vib.} \qquad (1.12)$$

In a liquid however, the total volume available to each molecule is not equivalent to the total volume of the system, and the volume V, must be replaced by the free volume $V_f (V_f < V)$; further, the potential energy of the liquid due to molecular interaction, expressed by the configurational integral β (see eqn. 1.8), must be considered. This problem is over-come by considering the liquid as though it were composed of individual molecules moving in an average potential field due to their neighbours. (If the liquid consists of molecules which are far from spherically symmetrical like those studied in this present work, this average potential field becomes extremely difficult to define:- see this chapter section 1.5). The energy required to remove a molecule from the potential field will be equivalent to the molecular energy of evaporation E_o. Hence, the configurational integral β may be written:

$$\beta = \exp - E_o/kT \qquad (1.13)$$

and the total partition function:

$$Z_{Total} = \frac{(2\pi mkT)^{3/2}}{h^3} \cdot V_f \cdot Z_{Rot.} \cdot Z_{Vib.} \exp - E_o/kT \qquad (1.14)$$

provided that the internal partition functions remain the same in both the liquid and the gas. (Again this is an assumption justified only in the case of molecules which are approximately spherically symmetrical where molecular rotation is virtually uninhibited in the liquid far from the critical point). In this way, difficulties arising from a consideration of single intermolecular potentials are obviated, and the problem again devolves upon the free volume V_f. If the free volume is considered, according to the simple cell theory, as the volume available to a molecule within its own cell, then the free volume can be simply related to the total volume of the system by considering the geometry of the cell; e.g. for a cubic close-packed arrangement the free volume can be expressed as follows:

$$V_f = 8\,(V^{1/3} - d)^3 \qquad (1.15)$$

where d is the molecular collision diameter, and V, the total volume of the system*. This evaluation of V_f fails to account for the communal entropy mentioned earlier (pp. 55) and Eyring et. al. have considered that the appearance of holes in a

---

* For molecules which are complex in shape, the true geometry of the cell may prove difficult to estimate; as indeed would be a realistic value of d.

liquid described by the cell model would facilitate the movement of a molecule from one site to another, in which case the communal entropy, which is introduced at the melting point, would be R (i.e. 1.98 e.u.). This concept forms the basis of the Eyring hole theory (1936)[10] and accounts for the fluid properties of the liquid state. (See also chapter 2, page 46). That all the communal entropy should be introduced at the melting point is clearly unrealistic, and at temperatures far from the critical temperature would be expected to lead to values of the entropy which are too high. Liquids, just above their melting points, often retain the basic matrix of the corresponding solid structure together with considerable long-range order. (See chapter 4, page 127). Consequently, individual molecules cannot claim access to the total free volume until the critical temperature is approached, when the total entropy is finally gained. However, experimental values of entropies of fusion for a variety of elements and compounds tend to be rather erratic, and often have values greater than R, even in the case of the solid inert gases (See table 1.1).

Quantitative developments of these simple cell theories do not, in their present form, match experiment closely, probably because this model fails to yield the solid state parameters adequately. After all, the entropy of fusion is simply expressed

TABLE 1.1[20]

Molecule	Entropy of fusion, S_f
Ne	3.26 e.u.
A	3.35 "
Kr	3.36 "
Xe	3.40 "
CH_4	2.47 "
$C(CH_3)_4$	3.0 "

as the quotient of the heat of fusion and melting temperature (i.e. $\Delta H_f/T$). The former will depend to some extent upon the nature of the solid lattice since:

$$\Delta H_f = [H]_{Liquid} - [H]_{Solid}$$

One of the most significant developments of the cell theory is due to Lennard-Jones and Devonshire (1938-39)[11,12]. The theory considers an assembly of N molecules moving in a volume V, which is divided into N identical cells arranged in a regular lattice. The following assumptions are then made with regard to molecular motion and molecular interaction.

(i) Each molecule is confined within the matrix of its own cell by its immediate neighbours.

(ii) Each cell can accommodate one molecule only and

the partition function of the liquid assembly can be expressed as a product of the partition functions for each individual molecule; i.e. the molecules can be regarded as moving independently in their cells.

(iii) The average field* in which any one molecule moves is that due to its immediate neighbours when each is in the centre of its own cell.

(iv) Atomic interactions fall off rapidly with distance, and only nearest neighbours need be considered; and if the number of nearest neighbours is large (generally twelve) the field within the cell will possess a high degree of symmetry, and may be regarded as spherically symmetrical about the centre of the cell*.

The main distinguishing feature of the Lennard-Jones and Devonshire theory is that the potential energy of the system can be approximated by a sum of terms each depending upon the position of one molecule. Thus, the potential energy of the system may be written:

$$U = U_o + \sum_i \left[\psi(r_i) - \psi(o) \right] \qquad (1.16)$$

where r_i is the vector displacement of molecule i from the

---

* See page 9 and section 1.5 of this chapter with regard to the difficulties attendant upon the estimation of the average potential field and the nature of intermolecular potentials within the context of very non-spherically symmetrical molecules.

centre of its cell, and U_o the potential energy of the system when all the molecules are at the centre of their cells. This leads to the following expression for the configurational integral:

$$\beta = \exp(-U_o/kT)\, V_f \qquad (1.17)$$

The free volume V_f is then defined in terms of the potential of a molecule within its cell:

$$V_f = \int \exp\left\{-\left[\psi(r_i) - \psi(o)\right]/kT\right\} dr_i \qquad (1.18)$$

The integration is taken throughout the interior of the cell.

For spherical molecules arranged in a face centred cubic lattice (co-ordination number 12), the mutual interaction $U(r)$ between any two molecules is of the form:

$$U(r) = U_o\left[\left(\frac{r_o}{r}\right)^{12} - 2\left(\frac{r_o}{r}\right)^{6}\right] \qquad (1.19)$$

U_o is the minimum value of $U(r)$ and r_o the value of r at which this is a minimum (See fig. 1.1).

On the basis of the above assumptions an expression may be derived for the configurational integral per molecule in terms of U_o and r_o, together with certain geometric constants relating to the nature of the lattice chosen. Thus, the molecular partition function for the external degrees of freedom is given by:

$$f_T = \frac{(2\pi mkT)^{3/2}}{h^3}\,\beta \qquad (1.20)$$

and the configurational integral of the system Ω (T):

$$\Omega(T) = [\beta]^N \qquad (1.21)$$

FIGURE 1.1

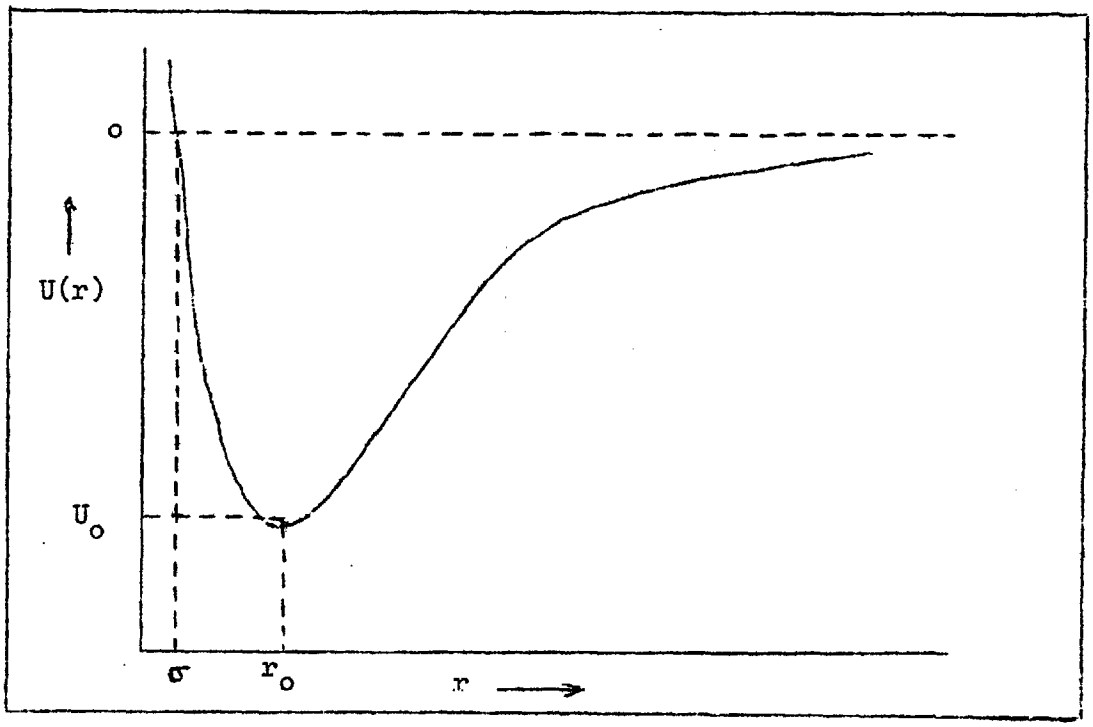

As in the case of the Eyring theory, no allowance has been made for the communal entropy, but if it is assumed that the total communal entropy is introduced at the melting point, it will be independent of volume and will not affect the equation of state. The total entropy will, as before, be modified by a factor R.

Attempts have been made to overcome the difficulties

arising from the communal entropy by modifying the model to accommodate more cells than molecules[13], and by introducing the idea of cell clusters[14]. The results have however, proved disappointing, particularly at the critical point where the advantage of the modifications should be most strongly manifest. A further weakness inherent in the theories mentioned so far, lies in the neglect of correlations between the motions of molecules. Attempts to overcome this restriction have been made, but the mathematical difficulties involved have so far proved insoluble and no results have been obtained[15].

The Lennard-Jones and Devonshire theory, by virtue of the inherent assumptions tends to describe the solid phase. Although a critical isotherm is predicted, the phase transition which disappears at the critical point given by the theory is neither a solid-gas transition nor a liquid-gas transition but a hypothetical transition from a condensed ordered phase to an expanded ordered phase (See this chapter, section 1.5, page: 26)

The Cohen and Turnbull Free Volume Theory[16].

Essentially this theory is based upon the quasi-crystalline model of Lennard-Jones and Devonshire mentioned above. The difference lies in the concept of free volume which, in this theory, is not associated equally with each cell, but is thermally

distributed over the whole volume. The theory is discussed more fully in connection with the influence of molecular shape upon transport properties and glass formation in chapters 2 and 4 respectively.

1.4. Radial Distribution Theories of the Liquid State[17,18]

A molecular distribution function defines the probability of the occurrence of a particular arrangement of molecules in an assembly of a fixed number, N, and fixed volume, V. The first function represents the probability of finding a molecule in a small element of volume, dr_1, at a position whose co-ordinates are defined from any arbitrary fixed point by the vector r_1. This probability is proportional to dr_1, and may be denoted as follows:

$$n^{(1)}(r_1)\, dr_1 \qquad (1.22)$$

In an isotropic fluid this first distribution function is simply the density.

$$n^{(1)} = N/V \qquad (1.23)$$

A pair distribution function defines the probability of finding simultaneously molecules at positions r_1 and r_2, and this function is related to the molecular distribution function according to the following integral equation:

$$\iiint n^{(2)}(r_1,r_2)\, dr_2 = n^{(1)}(r_1).(N-1) \qquad (1.24)$$

Distribution functions of higher order may be defined similarly, and a distribution function of order $h + 1$, may be related to a distribution function of order h according to the following general equation:

$$\iiint n^{(h+1)} dr_{h+1} = (N-h)\, n^{(h)} \qquad (1.25)$$

A set of integral equations for N distribution functions can thus be defined. If a complete solution of these equations could be achieved, an exact equation of state for the fluid could be obtained. The theory has been developed for simple liquids upon the basis of mathematical assumptions permitting a solution of the set of integral equations. One such assumption is the superposition approximation due to Kirkwood, which states that the probability of the simultaneous presence of molecules at r_1, r_2, and r_3 is the product of the independent occurrence of pairs at r_1 and r_2, r_1 and r_3, and r_2 and r_3. In this way a solution for the pair distribution function may be obtained without a knowledge of the triplet and higher order functions.

The radial distribution function theories of the liquid state can claim the theoretical advantage of being independent of any type of assumed physical model. The mathematical complexity of the theories has, however, restricted their application to simple spherical molecules of the inert gas type.

1.5 Liquids Comprising Non-Spherically Symmetrical Molecules.

The number of different liquids which could be expected to fulfil the rather exacting requirements of statistical thermodynamics are extremely limited. The liquid inert gases are an obvious choice, since they consist of spherically symmetrical atoms in which effects due to molecular shape and atomic interactions, other than dispersion forces, are absent. Table 1.2 serves to illustrate the agreement with experiment achieved by the Lennard-Jones and Devonshire theory in the case of solid[19] and liquid[18] argon by comparing the properties of the zero pressure condensed phase. For the 12:6 potential, the constants U_o and r_o are taken as 119.8 k and 3.405 Å respectively. (See this chapter pages 20 and 21) As mentioned before the theory describes the solid phase rather more successfully than the liquid phase. (See page 23).

TABLE 1.2[19]

	Reduced volume V/V_o	Reduced excess energy E'/NU_o	Reduced entropy S'/Nk	Reduced Heat capacity Cv'/Nk
L-J-D	1.037	- 7.32	- 5.51	1.11
Expt. solid	1.035	- 7.14	- 5.33	1.41
Expt. liquid	1.186	- 5.96	- 3.64	0.85
Reduced Properties for Argon				

Regrettably, the liquid range T_b/T_f, of quasi-spherical molecules tends to be short at ordinary pressures (See table 1.3); full use of their possibilities calls for work at enhanced pressures, and this practical difficulty has tended to discourage work in this field.

TABLE 1.3[20]

	Inert gases	$T_f(^oK)$	T_b/T_f (1 atm)
Existance ranges of liquids based on the ratio T_b/T_f	Ne	24	1.11
	A	83	1.04
	Kr	116	1.03
	Xe	161	1.03

It is evident from the preceding sections of this chapter, that the greatest stumbling block to a satisfactory prediction of the thermodynamic properties of liquids comprising non-spherically symmetrical molecules is the estimation of the configurational integral β, (See page 13), which requires a precise knowledge of the intermolecular potentials, and of the nature of the potential field in which the molecule moves.

As mentioned in the introduction to this chapter, this thesis is concerned with the synthesis and properties of "model molecules" of specific shape, and it is hoped that a study based upon the controlled variation of this parameter, not yet amenable

to the rigourous mathematical treatment required by statistical mechanics, will assist in the rationalisation and understanding of its effects.

Non-polar, non-spherically symmetrical molecules may be divided into two classes distinguished by the nature of their respective repulsion envelopes, viz. flexible and rigid molecules. The force fields relating to both classes are similar to those extant in the liquid inert gases, but they are not spherically symmetrical.

1) Flexible molecules

These species may assume more than one configuration, all having much the same energy. Normal paraffins and their derivatives are typical examples (see Fig. 1.2), but many more complex organic molecules are flexible in this sense.

FIGURE 1.2

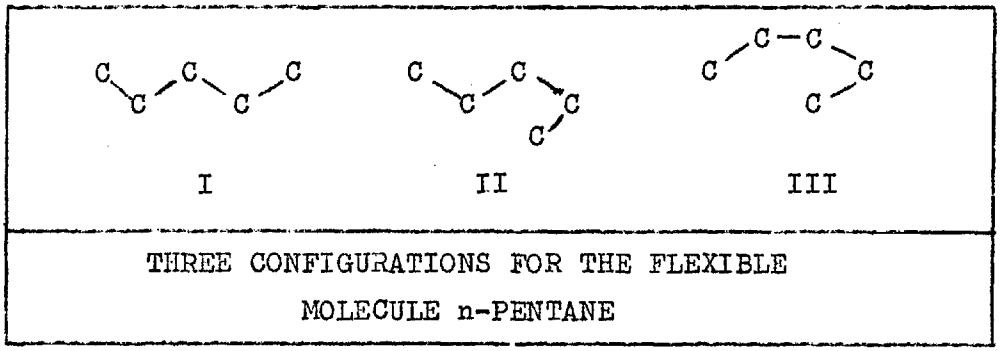

THREE CONFIGURATIONS FOR THE FLEXIBLE MOLECULE n-PENTANE

The shape of a molecule of this type may differ widely with each configuration adopted, and if the difference in energy is

small (i.e. 2-3 kT), and the potential energy barriers to the transformation are of the same order of magnitude, it is impracticable to treat the liquid as containing but one shape of repulsion envelope. In any case, such liquids are mixtures of configurational isomers, and will not be considered further in this present thesis.

2) Rigid Molecules

These species can assume but one configuration of minimum potential energy. Although the effective repulsion envelope changes somewhat with temperature, owing to intramolecular vibrations, to a first approximation they may be taken as constant. Pseudo-spherical and globular molecules display a general similarity in their thermodynamic properties, and in many cases show low entropies of fusion of the same order as the inert gases. They can be regarded as effectively free to rotate in the melt. This type includes neopentane, cyclopentane derivatives, and some globular terpenes derived from bicyclo 2,1,2 heptane, bicyclo 2,2,2 octane and dicyclopentadiene. (See table 1,1 page 19; reference (20), and Fig. 1.3, page 30). Rigid molecules of lower geometrical symmetry such as discs, rods, cog-wheels, and many other special shapes could, in principal, exhibit very special types of liquid behaviour.

Some of the "model molecules" selected for past work

FIGURE 1.3

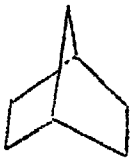	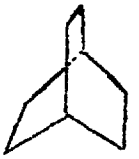	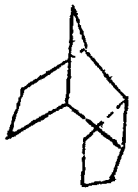
BICYCLO 2,1,2 HEPTANE	BICYCLO 2,2,2 OCTANE	α-DICYCLOPENTADIENE

have been of the polyphenyl type, e.g., o-, m- and p-terphenyl, 1:3:5 tri-α-naphthyl benzene, and 1:3:5 triphenyl benzene etc. These are not completely rigid in the strictest sense since the various substituent aryl groups are able to rotate somewhat within the restrictions imposed by atomic interaction and resonance energy. In the case of cog-wheel shaped molecules such as o-terphenyl, the 1:3:5 substituted benzenes, and the aromatic allenes studied in this present work, the resulting variations in the shape of their repulsion envelopes is comparatively small, and does permit the discussion of various anomalies in behaviour attributable to molecular shape. In some instances, the optimum orientation of substituents can be determined and the effects of the restricted rotation, upon volumes of molecular rotation, and upon the predisposition to molecular interlocking assessed.

A full discussion of the polyphenyls hitherto studied, and of the aromatic allenes, which are the subject of this present work, is reserved for the following chapters.

REFERENCES

1. Hazlewood, F.J., Ph.D. Thesis "The Physico-chemical Properties of Low Melting Salts", London, (1966).
2. Rushbrooke, G.S. "Introduction to Statistical Mechanics", O.U.P. (1949).
3. Fowler R. and Guggenheim, E.A., "Statistical Thermodynamics", C.U.P. (1949).
4. Buehler, R.J. Wentorf, R.H. Jr., Hirschfelder, J.O. and Curtiss, C.F., J. Chem. Phys., 19, 61 (1951).
5. Barker, J. A., "Lattice Theories of the Liquid State", Pergamon (1963).
6. Frenkel, J., Acta Physicochem, U.R.S.S. (1935), 3, 633 and 913.
7. Bresler, S.E. Acta Physicochem, U.R.S.S. (1939) 10, 491.
8. Eyring, H. and Hirschfelder, J.O., J. Phys. Chem., 41 249 (1937);
   Eyring, H. and Ewell, R.H., J. Chem. Phys., 5, 726 (1937).
9. Hirschfelder, J.O., Stevenson, D.P. and Eyring, H. J. Chem. Phys., 5, 896 (1937).
10. Eyring, H., J. Chem. Phys., 4, 283 (1936).
11. Lennard-Jones, A.F. and Devonshire, J.E., Proc. Roy. Soc., A.163, 53 (1937).
12. Lennard-Jones, A.F. and Devonshire, J.E., ibid., A.165, 1 (1938).

13. Cernuschi, F. and Eyring, H., J. Chem. Phys. 7, 547 (1939)
Ono, S., Mem. Faculty of Eng., Kyrushu Univ., 10, 190 (1947).
Peek, H.M. and Hill, T.L., J. Chem. Phys., 18, 1252 (1950).
Rowlinson, J.S. and Curtiss, C.F., J. Chem.Phys., 19, 1519 (1951).

14. De Boer, Physica, 20, 655 (1954).

15. Prigogine, I. and Janssens, P., Physica, 16, 895 (1950).
Pople, J.A., Phil. Mag., 41, 459 (1951).
Englert Chwoles, A., J. Chem. Phys., 20, 925 (1952).

16. Cohen, M.H. and Turnbull, D., J. Chem. Phys., 29, 1049 (1958).
" " ibid 31, 1164 (1959).
" " ibid 34, 120 (1961).

17. Mayer, J.E. and McMillan, W.G. Jr., J. Chem. Phys., 13, 276 (1945).
Kirkwood, J.G., Maun, E.K. and Alder, B.J., J. Chem. Phys., 18, 1040 (1950).
Kirkwood, J.G., J. Chem. Phys., 14, 180 (1946).
Green, H.S. "Molecular Theory of Fluids", N. Holland Publication Co. (1952).

18. Rowlinson, J.S. "Liquids and Liquid Mixtures, Butterworths (1959).

19. Dobbs, E.R. and Jones, G.O., Rep. Prog. Phys., 20, 516 (1957). (c.f. reference 5)

20. Ubbelohde, A.R. "Melting and Crystal Structure", Clarendon Press (1965).

CHAPTER 2.

THE VISCOSITY OF LIQUIDS

2.1. Definition of Viscosity[1]

The liquid state is characterised mechanically by an inability to sustain shearing stress. A stress applied tangentially to a mass of liquid will result in a velocity gradient perpendicular to the direction of the stress; the liquid displays resistance to the applied stress and is said to exhibit viscosity or internal friction. It was assumed by Newton that, for a liquid moving in parallel layers the shearing stress at any point is directly proportional to the velocity gradient, so that the frictional force per unit area, f, is given by:

$$f = \eta \frac{du}{dZ} \qquad (2.1)$$

where $\frac{du}{dZ}$ is the velocity gradient, and the constant of proportionality η is termed the coefficient of viscosity which is characteristic of the liquid at any particular temperature and pressure. Formally then, the coefficient of viscosity η , may be defined as the stress necessary to maintain unit velocity gradient in the liquid. Newton's law is found, by experiment, to hold when the motion of the liquid is stream-line, but it fails to hold for turbulence or disorderly flow. In most experiments devised to measure coefficients of

viscosity, stream-line flow is assumed to be present in which case the work done by the applied stress is dissipated solely in overcoming the viscous drag exerted by the liquid. On the other hand, when turbulent flow occurs, the energy applied to produce motion is used in producing eddy currents. Thus the onset of turbulence will depend upon the viscosity of the liquid, its density, and the nature of the channel through which it flows. Reynolds[2] has shown empirically that the critical velocity v is related to the density of the liquid ρ, its viscosity η, and the lateral dimension of the channel according to the following equation:

$$v_c = \frac{k\eta}{\rho r} \qquad (2.2)$$

For narrow tubes k, which is termed the Reynolds' number, is about 1000, when the velocity v_c reaches the critical value for turbulent flow. Further, if the liquid flow is not stream-line the coefficient of viscosity will vary with the applied stress, and this fact can be used to test for turbulence if the estimation of one or more of the parameters in the Reynolds equation is not practicable.

2.2 Viscosity and the Transfer of Momentum

Viscosity is one of the processes classified as transport phenomena, the others being diffusion and thermal conductivity. These three phenomena are related in that they each involve the

transport of a physical property through the medium under consideration. Viscosity involves the transport of momentum resulting from a velocity gradient in the medium, diffusion the transport of mass due to a concentration gradient, and thermal conductivity the transport of thermal energy due to a temperature gradient. Diffusion may be accounted for in terms of the movement of the molecules comprising the medium, but viscosity and thermal conductivity may also result from a mechanism involving molecular vibration. In addition to these simple processes, more complex mechanisms may contribute involving the flow and vibration of molecular clusters. No means have so far been devised with which it is possible to distinguish directly between the various mechanisms or to assess the contribution of any one in a complex process, but a number of theories of viscous flow have been presented upon the basis of assumed transfer mechanisms some of which will be discussed below.

2.3 Theories of Viscosity.

2.3.1. Maxwell's Relaxation Theory

Distortion or strain, s, is produced in a body by the application of a stress, f; in the case of a perfectly elastic body the stress is directly proportional to the strain, i.e.

$$f = \epsilon s \qquad (2.3)$$

where ϵ is a coefficient of elasticity. In a solid body,

free from viscosity, the strain produced will remain so long as the applied stress is maintained. Thus:

$$\frac{df}{dt} = \epsilon \frac{ds}{dt} \qquad (2.4)$$

where t is time. If the body is viscous it will fail to sustain the stress which will tend to disappear at a rate dependent upon the initial value of the stress and the nature of the body. If it is supposed, as a particularly simple assumption, that the rate at which the stress is dissipated is proportional to f, equation (2.4) may be rewritten:

$$\frac{df}{dt} = \epsilon \frac{ds}{dt} - \frac{f}{\tau} \qquad (2.5)$$

If the strain s remains constant equation (2.5) becomes, upon integrating:

$$f = \epsilon s \exp - \frac{t}{\tau} \qquad (2.6)$$

Hence the body, left to itself, loses internal stress and returns to the state of a fluid at rest. If ds/dt is constant, there is steady motion of the body and the displacement increases continuously. The following shows that under these conditions the stress f tends to a constant value depending upon the rate of displacement.

Rearranging equation (2.5):

$$f = \epsilon \tau \frac{ds}{dt} - \tau \frac{df}{dt} \qquad (2.7)$$

from equation (2.6)

$$\frac{df}{dt} = \frac{d}{dt}\left\{\epsilon s \exp - \frac{t}{\tau}\right\} = \epsilon \left[\frac{ds}{dt} - \frac{s}{\tau}\right] \exp - \frac{t}{\tau} \qquad (2.8)$$

Substituting into equation (2.7) and rearranging:

$$f = \epsilon \tau \frac{ds}{dt} + (\epsilon s - \epsilon \tau \frac{ds}{dt}) \exp - \frac{t}{\tau} \qquad (2.9)$$

Now, from equation (2.6), $\epsilon s \exp - \frac{t}{\tau}$ can be replaced by f_o which is the initial stress. Equation (2.9) may be rewritten:

$$f = \epsilon \tau \frac{ds}{dt} + K \exp - \frac{t}{\tau} \qquad (2.10)$$

where $K = f_o - \epsilon \tau \frac{ds}{dt}$.

The quantity $\epsilon \tau$ may be identified with the coefficient of viscosity η ; it is the product of a coefficient of elasticity ϵ , and a time τ termed the relaxation time for the elastic forces. For mobile liquids τ is a small fraction of a second but for very viscous liquids τ may be in the order of hours or days allowing velues of ϵ to be obtained experimentally. Thus, according to Maxwell, the phenomenon of viscosity arises from the fact that the response to an applied stress is not instantaneous, but is manifest after a time interval τ following the application of the stress. Maxwell's fundamental equation is:

$$\eta = \epsilon \tau \qquad (2.11)$$

In other words, a constant stress applied to a solid results in a constant deformation. In a fluid such a stress results in a deformation which increases with time. This conclusion may be illustrated by setting df/dt to zero in equations (2.4) and (2.5). In the latter case, the rate of change of strain (deformation) under constant stress is given by:

$$\frac{ds}{dt} = \frac{f}{\epsilon \tau} = \frac{f}{\eta} \qquad (2.12)$$

If the direction of the stress were to alternate with a frequency $\leqslant \tau$ the liquid would fail to exhibit viscous flow. The shearing stress in this case merely produces a shift of the equilibrium positions of all the particles within each layer of the liquid with respect to the adjacent layers in a manner similar to an elastic solid.

τ is therefore a measure of the rate at which a fluid loses internal stress. A physical interpretation of this factor will depend upon the nature of the particular mechanism proposed for flow. For example, in the case of a molecular vibration model, τ will be associated with the frequency of molecular vibration, and in the case of 'hole' theories τ will be associated with the kinetics of 'hole' formation and the subsequent movement of a molecule.

2.3.2. Frenkel's Theory of Viscous Flow[4]

This theory, closely similar in basic concepts and results to the Maxwell theory above, is evolved on a molecular basis. Each molecule is assumed to vibrate about its mean position with a period τ_o for a definite time τ subsequent to changing its position. Viscous flow will only occur when the stress f, is maintained for a period of time much greater than τ . The theory suggests that the transport of a molecule under the influence of the applied stress occurs in two stages. The first stage involves the transfer of a molecule from its site in the quasi-lattice to an interstitial position raising the potential energy to a value W which is the equivalent of the activation energy for the process; the second stage marks the return of the molecule from the high energy interstitial position to a new equilibrium position, when the kinetic energy released is distributed amongst the neighbouring molecules. In all, this is a characteristic 'hopping' mechanism in which each hop changes the equilibrium position. The theory further assumes, possibly by analogy with the Arrhenius rate equation, that the time spent by each molecule in an equilibrium position, i.e. τ is given by:

$$\tau = \tau_o \exp. W/kT \qquad (2.13)$$

where k is the Boltzmann constant. In order to relate the mean time τ to the relaxation time of the Maxwell theory

τ_m, the following relationship has been proposed:

$$\tau_m = \tau \frac{6kT}{\epsilon d^3} \qquad (2.14)$$

where ϵ is a modulus of rigidity and d, the distance between adjacent equilibrium positions. Hence the equation of the viscosity coefficient according to this theory is given by:

$$\eta = \frac{6\tau_o kT}{d^3} \exp W/kT \qquad (2.15)$$

If the pre-exponential term and activation energy are assumed independent of temperature, equation (2.15) bears a similarity to a relationship first proposed empirically by de Guzman[5] to explain the variation of viscosity with temperature:

$$\eta = A \exp B/T \qquad (2.16)$$

which holds good for a large range of non-associated liquids.

2.3.3. Andrade's Theory of Viscosity[6]

This theory is based upon the premise that momentum is transferred through a liquid under the influence of a shearing force according to a vibrational mechanism; the model of the liquid state assumed being similar to the cell models of Lennard-Jones and Devonshire, etc., described in Chapter 1.

In a liquid at rest each molecule vibrates about its equilibrium position which, unlike a solid, is displaced by time. Under the influence of stress a molecule located in one

layer of liquid may associate momentarily with another in a parallel layer moving past under the influence of the velocity gradient produced by the applied stress. The life-time of each association is very small but it is assumed that there is sufficient time to allow a sharing of momentum between the two molecules in the parallel layers. If it is further assumed that the vibrational frequency $(\nu_L)_f$ of each molecule at the freezing point is equal to that of the solid $(\nu_S)_f$ at the melting point, the following expression can be derived for the viscosity of the liquid at the freezing point:

$$\eta = \frac{4}{3} \cdot \frac{\nu_f m}{\sigma} \qquad (2.17)$$

where m and σ are the molecular mass and mean intermolecular distance respectively. The frequency ν_f may be given, upon the basis of the above assumptions by the Lindemann equation[7]:

$$\nu_f = k\sqrt{\frac{T_f}{MV^{1/3}}} \qquad (2.18)$$

where k is a constant, M, the molecular weight and V, the molecular volume, and T_f the freezing point. Hence expression (2.17) becomes:

$$\eta = \frac{4k}{3} \cdot \frac{(MT_f)^{1/2}}{(NV)^{2/3}} \qquad (2.19)$$

where $mN = M$ and $\sigma = \left(\frac{V}{N}\right)^{1/3}$.

In order to obtain an expression to describe the temperature dependence of viscosity it is necessary to make a few further assumptions:

(i) The transfer of momentum may only take place if the mutual potential energy of the approaching molecules is favourable. In the case of non-spherically symmetrical molecules, this mutual potential energy may be influenced by the relative orientations of the approaching molecules.

(ii) Under the influence of local intermolecular forces, the molecules tend to be similarly orientated within very small groups, the boundary and molecular population of each group being in a state of continual change.

(iii) The tendency for the molecules to assume an orientation favourable to interchange of momentum is disturbed by thermal agitation.

(iv) The number of molecules in possession of a favourable potential energy is determined by the Boltzmann distribution law. Hence the number of molecules possessing this energy ϵ at temperature T is given by:

$$n = e^{\epsilon/kT} \quad \text{and at } T', \quad n' = e^{\epsilon/kT'}$$

The ratio is: $e^{\epsilon/k\left(\frac{1}{T} - \frac{1}{T'}\right)}$.

If it assumed that the variation of molecular vibration can be neglected and that the dependence of viscosity upon temperature is determined principally by condition (iv) above, the dependence may be represented as follows:

$$\eta_T = \eta_{T'} \exp\left(-\frac{\epsilon}{kT'}\right) \exp\left(\frac{\epsilon}{kT}\right) = A \exp\left(\frac{c}{T}\right) \qquad (2.20)$$

where A and c are constants for a given liquid.

So far, the Andrade theory has failed to account for any effect arising from the change of volume of the liquid with temperature. Owing to normal expansion, the average distance between the molecules in the liquid will increase with temperature as $v^{1/3}$, where v is the specific volume, whilst the number of molecules per unit area will diminish as $v^{-2/3}$; hence the viscosity will diminish as $v^{-1/3}$. Further, the potential energy involved in the condition determining momentum transfer will also be a function of volume, i.e. f(v). These two effects may be taken into account by mod fying equation (2.20) to give:

$$\eta\, v^{1/3} = A' \exp\left\{\frac{c'f(v)}{T}\right\} \qquad (2.21)$$

Now, the average potential energy of a molecule is, to a first approximation, represented by the factor a in the a/v term of Van de Waals' equation. Andrade assumed that the part of the potential energy concerned in momentum transfer varies in a

similar manner yielding the following expression:

$$\eta\, v^{1/3} = A'' \exp (c''/vT) \qquad (2.22)$$

This formula agrees closely with experiment for a wide range of liquid types including some highly associated liquids like alcohols, acids and amines, particularly at temperatures well above the melting point. The satisfactory agreement with experiment which this theory affords may be due to the fact that the assumptions involved attribute momentum transfer to some kind of association governed by a simple temperature law not dissimilar to that describing the degree of association extant in the above liquid types.

2.3.4. The Reaction Rate Theory of Eyring[8]

This theory, due to Eyring and co-workers, is based upon a quasi-lattice model for the liquid in which a number of vacant sites or holes are present. Self-diffusion in liquids may be considered to result from the random movement of certain molecules from their equilibrium positions in their cells into adjoining vacant lattice sites. In order to change their location the molecules must overcome a potential energy barrier imposed by the proximity of the neighbouring molecules. According to the theory of absolute reaction rates, the frequency of movement of a molecule over such a barrier and hence the translation in any direction per second is given by:

$$K_s = \frac{kT}{h} \frac{Z^*}{Z} \exp - \frac{\epsilon_o}{kT} \qquad (2.23)$$

where Z^* and Z refer to the partition functions for unit volume of the molecule in the activated and initial states respectively, and ϵ_o, the height of the energy barrier. The equilibrium constant K^* of the process can be expressed as:

$$K^* = \frac{Z^*}{Z} \exp (- \epsilon_o/kT) \qquad (2.24)$$

and the Gibbs free energy of activation per mole as:

$$\Delta G^* = - RT \ln K^* \qquad (2.25)$$

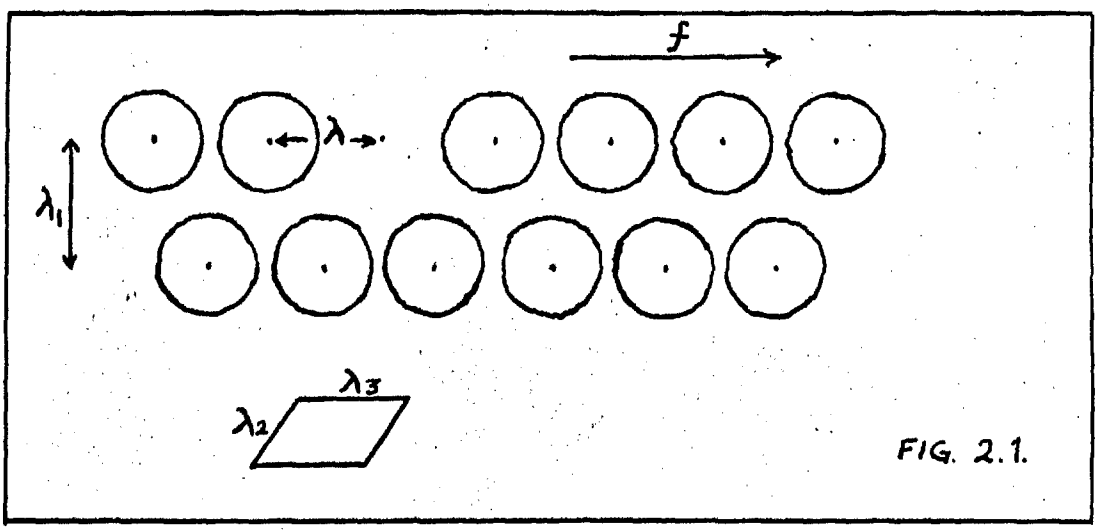

FIG. 2.1.

Viscous relaxation results from the application of an external stress which causes the diffusion process to occur in a

preferred direction.

Consider two layers of molecules in a liquid at a distance λ_1 apart. These layers slide past each other under the influence of an applied force f (See Fig. 2.1). If f is the force acting per unit area, and Δu represents the velocity difference between the two layers, then the viscosity η will be, by definition:

$$\eta = \frac{f \lambda_1}{\Delta u} \qquad (2.26)$$

The sliding of one layer of molecules over another is assumed to involve the movement of a molecule from one equilibrium position to another such position in the same layer, but in order that this movement may take place a suitable hole or vacant lattice site must be available, and an energy barrier overcome. If the distance between the initial and final equilibrium positions of the moving molecule is λ, the distance between neighbouring molecules in the same direction is λ_3 †, and the distance between molecules in a direction perpendicular to the direction of flow is λ_2, the applied force acting on a single molecule in the direction of flow is $f\lambda_2\lambda_3$ where $\lambda_2\lambda_3$ is the effective area of the molecule. It is reasonable to assume that the potential energy barrier is symmetrical, and that the peak of the barrier lies half way

---

† λ need not necessarily be equal to λ_3 since the presence of a hole may distort a lattice.

between the two equilibrium positions, its distance from either position being $\lambda/2$ (see Fig. 2.2). The energy the molecule has acquired from the applied force in moving from its equilibrium position to the peak of the energy barrier is $f\lambda_2\lambda_3\lambda/2$, which in effect reduces the height of the energy barrier, ϵ_o opposing the molecule's motion by that amount.

FIGURE 2.2

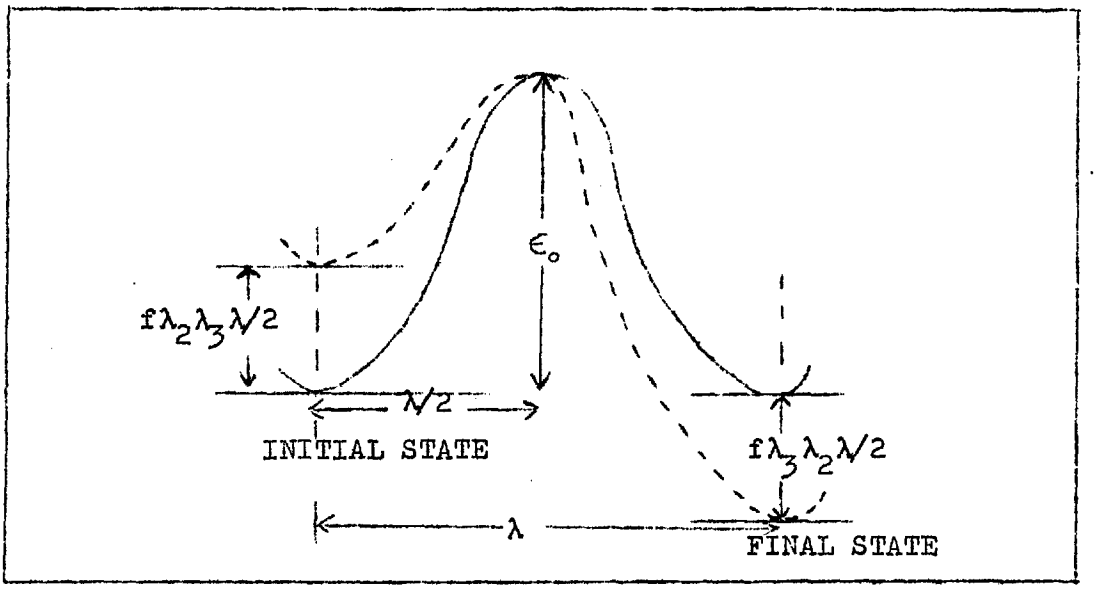

Thus, from equation (2.23) above, the number of times a molecule passes over the potential energy barrier per sec. is given by:

$$K = \frac{kT}{h} \cdot \frac{Z^*}{Z} \exp - (\epsilon_o - f\lambda_2\lambda_3\lambda/2)/kT \qquad (2.27)$$

Thus the rate of flow in the direction of the force is:

$$K_f = K_s \exp\left(\frac{f\lambda_2\lambda_3\lambda}{2kT}\right) \qquad (2.28)$$

and the rate of flow in the reverse direction is:

$$K_B = K_s \exp\left(-\frac{f\lambda_2\lambda_3\lambda}{2kT}\right) \qquad (2.29)$$

Every time a molecule cross the potential energy barrier it moves a distance λ, and since K_f and K_B represent the number of times this occurs per second in the forward and backward directions respectively, the rate of motion of the layer will be $K_f\lambda$ in the forward direction and $K_B\lambda$ in the backward direction. Thus the net rate of flow in the forward direction is $(K_f - K_B)\lambda$ which is by definition Δu. Hence, from equations (2.28) and (2.29), Δu is given by:

$$\Delta u = 2\lambda K \operatorname{Sinh} \frac{f\lambda_3\lambda_2\lambda}{2kT} \qquad (2.30)$$

From equation (2.26) the coefficient of viscosity is:

$$\eta = \frac{\lambda_1 f}{2\lambda K_s \operatorname{Sinh}(f\lambda_2\lambda_3\lambda/2kT)} \qquad (2.31)$$

For normal viscous flow $2kT \gg f\lambda_2\lambda_3\lambda$, since $f \approx 1$ dyne cm^{-2} and λ_2, λ_3, and $\lambda \approx 10^{-8}$ cm. Hence equation (2.31) may be simplified to give:

$$\eta = \frac{\lambda_1 kT}{\lambda_2 \lambda_3 \lambda^2 K_s} \qquad (2.32)$$

If the value for K_s given by equation (2.23) is inserted into equation (2.32) the expression becomes:

$$\eta = \frac{\lambda_1 h}{\lambda_2 \lambda_3 \lambda^2} \quad \frac{Z}{Z^*} \quad e^{\epsilon_o/kT} \qquad (2.33)$$

but since λ_1 is of the same order of magnitude as λ, equation (2.33) reduces to:

$$\eta = \frac{h}{\lambda_2 \lambda_3 \lambda_1} \quad \frac{Z}{Z^*} \quad \exp \ \epsilon_o/kT \qquad (2.34)$$

Now, $\lambda_2 \lambda_3 \lambda$ is approximately equal to the volume occupied by each molecule in the liquid, and may be replaced by V/N, where V is the molar volume and N the Avogadro number, hence:

$$\eta = \frac{hN}{V} \quad \frac{Z}{Z^*} \quad \exp \ \epsilon_o/kT \qquad (2.35)$$

According to equations 2.24 and 2.25):

$$K^* = \frac{Z^*}{Z} \quad \exp \ (-\epsilon_o/kT) \quad \text{and} \quad \Delta G^* = -RT \ln K^*$$

Hence:

$$\eta = \frac{hN}{V} \exp \frac{\Delta G^*}{RT} \qquad 2.36)$$

where ΔG^{*} is the free energy of activation. Since $\Delta G^{*} = \Delta H^{*} - T\Delta S^{*}$, equation (2.36) may be rewritten as follows:

$$\eta = \frac{hN}{V} \exp\left(-\frac{\Delta S^{*}}{R}\right) \exp\left(\frac{\Delta H^{*}}{RT}\right) \qquad (2.37)$$

or more simply:

$$\eta = A \exp \frac{\Delta H^{*}}{RT} = A \exp \frac{E\eta}{RT} \qquad (2.38)$$

It has become usual to identify the activation energy for viscous flow $E\eta$, with ΔH^{*}, when the pre-exponential term, A becomes a measure of the entropy of activation. The Eyring equation has been re-derived by A. R. Ubbelohde, et. al[9,10]. The derivation is identical in principal with the original, but the area associated with each molecule is defined as $1/n\delta$ (instead of $\lambda_2\lambda_3$) where n is the molecular concentration per unit volume and δ the distance between molecular layers. This gives the following expression:

$$\eta = \left(\frac{\delta}{a}\right)^{2} \frac{Nh}{V} \exp\left(-\frac{\Delta S^{*}}{R}\right) \exp\left(\frac{E\eta}{RT}\right) \qquad (2.39)$$

where a is the intermolecular distance in the direction of the applied stress. The advantage of this derivation lies in the term $\left(\frac{\delta}{a}\right)$ which can provide a measure of the anisotropy of the special molecules which are studied in this present work and which are discussed in the following section. Again

expression (2.38) reduces to:

$$\eta = A \exp E\eta/RT.$$

where $E\eta$ is the activation energy for viscous flow.

Van Velden[11] has pointed out that the theory presented above implies the assumption that E_η, ΔS^* and V are independent of temperature. Eyring[12] has suggested that for simple liquids* variations of these quantities with temperature tend to compensate each other, rendering $E\eta$ temperature independent. This general conclusion was later reached by McLaughlin[13], who stated that whilst $E\eta$, ΔS^*, and V are in fact temperature dependent, their temperature dependence is such that compensation occurs with the result that the viscosity/temperature behaviour may indeed be represented by equation (2.38). McLaughlin has further suggested that deviations from equation (2.38) may have their origin in effects associated with molecular shape (See this Chapter, section 2.4).

The Eyring Rate Theory affords one of the best theoretical descriptions of the temperature dependence of viscosity, and leads to a relationship of the type first proposed by de Guzman[5]. However, the theory can only be valid for liquids in which the molecules move individually; if the flow involves the movement of crystal clusters or molecular aggregates the relationship

---

* i.e. Liquids composed of non-polar molecules of high symmetry.

ceases to hold. This will be illustrated and discussed in section 2.4 of this chapter and in Chapter 4, section 4.2 in connection with liquids comprised of molecules of specialised shape.

It must be remembered however, that whilst the behaviour, with regard to the Eyring equation, of liquids comprising molecules of different shape or type may prove useful as a means of comparison or of correlation, a too specific interpretation of the values of E_η and $\Delta S^{\ddagger}$ should be avoided.

2.3.5. Theories Relating Viscosity to Free Volume

The first attempt to relate the viscosity η of a liquid to free volume was due to Batschinski[14] who, in 1913, proposed the following empirical relationship based upon a study of some 80 organic liquids:

$$\eta = \frac{c}{v - w} \qquad \text{or} \qquad \phi = \frac{v - w}{c} \tag{2.39}$$

where ϕ is the fluidity and $v - w$, a measure of the free volume of the liquid. The value of c is reasonably constant from liquid to liquid but it does show some variation which can be roughly correlated with molecular shape. This correlation is of particular importance in the present context and will be discussed more fully in section (2.4).

A further development of the Batschinski equation is due to MacLeod[15] who proposed the following relationship:

$$\eta = \frac{c}{(v - b)^n} \qquad (2.40)$$

in which n is a small number ranging from about 1.1 for non-associated liquids such as paraffins to about 3.5 for highly associated liquids such as alcohols, and b which may be loosely identified with the volume correction term 'b' in Van de Waals' equation. The definition of free volume implicit in these relationships is simply the difference between the molar volume of the liquid and the volume occupied by one mole of the molecules themselves. Doolittle[16] has shown that the dependence of fluidity upon free volume is satisfactorily described by the following expression over the glass transition region:

$$\phi = A \exp - (q\, V_o/V_f) \qquad (2.41)$$

where q is a constant in the order of unity, V_o the volume of a molecule, and v, the specific volume; the free volume V_f is then given by:

$$V_f = v - V_o \qquad (2.42)$$

The definition of free volume represented by equation (2.42) is essentially the same as the free volume defined by Batschinski and MacLeod above.

More recently, Cohen and Turnbull[17] have developed a theory to describe the viscosity of liquids based upon a rather

special concept of free volume. The primary object of their work was to provide a satisfactory explanation for the phenomenon of glass formation, but this aspect of their work together with a more detailed discussion of the theory is reserved for Chapter 4, section 4.3.

The theory is based upon a cell model for the liquid state. The free volume V_f represents that part of the cell in which the molecules may move freely with their gas kinetic energy velocity u ($u = (3kT/m)^{1/2}$). The most important premise of the theory is that when, upon raising the temperature, V_f exceeds a certain critical value, the free volume is no longer associated in equal portions with each molecule, but may be distributed in greater or smaller portions throughout the liquid. Thus the free volume may be redefined as that portion of the total volume which may be redistributed without any significant increase in energy, i.e. the activation energy for redistribution is small compared with kT. Transport may only take place when voids, having a volume greater than some critical volume V^*, are formed as a result of the redistribution into which a molecule may jump. Within the accuracy of the theory there is no necessity to allow for the movement of a molecule from its cell into a vacant space and then back again as in the case of diffusion in solids. The idea that the movement of molecules requires little

activation energy compared with kT, but before a molecule can move from its site a co-operative movement in several other degrees of freedom is necessary, appears in earlier theories due to Barrer[18] and Beuche[19], but the idea was not developed fully.

A consideration of the movement of the molecule in its cell, together with the statistically most probable distribution of free volume leads to an expression, similar in form to the Doolittle equation (equation 2.41), for the self-diffusion coefficient of the liquid:

$$D = g\, a^{*}\, u \exp - \frac{\gamma V^{*}}{V_f} \qquad (2.43)$$

D is the self-diffusion coefficient, g and γ are numerical factors allowing for the probability that a molecule is moving towards a site where diffusion could occur at the right time, and overlap of the various portions of free volume respectively; and a^{*} is the diameter of a void possessing the critical volume V^{*}, whilst u is the gas kinetic energy velocity defined above. The redefined free volume V_f is represented by the following equation:

$$V_f = \alpha \bar{V}_M (T - T_o)$$

where $\bar{V}_M$ is the average volume per molecule, and T_o the temperature at which the volume available for redistribution (i.e. V_f) is zero. T_o may be identified with the glass transition temperature (c.f. Chapter 4, section 4.3).

The viscosity of the material may be obtained from the diffusion coefficient by means of the Stokes-Einstein relationship, and this leads to an expression of the following type for the fluidity of a liquid.

$$\phi = \frac{1}{\eta} = A_\phi T^{-1/2} \exp - \frac{B_\phi}{(T - T_o)} \qquad (2.44)$$

Before proceeding further, it is necessary to comment upon the validity of the Stokes-Einstein relationship when applied to microscopic systems[20]. The original derivation of the Stokes equation considered the classical hydrodynamics of a sphere moving in a viscous continuum. Later derivations based upon a more realistic molecular model have led to an expression of the same form:

$$D_i = \frac{kT}{Aa_i \eta_i} \qquad (2.45)$$

where D_i is the self-diffusion coefficient of species i, and a_i the radius of the moving particle. The factor A is a molecular shape factor which for symmetrical molecules is in the order of unity, though in the original Stokes equation this constant was assigned the value 6π. Despite differences in this constant a simple proportional relationship does seem to apply.

An examination of equation (2.44) reveals a similarity to the Arrhenius type of equation but with a temperature dependence of the pre-exponential factor which does not contribute significantly if $T \gg T_o$. The greatest difficulty in applying the theory lies in the estimation of T_o, the glass transition temperature. It has been shown that the theory can describe

the temperature dependence of viscosity for a number of molten salts[21,22], T_o being estimated by extrapolating the η vs. T plot to $\eta = 10^{13}$ poise. The application of the analogous expression for electrical conductivity has also produced quite good agreement with experiment[21]. Hitherto no attempt has been made to test the theory within the context of organic liquids or melts, but the Doolittle equation (equation 2.41) has been shown to fit the fluidity data obtaining to a variety of organic liquids, particularly straight-chain hydrocarbons[16]. It would be interesting to see how the theory behaves within the context of the glass-forming melts considered in the present work.

2.4 Viscosity and Molecular Constitution.

This section is concerned with the influence of molecular shape upon the viscosity of organic liquids, particularly hydrocarbon melts.

The temperature dependence of viscosity is described quite well over a large range of temperature by an expression of the Eyring type (see equation 2.38) for a wide variety of compounds, both associated and non-associated, many of which comprise molecules which are far from spherical.

Over the past few years it has been found that the viscosity of a number of hydrocarbon melts, in which effects due to dipole interaction are minimised, increases at an anomalously high rate as the temperature of the melt is lowered

towards the solid phase melting point*. Anomalous behaviour of this type seems to be most marked in liquids consisting of "cog-wheel" shaped molecules, and this has been illustrated by comparing the viscosity/temperature behaviour of o-terphenyl and triphenylene[23, 9]. The volumes occupied by these molecules in space are almost identical, but in the case of o-terphenyl two phenyl groups are free to rotate, within the limites imposed by atomic interaction and resonance energy, with respect to the third, whilst triphenylene must necessarily remain in a planar configuration. (See Fig. 2.3 c and d). o-Terphenyl shows a marked increase in viscosity as the melting point is approached, whereas triphenylene displays no significant anomaly. (See Fig. 2.4 c and d). A further illustration of this correlation may be found by examining the viscosity/temperature behaviour of all three terphenyls[24], the magnitude of the anomaly increasing in the order p-terphenyl, m-terphenyl, o-terphenyl. (See figs. 2.3 a,b and c, 2.4 a,b and c). A number of other melts, consisting of molecules possessing an even more marked "cog-wheel" shape have been studied, and the results obtained serve to confirm the correlation mentioned above. These melts include 1:3:5 triphenyl benzene[10, 25], 2:2' biphenyl diphenyl[25] and 1:3:5 tri-α-naphthyl benzene[10, 25]; the latter compound,

---

* The term "freezing point" has been deliberately avoided since it becomes meaningless when applied to melts of this type which readily super-cool and occasionally congeal to glasses.

FIG. 2.3.

2.3a.

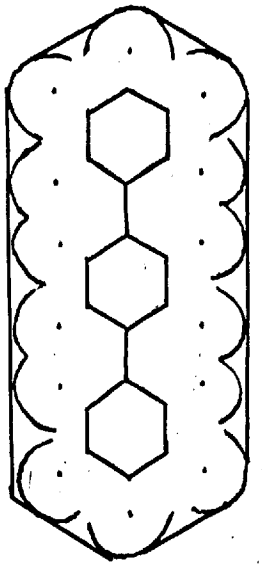

p-TERPHENYL.

2.3b.

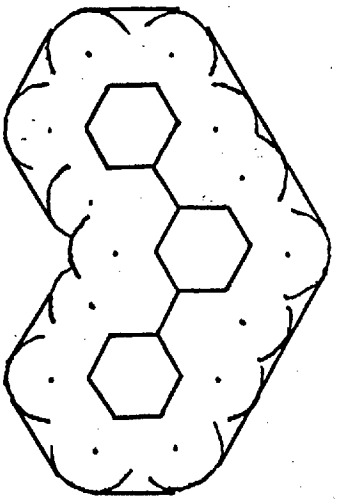

m-TERPHENYL.

2.3c.

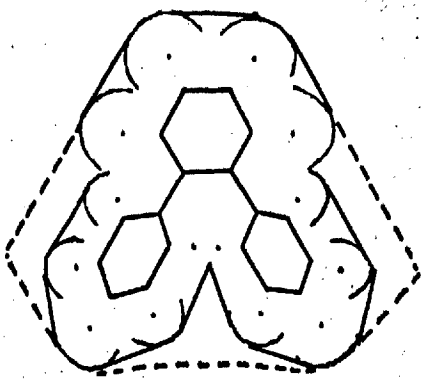

o-TERPHENYL.

2.3d.

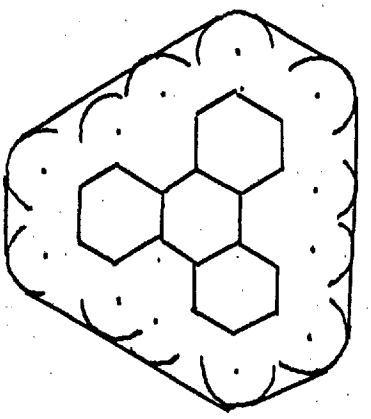

TRIPHENYLENE

VAN DE WAALS' ENVELOPES.

FIG. 2.4.

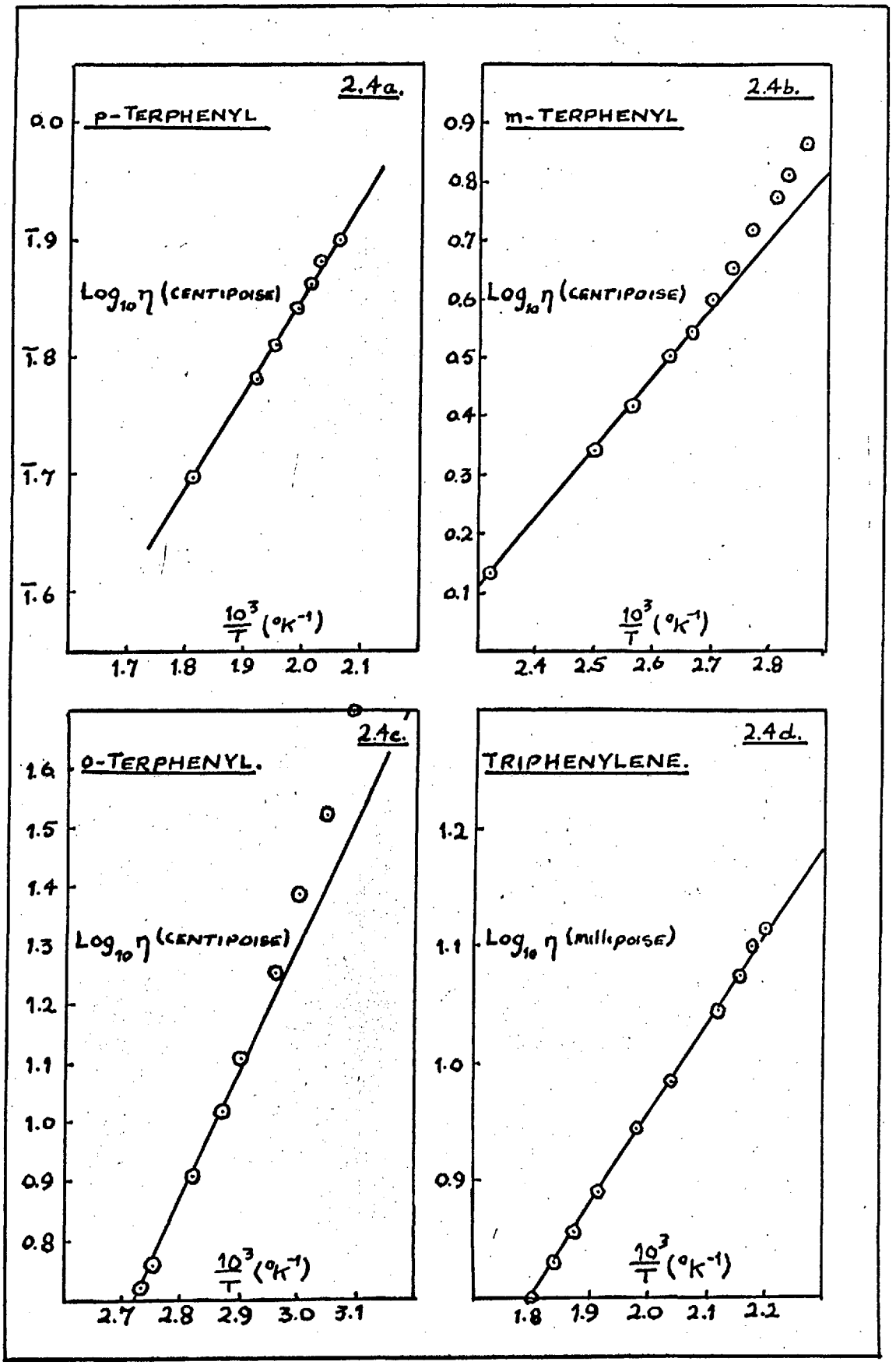
2.4a.
p-TERPHENYL
0.0
$\bar{1}.9$
$\bar{1}.8$
$\bar{1}.7$
$\bar{1}.6$
$\log_{10}\eta$ (CENTIPOISE)
$\frac{10^3}{T}$ ($^\circ K^{-1}$)
1.7 1.8 1.9 2.0 2.1
2.4b.
m-TERPHENYL
0.9 0.8 0.7 0.6 0.5 0.4 0.3 0.2 0.1
$\log_{10}\eta$ (CENTIPOISE)
$\frac{10^3}{T}$ ($^\circ K^{-1}$)
2.4 2.5 2.6 2.7 2.8
2.4c.
o-TERPHENYL.
1.6 1.5 1.4 1.3 1.2 1.1 1.0 0.9 0.8
$\log_{10}\eta$ (CENTIPOISE)
$\frac{10^3}{T}$ ($^\circ K^{-1}$)
2.7 2.8 2.9 3.0 3.1
2.4d.
TRIPHENYLENE.
1.2 1.1 1.0 0.9
$\log_{10}\eta$ (millipoise)
$\frac{10^3}{T}$ ($^\circ K^{-1}$)
1.8 1.9 2.0 2.1 2.2

which will readily congeal to a glass, has recently been examined in detail by Plazek and Magill[26] but the results obtained will be discussed more fully in Chapter 4.

There are two theories current at present which provide an explanation for the anomalous behaviour of these compounds. The first theory, and the most pertinent within the present context of "cog-wheel" shaped molecules is the cluster theory due to A.R. Ubbelohde and E. McLaughlin[23, 9, 10].

This theory is based upon the idea that the anomalous behaviour of liquids of the o-terphenyl type is due to the gradual appearance of molecular aggregates or anticrystalline clusters as the temperature is lowered towards the melting point; the formation of these clusters being favoured by the reduced free volume, mean free path, and thermal energy which accompany the drop in temperature. The nature of crystal clusters, the conditions which predispose their appearance and their significance in glass formation will be discussed more fully in Chapter 4, but it is possible to visualise clusters arising as a result of molecules of the "cog-wheel" type colliding and interlocking. The average size of the clusters will depend upon the molecular mean free path, the molecular shape, and the probability that any particular molecule will be favourably orientated when a collision occurs, either with another single molecule or with an already formed aggregate. At any particular temperature

the rate of formation and the rate of dissolution of clusters will be balanced, and the liquid will behave as if it were a colloidal solution in which clusters are suspended in a non-associated medium. The viscosity of the liquid will only be influenced by the presence of those clusters with a life time greater than the relaxation time for viscous flow, i.e. $t_{Cluster} \geqslant \tau$, in which case the transport will involve, as well as single molecules, clusters which will remain intact. Ubbelohde and McLaughlin[23] have developed the analogy between a liquid containing clusters and a colloidal solution on a quantitative basis. If Brownian motion is neglected, and provided that the density change accompanying cluster formation is small, the viscosity of the suspension η_i at any particular temperature T_i can be expressed as follows:

$$\frac{\eta_i}{\eta_{si}} = 1 + \alpha\phi_i + \beta\phi_i^2 \qquad (2.46)$$

where ϕ_i is the volume fraction per ml. of the suspension associated into clusters and η_{si} is the viscosity the melt would have if the clusters were absent. A value for η_{si} may be obtained by extrapolating the linear $\ln \eta$ vs. $1/T$ plot which is obeyed at higher temperatures. If the clusters are assumed to be spherical, the coefficients α and β are in the order of 2.5 and 7.0 respectively, though for particles of

variable shape their values may be rather different[27]. For concentrations of clusters not exceeding 0.3 the series represented by equation (2.45) may be terminated after the third term; the values of ϕ_i so obtained appear to obey a relationship of the following type:

$$\phi_i = A \exp. \frac{B}{T} \qquad (2.47)$$

where A and B are constants for a particular material. Ubbelohde and McLaughlin have evolved a method of estimating the heat of dissociation of the clusters and their mean size employing the values of ϕ_i obtained experimentally. The method is outlined below. The equilibrium at any temperature T between clusters and single molecules may be represented as follows:

$$Ag \rightleftharpoons gA \qquad (2.48)$$

where A denotes the molecular species and g the mean number of molecules per cluster. If the activity coefficients of the associated and non-associated components are assumed to be unity, the equilibrium constant K_x, may be expressed in terms of the mole fractions:

$$K_x = \left[x_A\right]^g / \left[x_{Ag}\right] \qquad (2.49)$$

where x_A and x_{Ag} represent the mole fractions of the non-associated and associated components respectively. Consider

1 mole of clusters of which, at equilibrium, y have dissociated to give gy moles of single molecules. The total number of moles present at equilibrium is therefore 1 - y + gy. The equilibrium constant K_x may then be rewritten as follows:

$$K_x = \left[\frac{gy}{1-y+gy}\right]^g \Big/ \frac{1-y}{1-y+gy}$$

which reduces to:

$$K_x = \left[gy\right]^g \Big/ \left[(1-y)(1-y+gy)^{g-1}\right] \qquad (2.50)$$

or in terms of concentration (moles/litre):

$$K_c = \left[gy\right]^g \Big/ \left[(1-y)\, V^{g-1}\right] \qquad (2.51)$$

where V is the total volume of the system. Since it is assumed that no change in density accompanies cluster formation, the total volume of the system containing 1+y+gy moles of both components is equal to $g\,V_m$, where V_m is the molar volume of the liquid. As y is the fraction of "gmer" clusters dissociated, (1-y) may be identified with ϕ_i, and the equilibrium constant rewritten as follows:

$$K_x = \left[g(1-\phi_i)\right]^g \Big/ \phi_i\left[\phi_i+g(1-\phi_i)\right]^{g-1} \qquad (2.52)$$

or

$$K_x = K_c \frac{gV_m}{\left[\phi_i+g(1-\phi_i)\right]^{g-1}} \qquad (2.53)$$

By using equations (2.47) and (2.52) values of K_x for assumed

cluster sizes may be calculated throughout the pre-freezing region. From each set of values, the heat of dissociation ΔHg per mole of clusters of that size may be evaluated graphically from the standard relationship:

$$\frac{d \ln K_x}{dT} = \frac{\Delta Hg}{RT^2} \qquad (2.54)$$

Alternatively, ΔHg may be calculated from the expression:

$$\Delta Hg = RAB \exp (B/T) \left[\frac{-g}{(1-\phi_i)(\phi_i)(\phi_i+g-g\phi_i)} \right] \qquad (2.55)$$

derived from equations (2.47), (2.52) and (2.54). Thus, if the heat of dissociation of the clusters could be determined by an independent method, a comparison of the value so obtained with those given by either of the above expressions should provide an estimate of the number of molecules in each cluster. One method of assessing this value is by using the expression:

$$\Delta Hg = N\epsilon^* \left[\frac{g!}{(g-2)!2!} \right] \qquad (2.56)$$

where ϵ^* is the force constant for the molecular interaction. If the molecules were to interact with a potential of the Lennard-Jones type, the value of ϵ^* could be estimated from the empirical rule[25]:

$$\epsilon^*/k = 1.15\ T_b \qquad (2.57)$$

where T_b is the boiling point. The nature of the potential operative between molecules of the interlocking type considered here is not known and would prove very difficult to estimate, though the values of ϵ^*/k for these liquids would probably be greater than those which obey the Hirschfelder rule.

As the value of ΔHg has been found to be insensitive to the number of molecules per cluster, the accuracy of such indirect calculations is insufficient to permit an assessment of the number of molecules per cluster to be made (see Table 2.1). Values of ϕ_i, the blocked volume, are listed in table 2.2 for a number of compounds discussed above, and it can be seen that there is a marked correlation between the value of ϕ_i for each compound and the extent of the anomaly observed in the respective viscosity.

TABLE 2.1

SUBSTANCE	ΔHg		
	g = 2	g = 5	g = 50
o-TERPHENYL	10.7	11.2	11.5
2-2' DIPHENYL-DIPHENYL	13.9	14.4	14.9
1-3-5 TRIPHENYL BENZENE	15.5	15.7	15.9
VARIATION OF ΔHg WITH CLUSTER SIZE			

TABLE 2.2

Substance	M.Pt.	ϕ_i at M.Pt.
o-TERPHENYL	55.5°C	0.58
1:3:5 TRI-α-NAPHTHYL BENZENE	197.3°C	0.40
2-2' DEPHENYL-DIPHENYL	118.0°C	0.23
1:3:5 TRI-p-DIPHENYL BENZENE	232.5°C	0.074
1:3:5 TRIPHENYL BENZENE	176.5°C	0.043

Greatest anomaly in η ↓ Least anomaly in η

Until recently the study of melts comprising "cog-wheel" type molecules has progressively evolved from the original work on o-terphenyl towards more complex molecules, but Binns and Squire[29] have shown that whilst 2-phenyl naphthalene and 2:2' dinaphthyl behave normally, 1-phenyl naphthalene and 1-1' dinaphthyl begin to show the same type of anomalies which characterise the more complex polyphenyls. This work has provided an important link in the rationalisation of the phenomena described above and proffers a clue as to the nature of a critical structure in which these anomalies first became manifest. Scale models of 1-1' dinaphthyl and 2-2' dinaphthyl reveal that in the former the naphthyl groups are placed perpendicular to each other; in the latter the groups are free to assume a coplanar configuration without atomic interaction which is compatable with maximum resonance energy. More evidence has been provided for the

structure of these two compounds through the medium of ultra-violet spectroscopy.

During the above discussion the normal viscosity/temperature behaviour of liquids has been identified with the Eyring equation (Equation 2.38), and anomalies have been assessed in terms of departures from the $\ln \eta$ vs. $1/T$ plots which are linear at high temperatures. Values of the parameter $E\eta$ which Eyring identifies with an activation energy for viscous flow, may also be correlated with molecular structure. Over the linear section of the $\ln \eta$ vs. $1/T$ plot $E\eta$ is of course constant, but at low temperatures, when anomalous behaviour becomes manifest values may be obtained by drawing tangents to the curve at the required temperatures. Values of $E\eta$ are listed in table 2.3 for a number of polyphenyl molecules, both at high temperatures and at their melting points.

TABLE 2.3

SUBSTANCE	$E\eta$ (K.Cal/mole)	
	At M. Pt.	Well above M. Pt.
o-TERPHENYL	16.04	7.93
m-TERPHENYL	7.40	5.34
p-TERPHENYL	3.76	3.76
TRIPHENYLENE	6.16	4.57
1:3:5 TRIPHENYLBENZENE	7.34	5.66
1:3:5 TRI-ρ-DIPHENYLBENZENE	16.63	10.00
1:3:5 TRI-α-NAPHTHYLBENZENE	20.78	7.32

From table (2.3) it can be seen that E_η shows a marked dependence upon molecular shape. Most striking is the difference between the values obtaining to the high temperature linear plot and those values corresponding to the melting points. The deviations of the viscosity plots from linearity is most striking for tri-α-naphthyl benzene compared with the other two 1:3:5 substituted benzenes. O-terphenyl, which is also highly sterically hindered, shows an abnormally high value of E_η at the melting point.

The corresponding values of the pre-exponential term A are listed in table 2.4, together with those values of the entropy of activation $\Delta S^{\ddagger}$ which are available. The latter have been calculated from equation (2.39) taking the value of δ/a as unity as this assumption permits justifiable comparisons between fairly similar molecules[9].

TABLE 2.4

SUBSTANCE	A(POISE)		$\Delta S^{\ddagger}$ (Cal/mole deg)	
	At M.Pt.	Well above M.Pt	At M.Pt.	Well above M.Pt
o-TERPHENYL	7.41×10^{-13}	9.95×10^{-8}	29.3	5.71
m-TERPHENYL	1.73×10^{-4}	2.70×10^{-3}	4.65	-0.84
p-TERPHENYL	1.64×10^{-2}	1.64×10^{-2}	-4.59	-4.59
TRIPHENYLENE	1.96×10^{-5}	1.10×10^{-4}	-0.06	-3.52
1:3:5 TRIPHENYLBENZENE	8.28×10^{-6}	4.96×10^{-5}	9.33	-2.70
1:3:5 TRI-p-DIPHENYLBENZENE	1.23×10^{-8}	7.26×10^{-6}	12.80	0.50
1:3:5 TRI-α-NAPHTHYLBENZENE	9.71×10^{-11}	5.19×10^{-5}	22.82	-3.46

It can be seen from table 2.4 that in the region of their respective melting points ΔS^{*} is negative for both the planar aromatic molecules, characterised by triphenylene, and the linear polyphenyls characterised by p-terphenyl. For molecules of the "cog-wheel" type the values of ΔS^{*} are large and positive. This is in accordance with the concept that such large entropy values are a consequence of molecular interlocking and cluster formation, a conclusion compatable with the correspondingly high values for E_η which suggest that transport involves aggregates rather than single molecules alone.

Like the Eyring equation, which describes the temperature dependence of viscosity, the Batschinski equation, which relates fluidity and free volume, holds quite well for a variety of liquids. The factor c, tends to vary somewhat from liquid to liquid, but the variations become more marked in the case of liquids comprised of interlocking molecules. Not only does the absolute value of c depend upon molecular shape but with the interlocking molecules the fluidity vs. specific volume plots show a marked deviation at temperatures approaching the melting point.

Herzog and Kudar[30,31] have derived the following equation for the fluidity of a liquid, consisting of spherically symmetrical molecules capable of molecular rotations, in terms of its free volume:

$$\phi = \frac{1}{\eta} = \frac{2.4 \times 10^{4}}{V^{1/3}} \sqrt{\frac{M}{T}} \, (v-w) \qquad (2.58)$$

from which it follows that the Batschinski constant c is:

$$c = \frac{V^{1/3}}{2.4 \times 10^{4}} \sqrt{\frac{T}{M}} \qquad (2.59)$$

where V is the molecular volume. For cases in which molecular rotation is inhibited Herzog and Kudar have modified equation (2.57) to:

$$1/\eta = \frac{1.3 \times 10^{4}}{V^{1/3}} \sqrt{\frac{M}{T}} \; (v - w) \qquad (2.60)$$

from which

$$c = \frac{V^{1/3}}{1.3 \times 10^{4}} \sqrt{\frac{T}{M}} \qquad (2.61)$$

It is evident upon the basis of this theory, that the inhibition of molecular rotation should cause a marked increase in the value of c; and since the formation of clusters in a melt will necessarily inhibit molecular rotations, the appearance of such groups will be evident in the increased values of c. Values of the Batschinski fluidity parameters for some polyphenyls are listed in table (2.5)

An inspection of table (2.5) reveals that for o- and m-terphenyl there is in fact a marked increase in c as the melting point is approached, and that this is accompanied by a decrease in the value of w. The term w has been identified with the factor 'b' in van de Waals' equation and roughly represents the volume occupied by the molecules themselves. It is probable that the appearance of clusters, which would give

TABLE 2.5[45]

BATSCHINSKI FLUIDITY PARAMETERS FOR POLYPHENYLS

Substance	Well above M.Pt		Close to M.Pt.	
	w	c	w	c
Benzene	1.05	5.75×10^{-4}	1.04	6.21×10^{-4}
Diphenyl	0.959	6.82×10^{-4}	0.959	6.82×10^{-4}
p-Terphenyl	0.932	8.01×10^{-4}	0.932	8.01×10^{-4}
m-Terphenyl	0.952	7.40×10^{-4}	0.938	12.15×10^{-4}
o-Terphenyl	0.958	10.50×10^{-4}	0.934	37.00×10^{-4}

rise to regions of higher density, would result in a decrease in the average volume occupied by each molecule.

In further support of this hypothesis it may be observed that in the case of substances which form liquid crystalline phases the liquid crystalline phase has a higher value of c and a lower value of w than the corresponding isotropic phase[45].

Recently attention has been directed towards the influence upon viscosity of inhibited molecular rotation. In particular Davies and Matheson[32] have interpreted deviations from the linear $\ln \eta$ vs. 1/T plot in terms of restricted molecular rotation. They suggest that if the ratio of the longest to the shortest van de Waals' radii of the molecules σ, is less than 1.5, the molecules will behave as if they were spherical, and obey

the Eyring-type equation. In cases where σ is large, the molecule will be unable to rotate freely about all three axes as the temperature is lowered towards the melting point, and the energy required to effect transport will increase as the molecules are pushed past their neighbours. They further suggest that in the non-Arrhenius region rotation about the short molecular axis occurs less frequently than molecular transport, but in the high-temperature linear region the molecule must rotate freely about one or more axes several times during the transport process:

i.e. $\tau_{\text{Rotn.}} \ll \tau_{\eta}$

The examples quoted do however cover a wide range of liquid types, polar and non-polar, in which intermolecular forces acting may differ considerably. Nevertheless, there does seem to be some correlation between the magnitude of σ and non-Arrhenius behaviour in the examples quoted, but the present author considers that this correlation does not obtain to molecules of the polyphenyl type. For example, Davies and Matheson cite benzene as a non-Arrhenius liquid with a σ value of 2.0*. However, the extent of the deviation from the Eyring equation at the melting point in the case of benzene is small when compared with

---

* Presumably this value is simply the quotient of the distance from the centre of the phenyl ring to the extremity of a hydrogen atom repulsion envelope, and half the "thickness" of the phenyl ring:- upon this basis, using scale molecular models, the present author has obtained a σ value of 2.6.

some of the polyphenyls mentioned earlier in this section. Upon the same basis, p-terphenyl has a σ value of 5.96, but the behaviour of this melt is nearly normal; o-terphenyl, which displays one of the largest anomalies, has a σ value not greater than 1.68 and not less than 1.65.

It would seem that values of σ have little significance within the context of interlocking molecules; the point being that once molecules of the "cog-wheel" type are locked together individual molecular rotation must necessarily be prohibited. Useful parameters are the volumes swept out by rotating the molecule about each axis. If all these quantities, computed from van de Waal's radii, are less than the volume per molecule of the liquid (i.e. V/N) then some degree of interlocking is implied, although freedom of rotation about any one axis does not rule out the possibility of aggregation - each case has to be considered separately bearing in mind the individual molecular shapes.

An alternative approach to the anomalous behaviour of these polyphenyl type molecules is due to Hildenbrand[33] who considers that, whilst at high temperatures, each molecule will rotate with little or no impedance, at low temperatures the molecules will roll over each other under the influence of stress engaging and disengaging like cog-wheels. At temperatures approaching the melting point, the decreased free volume will result in greater friction between engaging molecules, and

finally, at the glass point, the system will "sieze up". No attempt has been made to present this theory on a quantitative basis, but the physical picture presented does bear some similarities to the free volume theory of Cohen and Turnbull (see section 2.3.5.)

Qualitatively the main difference between the cluster theory and the theories of Cohen and Turnbull and Hildebrand is that the cluster theory implies regions of high density in the melt as clusters are formed, whilst the alternative theories predict a uniform contraction and congelation of the melt as the temperature is lowered, the density remaining homogeneous throughout. At the glass point all theories convey much the same picture. Regrettably, methods have not yet been devised to detect microscopic fluctuations in density, so that it is at present impossible to decide between the theories experimentally. The presence of liquid crystals in some melts adds weight to the cluster theory, but in the case of the few polyphenyl melts examined from this point of view, no liquid crystals have been detected[45].

2.5 The Viscosity of Liquid Mixtures

The earliest attempt to obtain an expression for the viscosity of a binary liquid mixture in terms of the viscosities of the pure components and the composition of the mixture was due to Arrhenius[34], who proposed the following empirical relationship:

$$\ln\eta_s = x_1 \ln\eta_1 + x_2 \ln\eta_2 \qquad (2.62)$$

where η_s is the viscosity of the mixture and η_1 and η_2 and x_1 and x_2 are the viscosities and mole fractions of components 1 and 2 respectively.

Since then many empirical equations have been proposed, but though each may apply to a specific system none are obeyed with any convincing generality[35, 36]. Typical of such relationships are those which have been proposed by the following authors:

(1) Bingham[37]:

$$\frac{1}{\eta_s} = \frac{V_1}{\eta_1} + \frac{V_2}{\eta_2} \qquad (2.63)$$

where V_1 and V_2 are the volume fractions of components 1 and 2 respectively. This expression is similar to one proposed by Lees in 1901[38].

(2) MacLeod[39]:

$$\eta_s = \frac{\eta_1 x_1 V_{f_1} + \eta_2 x_2 V_{f_2}}{V_f + c} \qquad (2.64)$$

where V_{f_1}, V_{f_2} and V_f are the free volumes of components 1 and 2 and the mixture respectively, and c the volume change upon mixing per ml.of solution. This expression has been modified by Bird and Daly[40] to give:

$$\frac{1}{\eta_s} = \left(\frac{V_1}{\eta_1} + \frac{V_2}{\eta_2}\right)\left(1 + \frac{c}{V_1 V_{f_1} + V_2 V_{f_2}}\right) \qquad (2.65)$$

This equation has been applied to mixtures of similar hydrocarbons (e.g., cis and trans decalin) but it fails when applied more generally.

(3) Kendall:[41, 36]

$$\ln\left(\frac{1}{\eta_s}\right) = x_1 \ln\left(\frac{1}{\eta_1}\right) + x_2 \ln\left(\frac{1}{\eta_2}\right) \qquad (2.66)$$

Equation (2.66) is Kendall's original expression, but by selecting mixtures comprising molecules of the same type though not necessarily of the same shape or size (e.g. Benzene/Naphthylene, Benzene/diphenyl, and Phenetole/Anisole) an expression of the following type was found to apply:[41]

$$\eta_s^{1/3} = x_1 \eta_1^{1/3} + x_2 \eta_2^{1/3} \qquad (2.67)$$

Expressions similar to equations (2.63) and (2.66) can however, on the basis of certain assumptions, be obtained by extension of the Eyring Reaction Rate Theory[8] (See section 2.3.4).

Thus if it is assumed that:

(a) the binary mixture is ideal, i.e. the interaction energies in the mixture can be written as $\epsilon_{11} = \epsilon_{12} = \epsilon_{22}$ and the molecular diameters as $r_{11} = r_{12} = r_{22}$;

(b) the molar volumes and molecular dimensions of the two species are equal;

(c) viscous flow involves the movement of one molecule at a time from one equilibrium position to the next; then from equations (2.21) and (2.30) it can be shown that

$$\frac{1}{\eta_s} = x_1\left(\frac{1}{\eta_1}\right) + x_2\left(\frac{1}{\eta_2}\right) \qquad (2.68)$$

(c.f. equation 2.63). Inherent in this derivation is the tacit assumption that the free energy of activation is the same in the mixture as in both the pure liquids. If an average value of this energy is used, i.e., $x_1 \Delta G^{*}_1 + x_2 \Delta G^{*}_2$, then the theory predicts an expression identical with equation (2.66).

Thus equation (2.66) can claim the advantage of some theoretical basis.

More recently Grunberg and Nissan[42] have suggested that the following equation is in better general agreement with experimental data:

$$\ln \eta_s = x_1 \ln \eta_1 + x_2 \ln \eta_2 + x_1 x_2 d \qquad (2.69)$$

where d is a constant characteristic of the particular mixture. The value of d is positive for systems which display negative deviations from Raoult's law and visa-versa; it is associated with the constant B in the simplified Margules equation:

$$\ln \gamma_1 = B x_2^2 \qquad (2.70)$$

where γ_1 is the activity coefficient for component 1, and B is given by:

$$Bc = d \qquad (2.71)$$

The factor c is expressed as:

$$c = \frac{\ln \eta}{\ln P_{Vap}} \qquad (2.72)$$

where P_{Vap} is the vapour pressure of the mixture at the temperature at which the viscosity measurements are carried out. In a later paper[43], devoted to the study of regular solutions, Grunberg has suggested that $d \propto w/RT$, where w is the interchange energy arising from the fact that although the molecules of the two components of a regular solution are interchangeable as far as size and shape are concerned, there is an increase in the "quasi-lattice" energy equal to $2w$ when a molecule of component 1 is introduced into the lattice of component 2.

The problems in providing a general expression for the viscosity of mixtures which has a convincing basis in theory are very complex. Bak and Andersen[44] have pioneered a new approach by applying the principle of corresponding states to the fluidities of liquid mixtures. The resulting expression bears some resemblance to the equations of Bingham and Eyring:

$$\frac{1}{\eta_s} = x_1\left(\frac{1}{\eta_1}\right) + x_2\left(\frac{1}{\eta_2}\right) + \left(\frac{1}{\eta_1} - \frac{1}{\eta_2}\right) \varrho\, x_1 x_2 \qquad (2.73)$$

$\varrho = 2\left(\frac{r_{22} - r_{11}}{r_{11} + r_{22}}\right)$ where r_{11} and r_{22} are the distances between molecules in pure component 1 and pure component 2 respectively. The theory was tested using mixtures CCl_4/CMe_4 in which both dipole and size effects are minimised, $CCl_4/CHCl_3$ in which dipole effects should predominate and, C_6H_6/CH_2Ph_2 and $C_7H_{16}/C_{16}H_{34}$ in which size effects

predominate. On the whole agreement with experiment was disappointing though attempts to assess the effects of dipole interaction in the case of the $CCl_4/CHCl_3$ mixture met with some success.

REFERENCES

1. Newman, F.H. and Searle, V.H.L., "The General Properties of Matter", Edward Arnold, London (1948).
2. Bingham, E.C., "Fluidity and Plasticity", McGraw-Hill, New York, (1922).
3. Maxwell, J.C., Phil. Mag. IV, 35, 134 (1868). See also: Moelwyn-Hughes, E.A. "Physical Chemistry", Oxford Clarendon Press.
4. Frenkel, J. "Kinetic Theory of Liquids", Dover Publications, New York (1955).
5. de Guzman, G., J. An. Soc. esp. Fis. Quim, 11, 355 (1913).
6. Andrade, E.N.daC., Nature, 125, 309, 582 (1930); Phil. Mag. VII, 17, 497, 698 (1934).
7. Lindemann, F.A., Phys. Z., 11, 609 (1911).
8. Glasstone, S., Laidler, K.J. and Eyring, H., "The Theory of Rate Processes", McGraw-Hill, New York, (1941).
9. McLaughlin, E. and Ubbelohde, A.R., Trans. Faraday Soc., 53, 628 (1957).
10. Magill, J.H. and Ubbelohde, A.R., Trans. Faraday Soc., 54, 1811 (1958).
11. Van Velden, P.F., Physica, 13, 529 (1947).
12. Ewell, R.H. and Eyring, H., J. Chem. Phys., 5, 726 (1937).
13. McLaughlin, E., Trans. Faraday Soc., 55, 29 (1959).
14. Batschinski, A.J., Z. Phys. Chem., 84, 645 (1913).
15. MacLeod, D.B., Trans. Faraday Soc., 19, 6 (1923).

16. Doolittle, A.K., J. Appl. Phys., 22, 1471 (1951).

17. Cohen, M.H. and Turnbull, D., J. Chem.Phys., 29, 1049 (1958).
" " ibid 31, 1164 (1959).
" " ibid 34, 120 (1961).

18. Barrer, R.M., Trans. Faraday Soc., 38, 322 (1942).
" ibid 39, 48 (1943).

19. Beuche, F., J. Chem. Phys., 21, 1850 (1953).
" ibid 24, 418 (1956).
" ibid 30, 748 (1959).

20. c.f. Bloom: Chapter 1, "Fused Salts", Ed. Sundheim, McGraw-Hill (1964).

21. Angell, C.A., J. Phys. Chem. 68, 1917 (1964).

22. Hazlewood, F.J., Thesis "The Physico-chemical Properties of Low Melting Salts", (1966).

23. McLaughlin, E. and Ubbelohde, A.R., Trans. Faraday Soc., 54, 1804 (1958).

24. Andrews, J.N. and Ubbelohde, A.R., Proc. Roy. Soc., A.228, 435 (1955).

25. Hind, R.K., Thesis, "Physical and Thermodynamic Properties of Polynuclear Aromatic Molecules" (1959).

26. Magill, J.H. and Plazek, D.J., J. Chem. Phys., 45, 3038 (1966).

27. Kynch, G.J., Proc. Roy. Soc., A.237, 90 (1956).

28. Hirschfelder, J.O., Curtiss, C.F. and Bird, R.B., "Molecular Theory of Gases and Liquids", Chapman & Hall, London, (1954.)

29. Binns, E.H. and Squire, K.H., Trans. Faraday Soc., 58, 762 (1962).

30. Herzog, R.O. and Kudar, H.C., Trans. Faraday Soc., 29, 1006 (1933).

31. Herzog, R.O. and Kudar, H.C., Z. Phys., 80, 217 (1933).

32. Davies, D.B. and Matheson, A.J., Trans. Faraday Soc., 63, 596 (1967). See also:

Barlow, A.J., Lamb, J. and Matheson, A.J., Proc. Roy. Soc., A.292, 322 (1966).

Davies, D.B., and Matheson, A.J., J. Chem. Phys., 45, 1000 (1966).

33. Hildebrand, J. and Smith, J. Chem. Phys., 40, 909 (1964)

34. Arrhenius, S., Z. Phys. Chem., 1, 285 (1887).

35. Hind, R.K., McLaughlin, E. and Ubbelohde, A.R., Trans. Faraday Soc., 56, 328 (1960).

36. Kendall, J. and Monroe, K.P., J. Amer. Chem. Soc., 39, 1802 (1917).

37. Bingham, E.C. and Jackson, Bull. Bur. Stand., 13, 309 (1916-17)

38. Lees, Ch., Phil. Mag., VI, 1, 139 (1901).

39. MacLeod, D.B., Trans. Faraday Soc., 20, 348 (1924).

40. Bird, L.H. and Daly, E.F., Trans. Faraday Soc., 35, 588 (1939).

41. Kendall, J. and Wright, A.H., J. Amer. Chem. Soc., 42, 1776 (1920);

Kendall, J. and Monroe, K.P., ibid , 43, 115 (1921).

42. Grunberg, L. and Nissan, A.H., Nature, 164, 799 (1949).

" " Trans. Faraday Soc., 45, 125 (1949).

43. Grunberg, L., Trans. Faraday Soc., 50, 1293 (1954).

44. Andersen, K. and Bak, T.A., Acta. Chem. Scand., 12, 1367 (1958).

45. Andrews, J.N., Thesis "Melting Mechanisms of the Polyphenyls", London (1956).

CHAPTER 3.

TWO COMPONENT LIQUID MIXTURES

3.1 Introduction and the Ideal Solution.

Throughout the years, experience has lead to a number of empirical rules with regard to the properties of liquid mixtures, and to the phenomenon of miscibility. In recent years, a theoretical foundation has been established for many of the axioms of the early chemists such as "like dissolves like" in terms of various types of molecular interaction into which modern experimental and theoretical techniques have permitted investigation.

In the present context, interest is focused principally upon the properties of binary mixtures.

Before discussing the various types of molecular interaction, and their influence upon the properties of liquid mixtures, it is desirable to describe an ideal solution in which these effects are minimised. An ideal solution therefore, is formed from its components with zero heat of mixing and no change in total volume. The ideal entropy of mixing is independent of temperature, and is a function of the mole fractions of the components only. It can be expressed as follows:

$$\Delta S_{Mixing} = Nk\,(x_1 \ln x_1 + x_2 \ln x_2) \qquad (3.1)$$

where x_1 and x_2 are the mole fractions of components 1 and 2 respectively, N is Avogadro's number, and k the Boltzmann constant. Thus, to produce an ideal solution, both components

must possess very similar force fields and molecular sizes. To replace one mole of component 1 by one mole of component 2 in an ideal solution should not effect any change in the potential energy of the system. This consideration leads to Raoult's law which, in its most simple form, states that the partial vapour pressure of component 1 in equilibrium with a mixture containing components 1 and 2 will be proportional to the mole fraction of component 1 in the mixture; the constant of proportionality is the vapour pressure of pure component 1.

$$\text{i.e.} \quad \text{V.P.}_{\text{Comp.1}} = P^{\circ}_1 x_1$$

$$\text{similarly,} \quad \text{V.P.}_{\text{Comp.2}} = P^{\circ}_2 x_2 \qquad (3.2)$$

The vapour pressure of a liquid is determined by the tendency of each molecule to escape from the matrix of its neighbours. If the addition of a second species, say component 2, leaves unchanged the forces existing between the molecules of component 1, the vapour pressure of component 1 over the solution will depend only upon the mole fraction of component 1 present. The same argument applies to component 2. Thus, an ideal solution is a solution which will obey Raoult's law over the full range of temperature and composition[1]. The type of vapour pressure vs. temperature plot to be expected from an ideal binary mixture is illustrated in Fig. 3.1.

Figure 3.1

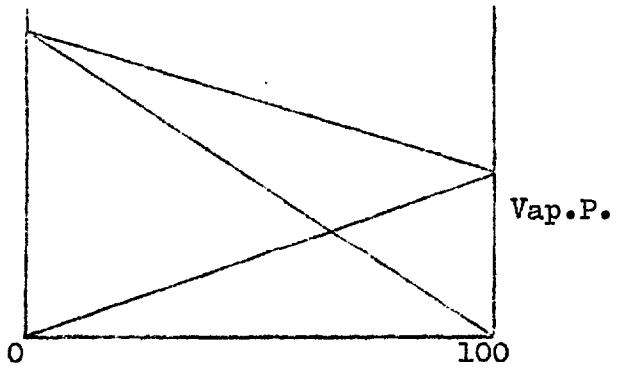

Having established the ideal solution as a yard-stick, it is possible to attempt an explanation of observed deviations from the ideal in terms of the various types of intermolecular forces involved. Considerations of the same forces can be extended to account for partial miscibility.

3.2. Intermolecular Forces and Non-Ideal Solutions.

3.2.1. Van de Waals' forces

Van de Waals' forces or London dispersion forces are always present, and can be expressed in terms of an attractive force and a repulsive force which, at equilibrium are balanced. In the case of molecules with spherically symmetric force fields the attractive force varies as approximately r^{-6}, and the repulsive force as r^{-12}, where r is the intermolecular distance. (See chapter 1, Fig. 1.1). If the molecules comprising each component of a binary mixture differ greatly in shape or size, then two possible factors may account for deviations from ideality. (2)

(a) If the mixing were to result in a weakening of the attractive forces, then the average separation of the molecules would begreater in the mixture than in the separate components. This would give rise to an increase in total volume on mixing since equilibrium must be maintained between the repulsive and attractive forces. A weakening in the attractive forces will mean that the molecules are less firmly held within the mixture and their tendency to escape will be enhanced. The vapour pressure of either component will increase upon mixing leading to a positive deviation from Raoult's law. If mixing were to result in an increase in the attractive forces precisely the opposite would occur, resulting in a negative deviation from Raoult's law and a decrease in total volume upon mixing. The balance between attractive and repulsive forces between molecules in a liquid give rise to what is termed the internal pressure P_i. This quantity, $(\frac{\partial E}{\partial V})_T\, dV$ is a measure of the change in internal energy accompanying an increase in volume at a constant temperature, and this is equal to the work done in overcoming the internal pressure during the volume change.

$$\text{Hence} \quad P_i dV = (\frac{\partial E}{\partial V})_T\, dV$$

$$\text{or} \quad P_i = (\frac{\partial E}{\partial V})_T \qquad (3.3)$$

Since the external pressure P is small compared with the internal pressure, the latter may be defined as:

$$P_i = T\left(\frac{\partial P}{\partial T}\right)_V = T\frac{\alpha}{\beta} \qquad (3.4)$$

where α is the coefficient of cubic expansion and β, the isothermal compressibility. Scatchard[3] has derived the following expression for the volume change on mixing two components to form a binary mixture by considering the mixing at constant volume followed by an expansion (or contraction) to restore the initial pressure:

$$\Delta V_M = -\beta_o V_o \left[\left(\frac{\partial E}{\partial V_o}\right)_T - \left(\frac{\partial E_o}{\partial V_o}\right)_T\right] \qquad (3.5)$$

where β_o, V_o and E_o represent the compressibility, volume and energy of the isolated components.* For a number of normal liquids, i.e. liquids in which molecular interaction is almost solely the result of dispersion forces, the quantity $\left(\frac{\partial E}{\partial V}\right)_T \approx -\frac{E}{V}$. Hence equation (3.5) may be rewritten:

$$\Delta V_M = -\beta_o V_o \left(-\frac{E}{V_o} + \frac{E_o}{V_o}\right) = \beta_o \Delta E_V^M \qquad (3.6)$$

where ΔE_V^M is the energy of mixing at constant volume.

The most important conclusion to be inferred from equation (3.6) is that an increase in total volume on mixing must always be accompanied by a positive energy (or heat) of mixing, and that a decrease in total volume must always be accompanied

* V_o is the ideal volume of the mixture $N_1V_1+N_2V_2$ where N_1 and N_2 and V_1 and V_2 represent the number of moles and the molar volumes of components 1 and 2 respectively. $E_o = \phi_1 E_1 + \phi_2 E_2$, and $\beta_o = \phi_1\beta_1 + \phi_2\beta_2$ where ϕ_1 and ϕ_2 are the volume fractions of components 1 and 2 respectively.

$$\left(\phi_1 = \frac{N_1V_1}{N_1V_1+N_2V_2} \text{ and } \phi_2 = \frac{N_2V_2}{N_1V_1+N_2V_2}\right)$$

by a negative energy of mixing; further it is only when mixing is athermal that no change in total volume occurs (see ref. 9 for a detailed discussion).

(b) The above section is concerned with the effect of dispersion forces alone, but if the difference in shape and size of the molecules comprising the two liquids is large, then a geometrical rearrangement may result in a fresh structure. Thus, both a change in intermolecular forces and geometrical rearrangement may contribute to a volume change on mixing and to deviations from Raoult's law. If, as is frequently assumed, the interaction energy between a pair of unlike molecules is the geometric mean of the interaction between each molecule and another of its own kind, the total energy of molecular interaction is not greater in the mixture and the liquid will tend to expand on mixing*. Geometrical rearrangement, however, will tend to oppose this effect since a change in molecular arrangement will usually act so as to bring the molecules into closer contact over a "larger area of their surfaces". One example is the mixture benzene/neopentane. This has a positive heat of mixing but a negative volume change on mixing[4]. The negative volume change is probably due to a geometrical rearrangement.

Since, in the present work, species have been chosen in

---

* Whilst this statement may be generally true in connection with mixtures composed of relatively non-polar molecules; it may not hold for mixtures in which the dispersion forces are modified by strong dipole interactions. (See Section 3.2.2).

which factors other than dispersion forces and molecular geometry are minimised, the influence of these other factors will be discussed only briefly.

3.2.2. Dipole interactions and association.

Deviations from Raoult's law may occur as a result of dipole interaction. The dispersion forces acting between molecules in the liquid mixture are modified by the presence of attractive forces due to dipole interaction, and this usually results in a contraction in total volume and a decrease in vapour pressure of either component, leading to a negative deviation from Raoult's law. Association due to hydrogen bonding produces a similar effect, as also does compound formation, e.g. solvation of solute or the reaction of components to produce fresh species. It is possible to realise a situation in which a negative deviation from Raoult's law, due to dipole interaction or compound formation, is exactly compensated by a positive deviation due to changes in internal pressure: e.g. the ethyl acetate/water system behaves as if it were ideal in the vicinity of $0^{o}C$ [5]. If the pure components are highly associated, it is possible that the degree of association in the mixture could be less than in the pure components. This would lead to a higher vapour pressure for each component and a positive deviation from Raoult's law.

3.3 Partially Miscible Liquids.

It has already been mentioned that the properties of a binary liquid mixture and the phenomenon of miscibility are largely

determined by the type of molecular interaction extant in the pure components and in the mixture. If the cohesive forces acting between the molecules in the pure components are very large, then it is possible that the two components will not mix throughout the full range of composition. This would give rise to a two phase system in which one layer consists of a solution of component 1 in component 2, and the other layer, a solution of component 2 in component 1. The phases in a system of this type are termed conjugate solutions.

At equilibrium the chemical potential, μ of each component must be the same in both phases.

$$\text{i.e.} \quad {}^{\text{Phase 1}}\mu_{\text{Compt. 1}} = {}^{\text{Phase 2}}\mu_{\text{Compt.1}}$$

$$\text{and} \quad {}^{\text{Phase 1}}\mu_{\text{Compt. 2}} = {}^{\text{Phase 2}}\mu_{\text{Compt.2}} \qquad (3.7)$$

In many cases, two liquids which are only partially miscible differ, in their respective cohesive forces as a result of the presence of strong dipole interactions or hydrogen bonding in one or other of the liquids: e.g. paraffin/water system. For cases in which only dispersion forces are acting, the packing and geometry of the molecules will assume a greater importance since dipole interactions etc. are directional and often play a major part in molecular orientation. If the liquids are regarded as quasi-crystalline, the cohesive energy is analogous

to the lattice energy of a crystalline solid; the value of this quasi-lattice energy will be a complicated function of molecular geometry and intermolecular potential. If the mixing of two non-polar liquids were to result in a gross disruption of their respective lattices, it is possible that each component will only accept the number of foreign molecules compatable with the retention of its original basic structure. In other words, each lattice will only accommodate a limited amount of distortion resulting from the inclusion of foreign molecules. In the present context liquids comprising molecules greatly differing in shape and size have been considered, and it was thought that binary mixtures of these liquids might separate into two phases at some stage throughout the composition range.

3.4. Partial Molar Volumes and Excess Volumes of Mixing[6]

The various extensive properties of any system must vary with the quantities of constituents present; such a system, to and from which matter may be transferred, is termed an open system. The variation of any extensive property X, with the amounts of the constituents present may be represented as follows:

$$dX = \left(\frac{\partial X}{\partial T}\right)_{P,n_1,n_2\cdots} dT + \left(\frac{\partial X}{\partial P}\right)_{T,n_1,n_2\cdots} dP + \left(\frac{\partial X}{\partial n_1}\right)_{T,P,n_2\cdots} dn_1 + \left(\frac{\partial X}{\partial n_2}\right)_{T,P,n_1\cdots} dn_2 \qquad (3.8)$$

or at constant pressure and temperature:

$$dX = \left(\frac{\partial X}{\partial n_1}\right)_{n_2,T,P} dn_1 + \left(\frac{\partial X}{\partial n_2}\right)_{T,P,n_1\cdots} dn_2 + \cdots\cdots \qquad (3.9)$$

where n_1, n_2 etc. are the numbers of moles of the various constituents.

The quantities $\left(\frac{\partial X}{\partial n_1}\right)_{T,P,n_2\cdots} = \bar{X}_1$ are termed partial molar quanties and can be regarded as the contribution per mole of each particular constituent to the value of the property X in the system under consideration. It follows that at constant temperature and pressure:

$$n_1 d\,\bar{X}_1 + n_2 d\,\bar{X}_2 + \cdots\cdots = 0 \qquad (3.10)$$

or in a mixture of two components:

$$n_1 d\,X_1 = - n_2 d\,X_2 \qquad (3.11)$$

also the total value of X is :

$$n_1\,\bar{X}_1 + n_2\,\bar{X}_2 + \cdots\cdots = X \qquad (3.12)$$

Since, in this present work, interest has been directed towards volumes of mixing, the property X, in the above equations may be replaced by V, when $\bar{V}_1 \left(=\left(\frac{\partial V}{\partial n_1}\right)_{T,\,P,\,n_2}\right)$ is the partial molar volume of component 1 in a binary mixture.

For an ideal solution, the total volume of the solution is simply the sum of the volumes of the constituents before mixing.

The volume vs. composition plot for an ideal binary mixture is illustrated in Fig. 3.2.

Figure 3.2

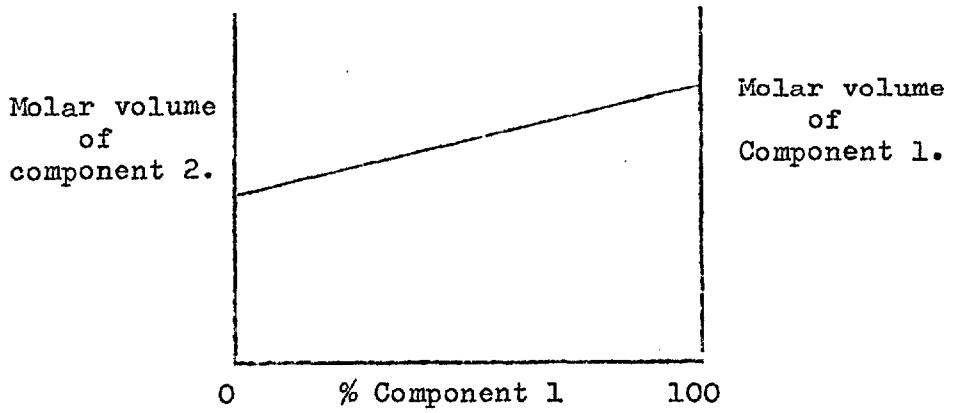

For binary mixtures of comparatively simple molecules, positive or negative excess volumes of mixing are generally symmetrical with respect to composition or very nearly so, and seldom exceed a maximum of 2% of the total volume; the variation of excess volume with temperature is rarely significant e.g. Benzene/cyclohexane system which has a positive, symmetrical volume of mixing independent of temperature from 20-70°C[7], and the benzene/neopentane system which was a negative symmetrical excess volume of mixing[4]. It will be seen, in a later chapter, that the mixtures studied in this present work, comprising molecules of a far more specialised shape than the examples cited above, display excess volumes of mixing which are nearly independent of temperature but unsymmetrical with respect to composition.

Before discussing methods available for the determination of partial molar volumes, a further development of the Scatchard equation (equation 3.6 above) for excess volumes of mixing provides the following expressions for the partial molar excess volumes in terms of the activity coefficients γ_1 and γ_2, of the two components, assuming the entropy of mixing to be ideal:

$$\begin{aligned} \Delta\bar{V}_1 &= \bar{V}_1 - V_1 = \beta_o \Delta\bar{F}^E = \beta_o RT \ln \gamma_1 \\ \Delta\bar{V}_2 &= \bar{V}_2 - V_2 = \beta_o \Delta\bar{F}_2^E = \beta_o RT \ln \gamma_2 \end{aligned} \qquad (3.13)$$

This does not represent the only attempt to correlate excess volumes of mixing with activities or mole fractions of components, since the following simple symmetrical relationship was proposed by Biron[5] as early as 1912[8].

$$\Delta V_M = k' x_1 x_2 \qquad (3.14)$$

or

$$\frac{\Delta V_M}{V} = k x_1 x_2 \qquad (3.15)$$

It can be shown that unless the molar volumes of the two components are equal or nearly so, k does not remain constant throughout the composition range. If, however, the volume fractions ϕ_1 and ϕ_2 are used in place of mole fractions this problem is obviated:

$$\frac{\Delta V_M}{V} = K \phi_1 \phi_2 \qquad (3.16)$$

N.B. $\phi_1 = \frac{N_1V_1}{N_1V_1 + N_2V_2}$; $\phi_2 = \frac{N_2V_2}{N_1V_1 + N_2V_2}$ where N_1 and N_2, and V_1 and V_2 refer to the number of moles and the molar volumes of the components present.

In many systems the activity coefficient vs. composition curves for the two components are nearly symmetrical and in such cases they may be represented by simple equations of the following form:

$$\ln \gamma_1 = B x_2^2$$
$$\ln \gamma_2 = B x_1^2 \qquad (3.17)$$

An equation possessing the same form as the Biron equation may be obtained by substituting the expression for $\ln \gamma_1$ and $\ln \gamma_2$ in equation (3.17) into equation (3.13).

There are several methods for the determination of partial molar properties, but the two methods described here are the most readily applicable to the molar volume and excess volumes of mixing data obtained in this present work.

Method 1.

The first part of the theory is quite general and obtains to any extensive property X.

Let X represent the observed value of the property, and X' the mean value of the property per mole of mixture.

Then: $X = (n_1 + n_2)\ X'$ (3.18)

where n_1 and n_2 are the number of moles of components 1 and 2

respectively.

Differentiation of equation (3.18) with respect to n_1, maintaining n_2, temperature and pressure constant yields:

$$\left(\frac{\partial X}{\partial n_2}\right)_{T,P,n_1} = \bar{X}_2 = X' + (n_1 + n_2)\left(\frac{\partial X'}{\partial n_2}\right)_{T,P,n_1} \qquad (3.19)$$

Now, the mole fraction of component 1 in the mixture is given by:

$$x_1 = \frac{n_1}{n_1 + n_2} \qquad (3.20)$$

Upon differentiation with respect to n_2, n_1 remaining constant gives:

$$dx_1 = - \frac{n_1\, dn_2}{(n_1 + n_2)^2} = - \frac{x_1\, dn_2}{n_1 + n_2}$$

which, upon rearrangement gives:

$$- \frac{x_1}{dx_1} = \frac{n_1 + n_2}{dn_2} \qquad (3.21)$$

Equation (3.21), upon substitution into equation (3.19) yields:

$$\bar{X}_2 = X' - x_1 \left(\frac{\partial X'}{\partial x_1}\right)_{n_1} \qquad (3.22)$$

Since x_1 is the mole fraction of component 1, it is unnecessary to maintain n_1 constant, hence:

$$\bar{X}_2 = X' - x_1 \left(\frac{\partial X'}{\partial x_1}\right) \qquad (3.23)$$

In the present context, partial molar volumes are to be

considered. The excess volume of mixing ΔV_M, can be expressed as follows:

$$\Delta V_M = V_T - (n_1V_1 + n_2V_2) \tag{3.24}$$

where V_T is the total volume of the mixture, and V_1 and V_2 the molar volumes of components 1 and 2 respectively. If both sides of equation (3.24) are divided by the total number of moles present, then the excess volume of mixing per mole of the mixture is given by:

$$\Delta V_M^m = V_T^m - (x_1V_1 + x_2V_2) \tag{3.25}$$

Since $x_2 = 1-x_1$, equation (3.25) can be rewritten as follows:

$$\Delta V_M^m = V_T^m - \{x_1V_1 + (1 - x_1) V_2\} \tag{3.26}$$

Differentiating equation (3.26) with respect to x_1, keeping temperature and pressure constant yields:

$$\left(\frac{\partial \Delta V_M^m}{\partial x_1}\right)_{T,P} = \left(\frac{\partial V_T^m}{\partial x_1}\right)_{T,P} + (V_2 - V_1) \tag{3.27}$$

or $$\left(\frac{\partial V_T^m}{\partial x_1}\right)_{T,P} = \left(\frac{\partial \Delta V_M^m}{\partial x_1}\right)_{T,P} - (V_2 - V_1) \tag{3.28}.$$

If, in equation (3.23), the general property X is replaced by the volume V, the equation becomes:

$$\bar{V}_2 = V_T^m - x_1\left(\frac{\partial V_T^m}{\partial x_1}\right) \tag{3.29}$$

Now, equation (3.26) may be rewritten as follows:

$$V_T^m = \Delta V_M^m + V_2 - x_1(V_2 - V_1) \qquad (3.30)$$

If equation (3.28) is multiplied by x_1 and substituted into equation (3.29) the resulting expression is:

$$\bar{V}_2 = V_T^m - x_1 \left(\frac{\partial \Delta V_M^m}{\partial x_1} \right)_{T,P} + x_1(V_2 - V_1) \qquad (3.31)$$

However, the value of V_T^m is given by equation (3.30) hence upon substitution into equation (3.31) the following expression is obtained:

$$\bar{V}_2 - V_2 = \Delta V_M^m - x_1 \left(\frac{\partial \Delta V_M^m}{\partial x_1} \right)_{T,P} \qquad (3.32)$$

Equation (3.32) provides the basis for the method of intercepts for the determination of partial molar volumes. The partial molar volumes of each component at a given composition x_1 may be obtained from the intercepts of the tangent to the ΔV_M^m vs. x_1 curve at that composition since the molar volumes of the pure components (i.e. V_1 and V_2) are known. See Fig. 3.2. The success of this method depends upon the accuracy with which tangents may be obtained to the ΔV_M^m vs. x_1 curve. Obviously, an analytical approach will obtain the best results from the data available, but if, as in the present case (see Fig. 9.1.7), the curve is unsymmetrical, containing several

Figure 3.2

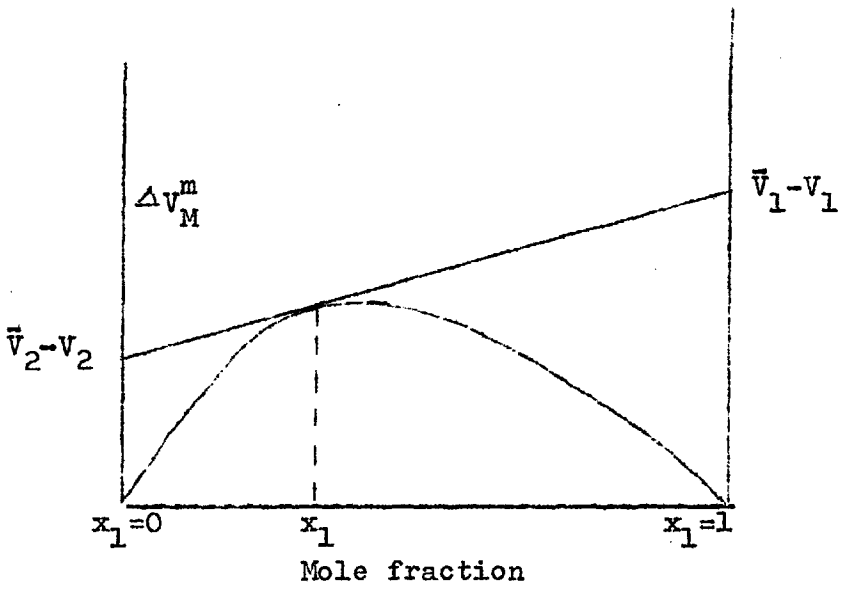

points of inflexion, it becomes very difficult to obtain a statistical fit for the curve especially if the boundary conditions (i.e. $\Delta V_M^m=0$ when $x_1 = 0$ and $\Delta V_M^m=0$ when $x_1=1$) are to be fulfilled. In such cases it is sometimes best to attempt to draw the curve by eye, constructing the tangents geometrically.

It will be seen later that this method of intercepts has proved particularly useful in the present context as plots of ΔV_M^m vs. composition have been obtained. Where the molar volumes of the two components differ widely it is often advantageous to quote values of $\bar{V}_1-V_1$ and $\bar{V}_2-V_2$ instead of the absolute partial molar volumes, particularly if the results are presented graphically. (See chapter 10).

Method 2.

This method is rather less useful in the present context, since all concentrations must be referred to one mole of component 1 or component 2.

Consider a mixture containing n_1 moles of component 1, molecular weight M_1, and 1 mole of component 2, molecular weight M_2. If the total volume of the mixture is V litres, then the density of the mixture ρ_M, is given by:

$$\rho_M = \frac{n_1 M_1 + M_2}{1000\ V} \tag{3.33}$$

or

$$n_1 = \frac{1000\ \rho_M V - M_2}{M_1} \tag{3.34}$$

Differentiation of equation (3.34) with respect to volume and density at constant temperature and pressure yeilds:

$$dn_1 = \frac{1000(\rho_M dV + V d\rho_M)}{M_1} \tag{3.35}$$

Hence:

$$\frac{dV}{dn_1} = \frac{M_1}{(\rho_M + V \frac{d\rho}{dV})1000} \tag{3.36}$$

Now, dV/dn_1 refers to a constant amount, i.e. 1 mole, of component 2.

Thus;

$$\frac{dV}{dn_1} = \left(\frac{\partial V}{\partial n_1}\right)_{n_2 \ldots} = \bar{V}_1$$

$$\text{and} \qquad \bar{V}_1 = \frac{M_1}{1000(\rho_M + V\frac{d\rho}{dV})} \tag{3.37}$$

If the concentration c_1 is expressed in moles per litre, then the volume V can be replaced by 1/c. It follows that

$$V(\frac{d\rho_M}{dV}) = -c\,(\frac{d\rho_M}{dc}) \tag{3.38}$$

Hence the partial molar volume of component 1 is:

$$\bar{V}_1 = \frac{M_1}{1000\,(\rho_M - c\,\frac{d\rho_M}{dc})} \tag{3.39}$$

Similarly, the partial molar volume of component 2 is:

$$\bar{V}_2 = \frac{M_2}{1000(\rho_M - c\,\frac{d\rho_M}{dc})} \tag{3.40}$$

Hence, the partial molar volumes of each component at a given concentration c, may be obtained from the tangent to the ρ_M vs. concentration curve at that point. The same problems exist in this method as in method 1 with regard to the construction of tangents to unsymmetrical curves.

3.5. Regular Solutions, Entropy of Athermal Mixing.

The factors relating to deviations from the ideal discussed in the preceeding sections of this chapter have assumed an ideal entropy of mixing. That is to say, the partial molar entropy of mixing for each component is given by:

$$\Delta\bar{S}_1 = -R \ln x_1$$
$$\Delta\bar{S}_2 = -R \ln x_2 \qquad (3.41)$$

Physically, this means the molecules in the mixture are distributed at random throughout the available volume, and that there is no preferred configuration and orientation with regard to either of the molecular species present. Many non-ideal solutions possess sufficient thermal energy to overcome the tendency to segregate due to different molecular fields and possess a nearly ideal entropy of mixing due to complete randomness from the point of view of spacial distribution and orientation. Solutions of this type have been termed by Hildebrand "regular solutions"[9]. Further it was pointed out by Guggenheim[10], that whilst a mixture may be formed with zero heat of mixing and zero change in total volume, it does not necessarily follow that it will have an ideal entropy of mixing. Solutions having zero heat of mixing, zero change in total volume, but a non-ideal entropy of mixing are termed "semi-ideal" solutions or more precisely "athermal solutions". Thus, in such cases, the free energy of mixing is determined by the entropy of mixing alone:

$$\Delta H_M = 0 \qquad (3.42)$$

$$\Delta F_M = -T \Delta S_M \qquad (3.43)$$

As stated in chapter 1, the Helmholtz free energy is related to the total partition function Z_T.

$$F = - kT \ln Z_T \qquad (3.44)$$

Thus, if the total partition functions for the pure components and for the mixture are Z_{T_1}, Z_{T_2} and Z_{T_M}, respectively, the change in free energy on mixing is:

$$\Delta F_M = -kT \ln \frac{Z_{T_M}}{Z_{T_1} Z_{T_2}} \qquad (3.45)$$

Hence:

$$\Delta S_M = + k \ln \frac{Z_{T_M}}{Z_{T_1} Z_{T_2}} \qquad (3.46)$$

for an athermal solution.

To evaluate the excess entropy of mixing must devolve upon the estimation of the partition functions which in turn depend upon the configurational integral β. (See chapter 1, section 1).

There are essentially three effects which may contribute to an excess entropy of mixing:

a) An effect due to a difference in the molar volumes of the two constituents.

b) An effect due to the spacial distribution of the molecules throughout the volume of the liquid.

c) An effect due to the orientation of the molecules. If the molecules behave as if they were spherically symmetrical this effect will be absent.

a) Volume effect

In a pure liquid each molecule enjoys a certain "free volume". Whether the free volume is defined, according to the lattice theory, as the volume available to each molecule moving within its own cell (see Chapter 1, section 1.3)or whether it is defined, according to the free volume theory, as the proportion of the excess volume (i.e. total volume minus volume of molecules) which may be redistributed without an accompanying increase in energy (see Chapter 1, section 1.3 & Chapter 4, p.135) need not effect the following argument: if, upon mixing the two liquids, the net free volume available to the molecular species present is altered, an excess entropy of mixing will be observed.

There have been several attempts to predict theoretically the effect upon entropy of mixing arising from differences in molecular size in athermal binary solutions. Although the mixtures studied in the present work are not athermal, the same arguments can often be applied, at least qualitatively. Two of the basic approaches to the problem are discussed here.

(1) The free volume approach

The advantage of this approach, due to Hildebrand[11], lies in the fact that it does not suffer from the limitations imposed by an artificial model for the liquid state.

Consider one mole of a liquid (or gas) contained in a vessel of volume V. The probability of finding a molecule in a

given place at a particular instant in time will be proportional to the number of molecules present, N (Avagadro's Number), the volume of the individual molecules v, and inversely proportional to the free volume, V-Nv since a small free volume will result in a short mean free path, and consequently a greater probability of locating a molecule at a certain place at a certain time.

$$\text{i.e.} \quad \text{probability} = \frac{Nv}{V - Nv} \ .$$

Hence, since entropy may be defined as:

$$S = R \ln \Omega$$

where Ω is the uncertainty of a particular arrangement, the change in entropy upon expanding the gas from volume V to volume V' is:

$$S' - S = R \ln \frac{V' - Nv}{V - Nv} \tag{3.47}$$

Suppose a solution is formed by mixing n_1 moles of component 1, and n_2 moles of component 2, the pure liquids occupying volumes V_1 and V_2 respectively. The probability of the instantaneous location of a molecule for the pure liquid is:

$$P_1 = \frac{Nv_1}{V_1 - Nv_1} \tag{3.48a}$$

and

$$P_2 = \frac{Nv_2}{V_2 - Nv_2} \tag{3.48b}$$

respectively.

If the total volume of the mixture is V, then the probability of the instant location of a molecule of component 1 in the solution will be:

$$P_1^S = \frac{n_1 N v_1}{V-(Nn_1v_1 + Nn_2v_2)} \qquad (3.49a)$$

Similarly, for a molecule of component 2:

$$P_2^S = \frac{n_2 N v_2}{V-(Nn_1v_1+Nn_2v_2)} \qquad (3.49b)$$

Thus, the increase in entropy on transferring n_1 and n_2 moles of the components from the pure liquids to solution can be derived from equations (3.48) and (3.49):

$$\Delta S = R\left\{ n_1 \ln \frac{V-N(n_1v_1+n_2v_2)}{n_1(V-Nv_1)} + n_2 \ln \frac{V-N(n_1v_1+n_2v_2)}{n_2(V_2-Nv_2)} \right\} \qquad (3.50)$$

For an athermal solution there is no excess volume of mixing, hence $V = n_1V_1 + n_2V_2$, and equation (3.50) becomes:

$$\Delta S = R\left\{ N_1 \ln \frac{N_1(V_1-Nv_1)+N_2(V_2-Nv_2)}{N_1(V_1-Nv_1)} + N_2 \ln \frac{N_1(V_1-Nv_1)+N_2(V_2-Nv_2)}{N_2(V_2-Nv_2)} \right\} \qquad (3.51)$$

Finally for an ideal solution $V_1=V_2$ and $v_1 = v_2$ and equation (3.51) reduces to:

$$\Delta S = -R\left\{ \ln x_1 + \ln x_2 \right\} \qquad (3.52)$$

which is the ideal entropy of mixing.

This approach of Hildebrand which essentially treats the two components as gases, neglects the fact that in liquids the free volume cannot be regarded as the difference between the total volume and the volume occupied by the actual molecules. In other words, the problem is that of communal entropy raised in Chapter 1 in connection with lattice theories of liquids in which molecules are confined by their neighbours to a comparatively small cell; under these circumstances the total free volume as defined above, is not freely available to each individual molecule. However, if it is assumed that the communal entropy is the same in the mixture as in the pure liquids, this factor will not appear in the expression for the entropy change on mixing.

(2) The quasi-lattice approach

The basis for this approach was first proposed by O. Stern in 1916[12]. The most simple model is one in which each available site in the quasi-lattice is occupied by a single molecule of either component. If the communal entropy is assumed to be the same for each pure liquid and the mixture, this factor will, as mentioned above, be absent from the expression for the entropy change upon mixing. The entropy is computed by counting the number of different ways in which the molecules of the two components may be distributed throughout the sites

available. The number of distinguishable arrangements Ω is, in the case of athermal solutions, proportional to the configurational integral β. If the entropies of the two pure components and the mixture are defined as:

$$S_1 = k \ln \Omega_1$$
$$S_2 = k \ln \Omega_2 \qquad (3.53)$$
and $$S_M = k \ln \Omega_M$$

respectively, then the entropy change on mixing will be:

$$\Delta S_M = k \left\{ \ln \Omega_M - \ln \Omega_1 - \ln \Omega_2 \right\} \qquad (3.54)$$

For a simple case in which one molecule of either species occupies one site Ω_M may be given as:

$$\Omega_M = \frac{(n_1+n_2)!}{n_1! n_2!} \qquad (3.55)$$

Ω_1 and Ω_2 are:

$$\Omega_1 = \frac{n_1!}{n_1!} \quad ; \quad \Omega_2 = \frac{n_2!}{n_2!} \qquad (3.56)$$

where n_1 and n_2 are the number of molecules of each component present.

Hence the entropy change on mixing may be given as:

$$\Delta S_M = k \left\{ \ln \frac{(n_1+n_2)!}{n_1! n_2!} \right\} \qquad (3.57)$$

Applying Stirling's theorem and differentiating we have:

$$\Delta \bar{S}_1 = - R \ln x_1 \quad ; \quad \Delta \bar{S}_2 = - R \ln x_2 \qquad (3.58)$$

which is the ideal entropy of mixing. The next development of the lattice approach was due to Fowler & Rushbrooke[13], though a more general solution was obtained by Chang[14]. A mixture is considered in which a molecule of one species occupies one lattice site, whilst a molecule of the second species occupies two sites. In this case the partial entropies of mixing are:

$$\Delta\bar{S}_1 = -R\left\{\ln \phi_1 - \frac{Z}{2}\ln\left(1 - \frac{1}{Z}\phi_2\right)\right\}$$

$$\Delta\bar{S}_2 = -R\left\{\ln \phi_2 - (Z-1)\ln\left(1 + \frac{1}{Z-1}\phi_1\right)\right\} \qquad (3.59)$$

where ϕ_1 and ϕ_2 are the volume fractions of components 1 and 2 respectively, and Z is the co-ordination number of the lattice. The theory has been further extended to include molecules occupying multiple sites[15-18], and this development has found particular application in polymer chemistry. More recently, an attempt has been made to assess the excess entropy of mixing of two liquids comprised of spherical molecules of different sizes by considering the following cycle[21]:

1) The pure liquids are converted to give gases of rigid spheres:- this is a hypothetical step in which the liquids are discharged of their entropy of evaporation. The total entropy change for the two pure liquids will then be:

$$\Delta S = n_1 \Delta S_1 - n_2 \Delta S_2$$

2) The pure compressed gases are expanded to pressures low enough to allow ideal behaviour.

3) The expanded gases are mixed at constant pressure, the entropy of mixing being ideal.

4) The gas mixture is compressed to the volume of the solution, and the entropy change accompanying this step is derived from the Lebowitz equation of state[22] for mixtures of rigid spheres.

5) The compressed mixture is recharged, i.e. the intermolecular attractive potential is restored and the repulsive potential is changed to that of the solution.

A rather lengthy expression is derived for the excess entropy of mixing in terms of composition, diameter of spheres and the total volume of the solution.

Agreement with experiment is satisfactory for binary mixtures of simple pseudo-spherical molecules such as argon, nitrogen, oxygen and carbon monoxide and methane. The applicability of the theory to mixtures of the very non-spherical molecules considered in this present work is doubtful.

b) Spacial distribution effect.

The preceeding section has dealt with the effect upon the entropy of mixing of differences in the molecular size of the two components assuming throughout that the mixing is random.

It is mentioned in chapter 4 (chapter 4, p.127) that in

a liquid consisting of molecules possessing a cog-wheel type of structure, the greater free volume and reduced symmetry of packing may result in the formation of molecular aggregates which may be either anti-crystalline clusters or cystal nuclei. If the cluster theory is accepted then any anomalies in the macroscopic properties such as excess viscosity may be explained as a result of the time averaged formation and dissolution of the clusters. If again the clusters arise from molecular collisions, the rate of formation of the cluster will depend upon both the molecular mean free path and the geometry of the collision. The latter factor will in turn depend upon the conformation of the molecules themselves, since only if the molecules possess the correct orientation with respect to each other or another aggregate will they interlock upon collision. In other words molecular orientation not only gives rise to an entropy effect in its own right, but it may influence the effects due to spacial distribution.

In a binary mixture clusters could comprise molecules of the same species, molecules of different species, or both. In the present work only one of the components in the mixtures chosen are likely to form clusters with sufficient cohesion to be significant, though the possibility of mixed clusters cannot be so readily discarded. However, if it is assumed that molecules of one species only are capable of cluster formation, one would expect the rate of cluster formation to be reduced in the mixture

if only as a result of the increased mean free path. Further, the volume excluded by the molecules of the second component may prevent the approach of molecules of the cluster forming type in comparatively dilute solution. It will be seen later that the dilution of the cog-wheel type molecules does result in a reduction of the anomalies in the macroscopic properties interpretable in terms of crystal clusters. The existance of crystal clusters in a mixture need not necessarily give rise to a low value for the entropy of mixing, since, if the dilution of the cluster forming component results in a marked decrease in cluster concentration there may well be a large positive entropy of mixing despite the existance of clusters in the mixture.

Most studies of the entropies of mixing have hitherto been directed towards mixtures of comparatively simple molecules in which the above mentioned factors are probably absent. If heat of mixing data were available for mixtures containing cog-wheel shaped molecules of the polyphenyl type it would be difficult to interpret any observed anomalies conclusively in terms of crystal clusters, since direct evidence for their existence is lacking (see Chapter 4, section 4.3). However the possibility that clusters do feature in liquids and liquid mixtures cannot be discounted, and in some instances the theory provides a quite convincing explanation of anomalies observed in transport properties and in excess parameters of mixing.

c) The effect of orientation[19]

The effect of incomplete randomness in molecular orientation upon entropy of mixing is the most difficult factor to assess quantitatively. There are two distinct types of molecular orientation, intermolecular orientation and intramolecular orientation which can operate either individually or in conjunction. The first factor is concerned with the rotations of each molecule within the volume it occupies in the liquid. The rotations of asymmetric molecules can be resolved along three perpendicular axes, but free rotation about either of these axes will necessarily depend upon the space available to each molecule; if a particular molecule is crowded by its neighbours to such an extend that rotation about either axis is inhibited by a large energy barrier ($\Delta E \gg kT$) then the orientation of that molecule will remain fixed. At higher temperatures, the increased free volume may permit the onset of rotation, consequently the entropy of mixing will tend to increase as the temperature at which the mixing takes place is raised. A more detailed discussion of the volume requirements for the rotation of molecules studied in the present work can be found in chapter 10 and the Appendix.

One of the first attempts to assess this effect quantitatively was due to Wood[19], by considering entropy of mixing data available for a number of binary mixtures selected from carbon tetrachloride, benzene, cyclohexane, and methanol.

Essentially the argument is based upon the idea that, at high dilution, the orientation of the solute molecules tends to be random, but this does not mean that in such solutions the effect due to preferred orientation is absent since in the mixtures considered by Wood, and, to an even larger extent the mixtures studied in the present work the orientation of solvent molecules has also to be considered. The introduction of a few solute molecules could well produce a large effect upon the orientational distribution of the solvent molecules throughout the liquid. By employing these ideas Wood has succeeded in showing that the behaviour of the mixtures mentioned above is compatable with the known properties of the pure components.

Although not directly related to liquid mixtures, attempts have been made to assess quantitatively the effect of molecular and group conformation upon the entropy of melting of some straight chain polymers; the principles involved may well find application in the context of liquid mixtures[20].

REFERENCES

1. Glasstone, S., "Text Book of Physical Chemistry", 2nd Edition, Macmillan and Co. (1955).

2. Mears, P., Trans. Faraday Soc., 45, 966 (1949).

3. Scatchard, G., Trans. Faraday Soc., 33, 160 (1937).

4. Mathot, V. and Desmyter, A., J. Chem. Phys., 21, 782 (1953) c.f., Rowlinson, J.S., "Liquids and Liquid Mixtures", Butterworths (1959).

5. Kendall, J. and King, C.V., J. Chem. Soc., 127, 1778 (1925).

6. Glasstone, S. "Thermodynamics for Chemists", D. Van Nostrand Co. Inc. (1947).

7a. Mathieson, A.R. and Thynne, J.C.J., J. Chem. Soc., 3708 (1956).

b. Wood, S.E. and Austin, A.E., J. Amer. Chem. Soc., 67, 480 (1945).

8. Biron, E., Russ. J. Phys. Chem. Soc., 44, 1264 (1912). c.f. Hildebrand, J.H. and Scott, R.L., "Solubility of Non-electrolytes", 3rd edition, Dover Publications Inc. (1964).

9. Hildebrand, J.H. and Scott, R.L., "Solubility of Non-electrolytes", 3rd Edition, Dover Publications Inc. (1964).

10. Guggenheim, E.A., Proc. Roy. Soc., 148.A., 304 (1935). c.f. Guggenheim, E.A., "Mixtures", O.U.P. (1952).

11. Hildebrand, J.H., J. Chem. Phys., 15, 225 (1947).

12. Stern, O., Ann. Physic., (4), 49, 823 (1916).

" ibid. 51, 237 (1916).

13. Fowler, R.H. and Rushbrooke, G.S., Trans. Faraday Soc., 33, 1272 (1937).

14. Chang, T.S., Proc. Roy. Soc., A.169, 512 (1939);
Proc. Camb. Phil. Soc., 35, 265 (1939).

15. Huggins, M.L., J. Chem. Phys., 9, 440 (1941).

16. Flory, P.J., J. Chem. Phys., 9, 660 (1941);
ibid, 10, 51 (1942).

17. Miller, A.R., Proc. Camb. Phil. Soc., 38, 109 (1942);
39, 154 (1943).

18. Guggenheim, E.A., Proc. Roy. Soc., A.183, 203 (1944).

19. Wood, S.E., J. Chem. Phys., 15, 358 (1947).

20. Starkweather, H.W. Jr. and Boyd, R.H., J. Phys. Chem., 64, 410 (1960). see also,
Lifson, S., J. Chem. Phys., 30, 964 (1959);
Flory, P.J., Proc. Roy. Soc., 234A., 60, (1956).

21. Yasim, S.J., J. Chem. Phys., 43, 286 (1965).

22. Lebowitz, J.L., Phys. Rev., 133, 4895 (1964).

CHAPTER 4.

PREMONITORY PHENOMENA, PRE-FREEZING PHENOMENA AND THE GLASSY STATE

4.1. Premonitory Phenomena

The earliest quantitative attempts to produce a theory to describe the melting process were due to Lindemann (1910)[1] and Sutherland (1891)[2]. According to Lindemann, the vibrations of molecules about their mean positions in the crystal lattice increase in amplitude as the temperature is raised, until a point is reached when the lattice is rendered unstable, and the crystal melts. Sutherland, on the other hand, has suggested that an increase in temperature results in a decrease in the crystal's resistance to shear, and at the melting point this resistance sinks to zero. Both these theories are one phase theories, and fail to account for the observed thermodynamic equilibrium between the solid and liquid states at the melting point. In their primitive forms they do not deal with any premonitory phenomena. Careful studies of the solid state, in particular the effect of rising temperature upon specific heat and molar volume, have shown that a variety of different crystal types display anomalous changes in these properties prior to melting. In other words, some anticipatory disordering takes place before the discontinuous changes occur at the melting point. The extent of this anticipatory disordering varies greatly from crystal to crystal.

In most molecular crystals two principal mechanisms of

disordering are available, viz: positional disordering and orientational disordering [3]. Positional disordering can arise for example, as the molecules in the expanding lattice occupy interstitial positions. This process is commenced before the melting point is reached, and may give rise to marked premonitory effects. On passing from crystal to melt, the change in volume incurred results in a large decrease in the energy required to form a defect. In consequence the fraction of those molecules occupying interstitial sites is comparable to unity in the melt at the freezing point. Positional disordering may also involve merely the formation of vacant sites in a crystal. The silver halides provide good examples of premonitory effects arising from positional disordering[4].

Orientational disordering occurs as a result of changes in molecular orientation within the expanding lattice. This may lead to a solid state transition at a particular temperature T_c, when the energy required for the molecule to adopt a fresh configuration, or to rotate, is $\leq kT$. Such a transition may involve the formation of a fresh crystal lattice of higher entropy and lower free energy. Usually, a solid state transition of this type is marked by sharp discontinuities in general properties, (e.g. entropy and volume) resulting from the intersection of the free energy surfaces of the two forms. The free energy G is a function both of pressure and temperature. Along the line of

intersection, the free energies of each form, (G_1 and G_2 respectively) are equal, and the two forms may co-exist in equilibrium. The discontinuities arise as a result of differences between the slopes of the two surfaces at the particular point under consideration in the line of intersection

$$\text{e.g.} \quad -\left(\frac{\partial G_2}{\partial T}\right)_P > -\left(\frac{\partial G_1}{\partial T}\right)_P$$

this implies a discontinuity in entropy since $\left(\frac{\partial G}{\partial T}\right)_P = -S$.

Similarly:

$$-\left(\frac{\partial G_2}{\partial P}\right)_T > -\left(\frac{\partial G_1}{\partial P}\right)_T$$

this implies a discontinuity in volume since $\left(\frac{\partial G}{\partial P}\right)_T = V$.

(NB. $\left(\frac{\partial G}{\partial T}\right)_P$ and $\left(\frac{\partial G}{\partial P}\right)_T$ are negative quantities, see Fig. 4.1a)

Figure 4.1a represents a section through the free energy surface at constant pressure, in which the difference between the slopes (represented by angle θ) is large. In some cases however, notably the crystalline ammonium halides [3,5], a continuous change in properties is observed in the transition region, extending over a range of temperature. The shape of specific heat curves arising from continuous thermodynamic transitions are reminiscent of the Greek letter lambda (λ), and it has become customary to refer to such phenomena as "lambda" phenomena (See Fig. 4.2). It has been suggested that these continuous changes result from the free energy surfaces of the two polymorphic forms not only intersecting but touching.

FIGURE 4.1.

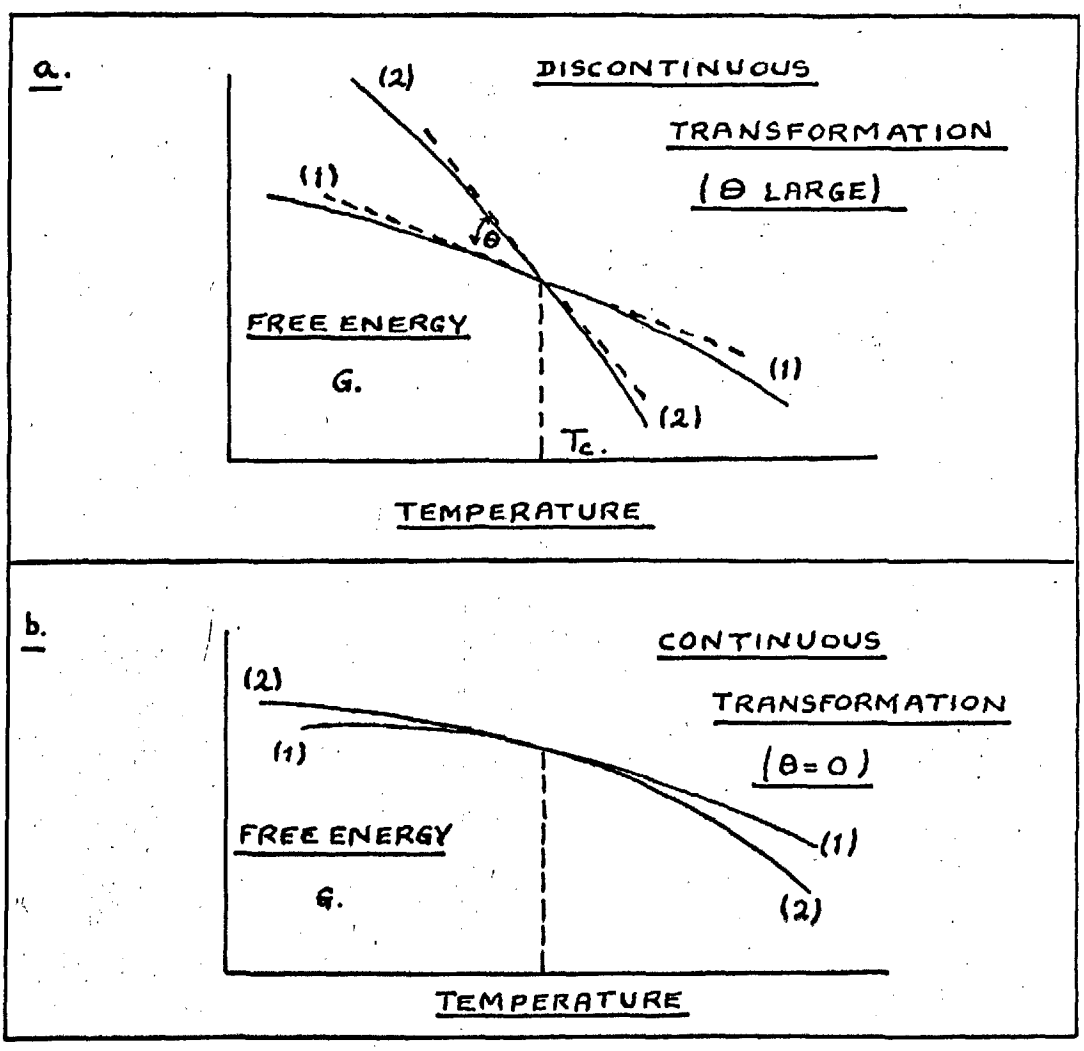

FIGURE 4.2.

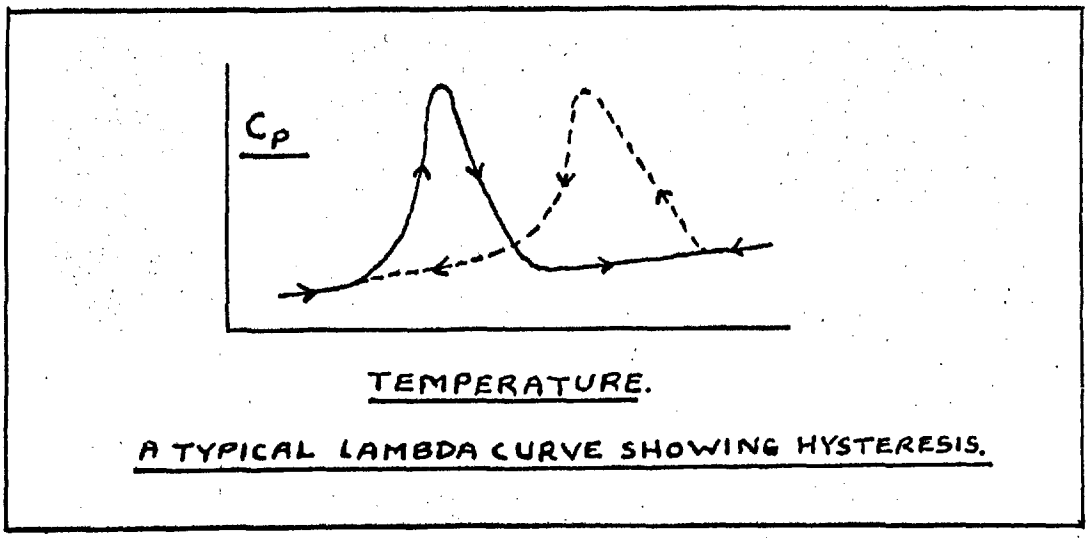

In other words, the angle θ between the slopes to the surfaces at the point or line of contact is zero (See Fig. 4.1b). Under these conditions:

$(\frac{\partial G_1}{\partial T})_P = (\frac{\partial G_2}{\partial T})_P$ and $(\frac{\partial G_1}{\partial P})_T = (\frac{\partial G_2}{\partial P})_T$. This implies that there is no discontinuity in either the entropy or the volume, since these quantities are the same for both forms at the transition point. X-ray studies of lambda transformations, using single crystal techniques, indicate that as the temperature is raised and the transition temperature T_c is approached, domains of the high temperature form begin to appear. In the vicinity of T_c, a hybrid crystal is produced in which the high and low temperature forms co-exist, both being present in significant proportions. Since the two forms are not identical, the hybrid state involves considerable mechanical strain as well as internal surface energy at the boundaries between domains of the two forms. If the temperature is cycled about T_c, marked hysteresis is often observed (see Fig. 4.2). A detailed discussion of lambda phenomena and their interpretation may be found in reference (3). With more complex molecules such as long chain paraffins[6], a number of these transformations may be observed, each associated with a fresh configuration (c.f. Chapter 1, section 1.5). It is generally true, within the broad context of orientational transformations, that for a single molecule to adopt a fresh configuration within an otherwise unperturbed lattice requires a fairly large amount of

energy compared with kT, but as an increasing fraction of molecules participate, the energy barrier is lowered and the lattice parameters expand. It should be emphasised that orientational transformations do not necessarily mark the onset of free rotation*, but more often the ability to assume new configurations. In many instances, in particular polynuclear aromatic hydrocarbons and polyphenyls, free rotation is denied even in the melt[7] (see Chapter 6, re. the molecules studied in this present work). The preceding discussion of positional and orientational disordering serves to illustrate some of the factors which may contribute, either jointly or singly, to the general disordering of a crystal lattice, of which the melting process is but a further stage.

Attempts have been made to produce a theory of melting which predicts a two phase equilibrium at the melting point by considering the introduction of interstitial defects with rising temperature. This approach was pioneered by Frenkel (1935)[8], and later developed by Lennard-Jones and Devonshire (1939)[9]. The latter workers proposed a model in which N molecules are distributed throughout a lattice of 2N sites, which are divided into two inter-penetrating sub-lattices each of N sites. In the ordered solid state, all N molecules lie on one of the two sub-lattices, whilst in the liquid state these molecules are

---

* A molecule is said to be free to rotate, when it is able to rotate about the three perpendicular axes through its centre of gravity within the space available in either the solid or the melt.

distributed, without long range order, over the total 2N sites. The process of distribution may be regarded as the gradual occupation of interstitial lattice sites as the temperature is raised. By considering the interaction between pairs of spherical molecules occupying adjacent sites on the same sub-lattice, and adjacent sites on different sub-lattices, they arrived at a modified equation of state predicting a two phase equilibrium at the melting point allowing for the observed phenomena of pre-melting. In the simple theory consideration is confined to spherical molecules possessed of a 6-12 intermolecular potential (see Chapter 1, page 21), and it is assumed that the vibrational frequency of the molecules remains unaltered throughout the disordering process. However, in this simple form, the theory predicts values of the volume and entropy change on melting for the solid inert gases, in which contributions due to orientational disordering are absent, in good agreement with experiment. The theory has been extended to include multiple interactions[10], but the agreement with experiment achieved is only marginally better than for the original theory.

Starting from the basic Lennard-Jones and Devonshire model, Karasz and Pople (1961)[11] have attempted to take some account of the influence of orientational disordering upon the melting process. Each molecule is allowed to assume two possible orientations α and β of different minima of potential energy.

With reference to the basic sub-lattice (lattice 1) corresponding to a solid state which is fully ordered positionally, the two possible orientations are designated α_1 and β_1. As the temperature is raised, molecules begin to occupy sites on the second sub-lattice (lattice 2) when they may again assume two possible orientations, α_2 and β_2 ($\alpha_1 \neq \alpha_2$, $\beta_1 \neq \beta_2$). The orientations α and β do not imply any particular relative orientation, e.g. that all the molecules are parallel, but are linked with solid angles within which the crystal axes lie. As mentioned above, the simple positional theory of melting considers pair interactions between molecules situated on the same sub-lattice and on different sub-lattices. The equation of state resulting from the present modification requires consideration of four pair interactions. A further repulsive term is introduced to enable an account to be made of the interactions between molecules possessing either the same or different orientations on the same sub-lattice or on different sub-lattices. Agreement with experiment is quite good for simple molecules such as the solid inert gases, methane, carbon monoxide and hydrogen chloride, but agreement is poor for more complex molecules such as cyclohexane. This is particularly regrettable since in molecules of low symmetry of the latter type, orientational factors must play a large part.

In the foregoing discussion of some theories of melting, mathematical detail and numerical examples have been omitted since

the wider aspects of the subject of melting only touches the main field of this thesis at certain parts. However a qualitative view of the melting process and of premonitory phenomena is helpful in considering the structure and behaviour of melts.

4.2 Prefreezing Phenomena

Just above the melting point the molecules of a melt may still retain considerable long-range order, and the basic matrix of the solid-state lattice. At temperatures well above the melting point, the long-range order of the melt is lost, and it is no longer realisitic to refer the liquid structure to a modified version of the original solid lattice. This reveals a further weakness in the above mentioned theories of melting since they fail to account for any further disordering (either positional or orientational) which might occur above the melting point.

The greater free volume and reduced symmetry of packing in a melt may permit the formation of clusters or molecular aggregates. These clusters may be divided into two distinct types, viz: those which comprise repeating units of structure, i.e. crystal nuclei, and those which comprise non-lattice conglomerations of molecules, i.e. anticrystalline clusters*. Both types possess very similar heat contents and specific volumes, provided that each contain but a few units; the unchecked growth of an

---

* See Chapter 2, page 61 .

anticrystalline cluster must necessarily involve the inclusion of voids and fronds, because of the absence of lattice packing. It must be pointed out that the cooling of a liquid to within a few degrees of its melting point may result in a large number of clusters of either type, in which case the concept of a quasi-crystalline structure for the melt is invalid. On the other hand, on heating a solid to just above its melting point may well result in a quasi-crystalline melt. In other words, in order to consider the possible structure of a liquid at any particular temperature it is necessary to take into account its previous history. Equally important from this point of view is the nature of the equilibrium configuration of the molecules, for example, they may behave as spheres, rods, discs, or cog-wheels. (c.f., Chapter 1, section 1.5). The formation of clusters may lead to a variety of prefreezing phenomena. For example, a variety of substances, including some molten alkali metals[12] and aliphatic hydrocarbons[13], display an anomalous increase in enthalpy as the temperature is lowered towards their melting points. The gradual formation of clusters may also be reflected in the viscosity/temperature relationships provided that the life-time of a cluster is longer than the relaxation time τ, for viscous flow (see Chapter 2, sections 2.3.1 and 2.4). The readiness with which a liquid will form clusters must necessarily depend upon the nature of the molecules of which it is comprised. There are

two principal factors which either singly or jointly favour the formation of clusters, viz: dipole interaction and molecular shape. There are many instances in which dipole interaction leads to cluster formation, e.g. phenols, ethers[14], carboxylic acids[15] and sugars, but as mentioned earlier, this thesis is concerned primarily with non-polar molecules* in which the effects of molecular shape are paramount. From this point of view, the tendency to cluster formation is greatest with rigid molecules possessing non-spherical force fields. (c.f. Chapter 1, section 1.5). For example, the "bog-wheel" shaped o-terphenyl, 1:3:5 triphenyl benzene, and 1:3:5 tri-α-naphthyl benzene all show anomalously high viscosities as their melting points are approached. All show marked super-cooling and 1:3:5 tri-α-naphthyl benzene finally sets to a glass**. With molecules of this type it is possible to visualize clusters arising from molecular interlocking. The influence of molecular shape and cluster formation upon viscosity is discussed in detail in Chapter 2, with particular reference to molecules of the polyphenyl type.

4.3. Glass Formation.

It was mentioned earlier (Chapter 2, section 2.4, and this chapter, section 4.2) that some polyphenyl melts display a

---

* See Chapter 6, section 6.3 for a discussion of dipole effects in aromatic hydrocarbons of the type studied in this present thesis.

** See section 4.3. for a discussion of the influence of cluster formation upon glass formation.

marked propensity towards glass formation. Both liquids and glasses are devoid of long-range order, and their fundamental difference is essentially kinetic. The macroscopic properties of liquids are manifestations of the time-averaged liquid structure, since the translational motion of the molecules is rapid with respect to the time of experiment. A glass, however, is similar to the solid crystalline phase in as much as each molecule is "locked" in its position in space. From the standpoint of statistical mechanics, a glass may be described as a localised liquid. It seems generally agreed that any pure liquid free from nucleating singularities, such as impurities or active surfaces, will not crystallise if the kinetic barrier to either crystal nucleation or crystal growth is very large; any liquid is capable of glass formation provided that crystallisation does not intervene. In fact very pure samples of liquids of different types such as toluene, some aliphatic alcohols, and iso-amyl bromide have been cooled to glasses[16, 17, 18]. Thus, the factors which determine the tendency for a liquid to form a glass are the rate at which nucleation occurs and the rate of crystal growth. In the case of inorganic glasses such as silica, comprising a three dimensional lattice of covalent bonds, re-orientation of each SiO_2 molecule to facilitate nucleation involves the cleavage of these bonds: i.e. the barrier to nucleation is very large[19]. In the present context of non-polar

interlocking organic molecules, the kinetics of aggregate formation and dispersion are the determining factors since it is possible to visualise a glass as a melt in which a large proportion of the total volume is involved in mutually interlocking aggregates. The point at which a super-cooled melt is termed a glass is not arbitrary. It was first shown by Tamman, in connection with silicate glasses, that marked changes occur in the general properties of the melt around a characteristic temperature T_g, known as the glass transition temperature, as the melt congeals to a glass. This behaviour appears quite general, and the viscosity of super-cooled melts in the vicinity of their glass transition temperatures, has a value $\eta \geq 10^{13}$ poise. Plots of molar heat capacity vs. temperature can provide a means of evaluating the excess entropy of a glass over the crystalline phase[20]. In the vicinity of their glass transition temperatures materials may also display critical changes in their thermal expansion, thermal conductivity, dielectric constant, and refractive index vs. temperature curves. In the present context the property particularly accessible for study is the molar volume V_m, since its variation with temperature may be determined by means of comparatively simple dilatometric techniques. Figure 4.3 represents a typical molar volume vs. temperature plot for a crystalline material which, after heating well above its melting point, congeals to a glass upon cooling.

Figure 4.3

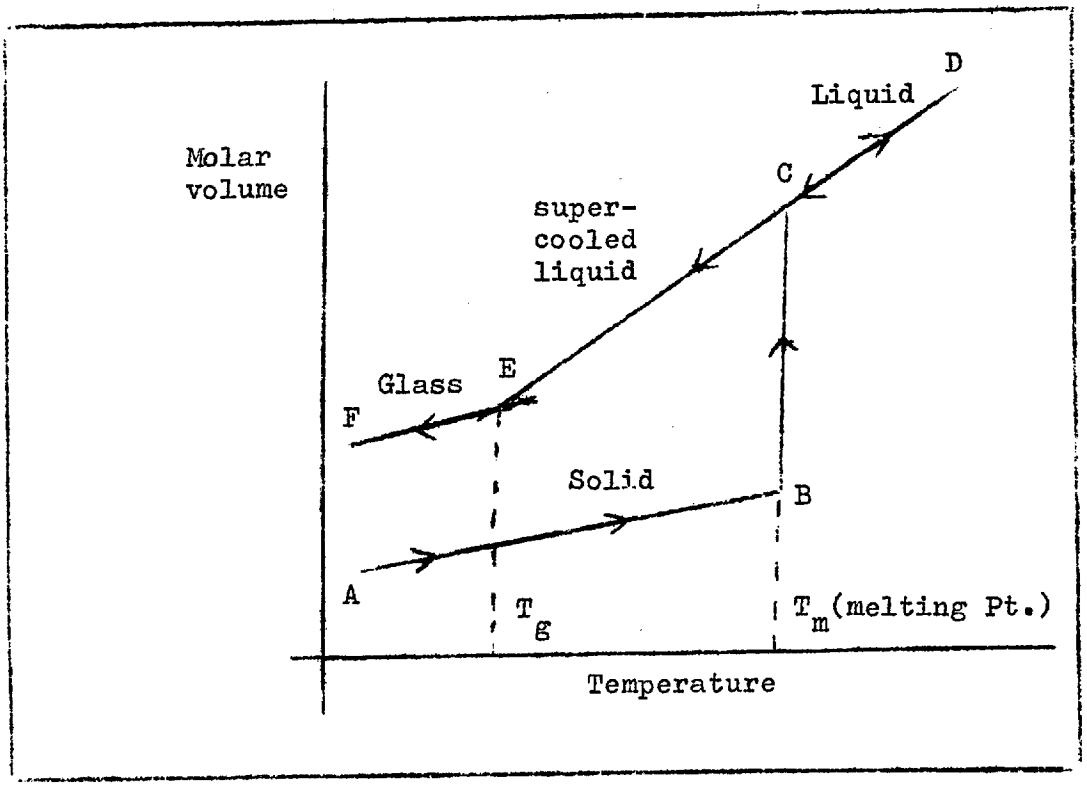

Section AB represents the solid crystalline phase, CD the melt, CE the super-cooled liquid, and FE the glass. It will be noticed that the slopes of the crystalline section AB, and the glass section FE are closely similar. The changes in volume displayed by melts with changing temperature may be roughly divided into configurational effects and vibrational effects.

$$\text{i.e.} \quad \frac{d\,V_{Liq}}{dT} = \left(\frac{\partial V}{\partial T}\right)_{Vib.} + \left(\frac{\partial V}{\partial T}\right)_{Config.} \qquad (4.1)$$

In both solids and glasses, the molecules are locked in their

positions in space (c.f. this chapter, page 130), and vibrational effects dominate. Small differences between the slopes of the crystalline and glass sections may arise as a result of differences in molecular environment which could influence the vibrational characteristics of the molecules. Fig. 4.3 illustrates a very simple example. In reality the crystalline section AB may well display orientational transformations and/or premonitory anomalies resulting from positional disordering (see this Chapter, page 120 et seq.).

Reference has been made to the glass forming properties of 1:3:5 tri-α-naphthyl benzene (see Chapter 2, section 2.4, and this chapter, section 4.2). This hydrocarbon, first investigated by Magill and Ubbelohde (1958)[21], provides one of the finest examples of a stable glass ($T_g \approx 70^{\circ}C$) formed as a result of cluster formation arising from molecular interlocking. More recently Plazek and Magill (1966)[22] have investigated some of the mechanical properties of this particular glass. It will be seen later, that this present work has resulted in the discovery of two more hydrocarbons which form stable glasses (see chapters 9 and 10).

Faucher and Koleske (1966)[18] have conducted an investigation into the glass forming properties of all the normal and isomeric aliphatic alcohols from C_1 to C_5 with a view to correlating their glass transition temperatures with

molecular weight and molecular shape. They have shown that, for normal alcohols, the glass transition temperature varies almost linearly with the reciprocal molecular weight. Perhaps the most interesting of their results, with regard to the present context, is the fact that in general the more branched the aliphatic chain, the higher the glass transition temperature. The highest glass transition temperatures are associated with t-butanol and neopentanol*. Faucher and Koleske have concluded that the more nearly spherical the molecule becomes, the greater is its tendency to form a glass. This interpretation would seem to contradict the mechanism of glass formation outlined above. The O-C bond in tertiary alcohols is weaker than in secondary and primary alcohols owing to hyperconjugation enhancing the dipole moment - a fact overlooked by the workers. The present author questions the statement that, within the context of glass formation, t-butanol may be regarded as almost spherical. The molecule is club shaped. Whilst it may be able to rotate in the melt at comparatively high temperatures, the reduced free volume of the glassy state may inhibit its motion. Further, branched alcohols in general are less flexible than corresponding normal alcohols (c.f. Chapter 1, section 1.5) , and they are less able to adopt alternative conformations. The present author considers

---

* All these glass transition temperatures are well below room temperature. The highest (for t-butanol) is -93°C.

that it may be the rigid nature of such molecules coupled, in the case of secondary and tertiary alcohols, with the enhanced dipole interactions which favour glass formation. The cluster theory of glass formation outlined above is one of two major theories current at present. The second theory, termed the "free volume" theory, was proposed by Cohen and Turnbull (1958-1961)[23]. According to these workers, the formation of a glass is the result of the decrease in the free volume of the amorphous phase below some critical value. Mention has already been made of this theory in chapter 2, section 2.3 in connection with theories relating viscosity and free volume, but the following brief summary will serve to illustrate its pertinence to the phenomenon of glass formation.

In the first instance the model chosen is essentially the same as the quasi-crystalline model of Lennard-Jones and Devonshire (see Chapter 1, section 1.3). The excess volume $\Delta \bar{V}$ resulting from the total thermal expansion of the quasi-crystal from $0^{\circ}K$ to the working temperature is divided into two parts:

$$\Delta \bar{V} = V_f + \Delta V_c \qquad (4.2)$$

The volume V_f represents the part of the cell in which the molecule may move freely with its gas kinetic energy velocity u. $\left[u = \left(\frac{3kT}{m}\right)^{1/2} \right]$. The volume ΔV_c represents the volume in the vicinity of the cell boundaries, to which the molecule is

denied access by virtue of the steeply rising potential energy barrier. The main premise of this theory is that above a certain temperature, the free volume is not associated in discrete portions with each molecule, but may be thermally distributed in greater or smaller portions throughout the liquid. Thus the free volume may be redefined as the proportion of the total volume which can be redistributed without a significant increase in energy compared with kT. The free volume V_f defined in this way is assumed to vary with temperature according to the following expression:

$$V_f = \alpha \bar{V}_m (T - T_o) \qquad (4.3)$$

where $\bar{V}_m$ is the average volume per molecule, and V_f, the total expansion of the liquid from a temperature T_o at which the volume available for redistribution is zero. A further premise is that transport will only occur when voids, having a volume greater than some critical volume V^*, are formed as a result of the redistribution of free volume into which a molecule may jump (c.f. Chapter 2, section 2.3). Since the free volume may be distributed throughout the liquid, the free energy of an amorphous phase in which this occurs will be least when this volume is distributed at random. In fact it is only in an amorphous phase that this randomisation can be achieved. Thus, if a liquid is cooled, the free volume available will decrease, and if no ordering redistribution takes place a point will be

reached when the free volume becomes too small to permit further redistribution without overcoming large energy barriers. The temperature at this point is the glass transition temperature and may be identified with T_o in equation 4.3 above. The molecules are locked in their positions in space in a disordered array. It may be seen that with very asymmetric molecules of the polyphenyl type which, in the crystalline state, possess lattices of low cohesive energy, the tendency towards glass formation is enhanced by virtue of the large energy barriers which must be overcome in order to achieve ordering distribution. As mentioned in Chapter 2 the main difference between the cluster theory and the free volume theory is that the former implies fluctuations in density throughout the melt as clusters are formed, whilst the latter theory predicts a uniform contraction and congelation of the melt as the temperature is lowered. At the glass point both theories convey much the same picture (c.f. Chapter 2, section 2.4).

Within the context of "model molecules" of specific shape, the cluster theory may claim the advantage over the free volume theory, since it provides a realistic explanation of the empirical correlation between molecular shape, pre-freezing phenomena, and glass formation. The free volume theory is concerned with hard sphere molecules with spherically symmetrical force fields. The factors of molecular shape are not considered.

REFERENCES

1. Lindemann, F.A., Phys. Z., 11, 609 (1910).
2. Sutherland, Phil. Mag., 32, 31, 215, 524 (1891).
3. Ubbelohde, A.R., "Melting and Crystal Structure", Clarendon Press (1965).
4. Wells, A.F., "Structural Inorganic Chemistry", 3rd ed. Oxford University Press (1962).
5. Ubbelohde, A.R., A. Rev. Chem. Soc., 36, 150 (1940).
6. Ubbelohde, A.R., Trans. Faraday Soc., 34, 289 (1938).
7. Andrews, J.N. and Ubbelohde, A.R., Proc. Roy. Soc. A.228, 435 (1955).
8. Frenkel, J., Acta Physiochem., U.R.S.S., 3, 633 and 913 (1935).
9. Lennard-Jones, J.E. and Devonshire, A.F., Proc. Roy. Soc., A.169, 317; A.170, 464 (1939).
10. Domb, C., Phil. Mag., 42, 1316 (1951).
11. Pople, J.A. and Karasz, J., Phys. Chem. Solids, (a) 18, 28 (b) 20, 294 (1961).
12. Schneider, A. and Hilmer, O., Z. anorg. chem., 286, 97 (1956).
13. Ubbelohde, A.R., Trans. Faraday Soc., 34, 292 (1938).
14. Hunter, A.N., Proc. Phys. Soc. Lond., 59B, 965 (1956).
15. Pilpel, N., Trans. Faraday Soc., 57, 1426 (1961).
16. de Nordwall, H.J. and Stavely, L.A.K., J. Chem. Soc., 224 (1954).
17. Kauzmann, W., Chem. Rev., 43, 219 (1948).

18. Faucher, J.A. and Koleske, J.V., Phys. and Chem. of Glasses, 7, 202 (1966).

19. Zachariasen, W.H., J. Amer. Chem. Soc., 58, 3841 (1932).

20. Jones, G.O. and Simon, F., Endeavour, 8, 175 (1949).

21. Magill, J.H. and Ubbelohde, A.R. Trans. Faraday,Soc., 54, 1811 (1958)

22. Plazek, D.J. and Magill, J.H., J. Chem. Phys., 45, 3038 (1966).

23. Cohen, M.H. and Turnbull, D., J. Chem. Phys., 29, 3841 (1958).
" " ibid 31, 1164 (1959).
" " ibid 34, 120 (1961).

CHAPTER 5

THE SOURCE, SYNTHESIS AND PURIFICATION OF MATERIALS

The sample of pyrene used was supplied by Rütgerswerk-Abtiengesellschaft, and was purified by chromatography using a silica gel column (Hopkin and Williams M.F.C.cat. no. 7555) and a mixture of redistilled benzene (3 vols) and redistilled petroleum spirit (2 vols, boiling range 66° - 74°C) as an eluent[1].

For all purification procedures, the technique of thin-layer chromatography was employed as a check for purity. In cases involving bulk chromatography the technique was particularly useful as a guide to the efficiency of the column. The thin-layer plates were prepared on clean microscope slides (8 cm.x 1 cm) using Kieselgel HF 254 Nach Stahl manufactured by E. Merck Ag. Darmstadt and supplied by Anderman & Co. Ltd. Different eluents were used as required, though iodine was employed throughout as an indicator[2].

The Allenes

Before describing the syntheses of the allenes studied in this present work, the following paragraphs may serve to provide a background to allenes in general.

Until quite recently (c.a. 1957) the allene or propane 1:2 diene $CH_2=C=CH_2$ structure was regarded by organic chemists, more upon the basis of intuition than experimental fact, as being intrinsically unstable. During the past decade however, an

increasing amount of interest has been directed towards the chemistry of allene and its homologues, and in many cases it has been shown that hydrocarbon allenes are more stable than their acetylene isomers; in fact tetrasubstituted aliphatic and aromatic allenes are remarkably stable thermally, and tend to resist rearrangement or polymerisation unless specific catalysts are employed[3]. The unique stereochemistry of the allene system is well known, and will be described in detail with regard to the present work in chapter 6, but there are two reactions of allenes which were borne in mind during this present study.

1) Acetylene-Allene rearrangement

This is usually a base catalysed rearrangement of terminal acetylenes:

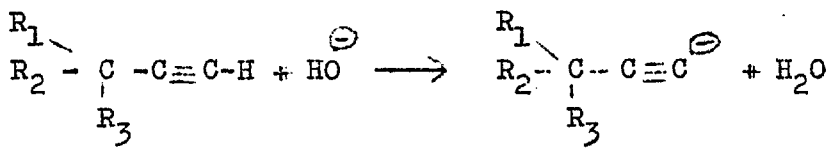

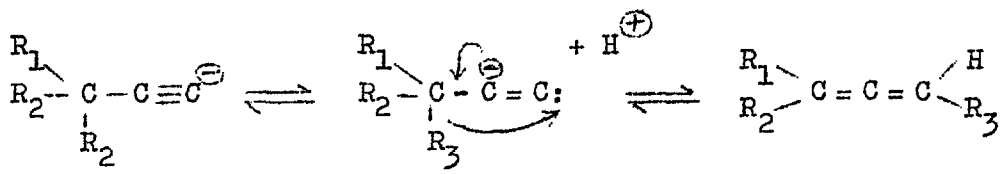

This is a reversible reaction, but usually the equilibrium lies on the acetylene side[3].

Although there is no precedence in the literature, the

---

* R_1, R_2 and R_3 = Aryl or alkyl.

following variation of the above reaction was considered as a possibility in the case of tetrasubstituted allenes; it would require neither acid nor base catalysis:

However, stability tests revealed the allenes studied in this present work to be sufficiently stable for study in the melt (See chapter 7, section 7.1).

2) Polymerisation.

There is no precedence in the literature for the uncatalysed polymerisation of tetrasubstituted allenes.

The electronic and vibrational spectra of allenes in general have hitherto defied detailed analysis, but the spectra of a number of aryl substituted allenes have been reported[5,6,7]. The spectra recorded for the first time in the present work have in fact proved quite useful by comparison with the data available in the literature, as diagnostic tests for structure. (See following section under individual syntheses).

The syntheses of tetraphenyl allene, triphenyl-α-naphthyl allene and triphenyl-4-biphenyl allene are described below.

Attempts were likewise made to synthesise tetra-α-naphthyl allene and tetra-4-biphenyl allene, but the yields obtained for the first stage were consistently poor (c.a. 6% for the variety of

different conditions tried, and it was decided that to produce the compounds in bulk would be impractible both on the score of cost and labour involved, and because of the high purity required in measurements of the physical properties.

The Synthesis of Tetraphenyl Allene

The method employed for the synthesis of tetraphenyl allene was originally derived from a study of the methods devised by Vörlander and Siebert (1906)[4] and Vörlander, Osterberg and Maye (1923)[8] for the synthesis of tetraphenyl allene; and Maitland and Mills (1936)[9] for the synthesis of di-α-naphthyl diphenyl allene. Various significant modifications introduced during this present work call for the detailed description cited below.

The two methods employed were basically four-stage syntheses differing only in their first stage; in both cases it was found preferable to carry the product of the first stage through without isolation.

Stage 1 :- 1,3,3 Triphenyl propan-3-ol-1-one.

Method A.

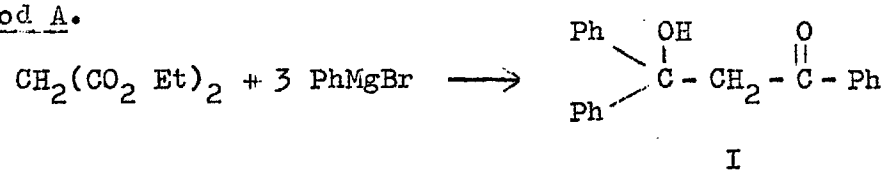

I

A solution of phenyl magnesium bromide was prepared in the usual way, by the dropwise addition of bromobenzene (78.6 ml, 118 g) dissolved in anhydrous ether (470 ml) to dry magnesium turnings(30g).

The reaction was initiated by the addition of a small quantity of iodine, and as far as possible oxygen was excluded from the reaction vessel by the passage of dry oxygen-free (White spot) nitrogen*.

The solution containing phenyl magnesium bromide was transferred to a dropping funnel by means of a syphon operated by the gas pressure provided by the cylinder of oxygen free nitrogen, and added slowly, with mechanical stirring, to diethyl malonate (30 g) dissolved in anhydrous ether (100 ml) and anhydrous benzene (100 ml) whilst maintaining the temperature of the reaction mixture between 0^{o} and 5^{o}C. The reaction mixture was allowed to warm to room temperature and left to stand overnight.

The reaction mixture was cooled to 0^{o}C and the excess Grignard reagent and the magnesium complex of 1.3.3 Triphenyl propan-3-ol-1-one were decomposed in the first instance by the addition of ice-cold saturated ammonium chloride solution. It was found later that, in this case, the decomposition could be effected more readily using cold dilute sulphuric acid (c.a. N). The resulting solution contained the 1.3.3 Triphenyl propan-3-ol-1-one (I).

---

* To ensure the absence of oxygen, the nitrogen was passed through a silver salt oxygen absorbing mixture before drying. See reference (11) for the composition of this mixture.

Method B

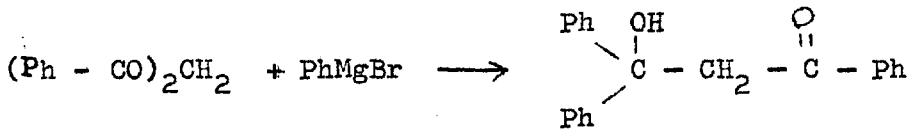

I

A solution of phenyl magnesium bromide was prepared as in Method A using bromo-benzene (41.9 ml; 63 g) dissolved in ether (240 ml) and magnesium turnings (15 g). The solution was syphoned into a clean vessel to separate unreacted magnesium, and then cooled to $0^{\circ}C$. To the cooled Grignard reagent dibenzoylmethane (41.7g) dissolved in benzene (50 ml) and ether (50 ml) was added dropwise. The mixture was allowed to warm to room temperature and was left to stand overnight. The excess Grignard reagent etc. was decomposed as above in method A. The theoretical yield of 1.3.3 triphenyl propan-3-ol-1-one obtaining to the quantities quoted is the same for both methods A and B, and in the following stages both resulting solutions are treated in the same way.*

Stage 2:- 1,3,3 Triphenyl Propan-2-ene-1-one

I II

---

* Method B was tried because there happened to be a stock of dibenzoyl methane available.

To the organic solution containing compound I, which had been separated from the aqueous acid layer, was added concentrated hydrochloric acid (250 ml) and water (250 ml). The mixture was warmed to allow the benzene/ether solvent to distil off; the remaining gum being boiled with the acid under reflux for 5 hrs. On cooling, the organic matter was extracted with ether, and the organic layer washed repeatedly first with saturated sodium bicarbonate solution and then with water. The bulk of the solvent was removed by distillation, and a little water added. The mixture was steam distilled continuously for 8 hours, removing the remaining solvent, unreacted bromobenzene, and diphenyl produced as a result of the coupling of some of the phenyl magnesium bromide. On cooling, the material was extracted with ether and the resulting solution dried over anhydrous sodium sulphate after which the solvent was distilled off leaving a brown gum which failed to crystallise on cooling. The gum was further cooled in an ice/salt freezing mixture, and by triturating with a little methanol a slurry of yellow crystals was produced. The crude product was recrystallised from ethanol giving pale greenish yellow crystals of the ketone (II). Melting point 90-91°C. The infra-red spectrum of the compound (in a nujol mull between sodium chloride plates) using a Cambridge S.P.200 spectrophotometer, featured a strong band at 1680 cm^{-1} corresponding to the conjugated carbonyl group, and a strong band

at 1603 cm^{-1} characteristic of mono-substituted phenyl groups.

Yield from Method A: 26g - 30g, 48% - 55%

with respect to diethyl malonate.

Yield from Method B: 23g - 25g, 42% - 46%

with respect to dibenzoyl methane.

The overall yields obtained by the methods described above are rather better than those obtained by earlier workers. This is probably due to the fact that no attempt was made in the present work to isolate the intermediate ketol (I). This compound loses water quite readily to give the ketone (II), and if isolation of ketol (I) were attempted any of the ketone (II) which may be formed during the process will be lost.

Stage 3:- Tetraphenyl Allyl Alcohol.

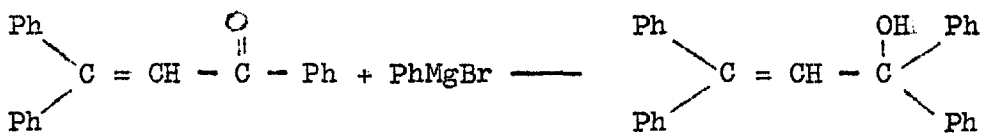

II III

A solution of phenyl magnesium bromide was prepared using bromobenzene (42 ml: 63 g) dissolved in ether (200 ml), and magnesium turnings (15 g). The solution was diluted with benzene (200 ml), decanted from unreacted magnesium, and cooled to below $0^{\circ}C$ in an ice/salt bath. To the cold Grignard reagent a solution of the ketone (II) (28.4 g) in benzene (180 ml) was added gradually over one hour, with mechanical stirring. The

temperature of the reaction mixture was allowed to rise to room temperature, and the mixture left overnight. The operations performed during this stage were conducted, as far as possible, in an oxygen free atmosphere (see page 144). The excess Grignard reagent etc. was decomposed by pouring the solution on to a mixture of ammonium chloride and ice, and the resulting organic layer was separated and dried over anhydrous sodium sulphate. The dry solution was distilled to a volume of about 100 ml., and upon cooling anhydrous ether was added (200 ml). The solution was left in a refrigerator over night when colourless crystals of the tetraphenyl allyl alcohol were formed. The crude material was recrystallised from benzene. Melting point 138-139°C . The infra-red spectrum of the compound, (in a nujol mull between sodium chloride plates), featured a sharp band at 3580 cm^{-1}, attributable to a free hydroxyl group, and a strong band at 1603 cm^{-1} characteristic of the mono-substituted phenyl groups.

Yield: 21g - 22.5 g, 59% - 62% theoretical yield with respect to ketone (II).

It was found that the yield of the allyl alcohol did not vary greatly with the quantity of Grignard reagent used provided that the latter was present in at least one mole excess. The quantities cited above seemed to give optimum results.

Stage 4 :- Tetraphenyl Allene

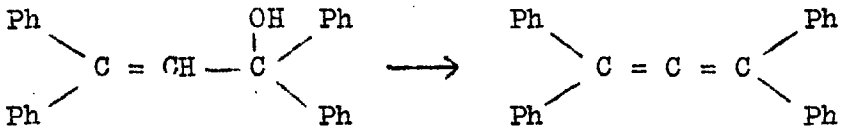

III IV

Tetraphenyl Allyl alcohol (III) (18 g) was dissolved in ethyl acetate (60 ml), and a trace of toluene-p-sulphonic acid was added as proton donating catalyst. The mixture was boiled under reflux for about 45 mins, during which time a purple colouration was observed at the interface between the boiling liquid and the glass vessel. The bulk of the liquid was reduced by distillation to about 40 ml and the solution allowed to stand over night. The tetraphenyl allene crystallised as colourless needles which were filtered off and recrystallised from ethyl acetate. Melting point* 165°-166°C (Lit. melting point 164° (4) and 166°C (8)).

Apart from the bands at 3100 cm^{-1} and 1603 cm^{-1} attributable to the aromatic C-H stretch and mono-substituted phenyl groups respectively, the infra-red spectrum (chloroform solution) displayed three fairly sharp bands of medium intensity at 1955 cm^{-1}, 1925 cm^{-1} and 1880 cm^{-1}, and two rather weaker bands at 1805 cm^{-1} and 1750 cm^{-1} . These five bands were also

---

* It was found advisable to warm the crystals in a water bath under vacuum (ca. 10^{-2} mm.Hg) prior to taking the melting point, since the crystals displayed a strong tendency to retain the solvent.

characteristic of the spectra of triphenyl-α-naphthyl allene, and triphenyl - 4 -biphenyl allene which syntheses are described later. The band at 1955 cm^{-1} may be identified with the band reported as characteristic of the allene system (asymmetric stretch) but it seems unlikely that all the remaining bands should be simply aromatic overtones since they are not all present in the spectrum of the allyl alcohol (III)[5]. The ultra-violet spectrum (using Unicam S.P.800) ir methanol shows a strong band at 266 mμ , $\epsilon = 34,000$.

Yield 13g - 14g, 78% - 80% theoretical yield with respect to the allyl alcohol (III).

The final purification of the tetraphenyl allene was achieved by chromatography. After trials with a variety of solvent systems, the following procedure was selected as the most satisfactory. The allene (12 g) was dissolved in a minimum amount of a mixture containing redistilled benzene (3 vols) and redistilled petroleum spirit (1 vol), (boiling range 66°-74°C) and eluted through a column containing silica gel (Hopkin and Williams, M.F.C. cat. No. 7555; 200 g) with a mixture of the pure benzene (2 vols) and pure petrol (1 vol). The progress of the elution was monitored by means of thin layer chromatography (see p. 140). The involatile nature of the compound prevented the use of high vacuum sublimation as a technique for purification. Finally, the purified material was warmed to about 100°C under

vacuum (ca. 10^{-2} mm.Hg) to remove the last traces of solvent.

The Synthesis of Triphenyl-α-naphthyl Allene.

Formally this is a four stage synthesis, but in the present research the ketone (II) i.e. 1,3,3 triphenyl propan-2-ene-1-one served as an intermediate.

Stage 1 - 1,3,3-Triphenyl-1-α-Naphthyl propan-2-ene-1-ol.

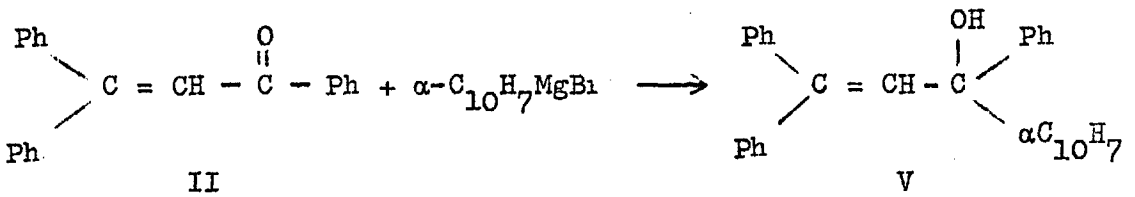

II V

A solution of α-Naphthyl magnesium bromide was produced from α-naphthyl bromide (154 g; 102 ml) dissolved in anhydrous ether (490 ml) and magnesium turnings (20 g). The Grignard reagent was decanted from the unreacted magnesium and cooled in an ice/salt freezing mixture. The ketone (II) (70g) was dissolved in dry benzene (500 ml) and added dropwise to the cooled Grignard reagent with mechanical stirring. The addition of the ketone was controlled to maintain the temperature of the reaction mixture between 0° and 5°C. The mixture was allowed to warm to room temperature and was left to stand overnight.

The excess Grignard reagent and the magnesium complex of the alcohol V were decomposed by pouring on to a mixture of ammonium chloride and ice; the resulting organic layer was dried over anhydrous sodium sulphate. The dry solution was

evaporated to low bulk (ca. 80 ml) and diluted with anhydrous ether (150 ml). The solution was left overnight and a crop of colourless crystals were filtered off. The product obtained was impure. The thin layer chromatographs revealed two compounds one of which, using a 1:1 benzene/petrol eluent, scarcely moved from the base line, whilst the other had an R_f value similar to tetraphenyl allene. The possibility of contamination with 1:1 dinaphthyl, produced as a result of the coupling of two moles of Grignard reagent, was dismissed by comparing the R_f values of the products with the R_f value of a characterised sample of 1:1 dinaphtyyl. It was tentatively supposed that the slow moving compound was the allyl alcohol V , and that even under the mild conditions of ammonium chloride/ice the allyl alcohol had to some extent decomposed to give the required allene. Thus it was decided to decompose the excess Grignard reagent etc. under stronger conditions (i.e. cold dilute sulphuric acid) in order to convert all the alcohol to the allene in situ. The alcohol (V) was therefore carried through to stage 2 without isolation.

Stage 2:- Triphenyl-α-naphthyl-allene.

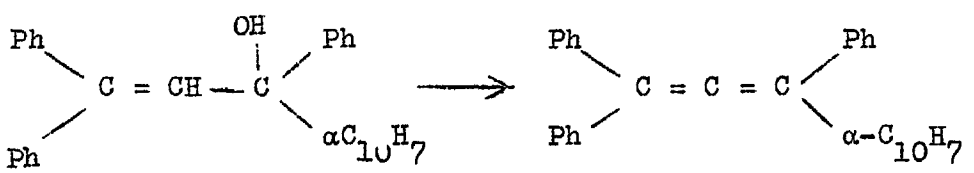

V VI

The solution obtained from stage 1 as a result of the addition of ketone (II) to the Grignard reagent α-naphthyl magnesium bromide

containing excess Grignard reagent and the magnesium complex of the alcohol V, was cooled to 0°C and decomposed with cold dilute sulphuric acid. The resulting organic layer was separated, dried over anhydrous sodium sulphate and reduced in bulk to about 60 ml. The solution was diluted with ether (150 ml.) and left overnight. The white crystals obtained were recrystallised from a mixture of benzene (1 Vol.) and petroleum spirit (1 vol). Melting point* 139°-140°C (192°).

Analysis: $C_{31}H_{22}$ requires C.94.3%; H. 5.62%

found C.94.19%; H. 5.69%

A mass spectrum confirmed that there was no compound present with a molecular weight greater than 394 which corresponds to $C_{31}H_{22}$; the infra-red spectrum was almost identical to that of tetraphenyl allene, showing the five characteristic bands (see p. 149), and the ultra-violet spectrum revealed two bands, the first at 266 mμ (ε = 29,000) in common with tetraphenyl allene, and the second at 284 mμ (ε = 20,000).

Yield 44g-48g, 45.3% - 49.4 % theoretical yield with respect to the ketone II.

The melting characteristics of this compound are rather unusual. When viewed on a Kofler block, under a microscope, the majority of the material melted sharply between 139° and 140°C leaving a few crystallites floating in the melt which finally

---

* See foot note, p. 149

disappeared at 192°C; on viewing through crossed nicols no evidence was found for the presence of liquid crystals. On heating a few milligrams of the material in a test-tube, the majority melted at 140°C giving a slightly milky melt which cleared at 192°C. At first it was suspected that this phenomenon was due to the presence of impurity despite the evidence supplied by the spectra and analysis; in any case the sensitivity of an infra-red spectrum to impurity will necessarily depend upon the nature of the impurity. However, thin layer chromatography (T.L.C.) using a variety of single and mixed solvents revealed the presence of only one compound, though attempts to effect separation using gas/liquid chromatography, which can produce an even better resolution, failed since the compound proved too involatile: to have raised the temperature of the column above 300°C would have probably decomposed the material, giving confusing results.

Since techniques involving solutions of the material failed to reveal the presence of impurity, efforts were directed towards a study of the melt itself.

The material (1g) was placed in a glass tube, sealed at one end, containing a fine sintered disc (see Fig. 5.1). The tube was immersed in an oil bath and heated to 150°C, when the melt (slightly milky) was sucked through the filter by means of a vacuum pump attached to a side arm situated beneath the disc. The filtrate was quite clear and on cooling congealed to a

FIGURE 5.1

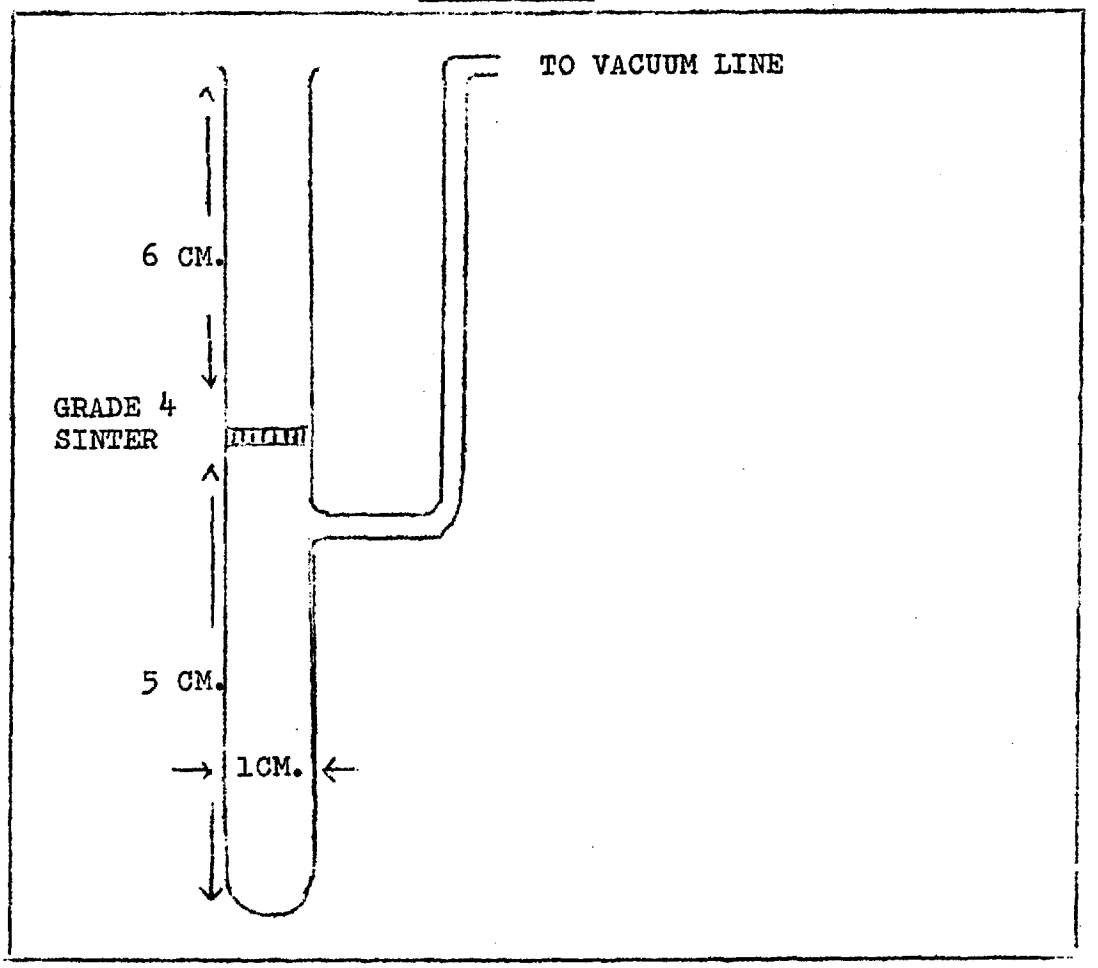

glass*. The tube was broken open and the filtrate dissolved in and recrystallised from benzene. The recrystallised material displayed the same anomalies in melting as before. Since there was insufficient material retained on the sinter to permit analysis

---

* The glass forming properties of this compound are discussed in chapters 9 and 10.

the experiment was repeated on a 4g scale using a larger version of the apparatus illustrated in Fig. 5.1. This time, about 7 mg. of material remained on the sinter, and this was dissolved in benzene, together with a little unmelted material retained on the wall of the tube, and analysed using T.L.C. Again the presence of one compound only was revealed, and that the same as the original. The infra-red spectrum (in chloroform) was identical with that obtained before.

The evidence would seem to suggest that the melting anomaly observed is due to some form of polymorphism, there being two crystalline forms. An explanation of this behaviour may rest in the geometry of the molecule, but this approach will be discussed in the following chapter. Working from the assumption that the unusual behaviour is due to polymorphism, attempts were made to isolate one or other of the forms by varying the solvents and conditions employed for recrystallisation. Out of about 25 different solvents and solvent mixtures only three proved satisfactory for the purpose of recrystallisation:- these were pure benzene, benzene/petroleum spirit, and chloroform/petroleum spirit. However, the material recovered from all the systems tried was tested, and all displayed the same anomaly in melting. Finally attention was again focussed on the melt. A sample was heated to 150°C and maintained at that temperature for several hours in the hope that all the material would convert to the high

melting form. This was repeated at 165°C and at 190°C, but the experiment was abandoned when, after being left overnight, the material showed signs of decomposition. On no occasion did the melt crystallise.

Attempts to maintain the solid at temperatures just below the primary melting point were not successful in converting all the material to the high melting form:- no change in behaviour was detected.

Since it was not possible to detect the presence of impurity, the evidence supplied by synthesis, analysis and spectra confirming the material as triphenyl-α-naphthyl allene was accepted.

The Synthesis of Triphenyl-4-biphenyl Allene.

As before this is formally a four stage synthesis, but the ketone (II) i.e. 1,3,3,triphenyl propan-2-ene-1-one served as an intermediate.

Stage 1 - 1,3,3,triphenyl-1-(4-biphenyl) propan-2-ene-1-ol.

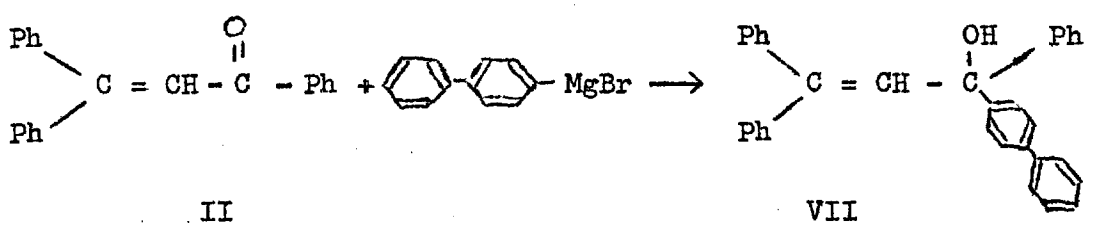

II VII

This synthesis involved the production of the Grignard reagent 4-biphenyl magnesium bromide. Diethyl ether was unsuitable for this preparation since the Grignard reagent proved insoluble in

this solvent and precipitated on the magnesium turnings, halting the reaction shortly after its initiation. The addition of anhydrous benzene to the ether failed to increase the solubility significantly. A number of other ethers were tried including di-n-butyl ether and anisole, but the most successful solvent was tetrahydrofuran (T.H.F.). Unfortunately this solvent displays a marked tendency to oxidise, yielding explosive peroxides, and the commercial product is supplied containing a suitable stabilising agent (e.g. hydroquinone); further, the solvent is very hygroscopic. The following procedure was adopted to remove the stabiliser and to produce an anhydrous sample.

The commercial T.H.F. (ca. 1.5 litres) was boiled under reflux for about 6 hrs. with potassium hydroxide pellets (50g). On cooling, the solvent was decanted from the pellets (now slightly yellow in colour) and transferred to a Winchester. Sodium wire was extruded into the Winchester of solvent which was allowed to stand overnight. The T.H.F. was transferred to a 3 litre round bottomed flask and Lithium Aluminium Hydride (L.A.H.) (c.a. 3g) was added. The mixture was boiled under reflux in a heating mantle for about 6 hrs. Samples were taken from time to time and tested by the addition of a few drops of water:- vigourous effervescence confirmed the presence of excess L.A.H. Since L.A.H. is fairly soluble in T.H.F. the solvent

was cautiously distilled into a dry receiver connected to a drying tower containing anhydrous calcium chloride*. The fraction boiling between 65° and 66°C was collected and transferred to a dry Winchester into which fresh sodium wire was then extruded. Although the Winchester was sealed with a plastic screw cap, it was deemed advisable to repeat the treatment with L.A.H. if the solvent were kept for longer than two weeks before use.

4-bromodiphenyl (23.3g), previously dried under vacuum, was dissolved in dry T.H.F. (160 ml), and added dropwise to magnesium turnings (3g). The reaction was initiated by the addition of a small trace of iodine and the reaction proceeded quite vigourously with gentle warming. The resulting solution of 4-diphenyl magnesium bromide was decanted from the unreacted magnesium turnings through a wad of glass wool into a fresh flask. The ketone II (14.2 g), dissolved in benzene (100 ml) was added dropwise with mechanical stirring, the temperature of the reaction mixture being maintained between 0°and 5°C. As far as possible all operations were conducted in an atmosphere of oxygen free nitrogen**. When all the ketone had been added, the mixture was allowed to warm to room temperature and was left

---

* The solvent was transferred to a smaller vessel when the liquid level in the flask fell below 2" from the rim of the heating mantle since L.A.H. can explode if overheated:- the present author was informed from a reliable source that negligence in this respect once resulted in an explosion producing a "fire-ball" which heavily damaged a laboratory and its occupants.

** (i.e. see page 144)

overnight. The excess Grignard Reagent was decomposed by pouring on to a mixture of ice and solid ammonium chloride. The resulting organic layer was separated and the aqueous layer extracted twice with benzene (100 ml); the extracts were added to the principal layer which was then dried over anhydrous sodium sulphate and evaporated to about 70 ml. The addition of ether failed to precipitate the alcohol so the mixture was cautiously evaporated to dryness under vacuum (water pump). The resulting oil was triturated with a mixture of methanol and ether when colourless crystals of the alcohol VII were produced. The crude product (10 g) was recrystallised twice from benzene. Melting point 127°-128°C. The infra-red spectrum of the compound, (in a nujol mull between sodium chloride plates) featured a sharp band at 3580 cm^{-1} attributable to a free O-H stretch, and a strong band at 1603 cm^{-1} characteristic of mono-substituted phenyl groups.

Yield: 8 g; 36.6 % theoretical yield

with respect to ketone II.

Stage 2 - Triphenyl-4-biphenyl allene.

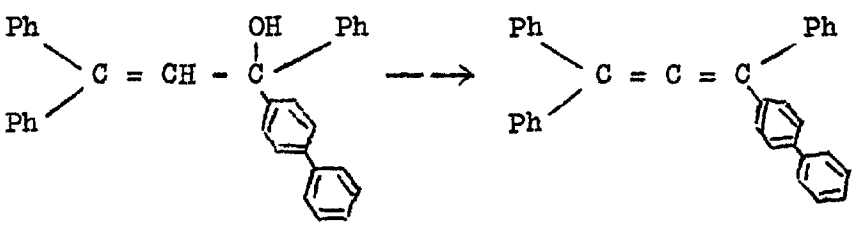

VII VIII

The alcohol VII (8 g) was dissolved in ethyl acetate (200 ml) and a trace of toluene-p-sulphonic acid was added. Immediately a transitory blue colour was produced. The solution was boiled under reflux for one hour and allowed to cool. No crystals formed but on evaporation to about 30 ml the solution assumed an intense blue colour which disappeared on dilution*. The solution was diluted with benzene (100 ml) and washed several times with dilute potassium carbonate solution and then with water to remove the acid. The solution was dried over anhydrous sodium sulphate and evaporated to dryness under vacuum. (At no stage was any blue colour observed). The pale yellow gum produced failed to crystallise and was dissolved in benzene (2 vols) and petroleum spirit (1 Vol) boiling range 66°-74°C, and chromatographed on a silica gel column. The eluted material, upon evaporation, yielded a colourless gum which, after drying under vacuum, congealed to a glass.

---

* It was thought that this colouration might be due to the stabilised carbonium ion 'X' resulting from the protonation and loss of the hydroxyl group. Perhaps under certain conditions the following equilibrium exists:

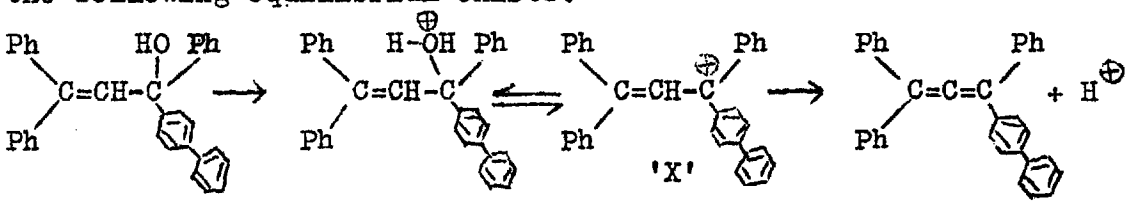

A similar explanation may serve for the transitory purple colour produced in the synthesis of tetraphenyl allene. See p. and reference (9).

T.L.C. revealed the presence of only one compound. The glass failed to crystallise despite trituration with a variety of solvents. However, after leaving for several months with occasional warming to 100°C, crystal nuclei appeared, after which trituration with petroleum spirit (boiling range 60°-80°C) accelerated total crystallisation of the bulk, giving colourless crystals of triphenyl-4-biphenyl allene. Melting point 105°-106°C.

Analysis: $C_{33}H_{24}$ requires C. 94.25% H 5.75%

found C. 94.08% H 5.81%

The infra-red spectrum was almost identical to that of tetraphenyl allene, showing the five characteristic bands (see p.149) and the ultra-violet spectrum revealed two bands, the first at 257 mμ (ϵ = 29,000) and the second at 280 mμ (ϵ = 27,000) with a trough at 267 mμ (ϵ = 26,000).

Yield 5.5 g; 72% theoretical yield with respect to alcohol VII.

REFERENCES

1. Linstead, R.P., Elvidge, J.A., and Walley, M., "Modern Techniques of Organic Chemistry", Butterworths (1955).
2. Elvidge, J.A. and Sammes, P.G., "A Course in Modern Techniques of Organic Chemistry". Butterworths (1966).
3. Taylor, D.R., Chem. Rev., 67, 317 (1967).
4. Vörlander, D. and Siebert, C., Chem. Ber. 39, 1024 (1906).
5. Jacobs, T.L., Dankner, D. and Singer, S., Tetrahedron, 20, 2177 (1964).
6. Jacobs, T.L. and Fenton, D.M., J. Org. Chem., 30, 1808 (1965).
7. Cross, R.D. "Introduction to Practical Infra-Red Spectroscopy", 2nd edition Butterworths (1964).
8. Vörlander, D., Osterberg, J. and Meye, O., Chem. Ber. 56, 1136 (1923).
9. Maitland, P. and Mills, W.H., J. Chem. Soc., 987 (1936).

CHAPTER 6.

THE STEREOCHEMISTRY, CONFORMATION AND DIPOLE MOMENTS OF TETRAPHENYL ALLENE, TRIPHENYL-α-NAPHTHYL ALLENE, AND TRIPHENYL-4-BIPHENYL ALLENE

6.1 The Molecular Structure and Stereochemistry of Allenes[1,2]

From the view point of molecular orbital theory, allenes may be regarded as a cross between olefins and acetylenes.

The outer electronic shell of the carbon atom (L shell) contains four electrons. The shell is divided into four atomic orbitals, one spherically symmetrical 2S orbital, and three equivalent dumb-bell shaped 2P orbitals of slightly higher energy, mutually disposed at right-angles along the X, Y and Z axes. In the ground state, two of the four available electrons, with opposing spins, fill the 2S orbital, whilst the remaining two electrons, with parallel spins, occupy the $2P_x$ and $2P_y$ orbitals respectively in accordance with the Pauli exclusion principal, leaving the $2P_z$ orbital vacant (See Fig. 6.1a).

The allene skeleton consists of three carbon atoms. The outer two carbon atoms are olefinic in nature. The 2S, $2P_x$, and $2P_y$ orbitals are hybridised to give three equivalent coplanar orbitals of relatively low energy pointing at angles of 120° in the XY plane, whilst the undisturbed $2P_z$ orbital is disposed at right-angles along the Z axis. (See Fig. 6.1b). The electrons are redisposed so that the three equivalent hybrid orbitals and

FIGURE 6.1 a. AND b.

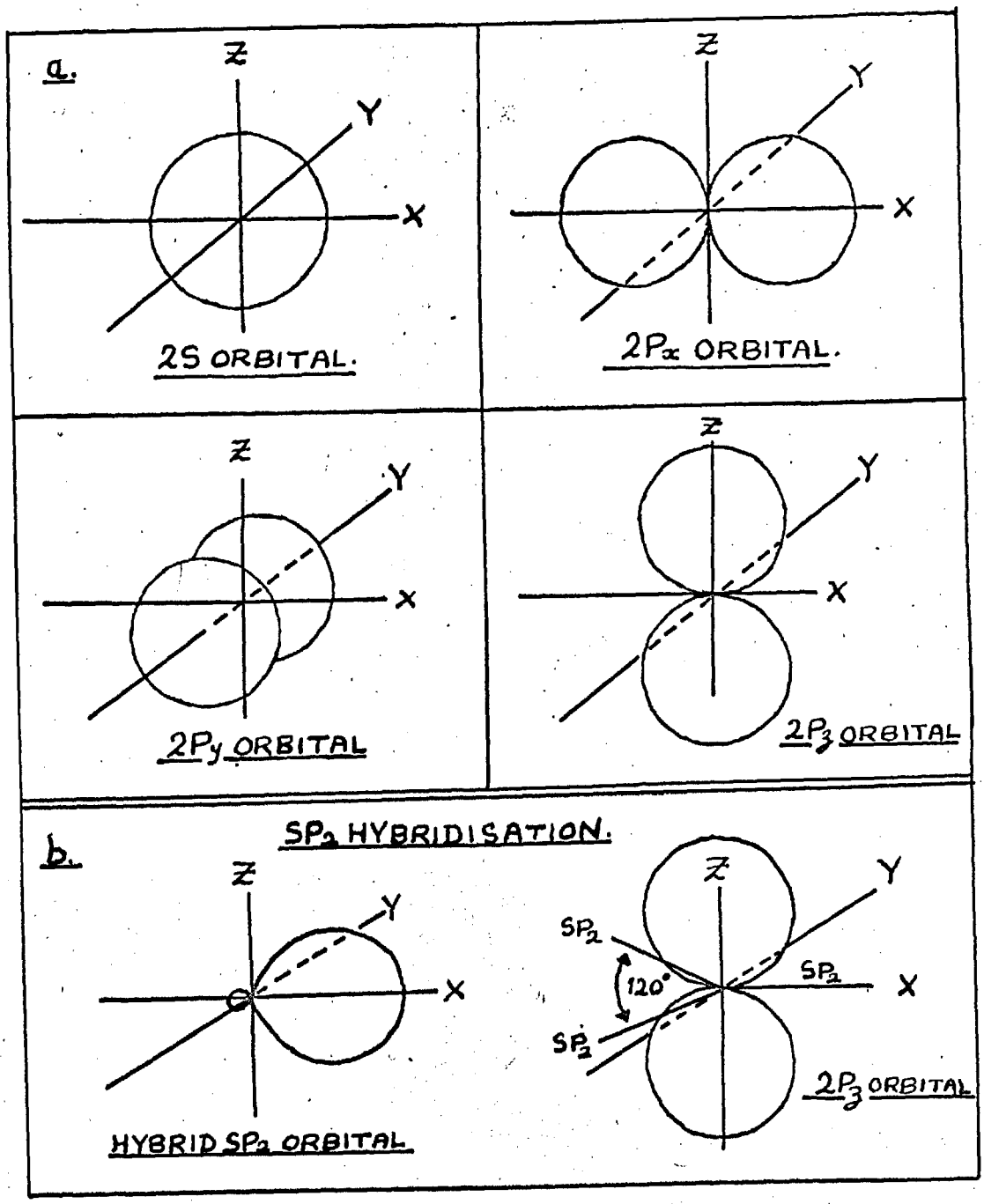

FIGURE 6.1. c, d, e, & f.

c.

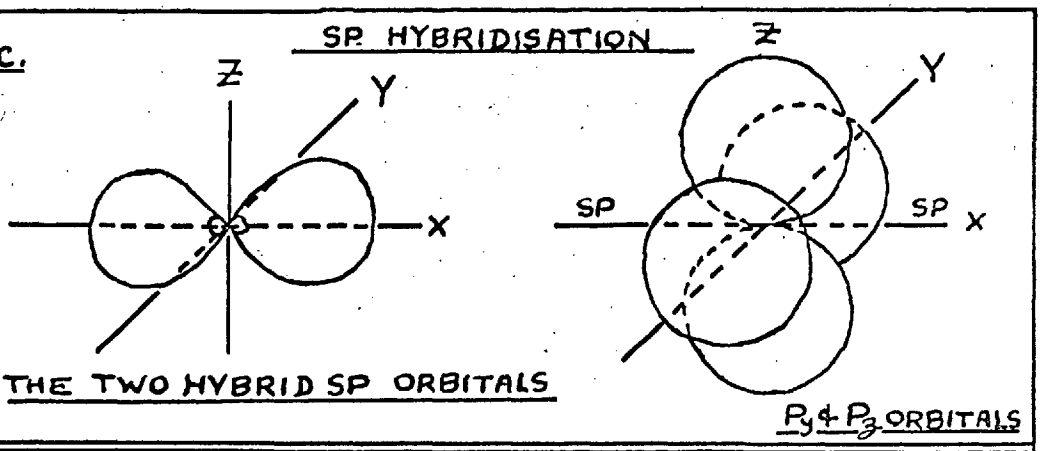

THE TWO HYBRID SP ORBITALS

P_y & P_z ORBITALS

d.

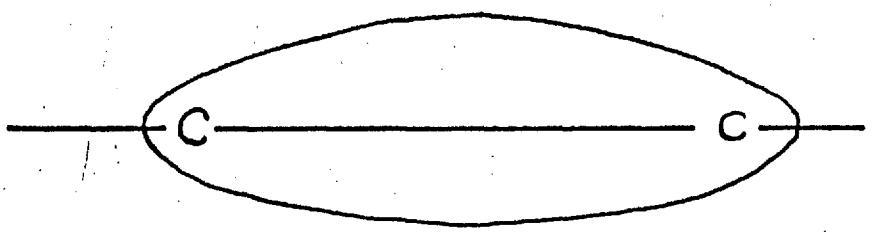

MOLECULAR ORBITAL OF A σ BOND (BONDING)

e.

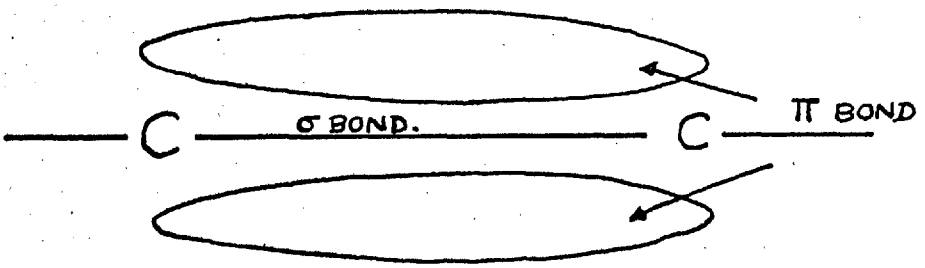

MOLECULAR ORBITAL OF A π BOND. (BONDING).

f.

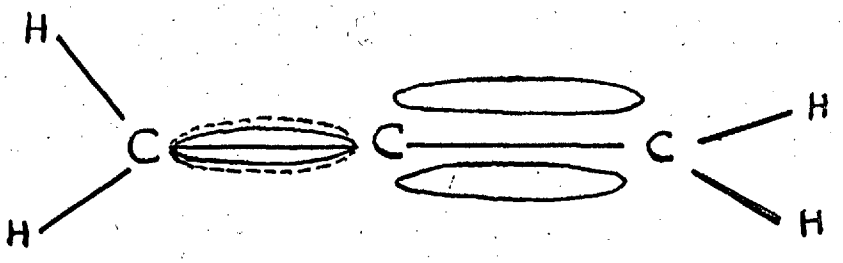

ALLENE

the undisturbed P orbital are each occupied by one electron. Hybridisation of this type is termed SP_2 hybridisation. The central carbon atom is acetylenic. The 2S and $2P_x$ orbitals are hybridised to give two equivalent collinear orbitals of relatively low energy, which lie along the X axis, whilst the undisturbed $2P_y$ and $2P_z$ orbitals are mutually disposed at right angles along the Y and Z axes respectively (See Fig. 6.1c). Again the electrons are redisposed so that each orbital is occupied by one electron. This type of hybridisation is termed SP hybridisation. If the overlap of hybrid SP_2 and/or SP atomic orbitals of two atoms results in a molecular orbital of relatively low energy, then a σ bond is formed. The molecular orbital is elliptical in shape and contains two electrons of opposing spins*. The foci of the ellipse are marked by the nuclei of the two contributing atoms. (See Fig. 6.1d). Overlap of the pure P orbitals result in a π molecular orbital*, in which the electron density is concentrated above and below the plane of the σ bond (see Fig. 6.1e). A pure σ bond may be rotated about an axis through the centres of the two atomic nuclei, giving rise to configurational isomers (i.e. the paraffins), but the presence of π bonds prohibits rotation in this sense, and accounts for the rigidity of the

---

* In fact two σ (or π) orbitals are formed, viz. a bonding orbital and an antibonding orbital. In the present context the antibonding orbitals are vacant of electrons and need not be considered.

ethylene "double" bond and the acetylene "triple" bond.

In the case of allenes, the P orbital of one of the outer carbon atoms overlaps with the P_y orbital of the central carbon atom, whilst the P orbital of the other outer carbon atom overlaps with the P_z orbital of the central carbon atom. This means that the planes of the two π bonds so formed are perpendicular, which in turn means that the planes of each pair of substituents are perpendicular. Fig. 6.1 f. illustrates the situation with regard to allene itself (C_3H_4). It follows that, since the planes of the two π bonds are perpendicular, there is no possibility of conjugation through the allene skeleton.

The fact that the planes of the two outer olefinic carbon atoms are perpendicular gives rise to unique stereochemistry. In materials containing an optically active centre, the two enantiomorphs are mirror images which cannot be superimposed. In all other physical and chemical respects they are identical, although the racemate (i.e. the equimolar mixture of both forms) may display very different physical properties (e.g. the melting points of the D and L tartaric acids are both 170°C; the melting point of the racemate, which crystallises from water as a hemihydrate, is 206°C). In other words the manner in which molecules in the solid racemate are packed may differ considerably from the packing arrangement in the solid enantiomorphs. In the realms of biochemistry, particularly enzymology, the presence of

FIGURE 6.2.

a.

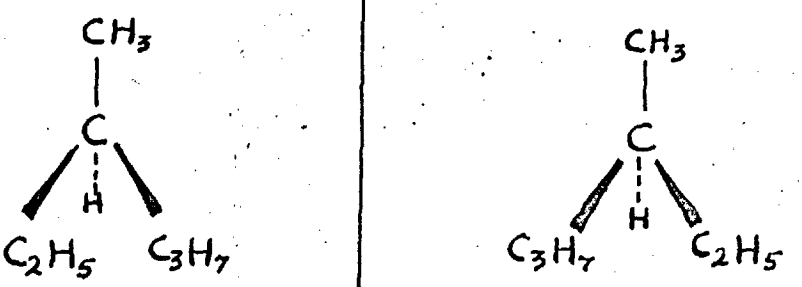

3-METHYL HEXANE AND ITS MIRROR IMAGE.

b.

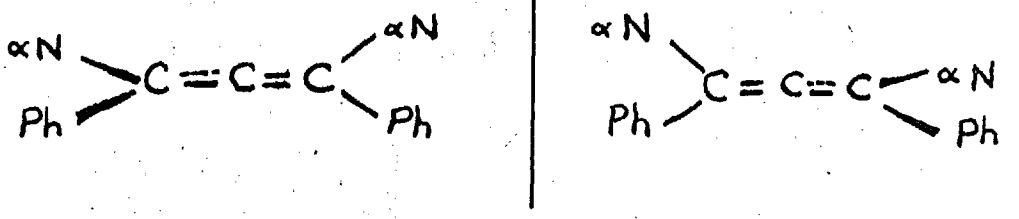

SYM-DIPHENYL-DI-α-NAPHTHYL ALLENE AND ITS MIRROR IMAGE.

PLATE 6.

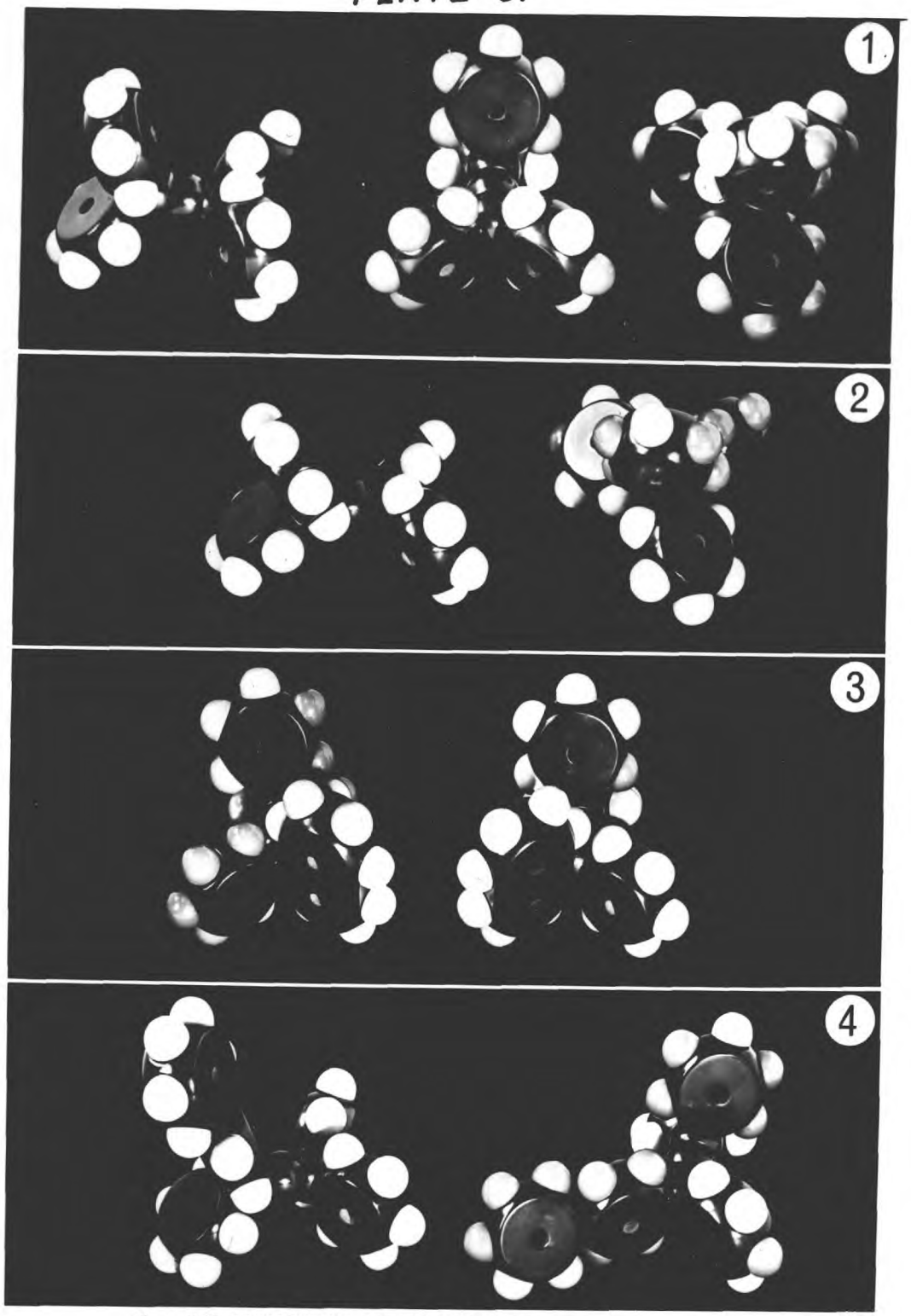

1. THE TETRAPHENYL ALLENE MOLECULE

2. THE TETRAPHENYL ALLENE MOLECULE WITH THE SUBSTITUENT PHENYL GROUPS TWISTED 30° OUT OF PLANE

3. A MOLECULE OF TRIPHENYL- α-NAPHTHYL ALLENE AND ITS MIRROR IMAGE

4. THE TRIPHENYL-4-BIPHENYL ALLENE MOLECULE

one or more optically active centres in a particular molecule is of paramount importance.

Apart from factors involving inhibited rotation arising from steric hinderance, the most simple examples of optical activity are to be found in compounds in which four different substituents are tetrahedrally disposed about a central carbon atom. An example of this is 3-methyl hexane. (see Fig. 6.2a). In allenes however, the substituents are not tetrahedrally disposed with respect to the central carbon atom, and it is only necessary for one pair of different substituents to be grouped at each end to result in a pair of enantiomorphs. This unique aspect of the allene structure was illustrated by Maitland and Mills in 1936[5], by the synthesis and isolation of the enantiomorphic forms of symmetrical diphenyl di-α-naphthyl allene (see Fig. 6.2b).

6.2 The Structure of Tetraphenyl Allene, Triphenyl-α-Naphthyl Allene Triphenyl-4-Biphenyl Allene.

6.2.1. The tetraphenyl allene molecule.

Tetraphenyl allene is optically inactive. Plate 6.1 represents three views of a scale model of the molecule*. In this picture, the angle between the planes of the two phenyl groups comprising each pair of substituents is about 120°. This orientation is the most favourable for molecular interlocking and cluster formation, but in this conformation there is no

---

* This model, and the other models illustrated in Plate 6, were assembled from 'Catalin' scale molecular models.

overlap of the π orbitals of each pair of phyenyl groups and those of the double bond to which they are attached.

Plate 6.2 represents the tetraphenyl allene molecule with the planes of the substituent phenyl groups twisted 30°. Although there is no possibility of conjugation through the allene skeleton, there is a possibility of some cross-conjugation between adjacent phenyl groups through the double bond to which they are both attached. To twist the groups through 30° would, according to the scale models, achieve the optimum balance between an increase in resonance energy accompanying some π orbital overlap, and steric repulsion. There is however, some indirect evidence to support the figure of 30°. Coates and Sutton (1942)[3] have estimated the angle through which the planes of the phenyl groups are twisted in 1:1 diphenyl ethylene ($\begin{matrix}Ph\\Ph\end{matrix}\!\!>\!C = CH_2$) to be 30°, from dipole moment data. Moriconi, O'Connor and Forbes (1960)[4] have arrived at a similar figure by similar means for benzophenone ($\begin{matrix}Ph\\Ph\end{matrix}\!\!>\!C = O$). Both these molecules are similar to tetraphenyl allene with regard to the conformation of their phenyl groups, and it is reasonable to suppose that the phenyl groups in tetraphenyl allene are twisted through the same angle i.e. 30°.

6.2.2. <u>The triphenyl-α-naphthyl molecule.</u>

Plate 6.3 represents a view of a scale model of the triphenyl-α-naphthyl allene molecule, and its mirror image.

The scale model of the molecule reveals that the α-naphthyl group and the adjacent phenyl group have less freedom of movement than the pair of phenyl groups at the further end of the molecule, and it is likely that their respective planes will remain at an angle of 120° as illustrated, ensuring the most favourable orientation for molecular interlocking. It will be seen from Plate 6.3 that the mirror images are not superimposable if the α-naphthyl group is unable to rotate. The presence of optical isomers must be considered as a possibility if the energy barrier to rotation is large compared with kT.

It was mentioned earlier in this chapter (page 170) that Maitland and Mills had succeeded in isolating the two enantiomorphs of symmetrical diphenyl di-α-naphthyl allene. If restricted rotation of the α-naphthyl group leads to an optically active centre then there should be eight pairs of enantiomorphs. However, the above authors obtained only one pair of enantiomorphs by means of a partially stereospecific synthesis. They did not attempt to resolve the racemic mixture. Having succeeded in obtaining the enantiomorphs associated with the asymmetry of the allene structure, it could be that each of these enantiomorphs is a mixture of racemates and pairs of diastereoisomers associated with the asymmetry arising from restricted rotation. This is of course pure conjecture based upon an examination of the scale molecular model.

There are a variety of compounds, notable amongst which are some biphenyl derivatives*, in which restricted rotation leads to a centre of asymmetry. In most cases the energy barrier to rotation is too low to permit resolution of the enantiomorphs, but occasionally the energy barrier is in the order of kT which would permit resolution at low temperatures, though on heating each enantiomorph would racemise. 6-nitrodiphenyl 2:2' dicarboxylic acid is a case in point[6]*. The sample of triphenyl-α-naphthyl allene studied in this present work was certainly optically inactive, since a solution of the compound failed to rotate the plane of polarised light when examined in a polarimeter. There was however no way of determining whether the sample was a racemate, short of an attempt at resolution. (This is very difficult in the case of pure hydrocarbons bearing no functional groups). Although the properties of a racemate may differ greatly from those of the pure enantiomorphs it seems unlikely that the unusual melting properties of this compound can be explained in terms of optical isomerism (see Chapter 5, page 153). Had the sample been optically active, it would have suggested that it was rich in one or other of the enantiomorphs. A situation of this type could possibly lead to anomalous melting provided that the thermal energy at the melting point is

---

* E.g. 6-nitrodiphenyl 2:2' dicarboxylic acid[6].

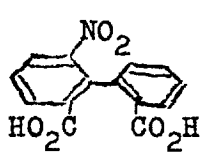

insufficient to overcome the energy barrier to rotation of the α-naphthyl group. However, the onset of rotation of this group could result in a change in the molecular packing arrangement, and become manifest in a solid-state transition. It will be seen in chapters 9 part II and chapter 10 section 10.3.1.2. that the nature of the molar-volume vs. temperature plot for the solid material was anomalous though difficulties arising from the experimental technique may be in part responsible.

6.2.3. The triphenyl-4-biphenyl allene molecule.

Triphenyl-4-biphenyl allene is optically inactive.

Plate 6.4 represents two views of a scale model of the molecule, the main features of which are similar to tetraphenyl allene which is discussed in section 6.2.1 of this chapter. The two phenyl rings constituting the biphenyl group prefer an almost coplanar configuration in order to achieve maximum overlap of their respective π orbitals.

The effect of the specific shape of each molecule upon its respective physical properties and propensity to glass-formation will be examined in the discussion section of this thesis.

6.3. The Dipole Moments of Hydrocarbons.

It has been mentioned in earlier chapters, that one of the principal reasons for selecting hydrocarbons as suitable subjects for an investigation into the influence of molecular shape upon physical properties, is that effects due to dipole interaction are minimised.

The dipole moment of a polar molecule can be represented as the product of a fractional electronic charge separation, and a distance between the charges (i.e. positive and negative centres). It is a vector quantity. The dipole moment of any symmetrical molecule will be zero even if it contains strongly polar bonds[7,8]. The value of a dipole moment depends upon the relative electron affinity (or electronegativity of the constituent atoms, the nature of the bonding (e.g. the type of hybridisation) and the molecular symmetry.

6.3.1. Dipole moments and hybridisation.

The more 'S' character a hybrid bond possesses, the more electronegative the carbon atom becomes[9]. For example:

a) SP_3 hybridised carbon.

In paraffin C-H bonds, the hydrogen atom is more electronegative than the carbon atom, and the bond is polarised in the following sense: $C^{\delta(+)} - H^{\delta(-)}$. An isolated C-H bond in methane has a dipole moment of 0.3D. This is not very significant when compared with aliphatic halides, and other polar molecules. Dipole moments of the aliphatic halides range from about 3D to 5D[10].

b) SP_2 hybridised carbon.

In olefins the carbon atom is more electronegative than the hydrogen atom, and the C-H bond is polarised in the following sense : $C^{\delta(-)} - H^{\delta(+)}$. An isolated C-H bond in ethylene has a dipole moment of 0.4D.

c) SP hybridised carbon.

In acetylene the C-H bond is strongly polarised and possesses considerable ionic character (viz. the existance of metallic acetylides). The dipole moment of an isolated acetylenic C-H bond must almost certainly be larger still:- surprisingly, a search in the literature for a value for an isolated bond was not fruitful.

6.3.2. Dipole moments of allene hydrocarbons:

Tetraphenyl allene is symmetrical, and like tetraphenyl ethylene, will have a dipole moment of zero. The question is whether the effect of replacing a phenyl group with an α-naphthyl group (as in triphenyl-α-naphthyl allene) or a biphenyl group (as in triphenyl-4-biphenyl allene) will increase the dipole moment significantly. Unfortunately, there are no analogous examples in the literature from which the effect of replacing a phenyl group by an α-naphthyl group, or by a biphenyl group, can be estimated. There are however, some examples in the literature which allow an order of magnitude to be estimated in this respect. In table 6.1 are listed the values of the dipole moments of tetra, tri, and unsymmetrical diphenyl ethylene. It may be seen that the increase in dipole moment accompanying the replacement of one or two phenyl groups by hydrogen in tetraphenyl ethylene is quite small.

TABLE 6.1

Compound	Dipole Moment (D)
Tetraphenyl Ethylene[11]	0
Triphenyl Ethylene[11]	0.63D (10°C); 0.51(70°C).
1:1 Diphenyl Ethylene[10]	0.38 D.

Further, Shorygin and Egorova (1957)[12], have shown that conjugated groups such as vinyl and phenyl have little effect in monosubstituted benzenes with regard to a change in dipole moments. The change in moment is rarely greater than 0.2D, which is hardly significant. In the light of this evidence, it would be reasonable to assume that any effects due to dipole interaction in the three allenes considered in the present work will be small, and will be dwarfed by the effects of molecular shape. It may also be noted in this connection that one of the properties most sensitive to molecular shape is viscosity. Many liquids comprising very polar molecules show little or no anomaly in their Eyring or Batschinski plots (see Chapter 2, section 2). Two extreme examples will serve to illustrate the point viz: 2-nitro-2-methyl propane 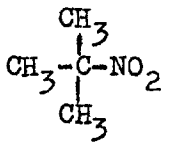 and 1,1,1 trichloro-ethane ($CH_3.CCl_3$)[13]. Compounds like glycerol and sugars require separate consideration since cumulative directional hydrogen bonding is involved.

REFERENCES

1. Cartmell, E. and Fowles, G.W.A., "Valency and Molecular Structure", Butterworths, London (1956).
2. Finar, I.L. "Organic Chemistry", Vol. I, 3rd. Ed., Longmans, London (1959).
3. Coates, G.E. and Sutton, L.E., J. Chem. Soc., 567 (1942).
4. Moriconi, E.J., O'Connor, W.F. and Forbes, W.F., J. Amer. Chem. Soc., 82, 5454 (1960).
5. Mailtand, P. and Mills, W.H., J. Chem. Soc., 987 (1936).
6. Barton, D.H.R., Private communication.
7. Debye, P., "Dipole Moment and Chemical Structure", Blackie and Son Ltd., London (1932).
8. Smith, J.W. "Electric Dipole Moments", Butterworths, London, (1955).
9. Walsh, A.D., Trans. Faraday Soc., 43, 60 (1947).
10. Sidgwick, D.V., Trans. Faraday Soc., 30, appendix (1934).
11. Smyth, C.P. and Dornte, R.W., J. Amer. Chem. Soc., 53, 1296 (1931).
12. Shorygin, P.P. and Egorova, Z.S., Doklady Akad. Nauk., S.S.S.R., 117 856 (1957).
13. Davies, D.B. and Matheson, A.J., Trans. Faraday Soc., 63, 596 (1967).

CHAPTER 7.

GENERAL EXPERIMENTAL TECHNIQUES

7.1 Preliminary Experiments.

It was mentioned in Chapter 5 that tetraphenyl allene has been synthesised before (1906), but, with the exception of its melting point, no physical properties had been studied. Triphenyl-α-naphthyl allene, and triphenyl-4-biphenyl allene are new compounds. The general properties of pyrene are well known and its stability in the solid and in the melt has been established[1,2]. In considering the design of the apparatus required for the determination of the viscosities and molar volumes of the molten allenes, it was necessary to verify adequate stability of the melts. In conducting stability tests the following three questions required consideration in view of the time required to complete the measurements described.

(1) Do the compounds polymerise or undergo chemical rearrangement in the melt?

(2) Do the compounds decompose and char, either in air or even in an inert atmosphere such as nitrogen? If such decomposition does occur in the melt, is the rate of decomposition sufficiently slow, compared with the time of experiment, to allow reproducible results to be obtained?

(3) In the light of an answer to questions one and two, over what temperature range are the melts stable?

The stability tests, and the results obtained for each compound are described below.

7.1.1. The stability of tetraphenyl allene (M. Pt. 165°-166°C)

Two samples of tetraphenyl allene, each of about 0.3 g., were selected from the bulk. One sample was placed in an open test tube. The other sample was placed in a test tube closed with a bung through which were passed two tubes allowing the passage of "white spot" nitrogen . The tube connected to the nitrogen cylinder was drawn out into a fine capillary (see Fig. 7.1). After the closed tube had been flushed out with nitrogen, the two test tubes were immersed in a thermostat oil bath* maintained at 175°C. When the samples had melted, the height of the capillary in the closed tube was adjusted to a level just below the surface of the melt (See Fig. 7.1). The flow of nitrogen was regulated to allow the gas to bubble gently through the melt. (c.a. thirty bubbles per minute). Neither sample showed any immediate discolouration upon melting, but after about four hours the sample contained in the open tube had assumed a light brown colouration. The sample maintained in the atmosphere of nitrogen was only very slightly discoloured. At this point small samples

---

* See this chapter section 7.3 for a description of the thermostat bath.

FIGURE 7.1

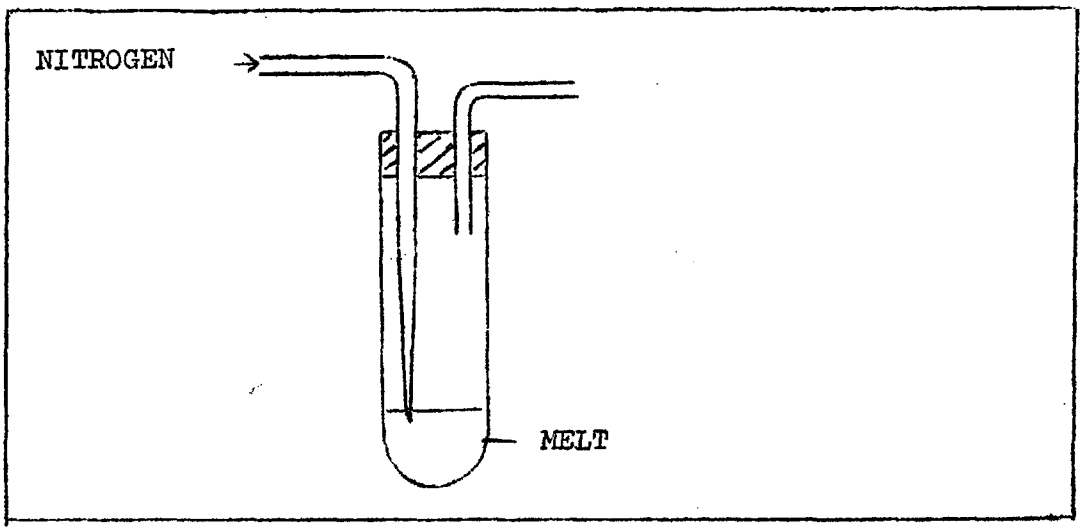

were removed from each tube, and the temperature of the bath was increased to 200°C. Both the small samples removed from the tubes at 175°C crystallised on cooling. The melting point of the sample maintained under nitrogen was sharp, and identical with that of the original material. The melting point of the sample removed from the open tube was less sharp and slightly depressed, melting over a range of three degrees from 162° to 165°C. As a further check, both samples were dissolved in benzene, and their R_f values compared with that of the original compound by means of thin-layer chromatography (see chapter 5 for details of this technique). The sample which had been maintained under nitrogen showed only one spot, the R_f value of which was identical with that of the original material. The sample taken from the open

tube showed two spots, viz. an intense spot corresponding to the original material, and a weak spot situated on the base line, corresponding to decomposition products. No charring was observed.

After being maintained at 200°C for about three hours, both tubes were removed from the thermostat bath. Again both samples crystallised on cooling. The sample from the open tube had darkened still further, but the sample maintained under nitrogen was still only slightly discoloured. The melting point of the sample maintained under nitrogen was slightly less sharp than before, melting between 164.5° and 166°C, but the melting point of the sample from the open tube was still further depressed, melting over a range of four degrees from 160-164°C. The R_f values of both samples were again compared with that of the original. The sample maintained under nitrogen showed only one spot, with an R_f value identical with that of the original. The sample taken from the open tube showed two spots viz. an intense spot corresponding to the original material, and a second spot, rather stronger than before, situated on the base line.

These results indicate that, in the absence of oxygen, molten tetraphenyl allene should be sufficiently stable over a temperature range of about 50°C, to permit fully reproducible results to be obtained. The conditions under which the stability tests were carried out were extreme. The experimental

proceedures adopted did not require the melt to be maintained at temperatures in the region of 200°C for as long as three hours. It will be seen in a later chapter that the viscosity and molar volume data obtained for tetraphenyl allene under varying temperature conditions were reproducible to within the limits of experimental error. It was, however, deemed advisable to use fresh or repurified material for each new set of independant measurements.

The melting point apparatus used in this work was a Kofler block. Although this is one of the more reliable varieties of melting point apparati, it is difficult to determine a melting point to better than $\pm$ 0.5°C. A few crystals of the material are placed between two thin-glass microscope slides. The sample is placed on an insulated heating block and observed through a low power microscope. As the melting point is approached the heating rate is regulated to about 1° per minute. Cooling the melt under these conditions resulted in some super-cooling ($\sim$10°) which prevented an estimate to be made of the depression of freezing point due to the presence of decomposition products. Once the sample had crystallised it could be remelted at the same temperature as before. Because of the inaccuracy inherent in the method, it has become customary for organic chemists to quote melting points over a range of temperature. As already stated, as a result of maintaining the melt under

nitrogen in a thermostat bath for seven hours, the melting range of the crystallised sample had increased by about 0.5°C. If it is assumed that this represents the depression of freezing point resulting from the presence of decomposition products, it is possible, with the aid of further assumptions, to attempt an estimate of the concentration of impurities present.

One form of the Van't Hoff equation for the depression of freezing point for ideal binary mixtures may be expressed as follows:

$$T_m - T = \Delta T = \frac{RT_m^2}{\Delta H_f} \left(\frac{N_2}{N_1 + N_2} \right) \qquad (7.1)$$

where T_m is the melting point of the pure material, ΔT the depression of freezing point, ΔH_f the heat of fusion for the pure material, and N_1 and N_2 the number of moles of the pure material and of impurity respectively[3]. Since it may be safely assumed that $N_2 \ll N_1$, equation (7.1) may be rewritten as follows:

$$\Delta T = \frac{R T_m^2}{\Delta H_f} \left(\frac{N_2}{N_1} \right) \qquad (7.2)$$

An average molecular weight for the impurities is not known*, but if the estimate is sought in terms of the mole % concentration of impurity, a knowledge of molecular weights is unnecessary.

---

* The low R_f value for the impurities detected in the sample from the open tube does not necessarily imply a high molecular weight. Since the decomposition occurs in the presence of oxygen the impurity may consist of polar oxygen containing molecules of comparatively low molecular weight.

Unfortunately there is no heat of fusion data available which would allow an accurate value for S_f for tetraphenyl allene to be estimated. However, molecules of similar shape appear to exhibit closely similar entropies of fusion (S_f) (See chapter 1, section 1.5). For example, plate-like molecules exhibit entropies of fusion in the order of 13 e.u. (See table 7.1), whilst spherical or pseudo-spherical molecules, including the inert gases and some globular terpenes, exhibit entropies of fusion in the order of 3 e.u. (See Chapter 1, section 1.5, table 1.2). The dumb-bell shaped mercury halides, which are largely covalent in character, exhibit entropies of fusion in the order of 8 e.u. (See table 7.1).

TABLE 7.1[4]

PLATE-LIKE MOLECULES		MERCURY HALIDES	
COMPOUND	ENTROPY OF FUSION S_f(e.u.)	HALIDE	ENTROPY OF FUSION S_f(e.u)
Naphthalene	13.1	$HgCl_2$	7.5
Acenaphene	13.6	$HgBr_2$	8.4
Anthracene	14.1	HgI_2	8.6
Phenanthrene	12.1		

Since tetraphenyl allene is roughly dumb-bell in shape (See Chapter 6, plate 6.1), it will probably exhibit an entropy of fusion which lies between 3 e.u. (for spherical molecules) and 13 e.u. (for plate-like molecules). The average of these values

is 8 e.u. which corresponds to the dumb-bell shaped mercury halides. However, liquids comprising interlocking molecules of the tetraphenyl allene type often display some long-range order when heated to just above the melting point (See Chapter 4, page 127), and a value of 8 e.u. for the entropy of fusion may be rather high. For the present purpose a value of 7 e.u. will be selected as a reasonable estimate for the entropy of fusion for tetraphenyl allene.

The heat of fusion ΔH_f may be expressed as follows:

$$\Delta H_f = T_m S_f \qquad (7.3)$$

Hence equation (7.2) may be rewritten as:

$$\Delta T = \frac{R\, T_m}{S_f} \left(\frac{N_2}{N_1} \right) \qquad (7.4)$$

Since $R = 1.987$ cal. deg^{-1} mole^{-1}, $T_m = 439.2^{\circ}K$, and it is assumed that $\Delta T = 0.5^{\circ}$, and that $S_f = 7$ e.u., the mole % impurity may be roughly estimated as 0.4 %

If the above assumptions are accepted as reasonable, the amount of impurity present as a result of decomposition will not exceed 0.4 mole % for any sets of measurements obtained in this work using tetraphenyl allene. It may also be noted in this connection that concentrations of impurities greater than about 1 % by weight should be detected by the technique of thin-layer chromatography, although the sensitiveness of the technique may

depend upon the readiness with which the materials absorb the iodine indicator* (See Chapter 5).

7.1.2. The stability of triphenyl-α-naphthyl allene (M.pt. 139°-140°C (192°)).

The unusual melting characteristics of this compound have been described in detail in Chapter 5. The majority of the sample melts between 139° and 140°C, giving a cloudy melt which finally clears at 192°C. This phenomenon was believed at first to be due to the presence of impurity. Extensive tests (described in detail in Chapter 5, page 153 et seq.) failed to reveal the presence of impurity, and the phenomenon was tentatively attributed to a variety of polymorphism. (See Chapter 5, page 156 et seq; Chapter 6, section 6.2.2., and Chapter 10., section 10.3.1.2 for a detailed discussion). At the same time attempts were made to isolate the solid material suspended in the melt. A sample of the material was melted, heated to 150°C and filtered. Analysis of the filtrate and the material retained on the filter indicated that they were the same compound. This test, the details of which are described in Chapter 5, page 154 et seq., was not designed to investigate the stability of the melt over a temperature range. The stability tests described in the following paragraphs were carried out subsequently, after it had been established that

---

* Owing to the comparatively inert character of hydrocarbons of this type, the absorption of iodine provides one of the most satisfactory methods of detection.

the material was a single compound and not a mixture.

The procedure adopted to test the stability of the melt was closely similar to that described above for tetraphenyl allene. Again, two samples were selected. One was placed in an open tube, and the other was placed in a tube sealed from the air, through which "white spot" nitrogen was passed. The two tubes were placed in a thermostat bath, and maintained at a temperature of 165°C for four hours. As before a sample was removed from each tube, and the temperature of the bath was raised to 200°C*. Molten triphenyl-α-naphthyl allene will not crystallise on cooling, but congeals to a glass**. Since the material may only be induced to crystallise by trituration with a little solvent (e.g. benzene), the melting point could not be used as a criterion of purity. Neither sample showed very much discolouring, but the sample maintained under nitrogen was noticeably less discoloured than the sample taken from the open tube. Both samples were dissolved in chloroform and their R_f values compared

---

* Similar tests were carried out later, but for a different purpose. Working on the assumption that the anomalous melting characteristics of triphenyl-α-naphthyl allene are due to polymorphism, attempts were made to convert a sample of the material into the high-melting form by maintaining the temperature of the melt at 150°C, and later at 165°C for several hours. The temperature was finally raised to 190°C and the sample left overnight (c.a. 14 hours). The experiment was abandoned when the melt showed signs of decomposition (See Chapter 5, page 153).

** See Chapter 5, page 154, and Chapters 9 and 10 for details of the glass forming properties of this compound.

that of the original material, again using thin-layer chromatography. The sample which had been maintained in an atmosphere of nitrogen showed only one spot, the R_f value of which was identical with that of the original material. The sample taken from the open tube showed two spots, viz. an intense spot corresponding to the original material and a very weak spot situated near the base line corresponding to the decomposition products. Infra-red spectra (chloroform solution) were used as a further check, but the spectra of both samples were identical to that of the original (See Chapter 5). After being maintained at 200°C for over three hours, both test tubes were removed from the thermostat bath. The sample maintained under nitrogen still showed little sign of decomposition. The sample in the open tube had darkened somewhat but no charring was observed. The same tests were carried out as before. The sample maintained under nitrogen showed only one spot on a thin-layer plate, corresponding to the original material. The sample from the open tube showed the same two spots as before, though the spot near the base line corresponding to the decomposition products had grown in intensity. The infra-red spectrum of the sample maintained under nitrogen showed no change, but the fine structure of the spectrum of the sample from the open tube showed some loss of definition.

These results indicate that molten triphenyl-α-naphthyl

allene is at least as stable as tetraphenyl allene provided that precautions are taken to exclude oxygen wherever possible.

7.1.3. The stability of triphenyl-4-biphenyl allene. M. pt. 105° - 106°C.

Only a small quantity of triphenyl-4-biphenyl allene was synthesised (c.a. 8 g). The stability tests, though similar to those described above for tetraphenyl allene and triphenyl-α-naphthyl allene, were conducted on a smaller scale. Two samples were selected from the bulk, each of about 0.1 g. One sample was placed in an open tube. The other sample was placed in a tube through which "white spot" nitrogen was passed. Both tubes were immersed in the thermostat bath and maintained at a temperature of 135°C. After about four hours, samples were taken from each tube, and the temperature of the bath was raised to 170°C. Since molten triphenyl-4-biphenyl allene will not crystallise on cooling, but congeals to a glass*, the melting point could not be used as a criterion of purity. A comparison between the R_f values and infra-red spectra of the two samples with those of the original served as a check for decomposition. After a further three hours, both tubes were removed from the thermostat bath, and the R_f values and spectra were again checked. A detailed description of these tests has been omitted, since they are closely similar in observation and inference to those carried

---

* See Chapter 5, page 161, and Chapters 9 and 10 for a discussion of the glass forming properties of this compound.

out with triphenyl-α-naphthyl allene. Provided that experiments are conducted in the absence of oxygen, the melt should be sufficiently stable to allow reproducible results to be obtained.

The possible loss of material from the melts by evaporation was considered. The involatile nature of these compounds was demonstrated, in the case of tetraphenyl allene and triphenyl-4-biphenyl allene, in attempts to use sublimation or molecular distillation techniques as a means of purification. The involatile nature of triphenyl-α-naphthyl allene was demonstrated in the unsuccessful attempts to use gas-phase chromatography as a check for purity (See Chapter 5). It will be seen later, from the results of molar volume measurements, that there is in fact no significant loss of material over the range of temperature studied in this work (See chapters 9 , parts I and II).

7.2 Preparation of the tetraphenyl allene-pyrene mixtures

Before preparing a mixture, the samples of tetraphenyl allene and pyrene to be used were each placed under vacuum (c.a. 10^{-2} mm. Hg) and repeatedly warmed to about 120°C and "shock-cooled" in liquid nitrogen, to remove any remaining traces of solvent (i.e. benzene and petroleum spirit). The apparatus employed for the preparation of the mixtures is illustrated in Fig. 7.2. The calculated quantities of tetraphenyl allene and pyrene required for a particular mixture were carefully weighed into vessel A. The total weight of each mixture prepared was

FIG. 7.2.

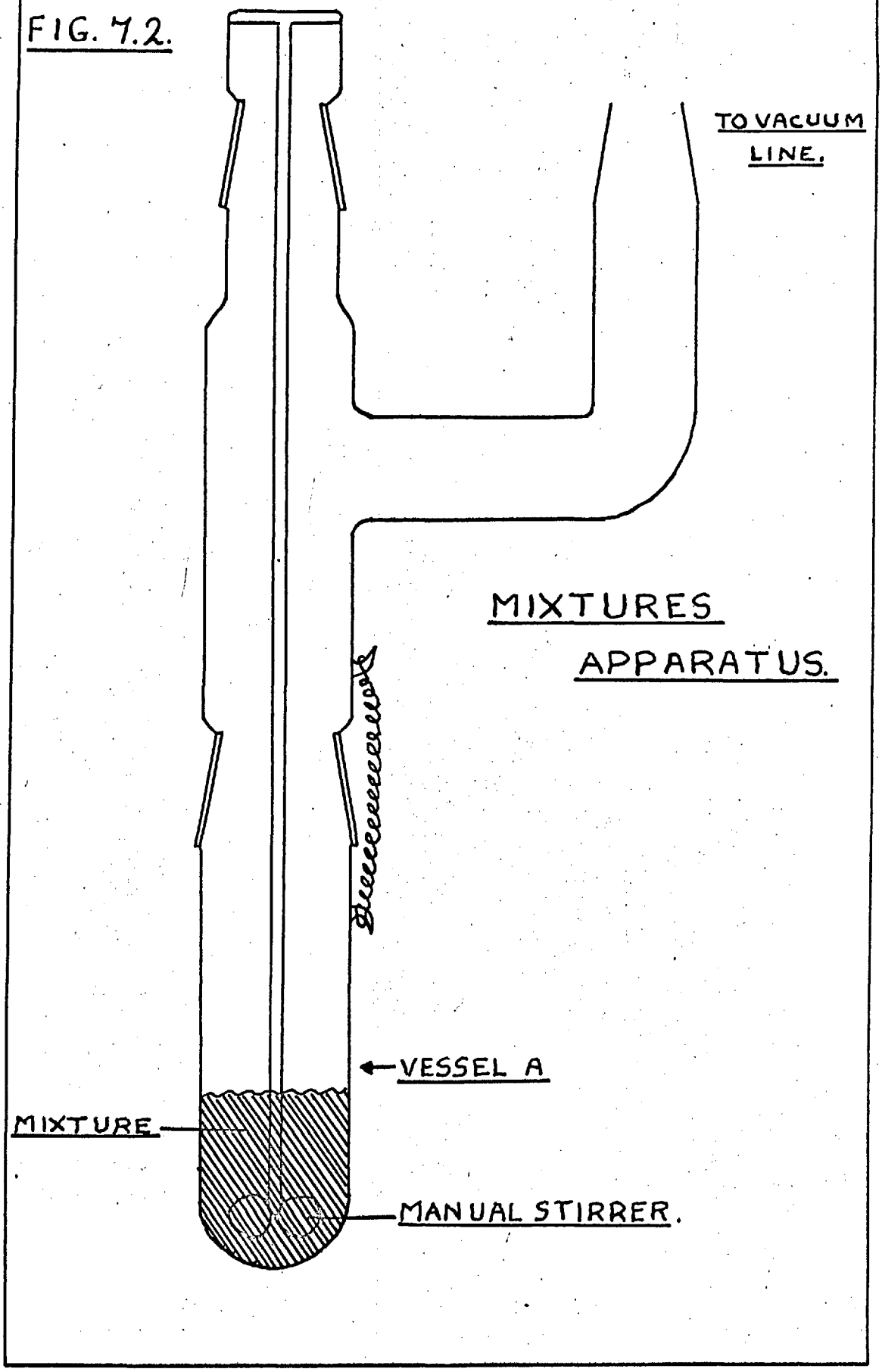
TO VACUUM LINE.
MIXTURES APPARATUS.
VESSEL A
MIXTURE
MANUAL STIRRER.

FIG. 7.3.

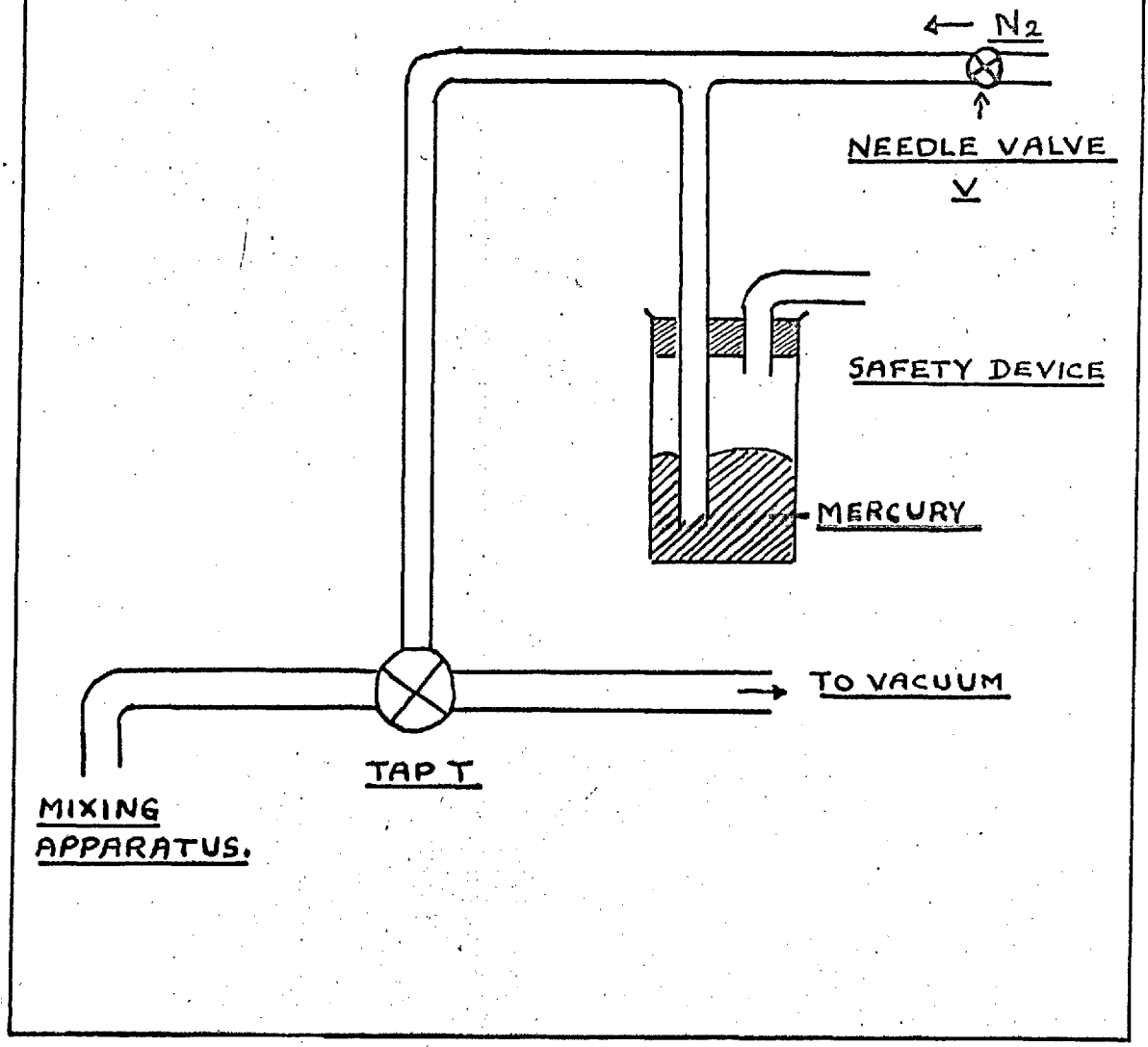
N2
NEEDLE VALVE
V
SAFETY DEVICE
MERCURY
TO VACUUM
TAP T
MIXING
APPARATUS.

about 5 g. The apparatus was assembled as indicated in Fig. 7.2 and attached to the limb of a vacuum line (See Fig. 7.3). The two-way vacuum tap T enabled the mixing apparatus to be opened to the vacuum system or to a supply of 'white-spot' nitrogen as required. A simple safety device was introduced between the nitrogen supply and tap T. The device consisted of a side-arm leading from the nitrogen supply line to a beaker of mercury. The end of the side-arm was immersed in the mercury to a depth of about 5 cm. This ensured that a positive pressure of nitrogen in the mixing apparatus would not exceed 5 cm. Hg. The mixing apparatus was evacuated (c.a. 10^{-3} mm.Hg) by opening tap T to the vacuum system. Before tap T was turned to seal off the vacuum system and to admit nitrogen into the evacuated mixing apparatus, the needle valve V was regulated to allow a stream of nitrogen to bubble vigourously through the mercury contained in the safety device. This ensured a positive pressure on the side of the tap closed to the evacuated mixing apparatus, and prevented mercury from the safety device from being drawn into the apparatus when tap T was opened to the nitrogen supply. After the apparatus had been filled with nitrogen, the process was repeated several times to ensure the absence of oxygen. The nitrogen filled mixing apparatus was finally isolated from both the vacuum system and the nitrogen supply, immersed in an oil bath to a level just above the contents, and warmed to a

temperature of 175°C. During the melting process the mixture was gently stirred. The stirring was continued until a homogeneous solution was obtained. After the stirrer had been removed, and tap T re-opened to the nitrogen supply (allowing nitrogen to flow through the upper section of the apparatus), the melt was quickly frozen by immersing the apparatus in a bath of cold water. This quenching process was adopted in order to freeze the melt quickly before any eutectic mixtures started to separate. When the apparatus had been dismantled and cleaned of oil and vacuum grease, the solid mixture was broken out of vessel A and ground to a powder with a pestle and mortar. In order to avoid contamination with dust, this grinding operation was carried out in a glove box. The powdered mixture was transferred to a dark bottle, sealed and stored for use*. Usually, each mixture was prepared from fresh samples of tetraphenyl allene and pyrene. For some repeat experiments, mixtures of new composition were prepared by the addition of fresh tetraphenyl allene or pyrene to a mixture which had already been used for one set of measurements. A mixture prepared in this way was always discarded after use.

---

* Mixtures containing a high proportion of tetraphenyl allene displayed a tendency to become electrostatically charged during the grinding process. This rendered handling difficult, and it was often necessary to leave the mixture in the glove box for several hours before attempting to transfer it to a bottle.

7.3 The Thermostat Baths.

For the majority of the measurements a thermostat bath, as illustrated in Fig. 7.4 was used to provide a constant temperature environment during the time of an experiment.

A 5 litre beaker formed the container for the M.S.550 silicone oil (supplied by Midland Silicones Ltd.) which was used as the heating fluid. The liquid is clear and may be maintained at temperatures up to 250°C without volatilisation or decomposition. The hot oil is not attacked by stainless steel, nickel, or copper, though prolonged contact with materials containing metallic lead or tin results in discolouration. The bath was insulated by a 2.5" thick layer of vermiculite. The heat was supplied by a 1500 watt iconel sheathed coil heater whose input was regulated by a bridge-type, half-wave saturable reactor temperature controller. The sensing element was a coiled 100 Ω platinum resistance thermometer, and the output from the temperature controller to the heater was monitored on an oscilloscope. A 50 Ω rheostat R was introduced between the output of the temperature controller and the heater. This enabled the output from the temperature controller to the heater to be reduced, permitting the controller to function efficiently at temperatures only slightly above the ambient. Althougn the bath was equipped with a water cooling coil (not shown in Fig. 7.4) its use as a heat sink for control at low temperatures

FIG. 7.4.

THE THERMOSTAT BATH

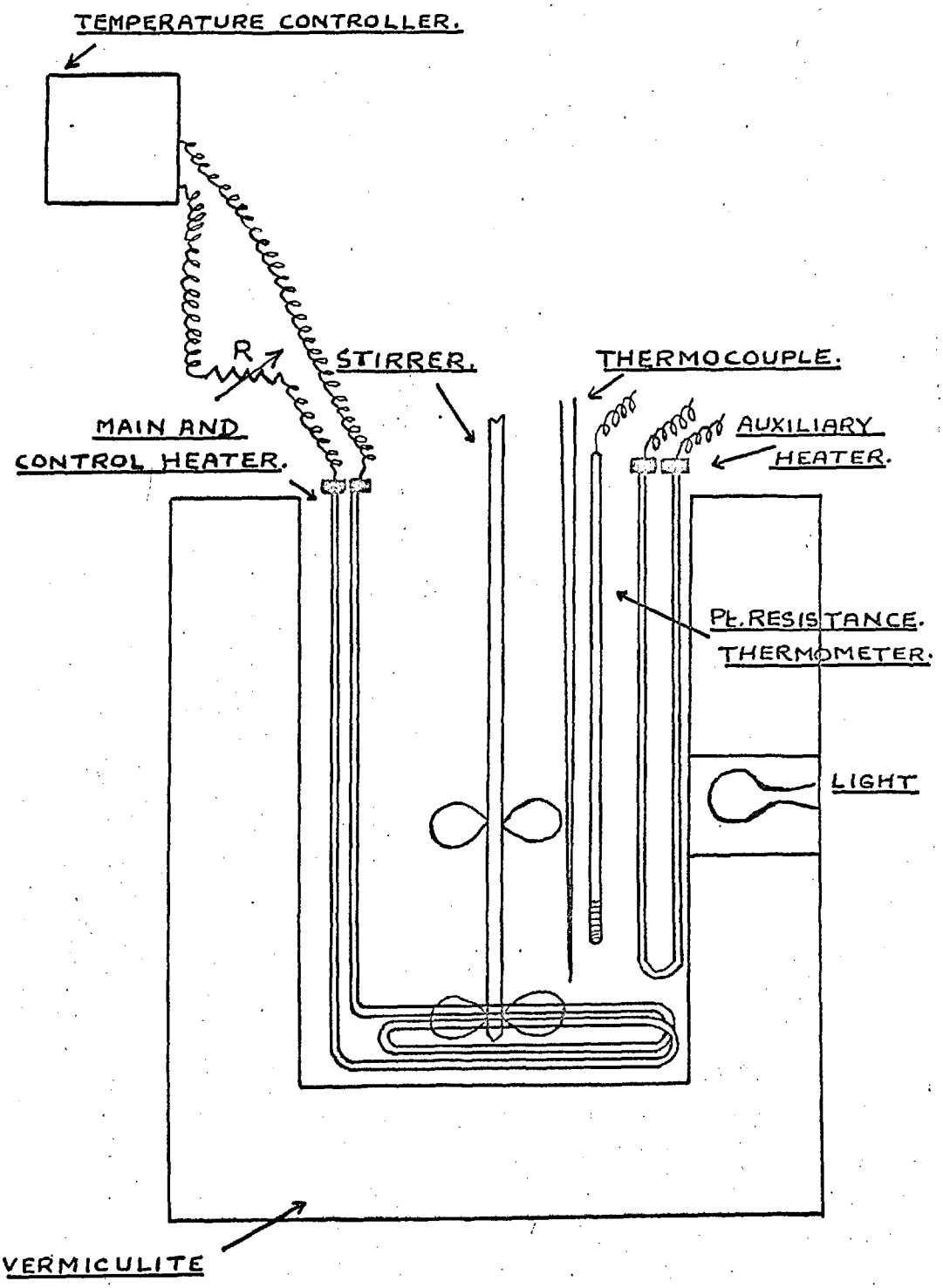

was obviated by the appropriate adjustment of the rheostat R. The cooling coil was used solely as a means of rapidly cooling the bath when required. For control at temperatures between 160°C and 210°C it was found advantageous to introduce a 110 volt, iconel sheathed, U-shaped auxiliary heater, controlled by a Variac transformer. Efficient stirring of the bath was achieved by means of a stainless steel shaft, inclined at an angle of 10° from the vertical, bearing two stainless steel propellers. The stirrer was driven by an induction motor controlled by a Variac. This allowed the rate of stirring to be maintained or adjusted as the viscosity of the heating liquid varied with temperature. A viewing slit was provided in the front of the insulation (not shown in Fig. 7.4) and the bath was illuminated by a 40 watt light bulb. At the higher temperatures, temperature fluctuations in the silicone oil bath amounted to no more than $\pm$ 0.03°C. after the bath had been allowed to equilibrate. At temperatures close to the ambient, fluctuations were somewhat greater amounting to $\pm$ 0.05°C.

For some calibration experiments conducted in the temperature range, ambient $\longrightarrow$ 50°C, a Townson and Mercer water thermostat bath was used. The specification of the water bath claimed a temperature control of $\pm$ 0.03°C. For temperatures in the range, ambient $\longrightarrow$ - 20°C, a Townson and Mercer "minus 70" bath was used. The specification of this bath claimed a

temperature control of $\pm$ 0.1°C.

7.4 The Measurement of Temperature

Johnson-Matthey 'Pallador' thermocouples (Pd/Au)(Pt/Ir) were used in the range, ambient $\longrightarrow$ 250°C. They were calibrated against an N.P.L. standardised platinum resistance thermometer reading to 0.01°C. Taking into account various errors in calibrating, and reading a thermocouple, the error in temperature measurement from this source was estimated at $\pm$ 0.05°C.

Since the thermocouple was only used intermittently, and temperatures did not exceed 250°C, it was considered that changes in e.m.f. resulting from diffusion at the hot junction would be small over the total period for which the thermocouple was used. However, it was deemed advisable to recalibrate the thermocouple after about 18 months. The change in e.m.f. amounted to an error of no more than 0.05°C.

For use with the Townson and Mercer water bath and "minus 70" bath, a mercury/thallium thermometer was used. This thermometer was calibrated in intervals of 0.2°C over a temperature range from -50°C to + 20°C.

REFERENCES

1. McLaughlin, E. and Ubbelohde, A.R., Trans. Faraday Soc., 54, 1804 (1958).

2. Hind, R.K., McLaughlin, E. and Ubbelohde, A.R., Trans. Faraday Soc., 56, 328 (1960).

3. Moelwyn-Hughes, E.A., "Physical Chemistry", Pergamon Press, London (1957).

4. Ubbelohde, A.R., "Melting and Crystal Structure", Clarendon Press, Oxford (1965).

CHAPTER 8.

VISCOMETRIC MEASUREMENTS

8.1 Types of Viscometer

There are five principal varieties of viscometer from which the choice of a suitable instrument may be made.

(1) A capillary viscometer in which the liquid flows through a capillary as a result of its hydrostatic head.

(2) A capillary viscometer in which the liquid is caused to flow through the capillary by means of an externally applied pressure.

(3) A viscometer of the Couette type in which the torque on an inner cylinder is measured when an outer concentric cylinder is rotated about it, the annular space between the cylinders being filled with the liquid under investigation.

(4) A viscometer of the falling sphere type.

(5) A viscometer of the oscillating type, in which a cylinder, sphere, or disc is suspended in the liquid by a torsion wire, and is allowed to oscillate. The logarithmic decrement of the oscillations is determined, providing a means of evaluating the viscosity of the liquid.

Where measurements of the highest accuracy are required, the choice should be made from methods (1-4), since the nature of the forces involved are rather less complex than in method (5). Method (4), the falling sphere method, has proved useful at high

temperatures in connection with molten salts[1,2]. Two of the principal drawbacks to its use in the present context are that the technique requires a considerable quantity of material, and that owing to errors in timing the fall of sphere, the technique is best employed for fairly viscous liquids such as glycerol where $\eta_l \sim 10$ poise.

Where, however, the experimental conditions render the use of methods (1-3) difficult or impossible (i.e. at temperatures above 300°C or at very low temperatures) a viscometer of the oscillatory type may be used.

Viscometers of the Couette type claim the advantage that the shearing rate may be readily varied over a wide range, and have proved useful in the investigation of the viscosity of thixotropic liquids and of liquids which have a micellar structure. The principal disadvantages of tnis method lie in the fact that they are difficult to thermostat at temperatures much in excess of ambient, and that it is difficult to conduct experiments in which the liquid is sealed from air. Capillary viscometers, cn the other hand, may be used up to temperatures in the order of 300°C, and their temperature may be controlled by immersion in a suitable thermostat bath (See chapter 7, section 7.3). Of the two types available, that in which the liquid is driven through the capillary by means of an externally applied pressure allows different rates of shear to be obtained by varying the applied

pressure. This advantage, coupled with the fact that, with a suitable design, it is possible to exclude air from the apparatus, indicated a viscometer of this type to be the most satisfactory for the present investigation.

8.2 The Viscous Flow of Liquids in Tubes

The basic expression relating the viscosity η of an incompressible fluid when flowing under an applied pressure P, to the volume V, which emerges from a capillary of radius r and length l, in time t is given by:-

$$\frac{V}{t} = \frac{\pi P r^4 t}{8 \eta l} \qquad (8.1)$$

This equation was first suggested empirically by Poiseuille (1840-41)[3], but was later derived by Hagenbach (1860)[4] on the basis of the following assumptions.

(a) The applied pressure is employed solely in overcoming the viscous resistance of the fluid.

(b) The flow is steady throughout the entire length of the capillary and is at all times parallel to the capillary axis.

(c) There is no slip between the fluid and the capillary wall.

Assumptions (b) and (c) result in a parabolic velocity distribution throughout all the cross-sections along the length of the capillary.

More detailed considerations of capillary flow by numerous authors have indicated that these assumptions are over-simplified, and that, under certain conditions, it is necessary to introduce the following corrections to equation 8.1.

(i) The kinetic energy correction.

The driving pressure, represented by the pressure difference between the ends of the capillary, is dissipated not only in overcoming viscous resistance as suggested in assumption (a), but also in imparting kinetic energy to the fluid[4]. On the basis of assumptions (b) and (c) the velocity head imposed on the liquid can be shown to be:

$$\frac{\rho V^2}{\pi r^4}$$

where ρ is the density of the fluid, r the radius of the capillary and V, the volume flowing through the tube in unit time. The effective pressure P_1 employed in overcoming the viscous resistance is given by:

$$P_1 = P - \frac{\rho V^2}{\pi r^4} \qquad (8.2)$$

where P is the actual pressure difference. A finite length is however required before the assumed parabolic velocity distribution is established in the capillary. To allow for this, a factor m is included in the correction term, i.e.

$$P_1 = P - \frac{m\rho V^2}{\pi r^4} \qquad (8.3)$$

The value of m is always nearly unity, but its precise value is largely dependent upon the shape of the capillary entrance. (See this Chapter, section 8.3).

(ii) The Couette correction.

At the entrace to the capillary, the different velocities of the converging streamlines in the liquid give rise to a viscous resistance additional to that caused by the capillary. The suggestion that Poiseuille's equation (equation 8.1) should be corrected for this extra resistance to flow was due to Couette (1890). It may be expressed in terms of a hypothetical addition, λ to the length of the capillary where:

$$n = \lambda/r \qquad (8.4)$$

n is a constant.

(iii) Slipping correction.

This correction arises from a consideration of assumption (c). Although attempts have been made to produce effects resulting from frictional slip between the fluid and the capillary wall, no evidence for its existance has been forthcoming. Assumption (c) is therefore taken as valid.

Introduction of these corrections into the original Poiseuille expression results in the vollowing relationship:

$$\eta = \frac{\pi r^4 P}{8V(l + nr)} - \frac{m\rho V}{8\pi(l + nr)} \qquad (8.5)$$

This equation provides an accurate description of capillary flow under streamline conditions.

As mentioned in Chapter 2, the criterion which determines that the flow through a capillary is streamline under any particular set of conditions was shown by Reynolds to be that the value of the dimensionless number $k \not> 1150$, where $k = v\rho r/\eta$. v is the linear velocity of the liquid, η its coefficient of viscosity, and r the capillary radius.

In order to measure the absolute viscosity of a fluid, the precise dimensions of the viscometer must be determined, and the coefficients m and n estimated.

8.3 Viscometers for Relative Determinations.

Since the dimensions of a capillary viscometer often prove difficult to determine accurately, most measurements are made relative to a standard liquid with which the instrument is calibrated. In the case of relative viscometers, in which the liquid is driven through the capillary by means of an external pressure, the density of the liquid ρ, appears only in the second term of equation (8.5).

For a viscometer of this type, the viscosity of the liquid under investigation η , relative to that of a standard liquid η_o, is given by the following expression:

$$\frac{\eta}{\eta_o} = \frac{k\,Pt - k'\,\rho/t}{k\,P_o t_o - k'\rho_o/t_o} \qquad (8.6)$$

where k and k' are constants for the viscometer, P the applied pressure, t the flow time under this pressure, and ρ the density of the liquid. The subscript 'o' designates the quantities relating to the calibration liquid. The densities of the liquids appear in only the second terms of the expression. If these terms are small compared with kPt and kP_ot_o or if $\eta \sim \eta_o$ equation (8.6) reduces to:

$$\frac{\eta}{\eta_o} = \frac{Pt}{P_o t_o} \qquad (8.7)$$

More usually this is rewritten as:

$$\eta = \frac{Pt}{C} \qquad (8.8)$$

where $\frac{P_o t_o}{\eta_o} = C$, and C is known as the calibration constant for the viscometer. By comparison with equation (8.1):

$$C = \frac{8Vl}{\pi r^4} \qquad (8.9)$$

The most reliable relative viscometer of this type is the Bingham and Jackson's[6] modification of the Ubbelohde[7] viscometer. A modified version of this design was used in the current work and is illustrated in Fig. 8.1. This particular design requires the use of comparatively little material (3-4 g), which is a considerable advantage if the material is scarce.

FIG. 8.1.

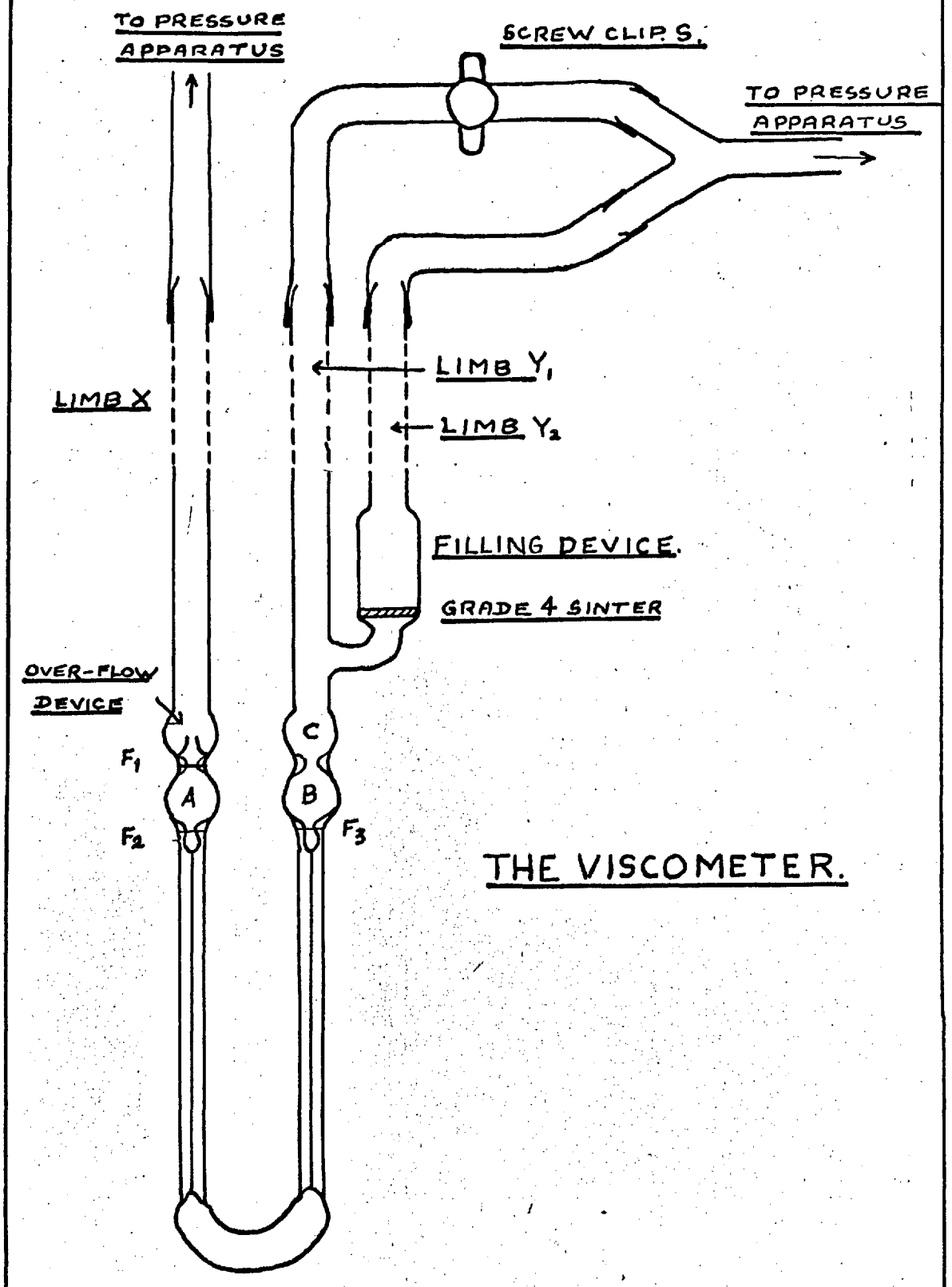

THE VISCOMETER.

The viscometer was constructed from two 10 cm. lengths of 0.3 mm. bore veridia capillary. In order to give a standard condition in which the kinetic energy correction may be calculated, the ends of the tubes should be ground flat. Alternatively, the correction is minimised by making the capillaries as long as possible and "belling-out" the ends[8]. This second procedure was adopted. It will be shown later that even under the least favourable conditions (i.e. low viscosity and high flow time) the introduction of a kinetic energy correction was unnecessary. The volumes of bulbs A and B were each about 1 ml. The size, shape, and height of these bulbs were kept as near as possible identical. In this way the effect of the hydrostatic pressure of the liquid as it is forced from bulb A to bulb B, in the first half of the flow-time, is exactly cancelled by the effect to be subtracted in the second half of the flow-time. Three fiducial marks were made on the viscometer F_1, F_2, and F_3 in the positions shown in Fig. 8.1 . The flow time was recorded in both directions viz. from F_1 to F_2 and from F_2 to F_1. These flow times should be identical within the limits of error in timing. Discrepancies were normally attributable to either a gas leak in the nitrogen pressure line (see section 8.4 below) or a partial blockage in the capillaries. The validity of the equation (8.6) rests on the total volume of the system remaining constant as the temperature varies. This condition was ensured

at each temperature by adjusting the volume of the liquid to that contained between mark F_3 and the tip T of the overflow device.

The limbs of the viscometer X and Y_1 and Y_2 were connected to the pressure system by means of 1/4 o.d. P.V.C. tubing. It was found from experience that a simple P.V.C./pyrex glass connection was reliable, and held positive pressures of nitrogen ($\not>$ 33 cm. Hg.) very well. Attempts to use ground glass joints, with or without 'teflon' sleeves, proved most unsatisfactory unless sealed with picene wax. The latter proved inconvenient to remove when attempts were made to recover the molten material from the viscometer. It will be seen from Fig. 8.1, that the viscometer was modified to accommodate a filling device. A description of this appendage together with an account of its use is reserved for section (8.5), following a description of the constant pressure apparatus.

8.4 The Constant Pressure Apparatus[6]

The apparatus used to obtain a constant driving pressure is illustrated in Fig. 8.2. This consisted of a series of glass tubes, C_1, C_2, C_3, and C_4 approximately 4 cm. in diameter and 1.5 metres in height. These were filled with water to the level shown. A 6 mm. bore tube was sealed into the top and bottom of each of these columns. A fine hole was pierced near the bottom of each of the 6 mm. bore tubes. Column C_1 was also joined to the glass line L which led through a liquid nitrogen cold trap B

FIG. 8.2.

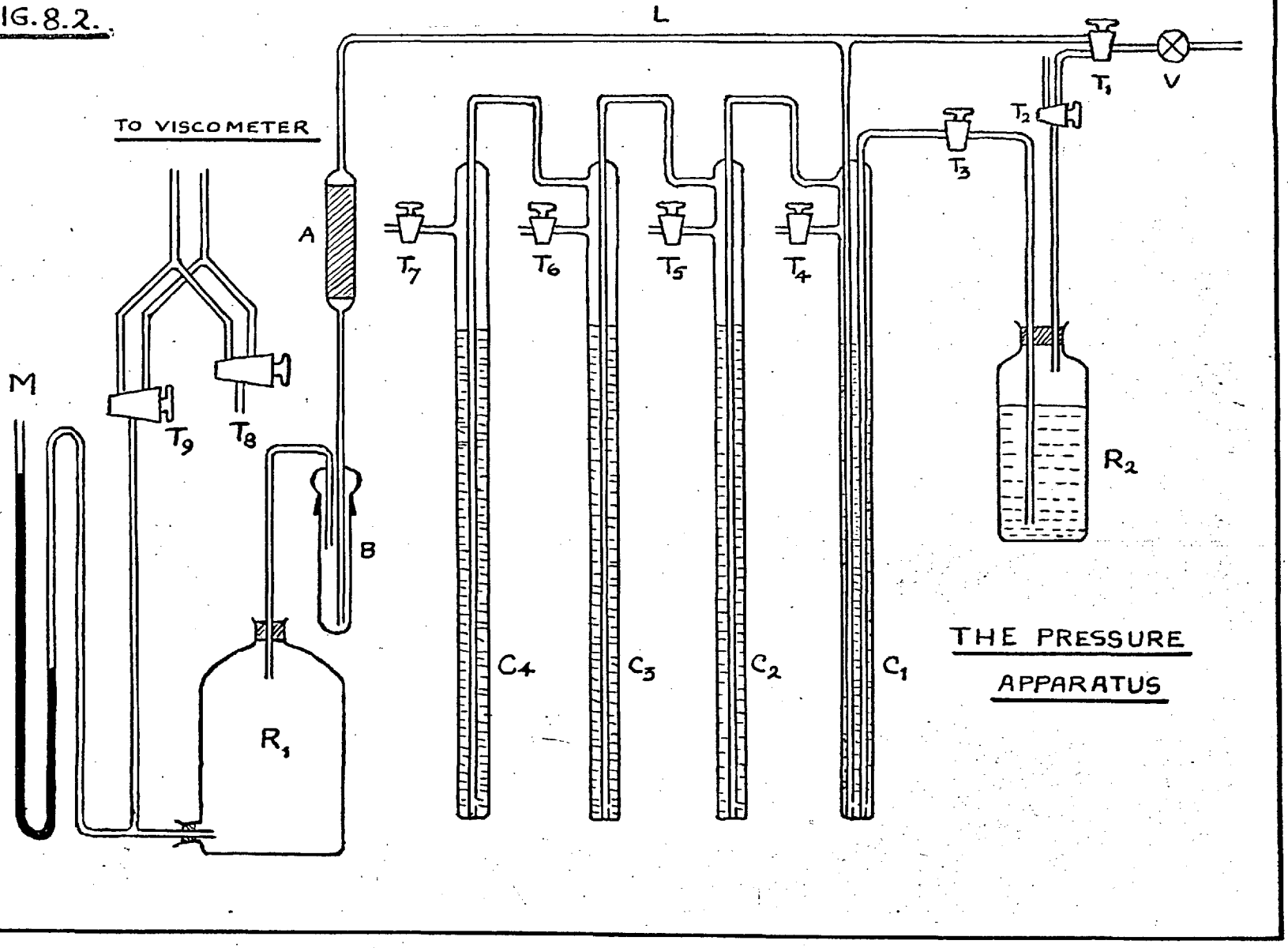

THE PRESSURE APPARATUS

and a cotton wool filter plug A into a twenty litre ballast reservoir R_1. An exit lead from this reservoir was taken to a manometer M, and a dual two-way tap system T_8 and T_9, and hence to either limb of the viscometer.

'White-spot' nitrogen was fed through a needle valve V from a cylinder. The valve was adjusted until, with tap T_1 open to the main apparatus, tap T_3 closed and taps T_4, T_5, T_6 and T_7 open to the atmosphere, a fine stream of bubbles were observed to rise in column C_1. The pressure in the apparatus was then equivalent to the head of water H_1 in that column. Any slight fluctuations in pressure were absorbed in the twenty litre aspirator R_1. A pressure equivalent to $H_1 + H_2$ was obtained by closing tap T_4 and adjusting the needle valve V until the gas overflow from column C_1 was sufficient to maintain a steady stream of bubbles in column C_2. Similarly, columns C_3 and C_4 could be brought into operation by closing taps T_5 and T_6 respectively.

To obtain any convenient value of the pressure, a siphon device was fitted to the apparatus as shown in the figure. The level of water in the first column could thus be varied to give any fractional height h equivalent to a pressure hH_1. This could be increased to $hH_1 + H_2$, etc. in the manner described above. When it was desired to return water to the first column, this was achieved by passing nitrogen from the cylinder, via taps

T_1 and T_2, into the syphon reservoir R_2. In this way water was forced back into the column via tap T_3.

Pressures were recorded to $\pm$ 0.002 cm. Hg, using a Pye cathetometer. No pressure fluctuations in excess of this value were detected in any of the determinations.

8.5. The Filling Device.

Since it was essential that the viscometer capillaries should not be blocked by any dust particles which, despite all precautions, may be present either in the material or introduced during the filling process, the viscometer was fitted with a filling device. (See Fig. 8.1)

This appendage consisted of an extra limb (Y_2), widened at the base, containing a grade 4 sintered disc filter. This extra limb was attached to limb Y_1 of the viscometer just above bulb C. The limbs Y_1 and Y_2 were both connected to the pressure apparatus via a 'Y' piece, thus ensuring no pressure difference across the sinter whilst the experiment was in progress. When immersed in the thermostat oil bath, the level of the sintered disc lay about 6 cm. below the surface of the oil in order that the volume between the sintered disc and the oil surface should not be less than the volume contained between marks F_1 and F_3. The general filling procedure is summarized in the tabulated sequence of operations which follow.

(i) Having connected the viscometer limbs to the constant pressure apparatus via taps T_8 and T_9 (see Fig. 8.2), the instrument was flushed out with nitrogen by connecting limb X to the nitrogen supply.

(ii) After about 5 minutes, the tube leading from limb Y_1 was closed by means of the screw clip S, allowing the nitrogen to flush out limb Y_2 which contained the sintered disc filter.

(iii) Limb Y_2 was then disconnected from the tube, and the approximate quantity of solid material required, when molten, to fill the viscometer was introduced on to the sinter through a funnel.

(iv) The tube was again connected to limb Y_2, and since clip S was still closed, the solid material was flushed out with nitrogen.

(v) After a few minutes, clip S was opened and the viscometer lowered into the thermostat bath which was maintained at a temperature about $5^{\circ}C$ above the melting point of the material. When the material had melted, clip S was again closed to allow nitrogen to bubble through the melt, ensuring the absence of oxygen. (This operation proved to be particularly useful in the case of tetraphenyl allene/pyrene mixtures. In mixtures of certain compositions, a low melting eutectic tended to melt first, but by bubbling nitrogen through the melt a homogeneous

solution was obtained before the mixture was admitted into the viscometer).

(vi) Whilst clip S was closed, the nitrogen pressure was transferred, using taps T_8 and T_9, to the limb Y_2, forcing the melt into the viscometer.

(vii) Clip S. was then opened and, by repeatedly transferring the pressure from limb X to limb Y and from limb Y to limb X, any gas bubbles trapped in the melt were removed. The volume of the liquid was adjusted to that contained between marks F_1 and F_3 by means of the overflow device.

There are three principal advantages of this filling technique.

(a) Handling of the material is reduced to a minimum.

(b) Any risk of overheating the melt during the filtering process is obviated.

(c) Oxygen may be excluded from the melt during the filling process.

Before each set of measurements, the viscometer was cleaned by filling with nitrating acid (conc.H_2SO_4/conc. HNO_3) and warming in a water bath to 100°C. The acid was removed by repeated flushing, first with distilled water and then with acetone. Finally the instrument was dried in an oven at 150°C.

8.6. Calibration of the Viscometer.

The constant C in the equation $\eta = Pt/C$ was found

by calibration with 40 % w/w sucrose solution at 25°C. The sucrose solutions were prepared gravimetrically, correcting all weights to vacuum. Freshly boiled distilled water was used and the solutions were not heated to aid solution of the sucrose since prolonged heating at elevated temperatures has been known to effect inversion of the sucrose. Several flow times in each direction were recorded using all the available driving pressures. The process was repeated twice with freshly prepared solutions. The viscometer constant, calculated as a mean of all results, was found to be 115.60 ± 0.25 cm.Hg.sec. millipoise^{-1}. Within this order of accuracy it is not necessary to correct the calibration constant for the thermal expansion of the viscometer. The different in temperature between the calibration and the experimental observations $\not> 200^{\circ}$C. A simple consideration of the Poiseuille equation indicates that there is no significant expansion effect[8].

$$\eta = \frac{\pi P r^4}{8Vl}$$

Let r_o and l_o be the radius and length of the capillaries, and V_o the volume flowing per second at the calibration temperature. The coefficient of expansion of glass is α. Then for a temperature rise ΔT,

$$\eta = \frac{\pi P\, r_o^4 (1 + \alpha \Delta T)^4}{8\, l_o V_o (1 + \alpha \Delta T)(1 + 3\alpha \Delta T)}$$

and $(1 + \alpha\Delta T)^4 = 1 + 4\alpha\Delta T$ ..... terms containing powers of α.

Thus for $\alpha \ll 1$:

$$(1 + \alpha\Delta T)^4 = (1 + \alpha\Delta T)(1 + 3\alpha\Delta T)$$

In other words, to a first approximation the change in viscosity resulting from expansion effects in the glass is fully compensated and the calibration is valid.

8.7. Viscosity Results.

The results obtained for tetraphenyl allene, pyrene, mixtures of tetraphenyl allene and pyrene (20, 25, 40, 60 and 80 mole % with respect to tetraphenyl allene) and triphenyl-α-naphthyl allene are listed in tables 8.1 to 8.5.

Measurements were carried out in the thermostat oil bath described in Chapter 7., section 7.2, and were generally commenced at the lowest temperature at which partial crystallisation did not occur. The volume at each temperature was adjusted to that contained between the fiducial mark F_3, and the tip of the overflow device. The flow times were noted to $\pm$ 0.1 sec., and were repeated four times (twice in each direction) for each set of pressure and temperature conditions, the reproducibility being 0.2 % or better. The driving pressures available ranged from 7 cm.Hg to 33 cm.Hg.

Ideally, flow times should be recorded using each of the four pressure heads available at every temperature selected. A linear

plot of applied pressure vs. reciprocal flow time which passes through the origin indicates that the flow is streamline and that a kinetic energy correction is unnecessary. In most cases however, it was deemed sufficient to carry out the full process for three or four temperatures only, distributed over the temperature range. As indicated in Chapter 7, section 7.1, it was desirable to reduce the time of experiment as far as possible in order to minimise decomposition. Further, the scarcity of the materials had always to be considered. Nonetheless, since the viscosity data for tetraphenyl allene was repeated several times (see tables 8.1a - 8.1c), it was possible to obtain pressure vs. reciprocal flow time isotherms for eight different temperatures. It will be seen from Figs. 8.4, 8.6, and 8.9 that the pressure vs. reciprocal flow time isotherms for tetraphenyl allene, pyrene, and triphenyl-α-naphthyl allene* are linear and pass through the origin. Linear plots were also obtained for the tetraphenyl allene/pryene mixtures, but since the data illustrated in Figs. 8.4, 8.6 and 8.9 represent extreme cases illustration of the pressure vs. reciprocal flow time isotherms for the mixtures is unnecessary.

---

* In the case of triphenyl-α-naphthyl allene, the two highest driving pressures (c.a. 24 cm.Hg. and 33 cm.Hg) only were used. The high viscosity of this melt rendered the flow times using the lower pressures (c.a. 7 cm.Hg and 16 cm.Hg) very long (> 1 hour even at higher temperatures) and the use of these pressures was abandoned in order to reduce the time of experiment.

Figs. 8.3, 8.5, 8.7 and 8.8 illustrate the $\log_{10} \eta$ vs. $1/T^{\circ}K$ plots for tetraphenyl allene, pyrene, tetraphenyl allene/pyrene mixtures and triphenyl-α-naphthyl allene respectively. The nature and interpretation of these plots are discussed in Chapter 10, sections 10.3.2 and 10.4.3.

It will be noticed that the viscosity measurements for tetraphenyl allene recorded in table 8.1b were commenced at the highest temperature. In order to investigate the viscosity of a liquid as the temperature is decreased, it was necessary to introduce fresh material for each reading in order to maintain the constant volume of liquid. In the super-cooled region this involved heating the liquid to above the solid state melting point in order to introduce material for each reading. After the material had been added the temperature was then lowered to the temperature selected, and the volume adjusted using the overflow device. Since the amount of fresh material introduced during the experiment, to compensate for thermal contraction, was small, it is safe to say that agreement with data obtained by raising the temperature indicates that the concentration of impurity resulting from decomposition is not sufficiently large to be significant. This agreement, illustrated in Fig. 8.3, serves to confirm the conclusions inferred from the stability tests described in Chapter 7, section 7.1., and indicates the reliability of the experimental technique.

TABLE 8.1.a.

VISCOSITY OF TETRAPHENYL ALLENE

Sample 1:-

LOW TEMPERATURE TO HIGH TEMPERATURE

Temperature ^{o}C	η Millipoise	$\frac{1}{T^{o}K} \times 10^{3}$	$\log_{10} \eta$ (Millipoise)
Super-Cooled Liquid			
164.1	43.73	2.2870	1.6408
Liquid			
166.7	41.42	2.2735	1.6172
169.9	38.71	2.2570	1.5879
171.3	37.43	2.2499	1.5732
175.4	34.56	2.2296	1.5386
178.1	32.86	2.2160	1.5166
182.7	30.18	2.1937	1.4797
188.8	27.08	2.1647	1.4326
194.6	24.69	2.1378	1.3925
200.3	22.64	2.1121	1.3549
204.3	21.30	2.0944	1.3284
209.3	19.88	2.0727	1.2985

TABLE 8.1.b.

Sample 2:-

HIGH TEMPERATURE TO LOW TEMPERATURE

Temperature °C	η Millipoise	$\frac{1}{T^{\circ}K} \times 10^{3}$	$\log_{10} \eta$ (Millipoise)
Liquid			
210.0	19.84	2.0697	1.2976
202.3	22.15	2.1032	1.3453
194.2	25.06	2.1397	1.3989
186.0	28.75	2.1779	1.4587
180.7	31.66	2.2036	1.5006
172.7	36.98	2.2431	1.5680
169.9	39.13	2.2570	1.5925
166.9	41.70	2.2724	1.6202
Supercooled liquid			
161.8	47.02	2.2993	1.6723
161.2	48.06	2.3022	1.6832
158.4	51.64	2.3171	1.7130
155.7	55.35	2.3310	1.7431

TABLE 8.1.c.

Sample 3:-

LOW TEMPERATURE TO HIGH TEMPERATURE

Temperature °C	η Millipoise	$\frac{1}{T^{o}K} \times 10^{3}$	$\log_{10}\eta$ (Millipoise)
Super-cooled liquid			
162.4	45.75	2.2959	1.6604
Liquid			
167.8	40.61	2.2678	1.6087
170.4	38.38	2.2545	1.5841
173.7	35.95	2.2381	1.5556
176.1	34.35	2.2259	1.5359
178.4	32.90	2.2148	1.5173
183.6	29.81	2.1893	1.4744
189.7	26.93	2.1605	1.4302
194.1	25.09	2.1404	1.3995
202.1	22.21	2.1041	1.3465
209.9	19.85	2.0701	1.2977
208.1	20.34	2.0779	1.3084

FIG. 8.3.

VISCOSITY OF TETRAPHENYL ALLENE.

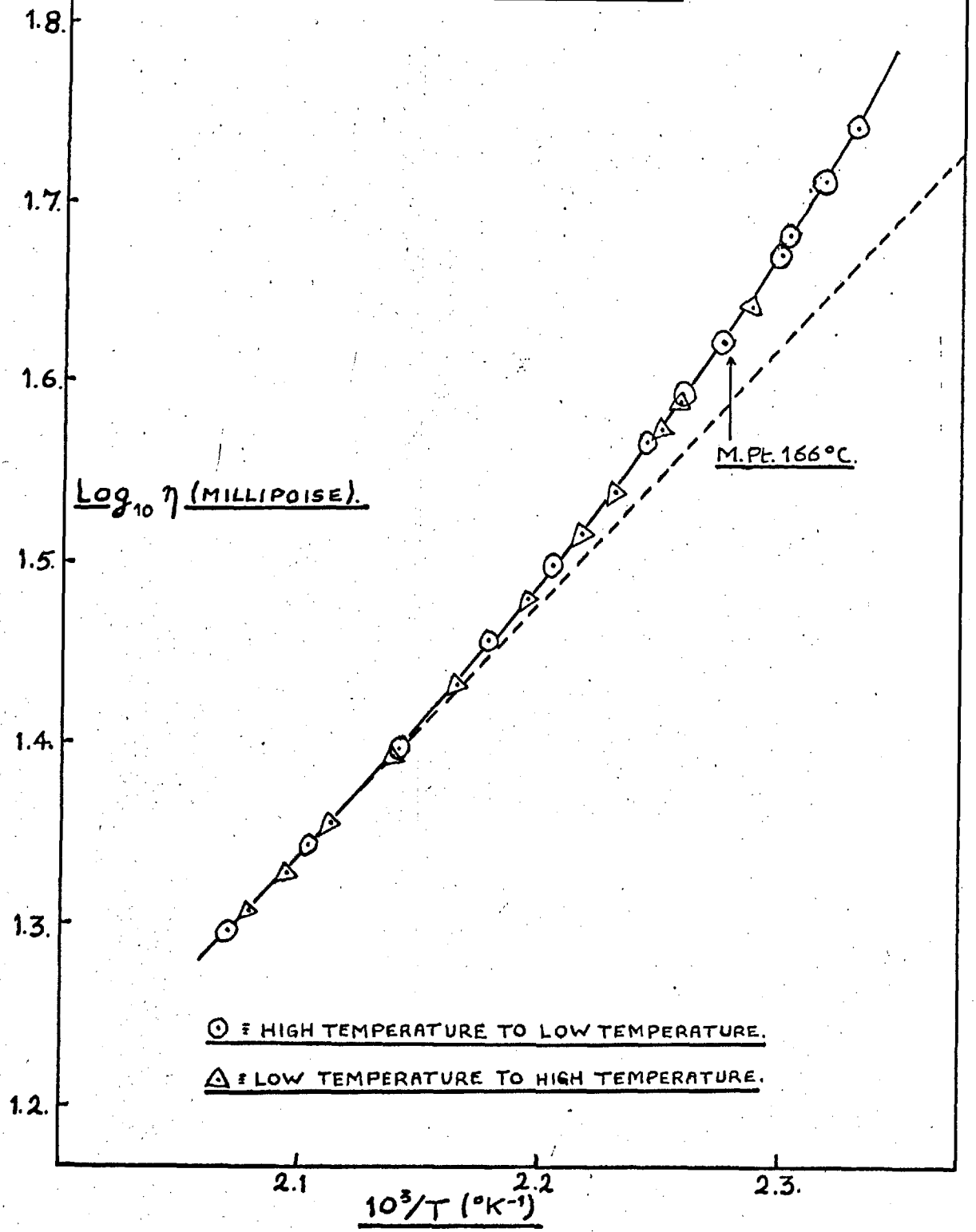

FIG. 8.4.

PRESSURE VS. RECIPROCAL FLOW TIME ISOTHERMS FOR TETRAPHENYL ALLENE.

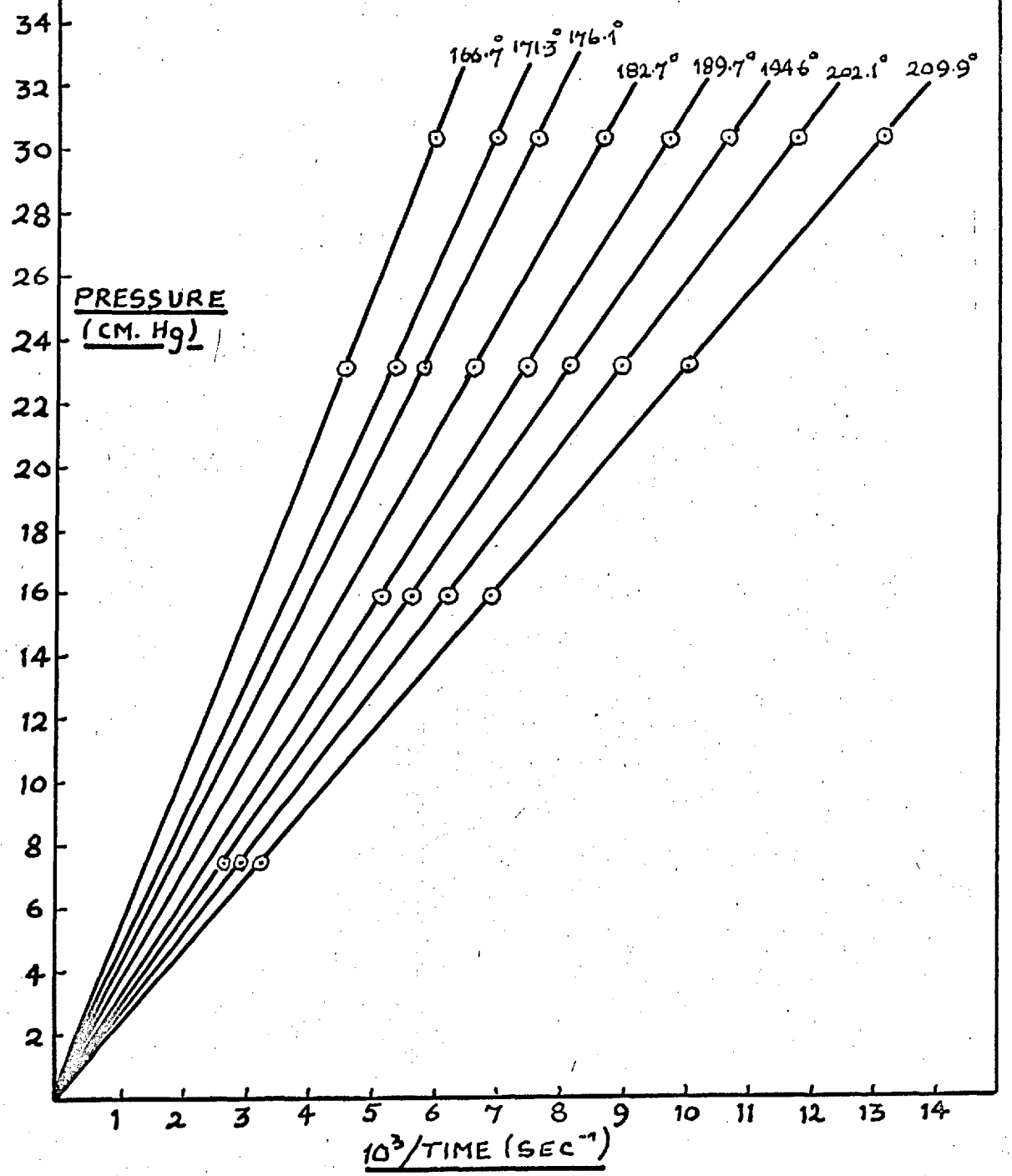

TABLE 8.2.a.

VISCOSITIES OF THE TETRAPHENYL ALLENE-PYRENE SYSTEM.

Mole % Tetraphenyl Allene = 0.00			
Temperature °C	η (Millipoise)	$10^3/T^\circ K$	$\log_{10}\eta$ (Millipoise)
152.3	18.00	2.3504	1.2553
160.7	16.22	2.3049	1.2101
169.5	14.67	2.2591	1.1665
177.4	13.54	2.2195	1.1314
181.9	12.84	2.1975	1.1085
187.3	12.17	2.1717	1.0853
193.1	11.52	2.1447	1.0613
200.7	10.77	2.1103	1.0321
208.9	10.00	2.0744	1.0000

Mole % Tetraphenyl Allene = 20.00			
Temperature °C	η (Millipoise)	$10^3/T^\circ K$	$\log_{10}\eta$ (Millipoise)
128.2	38.08	2.4916	1.5807
138.75	31.05	2.4278	1.4921
145.2	27.85	2.3903	1.4448
150.9	25.39	2.3582	1.4048
156.1	23.26	2.3296	1.3667
160.8	21.79	2.3044	1.3382
168.2	19.60	2.2660	1.2921
176.5	17.54	2.2239	1.2440
184.1	15.96	2.1869	1.2030
195.1	14.13	2.1365	1.1501

TABLE 8.2.b.

Mole % Tetraphenyl Allene = 25.00			
Temperature °C	η (Millipoise)	$10^3/T°K$	$\text{Log}_{10}\eta$ (Millipoise)
139.0	33.41	2.4262	1.5238
145.5	29.57	2.3886	1.4708
150.9	26.85	2.3582	1.4290
155.7	24.86	2.3320	1.3955
159.5	23.32	2.3116	1.3678
166.5	21.08	2.2745	1.3239
173.2	19.32	2.2403	1.2861
182.8	17.02	2.1932	1.2304
191.3	15.42	2.1530	1.1881
197.9	14.21	2.1229	1.1527

Mole % Tetraphenyl Allene = 40.00			
Temperature °C	η (Millipoise)	$10^3/T°K$	$\text{Log}_{10}\eta$ (Millipoise)
115.0	74.78	2.5763	1.8738
127.8	53.44	2.4940	1.7279
133.2	47.00	2.4612	1.6721
139.9	40.73	2.4212	1.6100
144.8	36.77	2.3926	1.5655
150.2	33.02	2.3623	1.5187
154.4	30.50	2.3391	1.4844
159.8	27.93	2.3100	1.4461
166.2	25.09	2.2760	1.3995
173.0	22.47	2.2413	1.3517
181.9	19.76	2.1975	1.2957
189.9	17.75	2.1595	1.2492
198.6	15.95	2.1197	1.2029

TABLE 8.2.c.

Mole % Tetraphenyl Allene = 60.00			
Temperature °C	η (Millipoise)	$10^3/T^\circ K$	$\log_{10}\eta$ (Millipoise)
123.3	82.62	2.5226	1.9171
143.9	48.23	2.3977	1.6833
148.4	43.29	2.3717	1.6364
151.5	39.00	2.3546	1.5911
158.3	35.33	2.3177	1.5481
162.2	32.79	2.2972	1.5157
165.8	30.61	2.2784	1.4858
171.4	27.66	2.2494	1.4419
175.6	25.76	2.2284	1.4111
182.0	23.16	2.1970	1.3648
185.2	22.06	2.1819	1.3435
189.7	20.71	2.1607	1.3163
195.5	19.08	2.1337	1.2806
200.2	17.87	2.1123	1.2520

TABLE 8.2.d.

Mole % Tetraphenyl Allene = 80.00			
Temperature ^{o}C	η (Millipoise)	$10^{3}/T^{o}K$	$Log_{10}\eta$ (Millipoise)
138.3	72.33	2.4304	1.8593
142.8	63.85	2.4041	1.8051
149.9	53.70	2.3637	1.7299
152.7	49.59	2.3482	1.6954
159.0	43.22	2.3140	1.6357
161.0	41.92	2.3033	1.6224
165.4	38.15	2.2802	1.5815
171.5	33.85	2.2489	1.5296
173.4	32.81	2.2393	1.5159
177.9	30.04	2.2170	1.4777
184.1	27.05	2.1869	1.4321
189.7	24.79	2.1605	1.3944
193.6	23.31	2.1424	1.3676

FIG. 8.5.

VISCOSITY OF PYRENE.

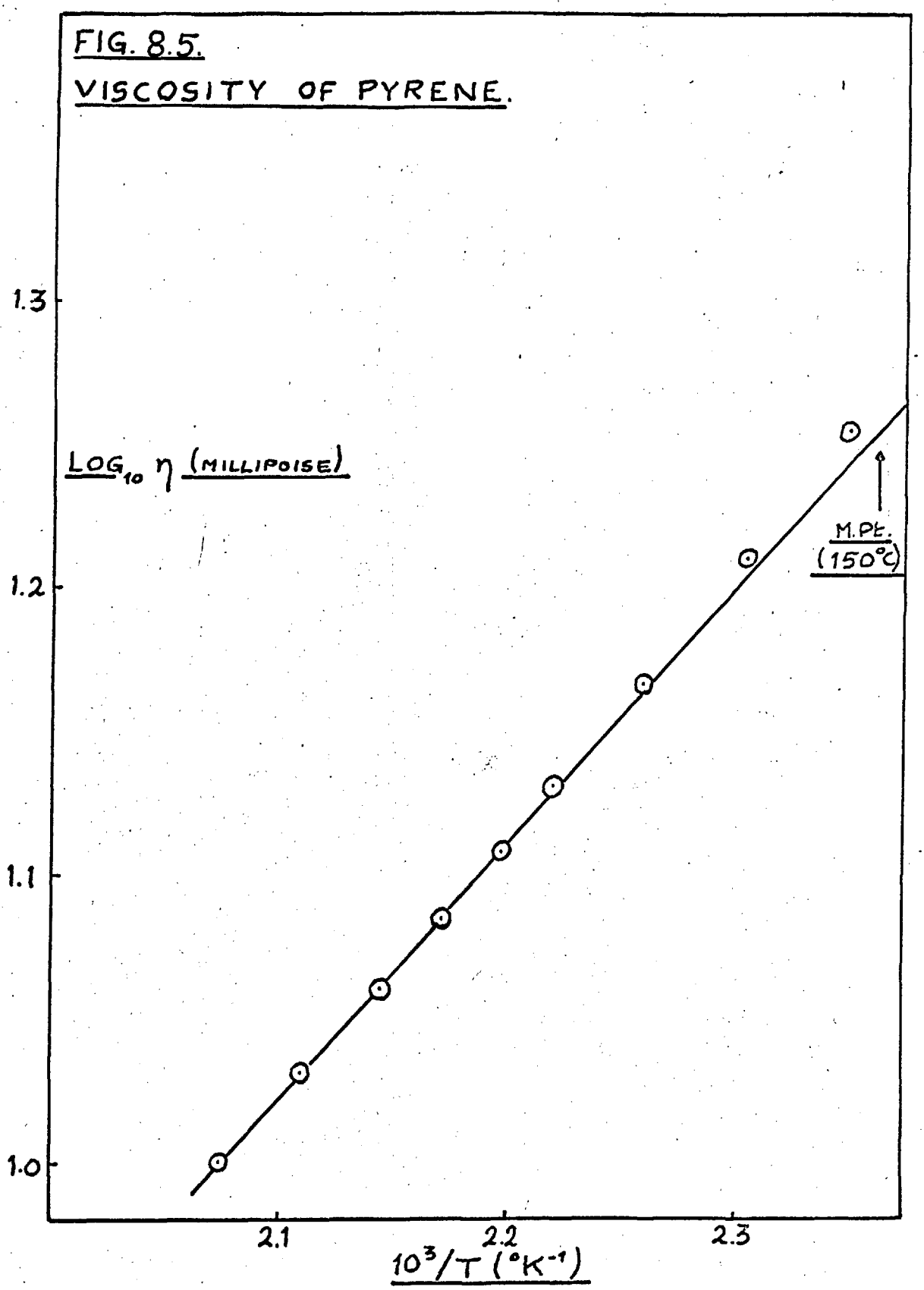

FIG. 8.6.

PRESSURE VS. RECIPROCAL FLOW-TIME ISOTHERMS FOR PYRENE.

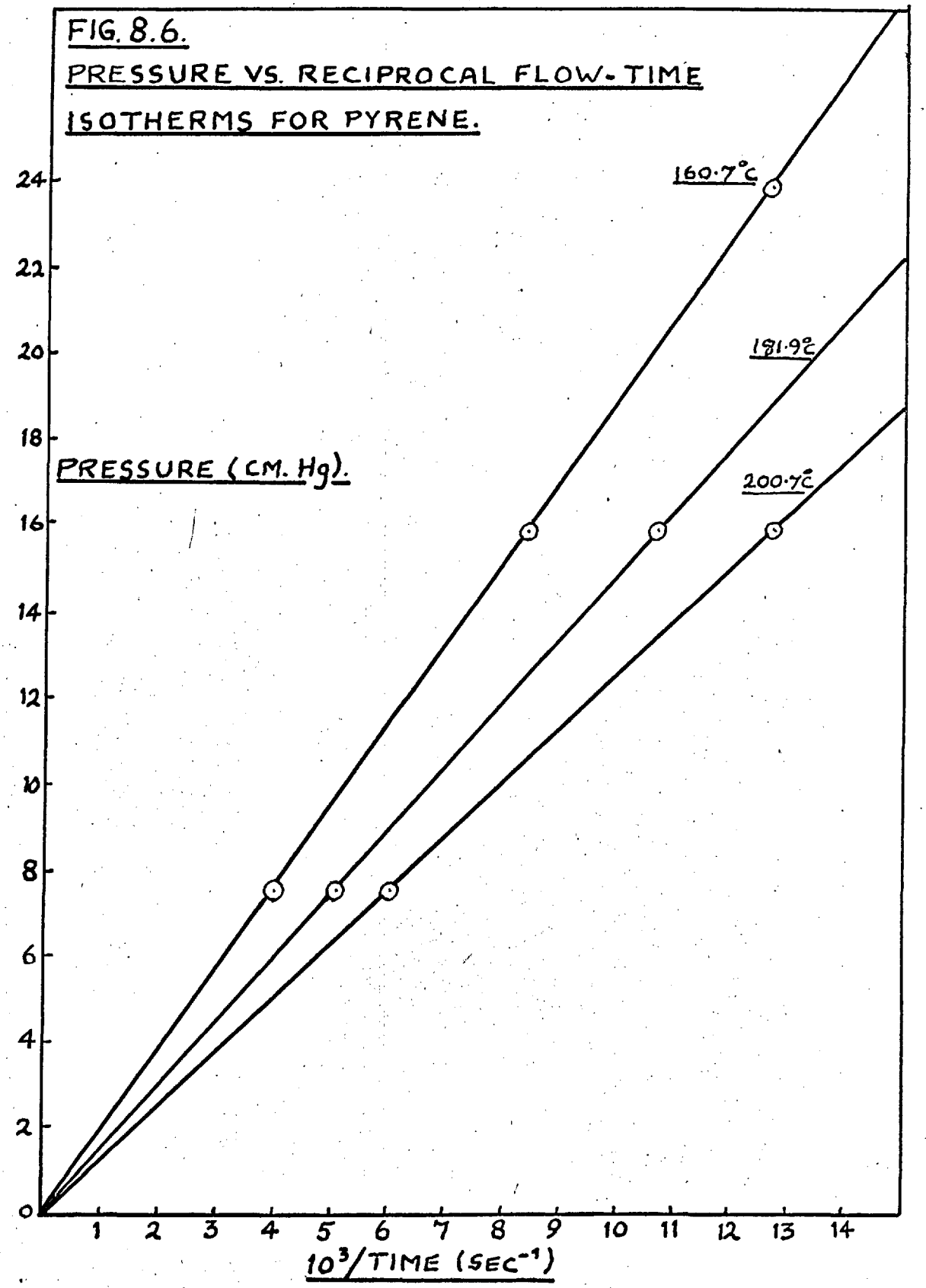

FIG. 8.7.

VISCOSITY OF TETRAPHENYL ALLENE - PYRENE MIXTURES

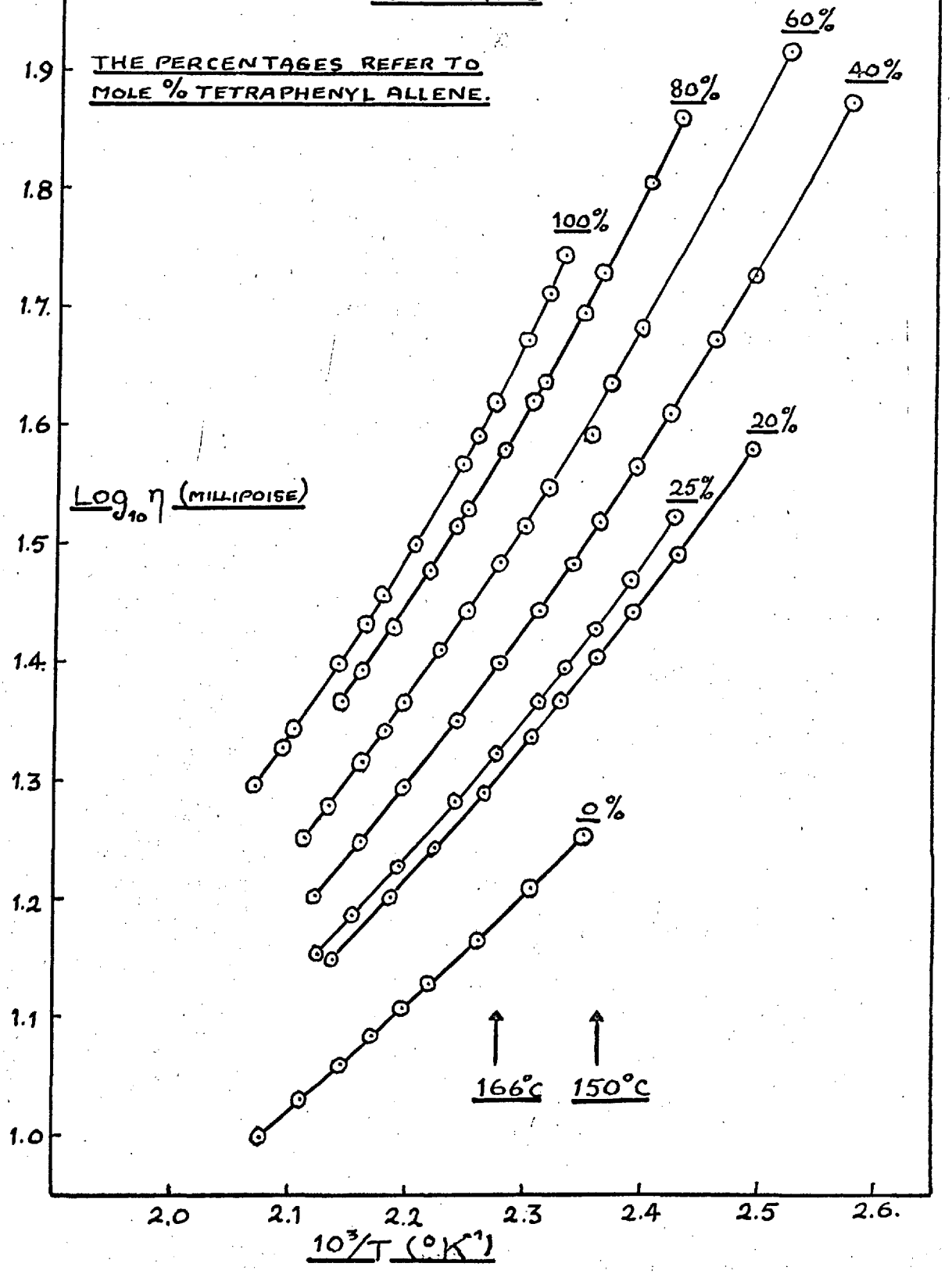

TABLE 8.3

VISCOSITY OF TRIPHENYL-α-NAPHTHYL ALLENE

Temperature °C	η (Millipoise)	$10^3/T°K$	$\log_{10}\eta$ (Millipoise)
Super-cooled liquid:			
135.7	773.52	2.4458	2.8886
137.7	668.34	2.4339	2.8250
Liquid:			
141.5	528.21	2.4116	2.7228
145.7	413.74	2.3874	2.6167
152.5	291.38	2.3493	2.4645
159.4	213.01	2.3118	2.3284
166.1	163.10	2.2768	2.2125
172.6	128.18	2.2434	2.1078
178.0	107.53	2.2165	2.0315
185.3	86.46	2.1812	1.9368
190.4	75.57	2.1572	1.8784
192.3	71.48	2.1484	1.8542

FIG. 8.8

VISCOSITY OF TRIPHENYL-α-NAPHTHYL ALLENE

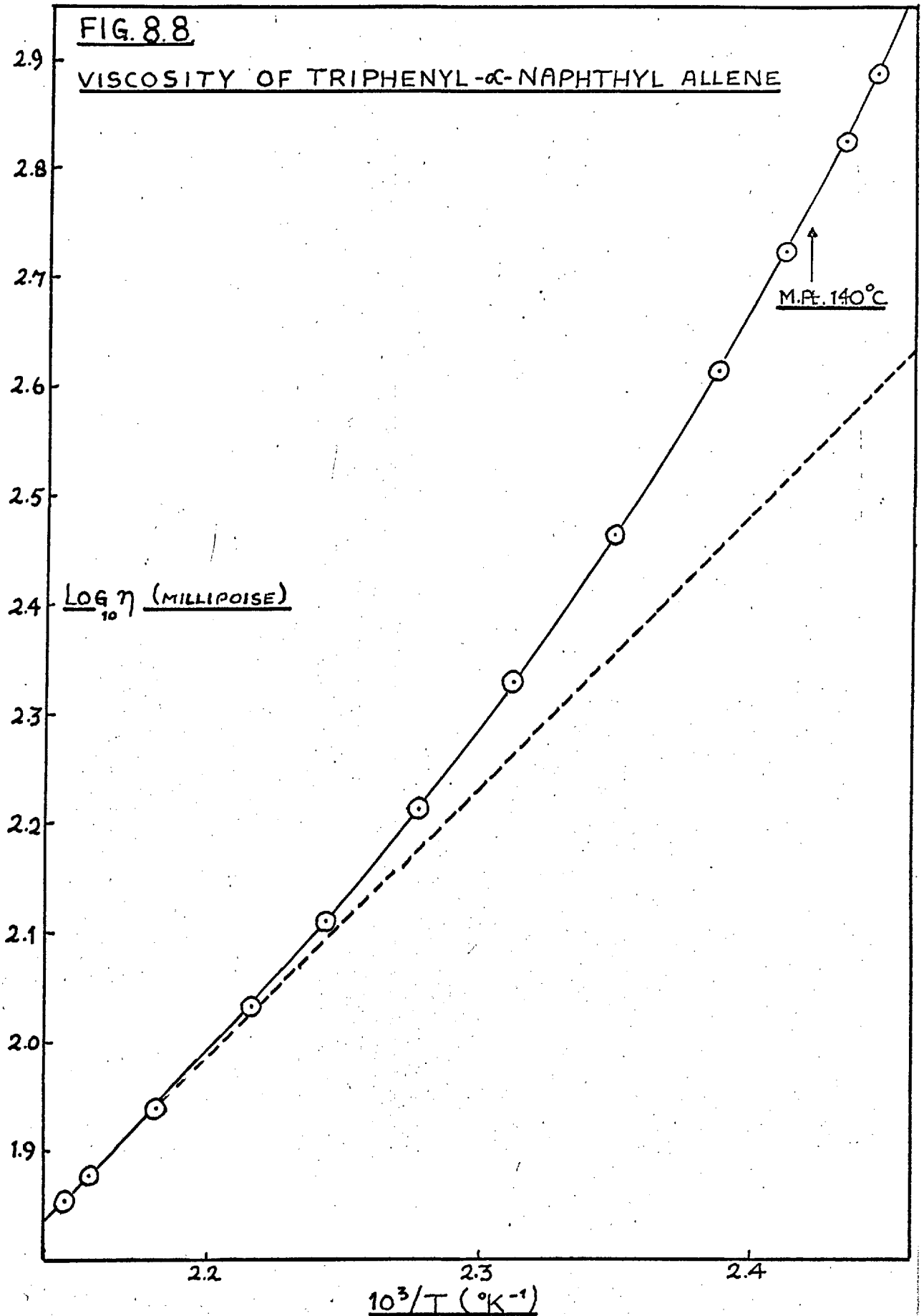

FIG. 8.9

PRESSURE VS. RECIPROCAL FLOW TIME ISOTHERMS FOR TRIPHENYL-α-NAPHTHYL ALLENE.

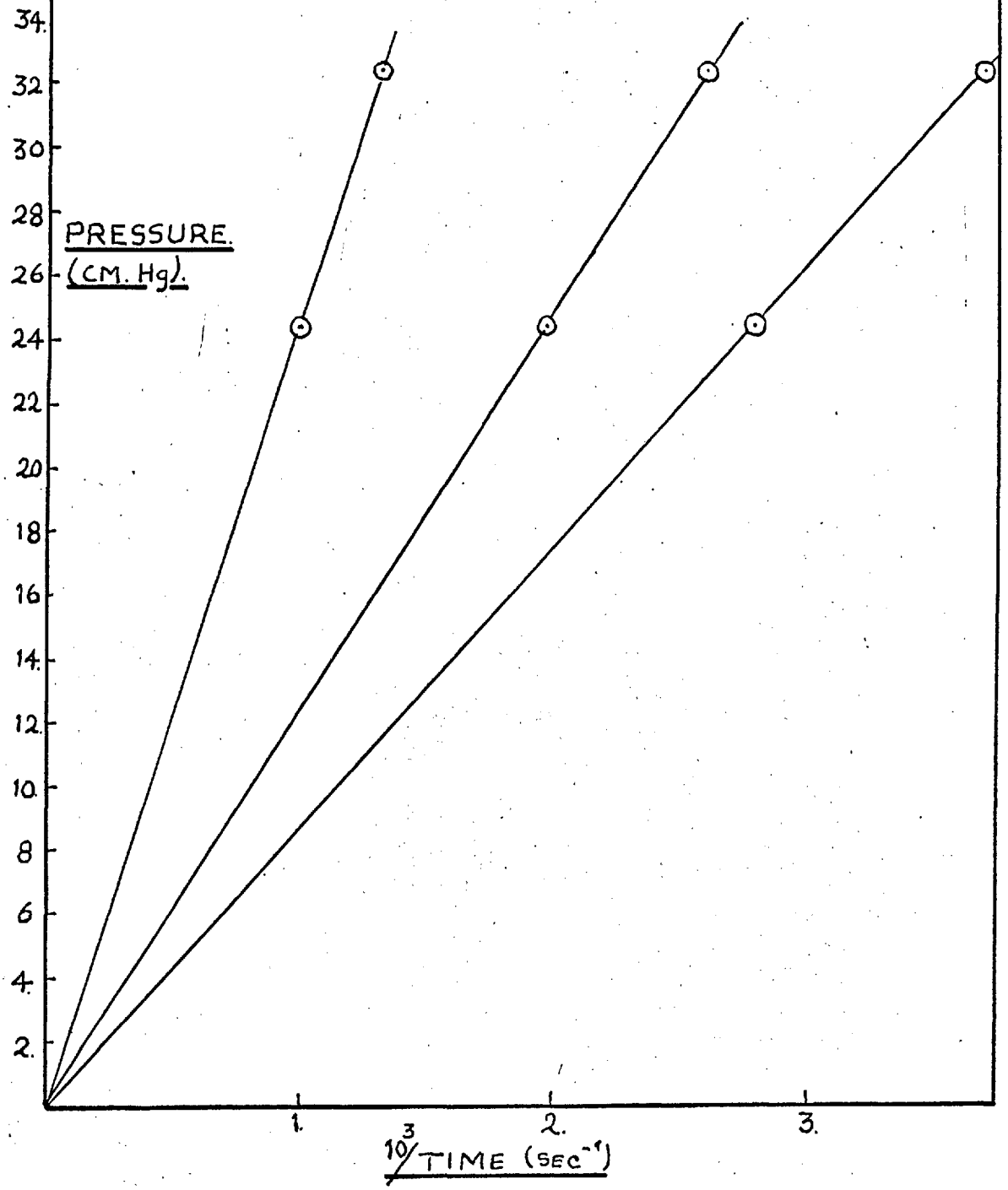

8.8 Experimental Accuracy of the Method.

The largest errors are encountered at high temperatures where the flow times are least, and where the kinetic energy correction attains it maximum value. The experimental quantities used in the following assessment of error obtain to this region and hence represent the maximum experimental error in the viscosity determinations.

In the equation

$$\eta = kPt - k'\rho/t \qquad (8.10)$$

c.f. Equation (8.6)

the term $k'\rho/t$ represents the kinetic energy correction. Bingham[6] asserts that the magnitude of this factor should never exceed 5% of the first term of the above equation. Provided that this condition is satisfied, the values of k' and ρ need only be known within an accuracy of 2% in order to permit the corrected viscosities to be determined to within $\pm$ 0.1 %.

The value of k is simply the reciprocal of the calibration constant C, the value and determination of which is described in section 8.6. The magnitude of k' is given by the expression

$$k' = \frac{1.12\ V}{8\ \pi\ l} \qquad (8.11)$$

c.f. equation(8.5).

V is the volume contained between the fiducial mark F_3 and the tip of the overflow device, l the total capillary length in centimetres and 1.12 represents an average value of the constant m

(see equation 8.5).

The volume V is also related to the calibration constant C, the capillary length l cm. and the radius r cm by the expression:

$$C = \frac{8Vl}{\pi r^4} \qquad (8.12)$$

As these quantities are known, V may be calculated

$$V = \frac{C\pi r^4}{8l} = \frac{115.6 \times 10^3 \times 981 \times 13.56 \times (0.015)^4 \times \pi}{8 \times 20}$$

$$= 1.52 \text{ mls.}$$

hence k' for the viscometer was:

$$k' = \frac{1.12 \times 1.52}{8 \times \pi \times 20} = 0.00338$$

and the kinetic energy correction, assuming a density of 1 $g.cm^{-3}$ and a minimum flow time of 80 secs. is given by:

$$0.00338 \times \frac{1}{80} = 0.000042 \text{ poise.}$$

The viscosity in this region is in the order of 10.0 millipoise. The maximum kinetic energy correction is thus in the order of 0.42 %.

The Couette correction is negligible provided the condition $l/r > 500$ is fulfilled, where l is the length of a single capillary. The ratio for this viscometer was 667 and therefore this correction can be neglected.

The Reynolds number of the liquid at the highest rate of

shear was calculated to be ~ 80. Since this is well below the critical value above which turbulent flow may commence (c.a. 1150) the flow was always streamline.

The maximum errors incurred in the measurement of pressure and flow time were in the order of 0.1 % and 0.25 % respectively. The experimental error in the determination of viscosity was therefore 0.35 %. Since this is exceeded by the maximum kinetic energy correction by only 0.07 %, the kinetic energy correction was not applied.

At lower temperatures the flow times and the applied pressures encountered increase; the experimental error decreases and the kinetic energy correction becomes insignificant. At no time was a viscosity of less than 10 millipoise recorded.

According to some authorities, the kinetic energy correction for the type of viscometer used in this work does not exceed 0.1 %[9,10]. In view of the calculations presented above, the present author considers that the kinetic energy correction must necessarily depend upon both the specific parameters of the viscometer used and upon the nature of the liquid under investigation.

REFERENCES

1. Rogers, S.E. and Ubbelohde, A.R., Trans. Faraday Soc., 46, 1051 (1950).
2. Ogawa, Kiyoichi, Japan Inst. Metals, B 14, 49 (1950).
3. Poiseuille, J.L.M., Compt. Rend. 11, 961, 1041 (1840). 12, 112 (1841).
4. Hagenbach, E., Pogg. Ann. 99, 221 (1856).
5. Couette, M., Ann. Chim. Phys., 21, 433 (1890).
6. Bingham, E.C. "Fluidity and Plasticity", McGraw Hill, New York (1922).
7. Ubbelohde, S.E., Handb. d. Chemie und Technologie d. Oele und Fette., Vol. I, Hinzel (1908).
8. Smith, W.E., Ph.D. Thesis, University of London (1965).
9. Stross, F.H. and Porter, P.E., Encyclopaedia of Chem. Tech., 14, 764 (1955).
10. Frame, J., Ph.D. Thesis, University of London, (1961).

CHAPTER 9.

THE MEASUREMENT OF MOLAR VOLUME

This chapter is divided into two parts. Part I is devoted to the techniques employed to determine the molar volumes of melts and the resulting data obtained. These melts include tetraphenyl allene, pyrene, tetraphenyl allene/pyrene mixtures, and triphenyl-α-naphthyl allene.

Part II deals with the dilatometric techniques used to determine the molar volumes of the crystalline, liquid, and glass regions of triphenyl-α-naphthyl allene, triphenyl-4-biphenyl allene, and the data so obtained.

PART I - THE MOLAR VOLUMES OF THE MELTS

9.1.1. The method involved the balancing of a hydrostatic head due to the liquid, against that due to a suitable reference liquid at room temperature. If the dimensions of the densitometer are accurately known, the change in hydrostatic pressure may be related to the change in volume of the liquid as the temperature is varied.

9.1.2. Construction of the Densitometer.

The densitometer was built to a design first proposed by Husband (1958)[1]. The original design has been modified by McAuley (1965)[2] and the instrument used in the present work was further modified to allow the use of comparatively small quantities of material (c.a. 4g).

The densitometer, illustrated in Fig. 9.1.1, consisted of a bulb Z surmounted by two lengths of 1 mm. precision bore veridia capillary tubing. As the temperature was raised, the liquid contained in the instrument was allowed to expand up the longer section of capillary which forms limb Y of the instrument. The liquid meniscus was maintained level with fiducial mark F_1 by the application of a suitable pressure of "white-spot" nitrogen to limb X.

Above the first fiducial mark (F_1) was a small bulb (B) and another short capillary section bearing fiducial mark (F_2). This allowed a larger temperature range to be covered. The volume of bulb (B) was adjusted to be as nearly equal as possible to the volume contained by the long capillary of limb Y. When the expansion from mark F_1 approached the top of limb Y, a change to mark F_2 allowed the process to be repeated. The bulb (A) and the surmounting capillary section bearing the fiducial mark F_3 allowed the temperature range to be extended still further.

The pressure required to bring the meniscus of the liquid to the appropriate fiducial mark was developed by the adjustable constant head device, also illustrated in Fig. 9.1.1. "White-spot" nitrogen was supplied through an overflow device, containing di-n-butyl phthalate*, which maintained the constant head; then

---

* This liquid was chosen because of its low volatility and chemical stability.

FIG. 9.1.1

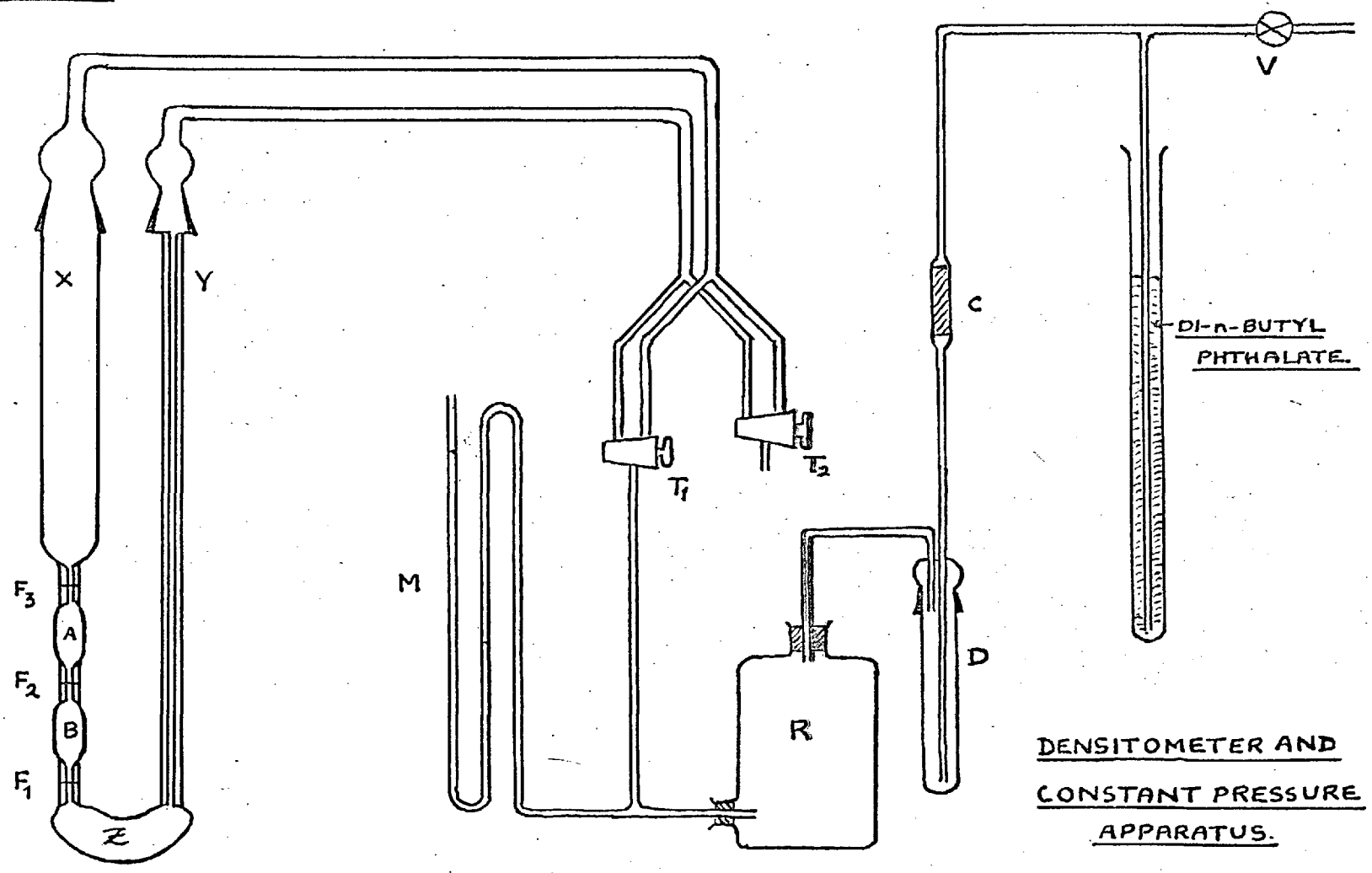

DENSITOMETER AND CONSTANT PRESSURE APPARATUS.

through a glass-wool plug C, a cold trap D and a 20 litre ballast volume R to the manometer M, which also contained di-n-butyl phthalate. The two-way tap system (taps T_1 and T_2) permitted pressure to be applied to either limb of the densitometer as required.

9.1.3. Derivation of Formula

The salient features of the densitometric technique are illustrated schematically in Fig. 9.1.2. below.

FIGURE 9.1.2

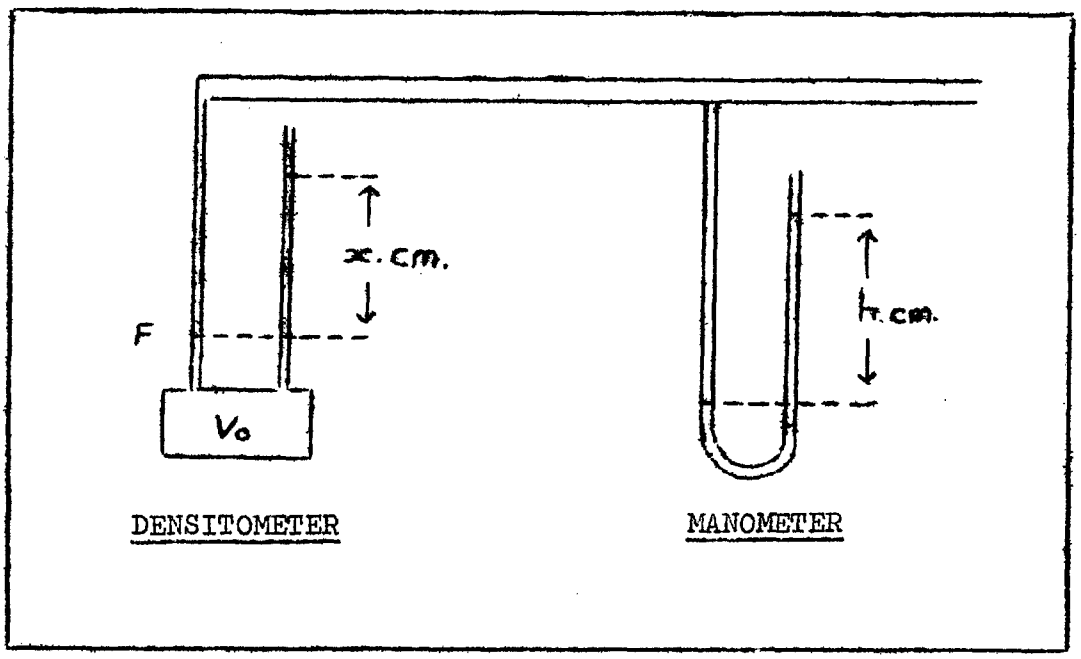

The excess pressure applied to support the column of liquid in the densitometer is given by:

$$p = x\rho = h\rho_o \qquad (9.1.11.)$$

where p is the applied pressure, x and h the differences in levels in the densitometer and manometer respectively, and ρ and ρ_o the densities of the liquids contained in the densitometer and the manometer respectively. The densitometer consists of a volume V_o surmounted by a precision bore capillary of cross-sectional area A cm^2, and the volume of liquid in this tube will be given by:

$$V = V_o + Ax \qquad (9.1.2.)$$

Therefore:

$$x = \frac{V - V_o}{A} \qquad (9.1.3)$$

Thus, from equation (9.1):

$$h\rho_o = \left(\frac{V - V_o}{A} \right) \rho \qquad (9.1.4)$$

Since $\rho = M/V$, where M is the weight of liquid contained in the volume V of the densitometer in use:

$$Ah\rho_o = M - \frac{MV_o}{V} \qquad (9.1.5)$$

Hence:
$$V = \frac{MV_o}{M - A\rho_o h} \qquad (9.1.6)$$

If the effective molecular weight of the liquid or liquid mixture is Wg., then its molar volume (V_m) is given by:

$$V_m = \frac{WV_o}{M - A\rho_o h} \qquad (9.1.7)$$

Thus, once the densitometer has been calibrated, only the

external pressure required to bring the liquid level to the appropriate mark in limb X needs to be measured. This pressure is considered positive if applied to limb X, and negative if applied to limb Y. With the densitometer used in the present work, the volumes of bulbs A and B were so nearly equal to the volume contained in limb Y that it was unnecessary to cover any overlap in volume by applying pressure to limb Y.

9.1.4. Calibration of the Densitometer.

The volume V_o was determined for each fiducial mark by filling to the mark with freshly distilled water. For the calibration, the densitometer was immersed in a Townson and Mercer water thermostat bath maintained at 25°C. (See Chapter 7 section 7.3). The values of V_o so obtained were corrected to each working temperature using a value of 9.90×10^{-6} for the coefficient of expansion of 'pyrex' glass[3].

The 1 mm. bore veridia capillary tubing was checked by weighing a thread of mercury of known length contained in the capillary. At room temperature the diameter was 1.0007 mm., well within the manufacturers tolerance of $\pm$ 0.01 mm. The capillary bore was corrected to each working temperature.

The values used for the density of di-n-butyl phthalate (supplied by B.D.H.) were those obtained by Cleaver[4] and later checked by McAuley[2], and are shown in Fig. 9.1.3.

FIG. 9.1.3.

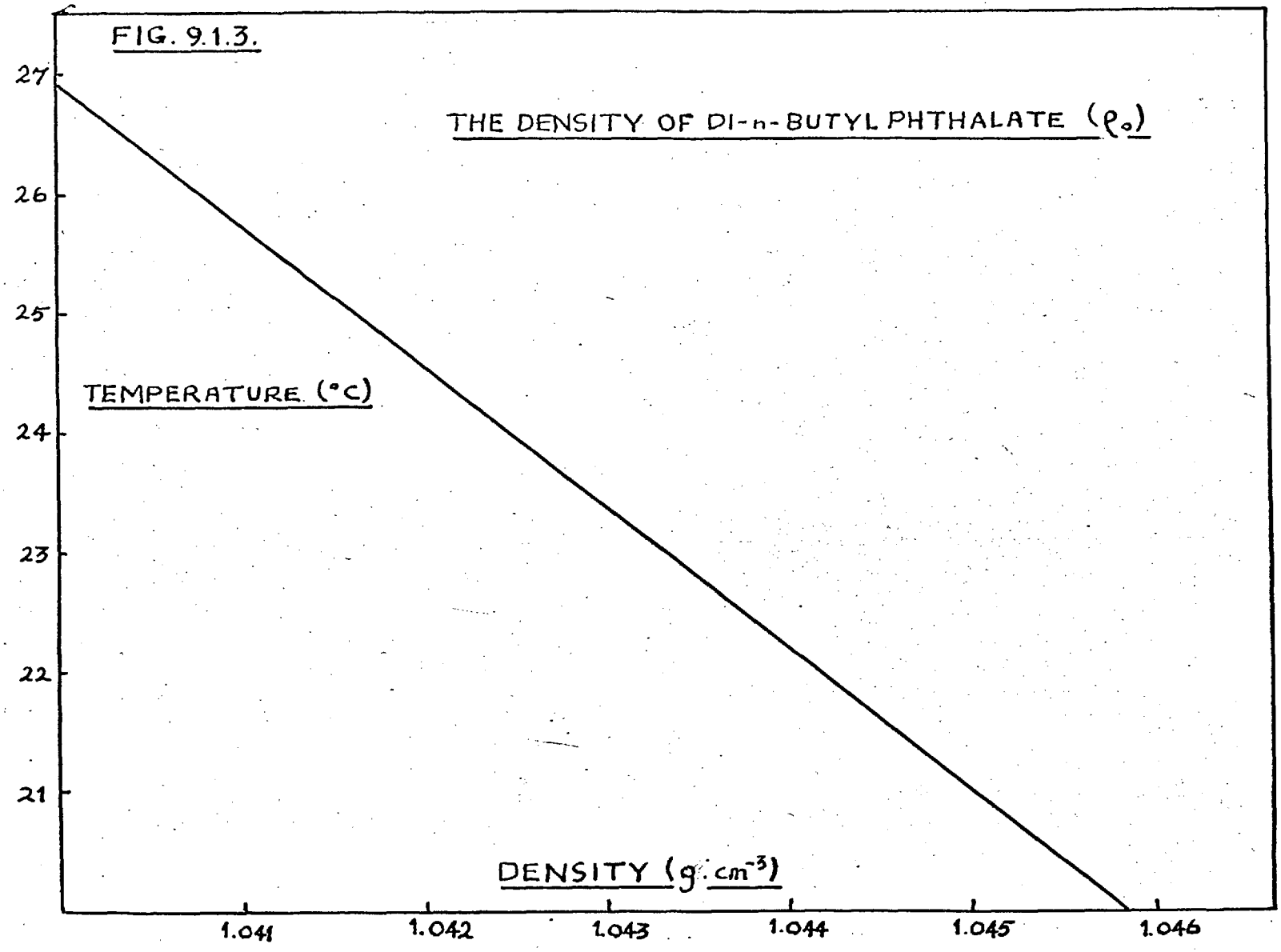
THE DENSITY OF DI-n-BUTYL PHTHALATE (ρ_o)
TEMPERATURE (°C)
27
26
25
24
23
22
21
DENSITY (g.cm^{-3})
1.041
1.042
1.043
1.044
1.045
1.046

9.1.5. The Measurement of Molar Volume of the Melts.

The molar volumes of tetraphenyl allene, pyrene, tetraphenyl allene/pyrene mixtures, and triphenyl-α-naphthyl allene were determined at various temperatures according to the following procedure.

The needle valve V was opened to the nitrogen supply, and the constant pressure device regulated to provide a pressure of about 10 cm. di-n-butyl phthalate. The densitometer was attached to the pressure apparatus as indicated in Fig. 9.1.1., and taps T_1 and T_2 adjusted to allow nitrogen to flow through limb Y, flushing out the instrument.

In order to avoid the retention of material on the sides of the wide section of limb X after the molten material had filled the densitometer, the simple filling device illustrated in Fig. 9.1.4. was used. This consisted of a tube just small enough to fit into the wide section of limb X of the densitometer. At one end of the tube was attached a socket, fitting the cone which formed the top of limb X. The other end of the tube was drawn out to a capillary extending into the neck of the upper section of capillary bearing the fiducial mark F_3. The approximate quantity of material required to fill the densitometer was introduced into the filling device via a funnel. The filling device was then inserted into limb X of the densitometer and attached to the pressure system as

FIGURE 9.1.4.

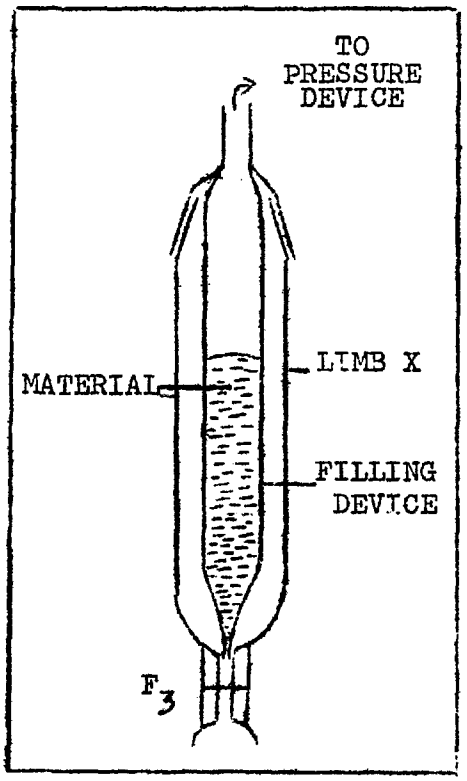

indicated in Fig. 9.1.4. The nitrogen supply connected to limb Y was then allowed to flush out the solid material contained in the filling device.

After a few minutes the densitometer was clamped to a steel support rod and lowered into the thermostat bath which was maintained at a temperature about 5°C above the melting point of the material. As the material melted, the variable head of the pressure apparatus was increased to allow nitrogen to

bubble very gently through the melt. This technique proved particularly useful when dealing with the tetraphenyl allene/pyrene mixtures in which a eutectic mixture tended to melt first. By increasing the pressure head it was possible to prevent the mixture from entering the densitometer until it was both molten and homogeneous. The melt was forced into the densitometer by transferring the pressure from limb Y to limb X. Gas bubbles trapped in bulb Z were removed by alternately transferring the applied pressure from limb X to limb Y. When the densitometer had been filled and the pressure reduced to a few millimetres of di-n-butyl phthalate applied to limb Y, the filling device was detached from the pressure apparatus and removed from limb X. Limb X was then directly attached to the pressure apparatus as indicated in Fig. 9.1.1. During this operation a stream of nitrogen from a source independent of the pressure apparatus was directed intc limb X to minimise the entry of atmospheric oxygen.

The data for each liquid were obtained by adjusting the overflow of the constant head device until a steady stream of bubbles emerged and the meniscus of the liquid in the densitometer was levelled at the appropriate fiducial mark. The applied pressure was measured on the manometer by means of a Pye cathetometer reading to 0.001 cm. Readings were obtained as the temperature was both raised and lowered.

After the temperature range had been covered, the melt was forced into limb X of the densitometer, and the bulk carefully emptied into a tared beaker. The beaker and its contents were allowed to cool in a desiccator, free from contamination with dust, and then weighed. The densitometer was cleaned externally and weighed*. From the combined weights, the weight of material used in the experiment was determined.

9.1.6. Results.

The molar volume data obtained for the tetraphenyl allene/pyrene mixtures are listed in tables 9.1.1a to 9.1.1h , and are illustrated in Fig. 9.1.5. The data obtained for triphenyl-α-naphthyl allene are listed in table 9.1.2. and illustrated in Fig. 9.1.8. Linear equations have been calculated to fit these lines, and the relevant equation for each set of data may be found at the head of each table. Fig. 9.1.6. illustrates the expansion parameters for the tetraphenyl allene/pyrene mixtures. The excess volumes of mixing and the percentage excess volumes of mixing at three different temperatures are represented in Figs. 9.1.7. and 9.1.7a. respectively. The nature and interpretation of these plots will be discussed in Chapter 10 section 10.4.2.

---

* A satisfactory solution for use in removing silicone oils from glass-wear was found to be a mixture containing equal volumes of acetone and chloroform. Before weighing, the densitometer was handled using a piece of chamois leather. Paper towels not only contaminate the apparatus with traces of cellulose but tend to electrostatically charge the glass surface.

TABLE 9.1.1.a.

MOLAR VOLUMES OF THE TETRAPHENYL ALLENE - PYRENE SYSTEM

Mole % tetraphenyl allene = 0.00		Mole % tetraphenyl allene = 10.00	
Least squares fit for line: $V_M = 0.1137\ T(^oK) + 136.4033$		Least squares fit for line: $V_M = 0.1276\ T(^oK) + 146.0680$	
Molar volume V_M (mls)	Temperature ^oC	Molar volume V_M (mls)	Temperature ^oC
		199.1699	143.2
185.0198	154.0	199.4668	145.4
185.5016	158.5	200.4558	152.8
186.6506	169.3	200.4205	153.0
187.5593	177.3	201.2572	159.9
188.4226	184.7	202.3263	168.0
189.3731	192.1	202.4046	168.4
190.9641	206.6	203.2564	175.4
		204.7814	187.2
		205.5313	192.8
Molecular weight of mixture = 202.240		Molecular weight of mixture = 216.459	

TABLE 9.1.1.b

Mole % tetraphenyl allene = 20.00		Mole % tetraphenyl allene = 25.00	
Least squares fit for line: V_M = 0.1429 T(^oK) + 155.2939		Least squares fit for line: V_M = 0.1496 T(^oK) + 160.2892	
Molar volume V_M (mls)	Temperature ^oC	Molar volume V_M (mls)	Temperature ^oC
214.7016	142.4	222.7801	144.1
215.9804	151.8	224.0430	153.5
217.0359	159.0	225.2902	161.5
218.2602	168.0	226.3737	168.9
219.9762	179.5	228.8245	185.3
220.6510	184.4	229.8931	192.3
221.6093	190.8	230.6618	196.9
Molecular weight of mixture = 230.678		Molecular weight of mixture = 237.788	

9.1.1.c.

Mole % tetraphenyl allene = 40.00		Mole % tetraphenyl allene = 45.00	
Least squares fit for line: V_M = 0.1765 T(°K) + 172.4086		Least squares fit for line: V_M = 0.1841 T(°K) + 177.0193	
Molar volume V_M (mls)	Temperature °C	Molar volume V_M (mls)	Temperature °C
245.2548	139.3	251.6925	130.9
246.3751	145.7	253.4000	140.8
247.2437	151.0	254.3034	146.4
248.3910	157.6	255.5638	153.5
249.8310	166.1	256.9946	161.5
251.3887	175.0	258.4588	169.5
252.3570	180.1	259.8263	176.5
253.5347	186.5	261.3343	184.8
254.5860	191.8	262.3527	190.3
Molecular weight of mixture = 259.116		Molecular weight of mixture = 266.226	

TABLE 9.1.1.d

Mole % tetraphenyl allene = 50.00		Mole % tetraphenyl allene = 55.00	
Least squares fit for line: V_M = 0.1950 T(°K) + 180.1922		Least squares fit for line: V_M = 0.1957 T(°K) + 188.0069	
Molar volume V_M (mls)	Temperature °C	Molar volume V_M (mls)	Temperature °C
262.7592	150.6	267.9639	134.7
263.7883	156.1	269.4504	142.8
264.8149	161.4	271.0049	151.3
265.6710	166.3	272.0945	156.9
266.6921	171.6	273.0125	161.7
269.0113	183.1	274.1224	166.9
269.9257	187.7	277.2552	182.6
270.9684	192.7	278.9613	191.3
Molecular weight of mixture = 273.335		Molecular weight of mixture = 280.445	

TABLE 9.1.1.e.

Mole % tetraphenyl allene = 60.00		Mole % tetraphenyl allene = 65.00	
Least squares fit for line: V_M = 0.2031 T(°K) + 192.8596		Least squares fit for line: V_M = 0.2118 T(°K) + 196.9375	
Molar volume V_M(mls)	Temperature °C	Molar volume V_M (mls)	Temperature °C
275.0109	130.4	286.6428	149.6
277.8313	145.3	287.8670	156.2
279.0265	151.5	288.1386	157.7
280.2371	157.4	289.3713	163.2
281.9122	166.0	289.7009	165.3
283.6484	174.2	291.4024	173.2
285.3350	182.1	293.2720	181.8
287.8359	193.7	294.4609	187.1
		295.2882	190.8
Molecular weight of mixture = 287.554		Molecular weight of mixture = 294.664	

TABLE 9.1.1.f.

Mole % tetraphenyl allene = 75.00		Mole % tetraphenyl allene = 80.00	
Least squares fit for line: V_M = 0.2300 T(°K) + 204.8798		Least squares fit for line: V_M = 0.2405 T(°K) + 208.0096	
Molar volume V_M(mls)	Temperature °C	Molar volume V_M(mls)	Temperature °C
301.1242	144.7	310.9056	154.1
302.8824	152.9	312.5255	161.9
304.2827	159.2	313.6669	166.4
304.6507	160.8	315.3556	173.5
306.0044	166.7	316.4079	177.7
306.0236	166.9	318.1235	184.6
307.8683	174.7	319.2425	189.2
309.7375	182.7	319.9958	192.5
311.1047	188.6		
311.9639	192.1		
Molecular weight of mixture = 308.883		Molecular weight of mixture = 315.992.	

TABLE 9.1.1.g.

Mole % tetraphenyl allene = 90.00		Mole % tetraphenyl allene = 95.00	
Least squares fit for line: V_M = 0.2639 T(^oK) + 213.3707		Least squares fit for line: V_M = 0.2614 T(^oK) + 222.0770	
Molar volume V_M(mls)	Temperature ^oC	Molar volume V_M(mls)	Temperature ^oC
327.7659	159.9	336.3339	164.0
329.3520	166.7	337.4821	168.5
330.6539	171.5	338.8843	173.6
331.9282	176.4	340.2001	179.0
333.3361	181.3	341.4846	183.7
334.3594	185.2	342.3470	186.0
335.3003	188.8	343.6134	191.9
336.3294	192.8		
Molecular weight of mixture = 330.211		Molecular weight of mixture = 337.321	

TABLE 9.1.1.h.

Mole % tetraphenyl allene = 100.00	
Least squares fit for line: $V_M = 0.2774\ T(^{\circ}K) + 221.5488$	
Molar volume V_M (mls)	Temperature $^{\circ}C$
344.1187	168.6
345.5791	173.7
346.7620	177.9
347.3109	180.0
347.8502	182.5
349.3800	188.0
351.0667	193.5
352.3922	198.2
Molecular weight of mixture = 344.430	

FIG. 9.1.5.

MOLAR VOLUME VS. TEMPERATURE PLOTS.

TETRAPHENYL ALLENE / PYRENE SYSTEM.

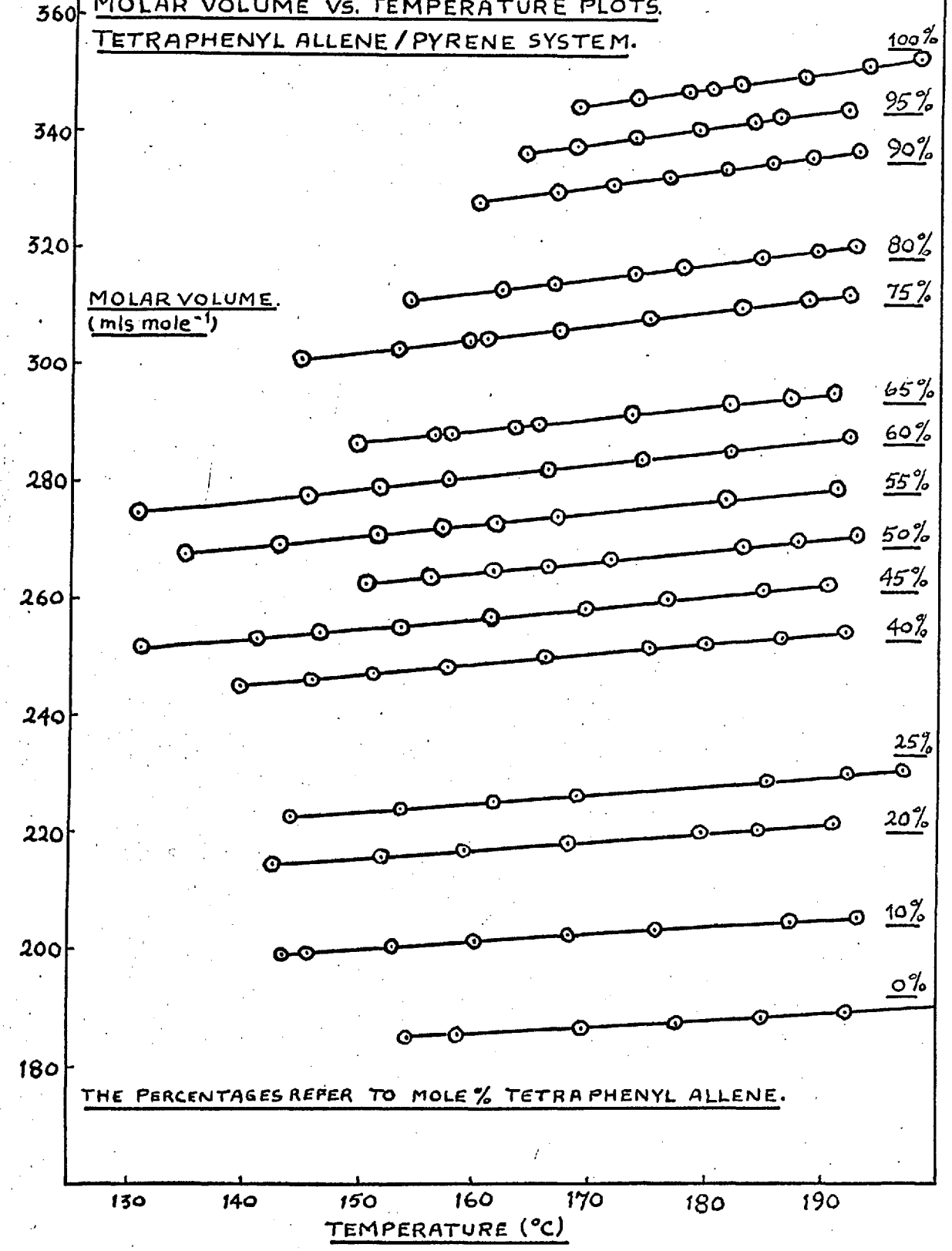

THE PERCENTAGES REFER TO MOLE % TETRAPHENYL ALLENE.

FIG. 9.1.6.

EXPANSION PARAMETER VS. COMPOSITION

(TETRAPHENYL ALLENE/PYRENE SYSTEM)

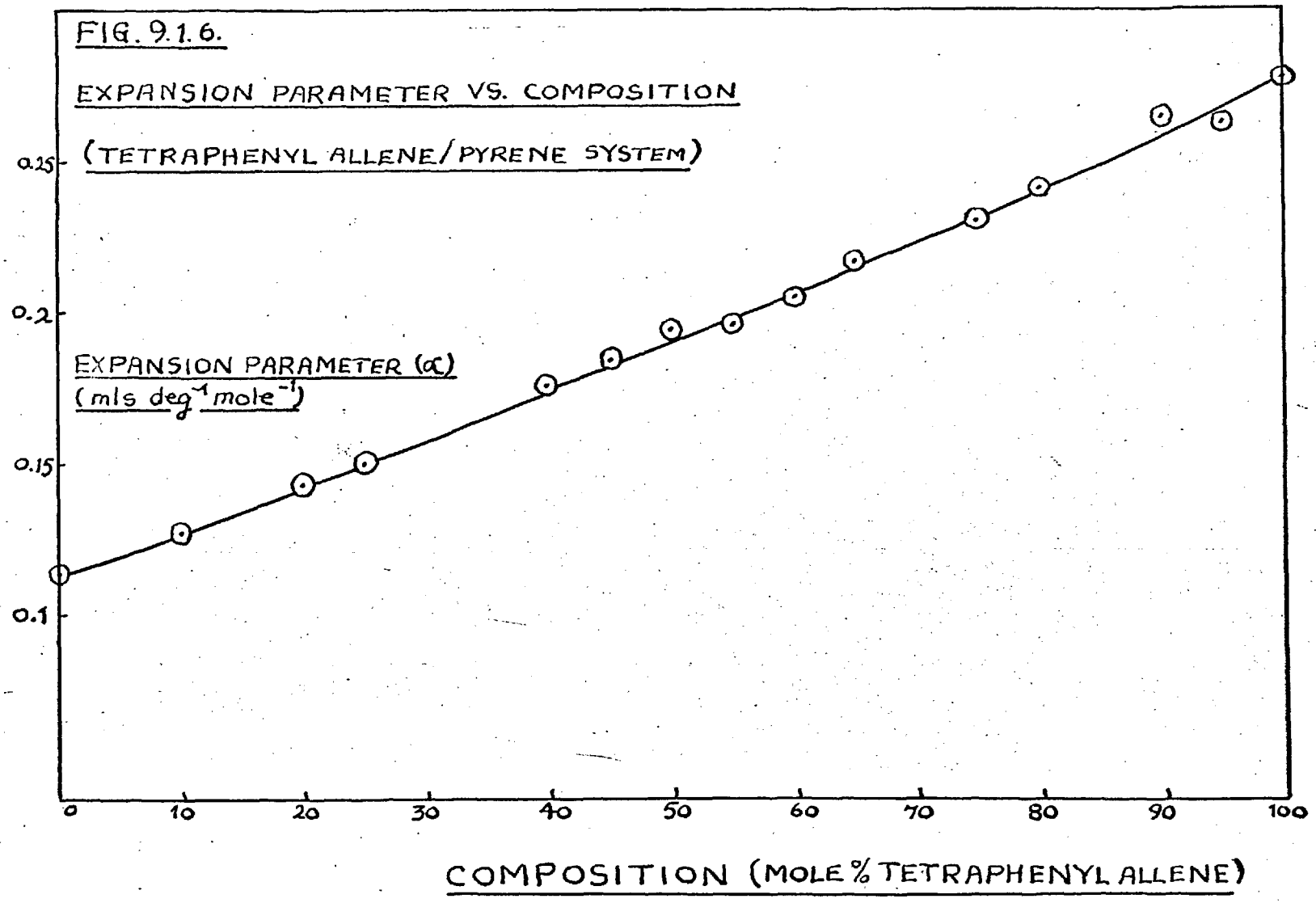

FIG. 9.1.7.

EXCESS VOLUMES OF MIXING :- TETRAPHENYL ALLENE / PYRENE SYSTEM.

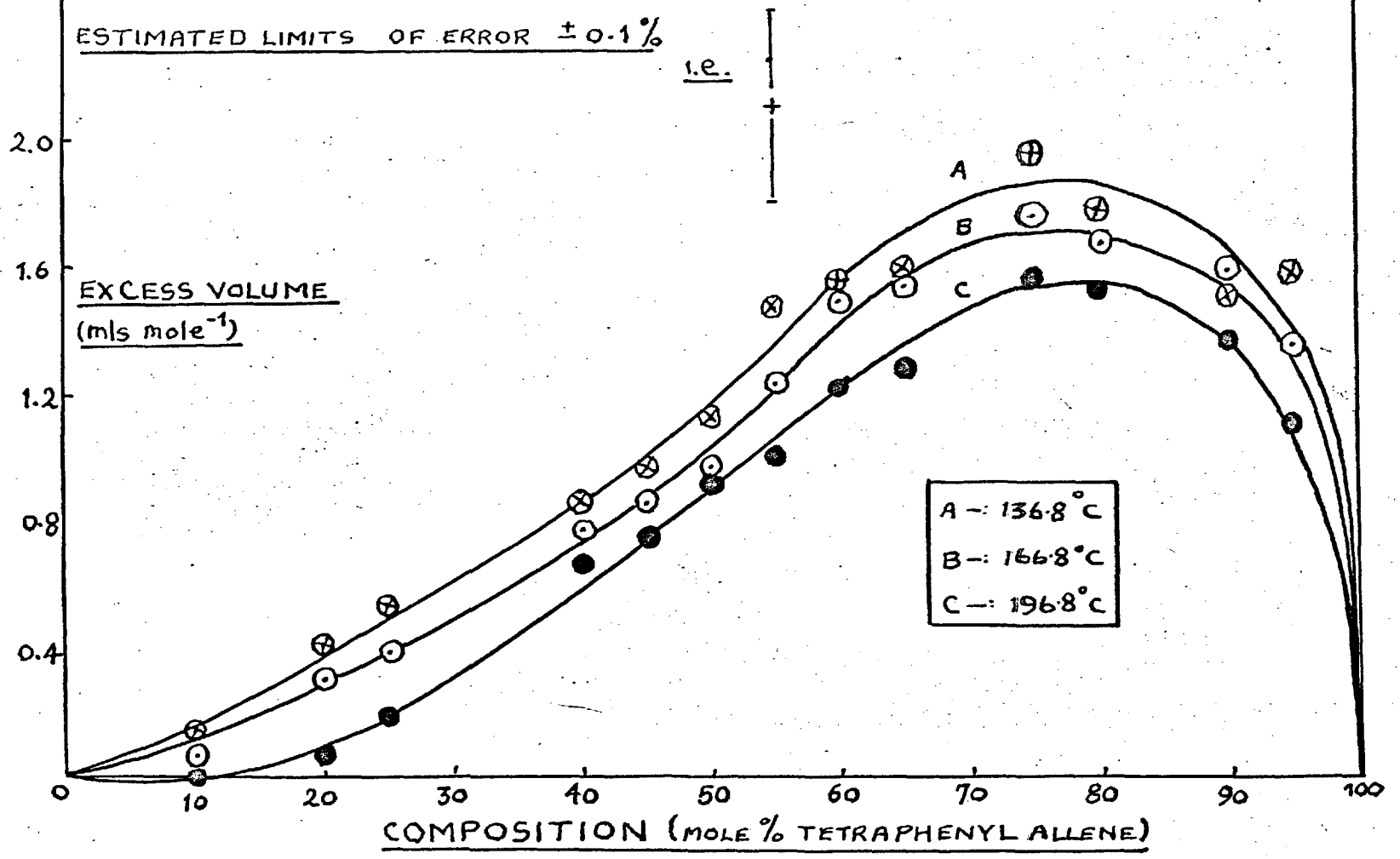

FIG. 9.1.7a.

PERCENTAGE EXCESS VOLUMES OF MIXING.
VS. COMPOSITION.

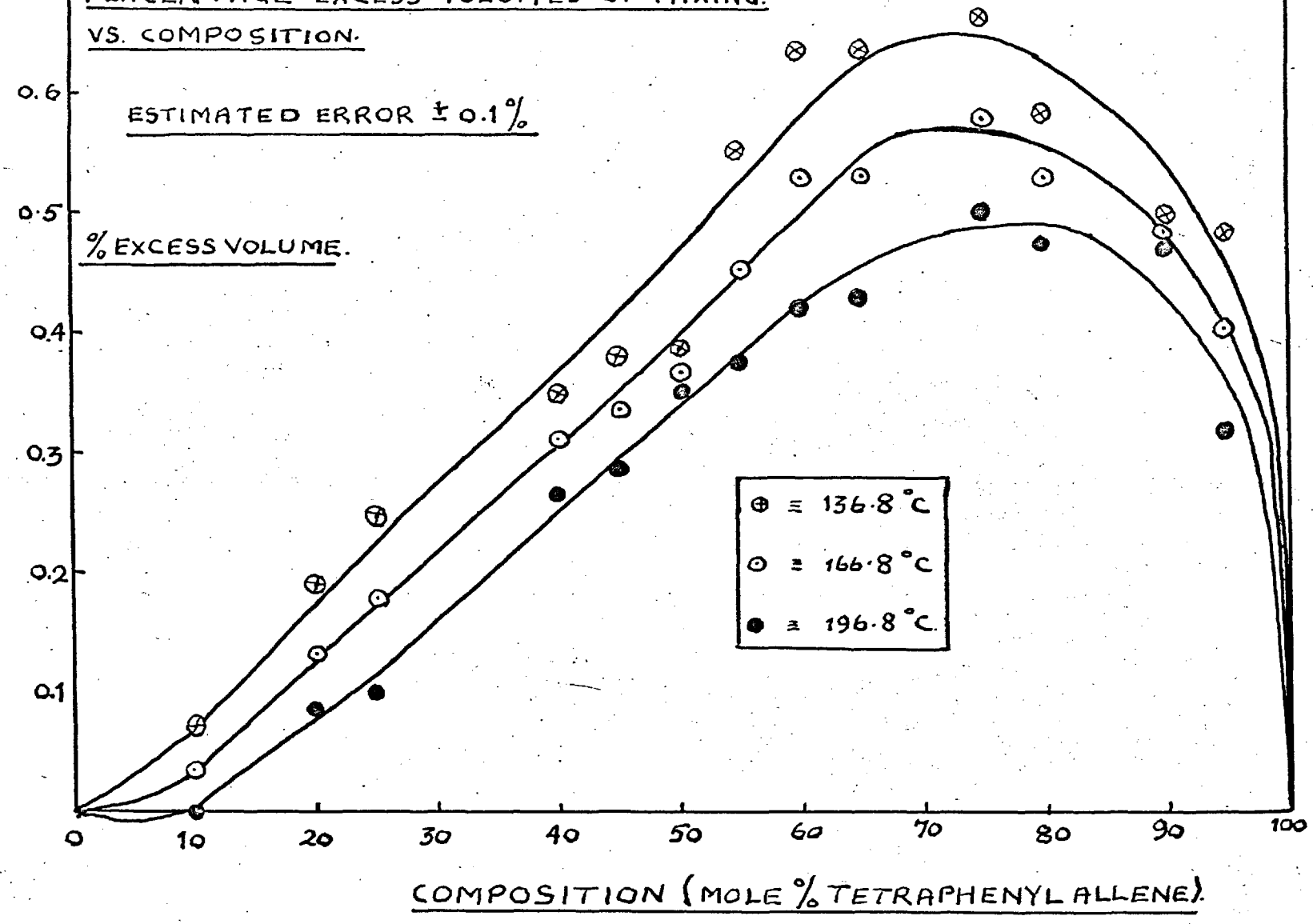

TABLE 9.1.2.

MOLAR VOLUME OF
TRIPHENYL-α-NAPHTHYL ALLENE

Least squares fit for line: $V_M = 0.2827\ T(^oK) + 258.1490$	
Molar volume V_M	Temperature ^oC
375.7509	142.8
378.0961	151.3
379.5953	156.8
381.2238	162.2
383.0979	169.1
384.5852	173.6
385.7538	178.7
387.3456	183.8
388.4922	189.2
Molecular weight = 394.486	

FIG. 9.1.8

MOLAR VOLUME VS. TEMPERATURE PLOT FOR TRIPHENYL-α-NAPHTHYL ALLENE.

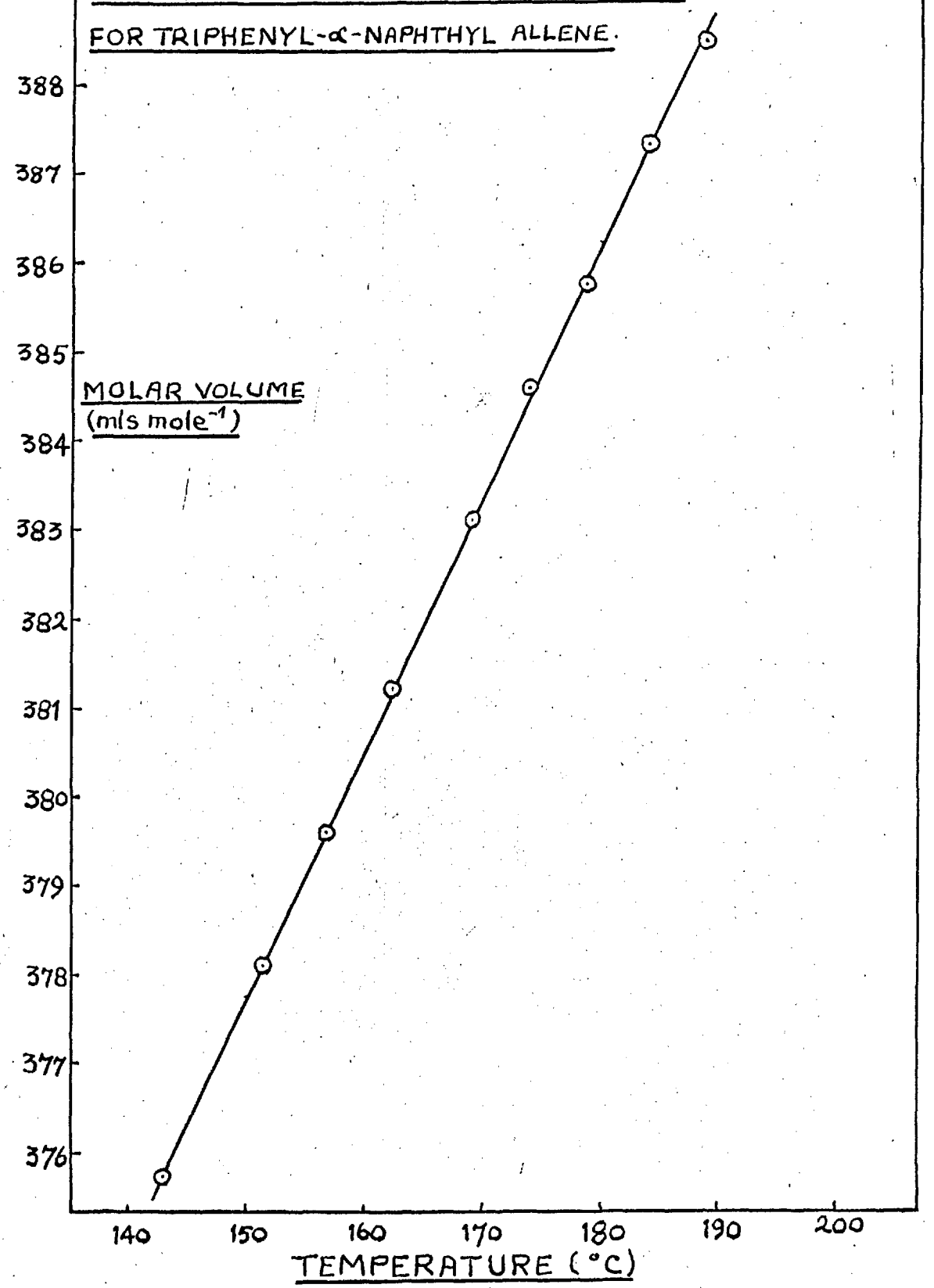

9.1.7. Errors

An error in the molar volume V_M arises from small errors in each of the quantities expressed in the right-hand side of equation 9.1.8 below:

$$V_M = \frac{WV_o}{M - A\rho_o h} \qquad (9.1.8)$$

(c.f. section 9.1.3).

The molecular weight W, of the material under investigation is independent of the measurements connected with the densitometer. Errors in the calibration volume V_o, the cross-sectional area of the capillary A, and the density of di-n-butyl phthalate ρ_o, are, to a first approximation, systematic errors applicable equally to the whole family of data. Errors in the mass M, of material are consistent for each particular set of data, and errors in the height h registered on the manometer give rise to the scatter of points about each line.

According to the Principle of Superposition of Errors, the cumulative error in V_M, δV_M may be expressed as follows:

$$\delta V_M \approx \frac{\partial V_M}{\partial V_o} \cdot \delta V_o + \frac{\partial V_M}{\partial A} \cdot \delta A + \frac{\partial V_M}{\partial h} \cdot \delta h + \frac{\partial V_M}{\partial \rho_o} \cdot \delta \rho_o + \frac{\partial V_M}{\partial M} \cdot \delta M \qquad (9.1.9)$$

If each error can have a value between $+\delta V_o$ and $-\delta V_o$, and $+\delta A$ and $-\delta A$ etc., then the most probable value of δV_M is given by:

$$(\delta V_M)^2 = \left(\frac{\partial V_M}{\partial V_o}\,\delta V_o\right)^2 + \left(\frac{\partial V_M}{\partial A}\,\delta A\right)^2 + \left(\frac{\partial V_M}{\partial h}\,\delta h\right)^2 + \left(\frac{\partial V_M}{\partial \rho_o}\,\delta \rho_o\right)^2 + \left(\frac{\partial V_M}{\partial M}\,\delta M\right)^2$$

The errors in M and V_o have been estimated as $\gtrless$ 0.1 % respectively. The maximum error in h occurs when h is small, and under these conditions is estimated at $\pm$ 1 %. Errors in A and ρ_o are assessed at 0.7 % and 0.1 % respectively. From these error assessments, the absolute error in V_M has been estimated as $\pm$ 0.2 %. About half this total error is due to the calibration volume V_o. Since this is a systematic error in common with all the data, a relative error of $\pm$ 0.1 % may be expected for values of the excess volumes of mixing. In fact, standard deviations derived from the statistical treatment of the points are $<$ 0.1 %, and this conclusion has been confirmed by examining each set of data when plotted on a large scale. Upon the basis of the discussion of errors above it is felt that an error of $\pm$ 0.1 % is a fair assessment of the errors in the excess volumes of mixing illustrated in Figs. 9.1.7 and 9.1.7a.

9.2. PART II - THE MOLAR VOLUMES OF THE CRYSTALLINE, LIQUID, AND GLASS REGIONS OF TRIPHENYL-α-NAPHTHYL ALLENE AND TRIPHENYL-4-BIPHENYL ALLENE

9.2.1. Introduction.

The principle behind the dilatometric technique used is very simple, and the most elementary variety of dilatometer is illustrated in Fig. 9.2.1a below. A bulb A is surmounted by a length of precision bore capillary tubing B. A tared sample

FIGURE 9.2.1.a.

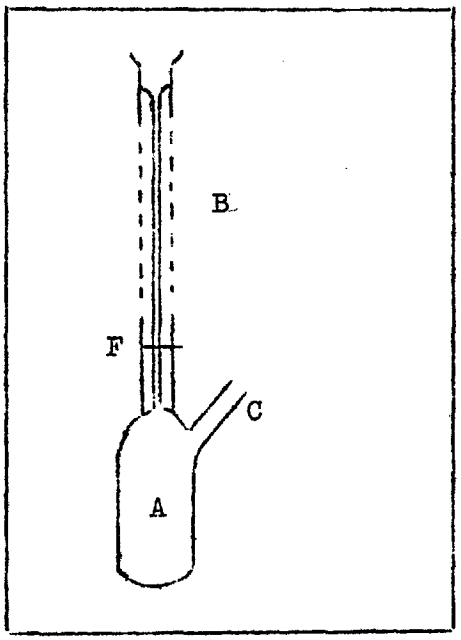

of the solid material is introduced into bulb A via the side-arm C of the weighed dilatometer. Side arm C is then sealed off, the apparatus evacuated, and filled with a suitable confining fluid. In order to remove any pockets of air

trapped in the sample it is usual to repeatedly melt and freeze the sample under vacuum before introducing the confining fluid. When filled, the level of the confining fluid is adjusted to the vicinity of the fiducial mark F. The apparatus plus the detached side arm is then reweighed and the weight of confining fluid determined. The instrument is immersed in a thermostat bath and the expansion of the confining fluid up the capillary tube is noted as the temperature is raised.

If the volume of the dilatometer up to the fiducial mark V_o, the density and coefficient of expansion of the confining fluid, and the area of cross-section of the capillary A, are known, the molar volume V_M of the material at a particular temperature T may be expressed as follows:

$$V_M = \frac{(V_o - V_f + Ah)W}{M} \qquad (9.2.1)$$

where V_f is the volume of the confining fluid, h the measured height of the liquid meniscus above the fiducial mark F, W the molecular weight of the material and M, the mass of material present in the dilatometer.

There were however a number of problems associated with the materials studied in the present work which required extensive modifications to be made in the general technique. The factors which required particular consideration within this context are listed below.

(1) Both triphenyl-α-naphthyl allene, and triphenyl-4-biphenyl allene will form stable glasses when their melts are cooled. Consequently it was not possible to employ the technique of repeatedly melting and freezing the material as a means of removing the last traces of air and/or solvent.

(2) The confining fluid chosen must be sufficiently involatile to be used up to 200°C, and it must not dissolve the materials.

(3) If the materials are present in a powdered or finely divided form, steps must be taken either to prevent or to account for loss of material during evacuation.

Several different designs of dilatometer were tried, but only the design which proved the most successful is described in the following section together with the general techniques adopted to solve the problems cited above.

9.2.2. The Dilatometer and the Techniques Employed in Its Use.

9.2.2.1. The dilatometer.

The dilatometer in its initial form is illustrated in Fig. 9.2.1.b. The tube contained between fiducial mark F_1 and point D consisted of a length (23 cm) of 1 mm. precision bore veridia capillary tubing. The inverted 'U' shaped section G, connecting the precision bore capillary to bulb A, consisted of a length (c.a. 8 cm) of ordinary 1 mm. bore capillary tubing. The bulb A (capacity c.a. 4 ml) was surmounted by a filling tube C, joined via a constriction K. Attached to the top

FIG. 9.2.1b.

THE DILATOMETER.

(FILLING AND EVACUATION)

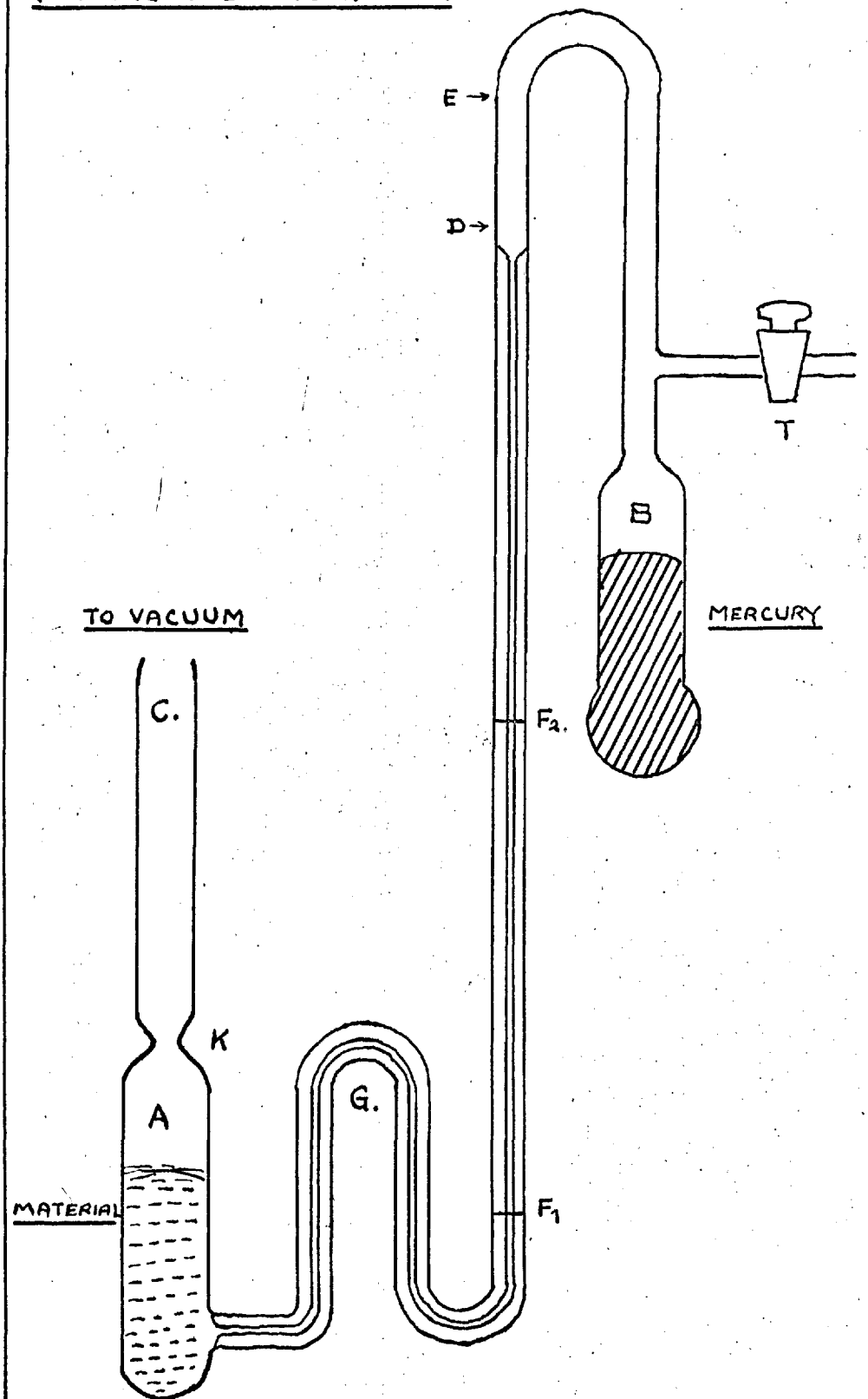

of the precision bore capillary was a length (c.a. 12 cm) of 6 mm. bore tubing which led to bulb B (capacity c.a. 4 ml). Situated just above bulb B was a side arm bearing the high-vacuum tap T.

9.2.2.2. The filling of the dilatometer.

Before use, each sample of the powdered material was placed under vacuum ($\sim 10^{-6}$ mm.Hg) and repeatedly heated to just below its melting point and "shock-cooled" in liquid nitrogen, in order to remove any remaining traces of solvent (i.e. benzene and petroleum spirit).

The dilatometer, as represented in Fig. 9.2.1.b., was cleaned and weighed. Sufficient of the powdered material (c.a. 1.5g) was introduced through tube C to fill about 80% of the volume contained in bulb A* . The inverted 'U' shaped section G, prevented any of the powder from entering the precision bore capillary section of the apparatus. The dilatometer plus the powder were weighed.

Since both triphenyl-α-naphthyl allene and triphenyl-4-biphenyl allene proved soluble in high boiling oils such as silicone oils, mercury was used as a confining liquid. The principal disadvantage of mercury lies in the fact that its high surface tension may prevent it from entering the smaller

---

* Attempts were made to introduce the material in pellet form but since the pellets produced crumbled on evacuation the practice was discontinued.

interstices in the powder. Bulb B was filled with "triple distilled" mercury via tap T by means of a fine capillary pipette. The dilatometer, containing the powdered material and the mercury was again weighed. At this stage the total weight of the apparatus W_T was given by:

$$W_T = W_D + W_M + W_{Hg} \qquad (9.2.2)$$

where W_D is the weight of the empty dilatometer, W_M the weight of material, and W_{Hg} the weight of mercury.

After tap T had been greased (Apiezon 'M' vacuum grease), the tap was closed to the atmosphere and the dilatometer plus contents attached to a vacuum line by means of tube C. The apparatus was first evacuated cautiously (to minimise loss of material into the vacuum line) to about 10^{-2} mm. Hg., and then, by means of a mercury diffusion pump, to about 10^{-6} mm.Hg. The vacuum was tested with a "Tesla" coil. The apparatus was tapped gently with a rubber policeman to remove any trapped air pockets, and left overnight under vacuum. The apparatus was sealed under vacuum at constriction K. The apparatus (minus tube C), now detached from the vacuum line, was cautiously inverted. This allowed the powdered material to fall to the sealed end of bulb A, and the mercury contained in bulb B to flow into the capillary section. With the apparatus in the

inverted position, the mercury meniscus was situated just below tap T. Tap T was then carefully opened to the atmosphere, allowing the mercury to enter the bulb A under atmospheric pressure. After tap T had been cleaned of grease, the whole apparatus was re-weighed together with the detached tube C which had been removed from the vacuum line and cleaned. If the weight of the apparatus plus contents obtained at this stage is W_T', then the weight of powder lost ΔW_M during the evacuation process is simply:

$$\Delta W_M = W_T - W_T' \qquad (9.2.3)$$

(c.f. equation (9.2.2).

The value of ΔW_M was usually in the order or 5 m.g.

The section containing bulb B and tap T was carefully removed from the apparatus at point E and weighed. At this stage the level of mercury in the remaining apparatus extended into the section contained between points D and E. The apparatus was warmed in an oil bath to within a few degrees of the melting point of the material. This procedure, by reducing the surface tension of the mercury, assisted its entry into the smaller interstices of the powder. After about one hour, the apparatus was removed from the oil bath, and when cooled, cleaned of oil. The level of mercury was adjusted to the vicinity of fiducial mark F_1 (see Fig. 9.2.1.c). Since the weights of the apparatus and of the powder were known, the

FIG. 9.2.1c.

THE DILATOMETER

(FILLED AND READY FOR EXPERIMENT)

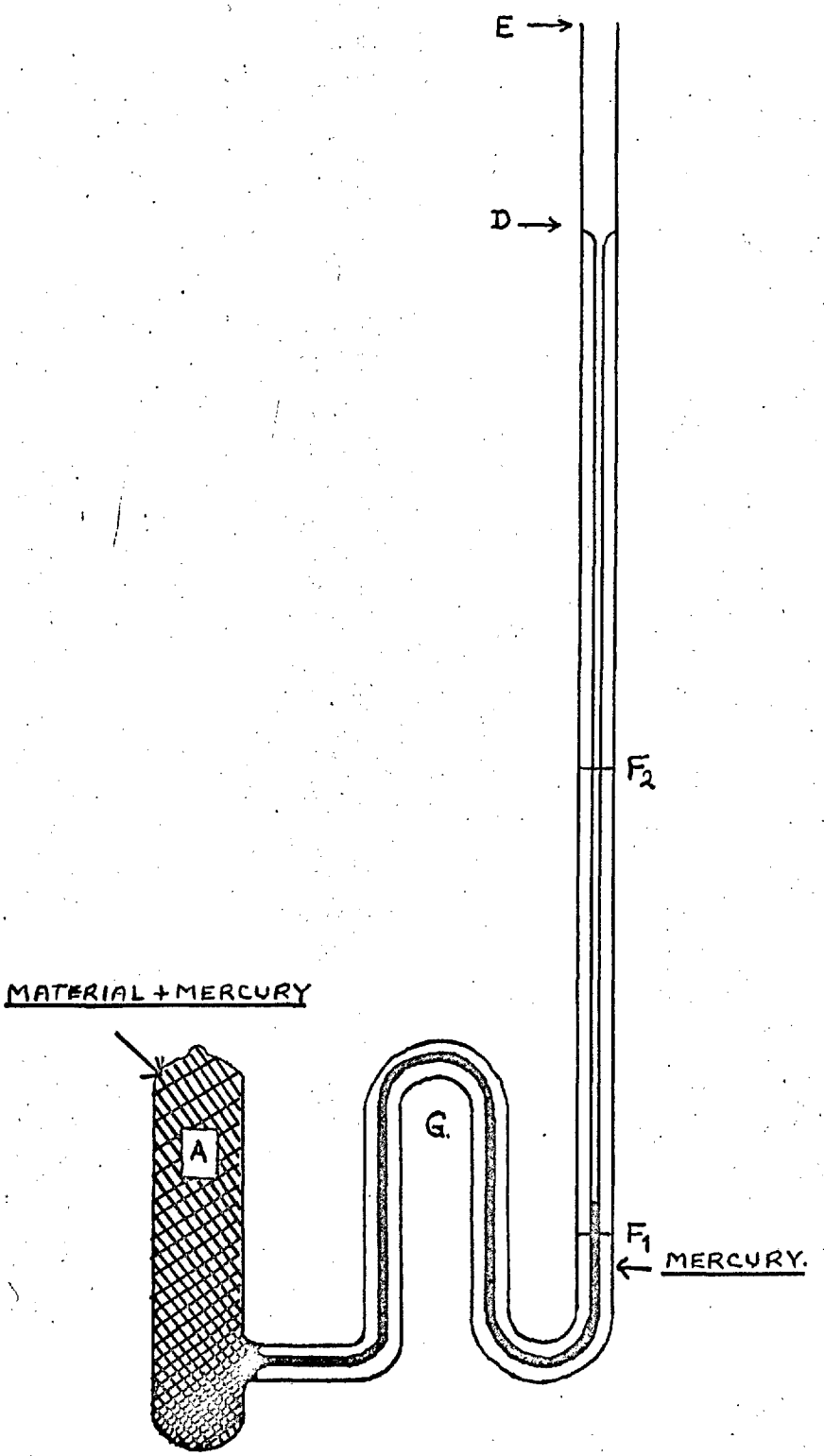

weight of mercury could be determined.

The apparatus was now ready for experiment.

9.2.2.3. The measurement of molar volume.

The determination of the volume V_o contained in bulb A up to the level of the fiducial mark F_1 (i.e. the calibration volume) was the final operation of the experiment, and is described in the next section.

The apparatus as illustrated in Fig. 9.2.1.c. was was attached to a steel support rod and immersed in the thermostat bath. At each temperature selected the apparatus was allowed about 15 minutes to reach equilibrium. The levels of the mercury meniscus and the fiducial mark were noted by means of a Pye cathetometer reading to 0.001 cm. The height of the fiducial mark was recorded for each temperature, obviating the application of a temperature correction for the linear expansion of glass in the value of h. (see equation 9.2.1). A temperature correction was of course applicable to the calibration volume V_o and the cross-sectional area of the capillary A. Since the height of the viewing slit in the bath was comparatively small (c.a. 15 cm.), it was necessary to lower the apparatus further into the bath as the mercury meniscus approached the top of the viewing slit. The meniscus height h was then referred to fiducial mark F_2 situated about half way up the precision bore capillary (c.a. 10 cm. above F_1).

On some occasions, particularly after the material had melted, the mercury meniscus approached the top of the precision bore capillary, and it was necessary to remove some of the mercury. This was achieved by using a teat pipette. The mercury was always removed at a stable temperature, and the height of the meniscus before and after removal was recorded. The weight of the mercury removed served as a check for the quantity removed as calculated from the difference in meniscus height. In lowering the temperature the reverse proceedure was adopted. This complication could have been avoided by choosing a wider bore capillary, but it was felt that the accompanying loss of sensitivity did not warrant its adoption.

Each experiment was divided into a study of the 4 "phases" of each material; viz. the crystalline phase (temperature ambient to melting point), the liquid phase (temperature range melting point T_m to about $T_m + 50^\circ$), super-cooled liquid phase (temperature range T_m to glass transition temperature T_g) and finally, the glass phase (temperature range from T_g to about $T_g - 10^\circ C$). For each section readings were obtained for both rising and dropping temperature. In the glass region, from ambient to $\sim -10^\circ C$ a Townson and Mercer "minus 70" thermostat bath was used. (See Chapter 7, section 7.3).

At the conclusion of each experiment, the apparatus, which had been cleaned of oil, was again weighed and the amount of mercury present assessed. The weight of mercury so obtained

should be equal to the sum of the initial weight of mercury and the subsequent subtractions and additions of mercury which were carried out during the experiment. A comparison of the weights before and after the experiment provided a further check to the assessment of the quantities of mercury added or removed during the experiment.

The absence of gas bubbles in the samples of molten triphenyl-α-naphthyl allene and triphenyl-4-biphenyl allene indicated that any remaining solvent and all the air had been removed during the pre-filling and filling procedures. The absence of gas bubbles also confirmed the absence of volatile decomposition products (c.f. chapter 7, section 7.1).

9.2.2.4. Calibration

For the first experiment using triphenyl-α- naphthyl allene, it was possible to evaluate the calibration volume V_o by using the molar volume data obtained for this compound using a densitometer (see Chapter 9, part I). The value of V_o was obtained at 164.5°C using equation (.9.2.1) above. The value of V_o was corrected to 25°C using the value of 9.90×10^{-6} for the coefficient of cubical expansion of pyrex glass[3]. Values for the specific volume of mercury were obtained from the International Critical Tables in which the following cubic equation for the specific volume V_T in terms of temperature T, is quoted:

$$V_T = V_o \left\{ 1 + 10^{-6}(181.456T + 0.009205\ T^2 + 0.000006608\ T^3) \right\}$$

V_o is the specific volume of mercury at 0^oC, and is quoted as 0.07355391 ml/g. The value of $V_o(25^o\ C)$ for the instrument used in this experiment was 3.5524(0) ml.

In all, three instruments were used, and in each case the 1 mm. precision bore capillary tubing was selected from the same batch as that used in the densitometer. (see Chapter 9, part I). The bore of each piece used fell well within the manufacturers tolerance of $\pm$ 0.01 mm.

For subsequent experiments using triphenyl-α-naphthyl allene and triphenyl-4-biphenyl allene, the following direct method of calibration was adopted. In order to calibrate the dilatometer it was necessary to remove the material and mercury from bulb A and to replace the mixture with pure mercury. When the necessary readings had been taken, as much mercury as possible was removed from the capillary by means of a fine capillary teat pipette. The dilatometer was then immersed in an oil bath and the temperature slowly raised. As the mercury expanded up the capillary it was removed. At about 180^oC the procedure was halted and the dilatometer cooled. The mercury contracted through the inverted 'U' shaped section G and into bulb A. Benzene was introduced into the length of tube contained between points D and E surmounting the capillary, and the instrument was gently warmed to allow the solvent to displace the

air in the capillary and in bulb A. The remaining mercury was gradually displaced from bulb A by the solvent and upon warming was forced up the capillary by the solvent vapour pressure and removed. By repeatedly removing solution and adding fresh solvent it was possible to remove all the material and to clean out the dilatometer. The dilatometer was finally flushed out with acetone and dried in an oven overnight.

The apparatus used to refill the dilatometer with fresh mercury is illustrated in Fig. 9.2.2.

The clean dilatometer was attached to the vacuum line by means of a length of pressure tubing R. The top of the dilatometer was pushed into the tubing until the tip of capillary K was situated within the section of dilatometer contained between points D and E and secured with a "Jubilee" screw clip. The capillary tube K was surmounted by a bulb B of approximately the same volume as bulb A, whilst the tube above bulb B divided, forming a 'Y' piece. The right-hand limb of the 'Y' piece could be opened to either the vacuum system or to the atmosphere by means of the two-way tap T. The left hand limb was attached to bulb C by means of the ground glass joint J. The volume of bulb C was constructed to be slightly larger than that contained in bulb A up to the fiducial mark F_1.

After the bulb C had been filled with mercury, the apparatus was assembled as indicated in Fig. 9.2.2. The tap T

FIG. 9.2.2.

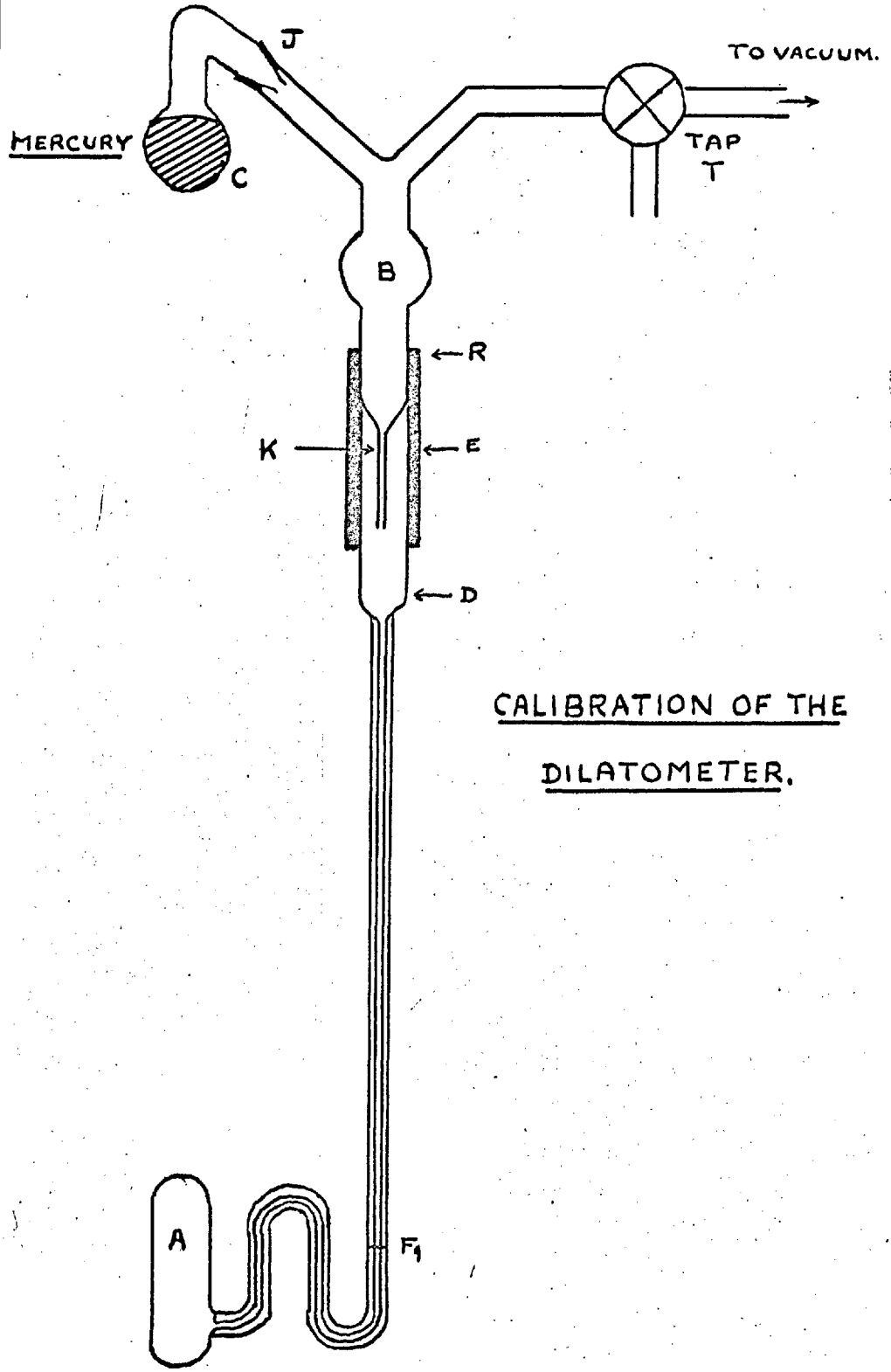

CALIBRATION OF THE DILATOMETER.

was opened to the vacuum system and the apparatus evacuated to about 10^{-6} mm.Hg. Since bulb A was being evacuated through the capillary section, the system was left to pump over-night. The vacuum was finally tested using a "Tesla" coil. Bulb C was carefully inverted by turning about joint J, allowing the mercury to flow down the left-hand limb of the 'Y' piece into bulb B. Tap T was then closed to the vacuum system and cautiously opened to the atmosphere. The mercury filled bulb A and the capillary section of the dilatometer. The apparatus was dismantled and the height of the mercury meniscus in the capillary adjusted to the vicinity of fiducial mark F_1. The dilatometer was immersed in a thermostat water bath (see Chapter 7, section 7.3) controlling, for the second dilatometer, at 25°C and for the third dilatometer at 20.3°C. The height h of the mercury meniscus above the fiducial mark F_1 was noted using a cathetometer. The dilatometer plus mercury was weighed and the weight of mercury assessed. The calibration volume V_o was given by the following expression:

$$V_o = MV_T + Ah \qquad (9.2.4)$$

where M is the weight of mercury, V_T the specific volume of mercury at the calibration temperature T, and A the cross-sectional area of the capillary at temperature T. The values of V_o for the second and third dilatometers were 3.3295(1) ml. (25°C) and 3.0308(9) ml. (20.3°C).

9.2.2.5. Results.

The molar volume results obtained for triphenyl-α-naphthyl allene and triphenyl-4-biphenyl allene using the dilatometric technique are listed in tables 9.2.1a, 9.2.1b and 9.2.2. and illustrated in Figs. 9.2.3. to 9.2.6.

It is necessary at this stage to proffer a few words of explanation with regard to some of the special features of these plots.

(i) The molar volumes of triphenyl-α-naphthyl allene (Figs. 9.2.3.a and b)

These figures illustrate results obtained from the two independent experiments conducted with triphenyl-α-naphthyl allene. The results obtaining to the liquid and supercooled liquid regions (contained between points G and E) are in good agreement. The results for the crystalline phase, contained between points A and B, differ widely. In experiment 1 the curve corresponding to the crystalline phase displays two maxima. The values of the molar volumes in this region are less than the corresponding values for the super-cooled liquid, and the line BC represents the solid/liquid transition at the melting point. In experiment 2 (Fig. 9.2.3.b), the values of the molar volumes are greater than those of the corresponding super-cooled liquid, and there are no maxima in the region A to B. At about 90°C, the mercury meniscus continued

TABLE 9.2.1.a

MOLAR VOLUMES OF TRIPHENYL-α-NAPHTHYL ALLENE

Experiment 1.

Molar volume V_M (mls)	Temperature (°C)	Molar volume V_M (mls)	Temperature (°C)
CRYSTALLINE PHASE:		352.1823	110.7
343.9362	22.6	354.4133	118.9
345.1788	29.2	357.9151	123.4
345.9413	33.4	357.4350	130.2
346.6755	38.0	352.0694	134.7
347.4662	43.0	370.4819	140.1
348.0875	47.6	MELT (RISING TEMPERATURE)	
348.6806	52.5	372.2892	145.4
349.2454	57.1	374.8026	151.7
349.9796	63.6	376.2994	155.4
350.2902	68.6	378.5303	160.6
350.4879	73.4	380.3972	164.8
350.5444	77.9	382.9076	169.0
350.0064	82.3	384.4043	174.2
347.4380	89.2	386.6635	182.1
348.0593	94.6	388.5201	191.0
349.0194	97.9	MELT (DROPPING TEMPERATURE)	
349.7819	102.4	383.3594	170.0

TABLE 9.2.1.a (Continued)

Molar volume V_M (mls)	Temperature (°C)	Molar volume V_M (mls)	Temperature (°C)
381.4108	163.2	356.1077	61.4
380.2247	158.7	354.5263	54.5
378.5586	153.0	353.7073	51.0
376.6947	146.2	352.5777	48.2
SUPER-COOLED LIQUID:		351.7305	44.5
375.0286	140.0	350.9398	39.2
374.1249	136.3	350.3750	37.8
372.9388	131.9	349.1324	34.1
371.5550	126.6	GLASS PHASE:	
369.9453	120.0	348.5958	31.3
368.4486	113.5	348.5560	30.6
366.7542	107.4	347.9463	27.85
365.7941	103.2	347.5792	24.3
364.1844	97.0	346.7602	22.8
362.9700	91.5	347.2121	18.1
361.9816	87.2	346.3084	14.1
360.7391	81.6	346.1672	11.6
359.7507	74.7	345.9695	9.0
358.9317	74.3	345.8283	6.8
357.2938	67.1	345.7153	5.1

TABLE 9.2.1.a (Continued)

Molar volume V_M (mls)	Temperature (^oC)	Molar volume V_M (mls)	Temperature (^oC)
345.5459	3.0	344.9246	- 6.0
345.1505	- 3.0	346.0825	10.1
345.2635	- 1.0		

TABLE 9.2.1.b

Experiment 2.

Molar volume V_M (mls)	Temperature (^oC)	Molar volume V_M (mls)	Temperature (^oC)
CRYSTALLINE PHASE:		361.4592	50.8
359.1647	22.6	361.9929	57.6
359.5353	27.1	362.7567	67.1
359.9877	32.2	363.0132	74.3
360.3554	36.9	362.1769	62.2
360.6594	40.8	362.6945	68.5
359.2851	22.6	363.2675	76.7
359.6903	28.4	363.8915	83.7
360.2070	34.5	364.6770	88.6
360.5488	39.5	365.3799	94.8
361.0371	45.9	366.1211	99.8

TABLE 9.2.1.b (Continued)

Molar volume V_M (mls)	Temperature (°C)
PARTIALLY MELTED MATERIAL	
(RISING TEMPERATURE)	
345.6788	20.8
345.8666	21.6
346.1305	26.5
346.6890	30.4
348.4039	35.2
349.6677	40.4
350.6655	45.7
352.2980	52.8
354.5937	63.0
356.8738	74.1
358.9588	83.9
361.1763	94.7
363.4671	104.8
365.4889	115.3
367.4006	126.1
371.3448	137.2
373.2971	145.0
376.9201	154.8
381.4670	166.8
384.6456	177.4
TEMPERATURE CYCLED:	
365.4315	115.3
383.6906	174.9
386.1158	182.8
387.2270	191.2
386.3566	182.2
384.3116	174.3
382.0266	166.4
380.4195	160.3
383.4212	171.1
389.4891	192.9
MELTED MATERIAL	
(DROPPING TEMPERATURE)	
391.6610	199.6
390.3176	195.3
388.6365	188.6
386.0456	179.2
384.0427	171.7

TABLE 9.2.1.b (Continued)

Molar volume V_M (mls)	Temperature (°C)
381.3528	163.1
379.0737	154.6
377.0521	145.9
SUPER-COOLED LIQUID	
374.7896	139.0
372.3003	130.2
370.0624	120.5
367.3927	109.9
367.4224	109.4
365.0256	100.2
362.7547	90.45
361.1093	83.3
358.8807	74.1
357.2250	66.0
355.5036	58.2
353.6193	50.5
354.7037	56.1
353.5103	50.5
351.5586	42.8
350.6537	38.1
350.1347	35.0
349.8398	33.1
GLASS PHASE:	
349.3431	30.0
346.5811	10.6
(TEMPERATURE CYCLED)	
347.4802	22.1
347.4668	20.0
347.4447	16.6
347.3541	14.1
347.2913	11.7
346.7545	8.4
346.6577	8.6
346.4491	5.9
346.1024	2.0
345.8688	- 1.5

FIG. 9.2.3a.

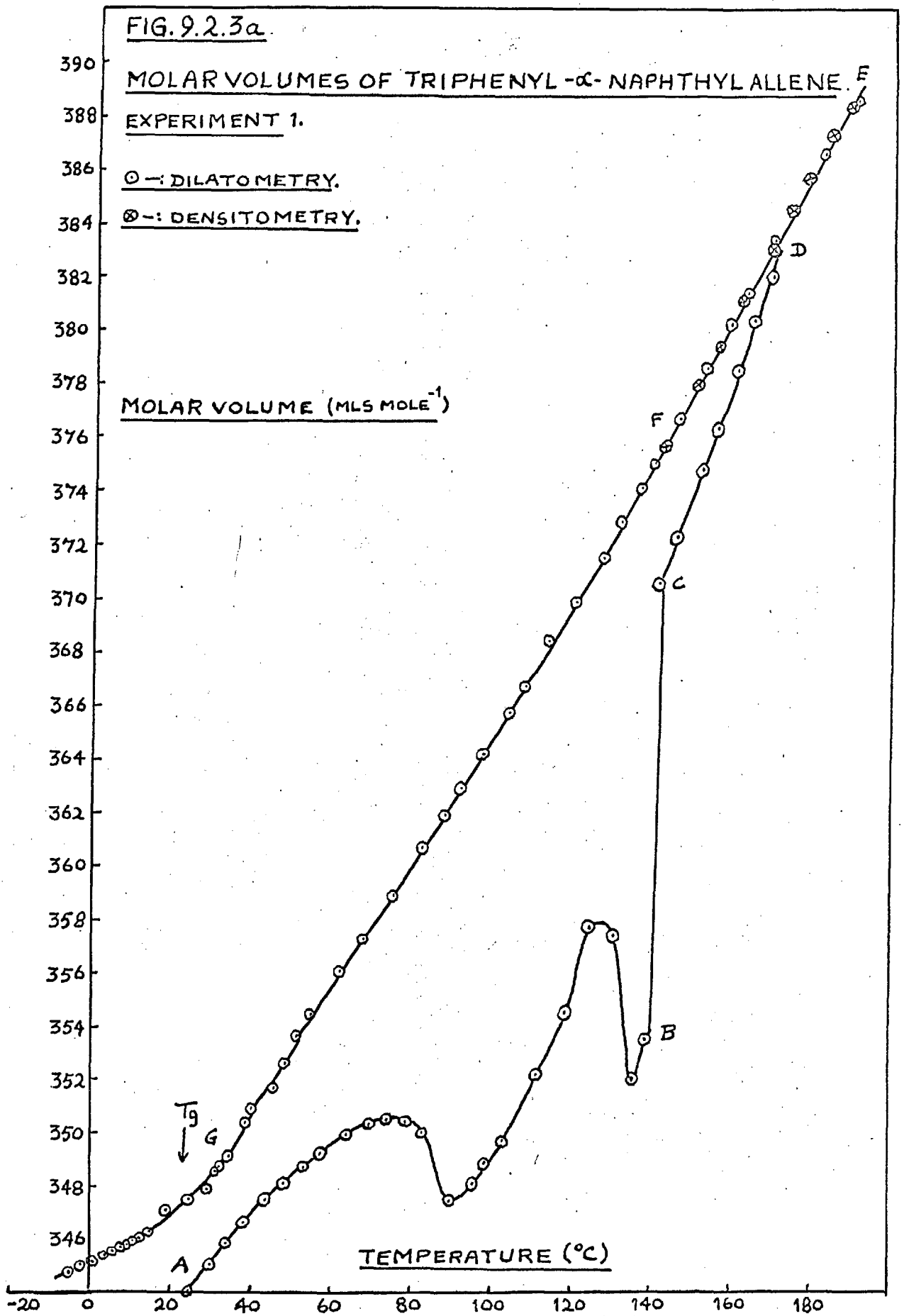
MOLAR VOLUMES OF TRIPHENYL-α-NAPHTHYL ALLENE.
EXPERIMENT 1.
⊙—: DILATOMETRY.
⊗—: DENSITOMETRY.
MOLAR VOLUME (MLS MOLE^{-1})
TEMPERATURE (°C)
390
388
386
384
382
380
378
376
374
372
370
368
366
364
362
360
358
356
354
352
350
348
346
-20
0
20
40
60
80
100
120
140
160
180
A
B
C
D
E
F
G
Tg

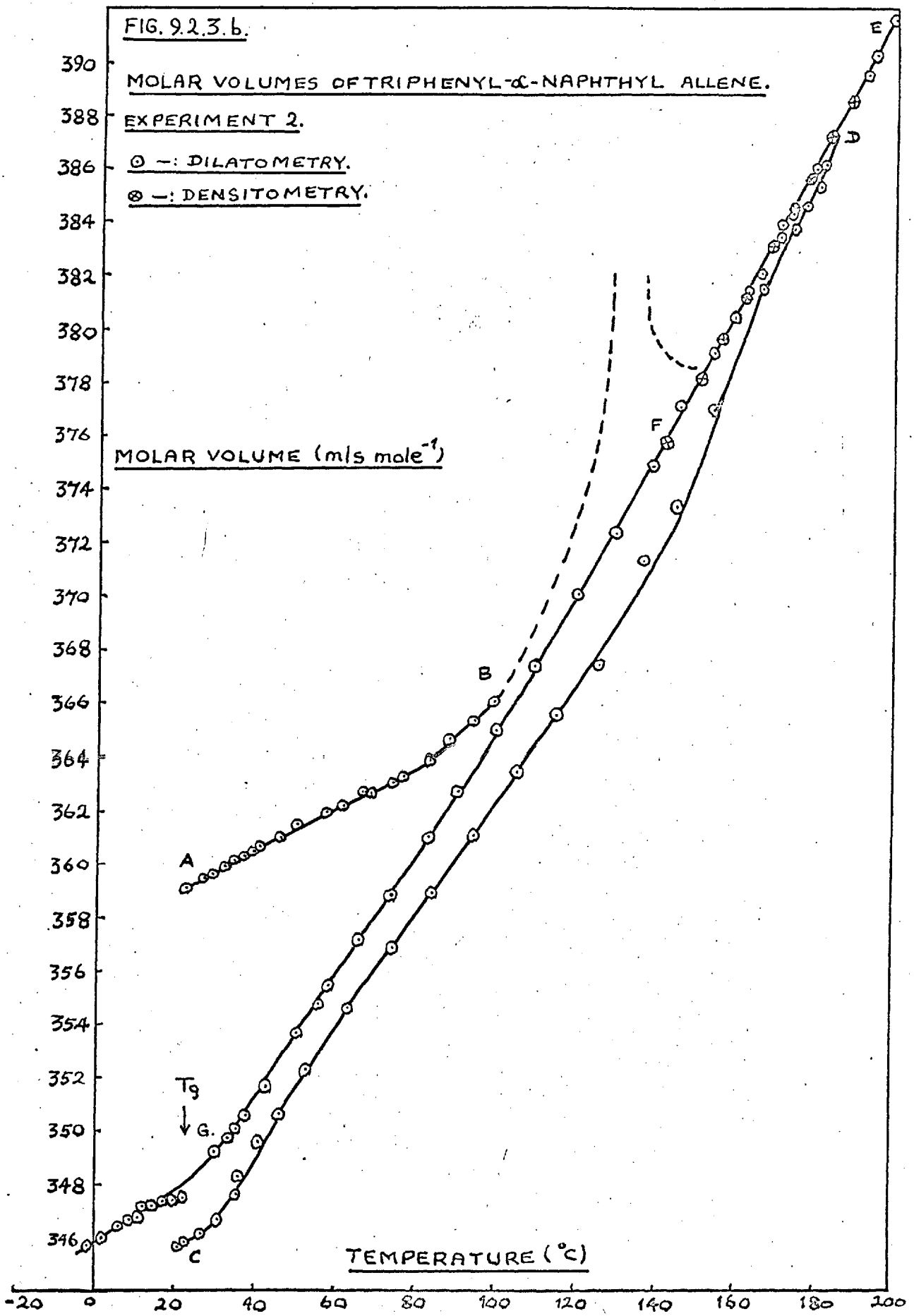
FIG. 9.2.3.b.
MOLAR VOLUMES OF TRIPHENYL-α-NAPHTHYL ALLENE.
EXPERIMENT 2.
⊙ —: DILATOMETRY.
⊗ —: DENSITOMETRY.
MOLAR VOLUME (m/s mole⁻¹)
TEMPERATURE (°C)
390
388
386
384
382
380
378
376
374
372
370
368
366
364
362
360
358
356
354
352
350
348
346
-20
0
20
40
60
80
100
120
140
160
180
200
A
B
C
D
E
F
G.
Tg

TABLE 9.2.2.

MOLAR VOLUMES OF TRIPHENYL-4-BIPHENYL ALLENE

Molar volume V_M (mls)	Temperature (°C)	Molar volume V_M (mls)	Temperature (°C)
CRYSTALLINE PHASE:		409.3042	111.9
383.1536	19.9	410.7610	117.5
383.6271	25.8	411.8901	121.7
384.1370	31.5	413.4927	126.0
385.1932	37.2	415.0588	130.6
386.1037	44.4	416.3335	137.8
387.1599	51.9	417.9177	143.4
388.2526	59.5	418.3352	144.8
389.2724	66.7	419.8163	150.0
390.1829	73.6	421.4642	156.6
390.9114	79.4	MELT (DROPPING TEMPERATURE)	
391.8219	86.8	419.9994	150.4
392.5139	92.2	418.0675	144.5
393.4609	98.5	415.4300	135.2
398.4870	103.1	414.0026	130.2
401.6231	104.0	412.5602	124.4
MELT (RISING TEMPERATURE)		410.8850	119.2
402.5103	104.6	409.6138	114.1
404.3509	104.8	407.3012	105.9

TABLE 9.2.2. (Continued)

Molar volume V_M (mls)	Temperature (°C)	Molar volume V_M (mls)	Temperature (°C)
405.0010	97.5	GLASS PHASE:	
404.9760	97.5	(TEMPERATURE CYCLED)	
402.9259	89.7	387.0623	22.15
400.9459	81.4	387.0418	18.8
399.0721	74.1	386.9675	15.2
396.9167	65.5	386.7249	12.3
394.9620	57.8	386.5677	9.4
387.3304	24.1	385.8702	6.8
387.4014	29.3	385.6382	4.7
387.8742	33.6	385.3529	2.8
390.2955	39.8	385.3654	2.9
391.7226	45.7	385.1357	0.2
393.0186	59.0	384.9790	0.8
393.8288	54.1	385.0607	2.2
395.8826	62.2	385.1090	3.0
397.4886	68.3	385.2293	5.0
389.5981	36.0	385.3571	6.4
388.8124	33.8	385.4913	7.8
388.3636	31.5	385.6013	10.0
387.5424	26.0	385.8071	13.2

TABLE 9.2.2. (Continued)

Molar volume V_M (mls)	Temperature (°C)	Molar volume V_M (mls)	Temperature (°C)
386.0106	15.7	386.1259	19.9
386.1361	17.1	384.8785	- 2.1
386.0203	18.4	384.6693	- 4.1
385.4425	10.8	384.5348	- 5.3

to rise up the capillary at constant temperature, and failed to stabilise after several weeks. This phenomenon is represented by the rising dotted line. At about 120°C the meniscus started to drop steadily. The peak represented by the dotted lines roughly corresponds to the second maximum observed in the crystalline region of experiment 1. It seems likely that the inconsistencies in this region are primarily due to the failure of the mercury to completely fill the interstices in the powdered solid (c.f. page 272). However, the possibility that the maxima in either curve are connected, at least in part, with a solid state transition cannot be dismissed (see Chapter 10, section 10.3.1.2.). It should be noted that the region corresponding to the crystalline phase of

FIG. 9.2.4.

MOLAR VOLUMES OF TRIPHENYL-4-BIPHENYL ALLENE.

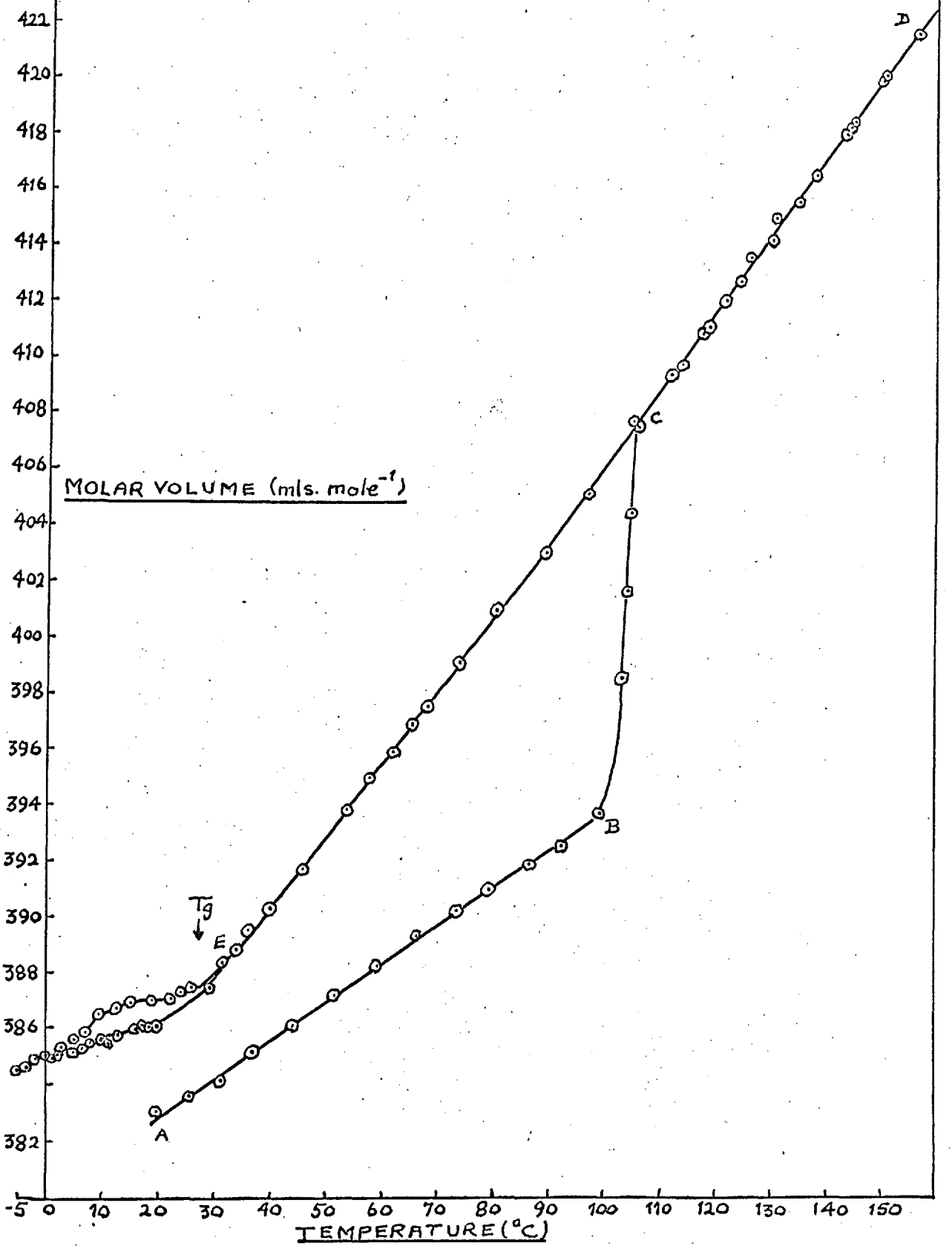

triphenyl-4-biphenyl allene shows no anomaly (see Fig. 9.2.4. and below). It was mentioned in chapters 5 and 7 that triphenyl-α-naphthyl allene displays unusual melting properties. The regions in Figs. 9.2.3 a and b contained between points C and D represent the partially melted material. This region is reproducible within experimental error. The curve CD meets the liquid curve EF at about 190°C, and this temperature corresponds to the final melting of the material. If, as has been tentatively suggested earlier, tne compound exists in two polymorphic forms α and β, the regions CD may represent a mixture of the molten (or super-cooled liquid) α form and solid β form.

The glass regions (from point G downward) are fairly reproducible. This region has been replotted on a larger scale in Fig. 9.2.5. Although the difference between the two sets of results is small ($\sim$ 0.3 %), it lies outside experimental error ($\pm$ 0.1 %, see following section). This discrepancy, like the hysteresis displayed in this region by triphenyl-4-biphenyl allene (see Fig. 9.2.6), may arise from two sources operating either singly or jointly. As the melt congeals to a glass, the material tends to draw away from the walls of the bulb leaving vacuoles which are slow to fill with mercury unless the temperature is cycled about the glass transition temperature, T_g. Evidence for the formation of such vacuoles was provided by

FIG. 9.2.5.

MOLAR VOLUMES OF TRIPHENYL-α-NAPHTHYL ALLENE.

GLASS REGION

⊗ —: EXPERIMENT 1.

⊙ —: EXPERIMENT 2.

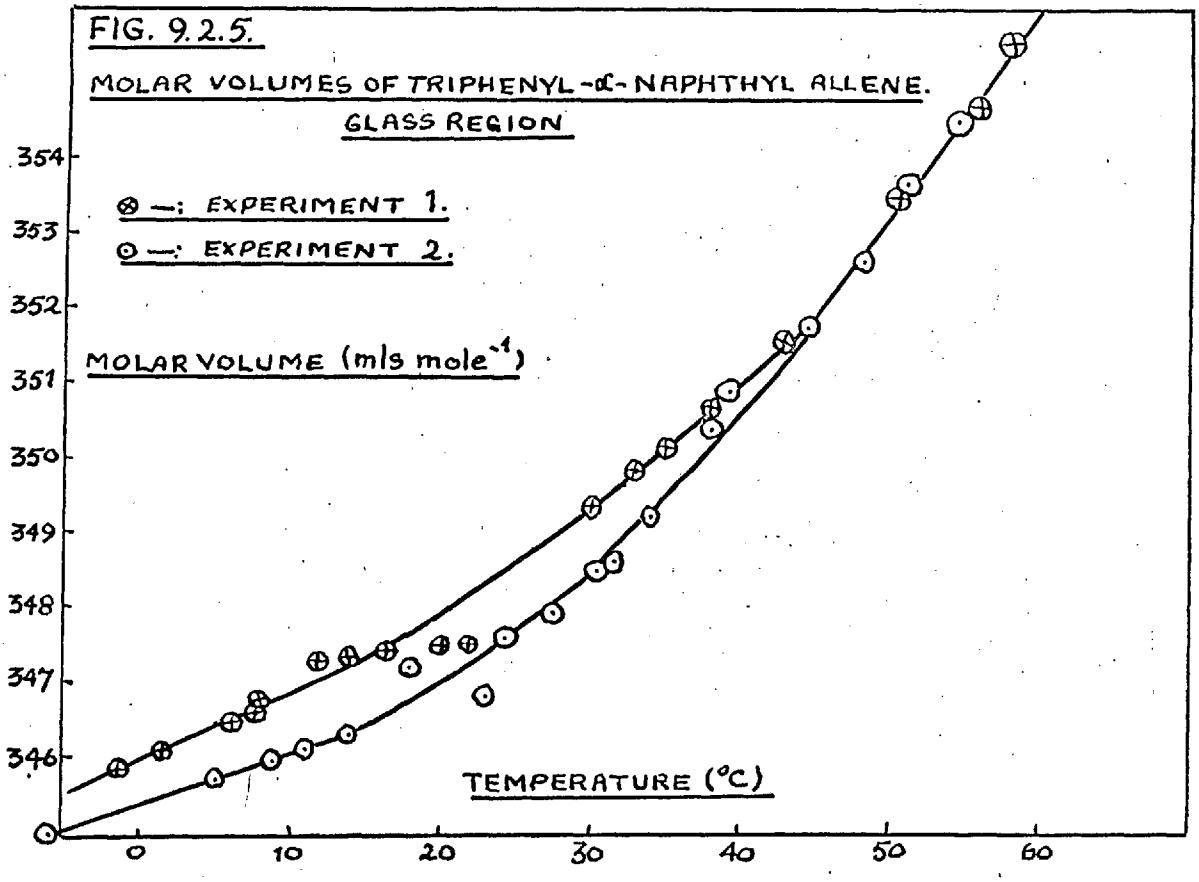

FIG. 9.2.6.

MOLAR VOLUMES OF TRIPHENYL-4-BIPHENYL ALLENE.

GLASS REGION.

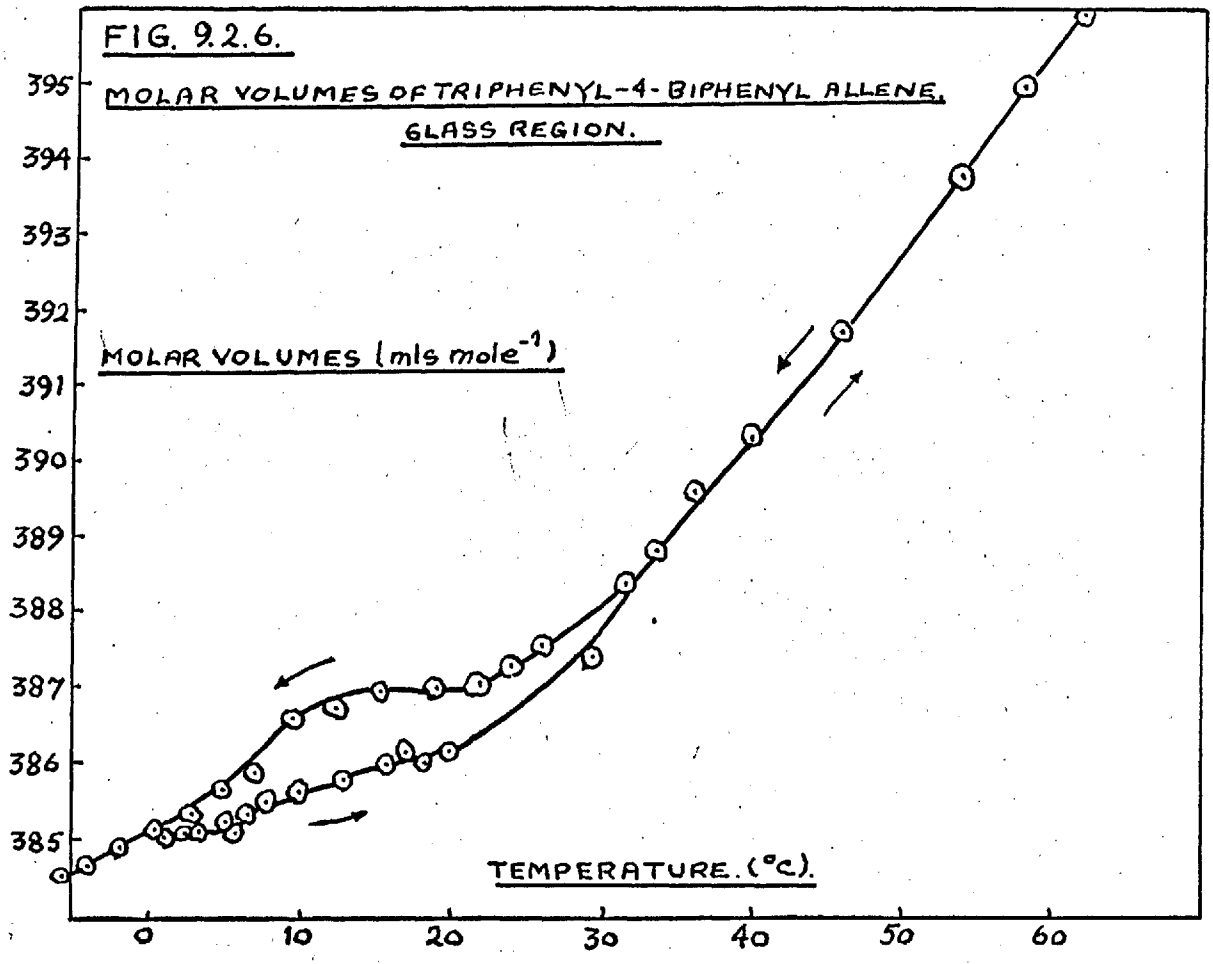

careful observation. The second possible cause may lie in the stresses set up in the material during congelation. The resulting strains may become manifest in the values of molar volume. The magnitude of stresses of this type will probably depend upon the previous history of the material. For example, in the vicinity of the glass point the relaxation time for flow will be very long, and if the rate of cooling over this region is comparatively rapid stresses will be "frozen" in.

However, both sets of data indicate quite clearly that the glass transition temperature for this compound lies between 32° and $35^{\circ}C$.

(ii) Triphenyl-4-biphenyl allene (Figs. 9.2.4 and 9.2.6)

The results obtained for triphenyl-4-biphenyl allene are typical of a glass forming compound and show no outstanding anomalies. Allusion has been made in the section above to the hysteresis displayed in the glass region.

The glass transition temperature for this compound lies between 32° and $34^{\circ}C$.

To recapitulate, it may be emphasised that the data obtaining to the liquid, super-cooled liquid, and glass regions of these compounds is significant and fully reliable (see following section). The validity of data obtained for the crystalline regions is subject to some doubt because of difficulties with dilatometry and because of peculiarities in the thermal behaviour

of the solids. Interpretation thereof can only be tentative.

An examination of the glass forming properties of these compounds with respect to molecular shape and structure is reserved for Chapter 10, section 10.3.1.

9.2.2.6. Errors

The experimental errors in the values of the molar volume V_M may be assessed by considering equation (9.2.1)

$$\text{i.e.} \quad V_M = \frac{W(V_o - V_f + Ah)}{M} \qquad \text{(see page 267)}$$

By employing the Principle of Superposition of Errors, the most probable error in V_M due to errors in V_o, V_f, A, h and M may be represented as follows:

$$(\delta V_M)^2 = (\frac{\partial V_o}{\partial V_M} \delta V_o)^2 + (\frac{\partial V_f}{\partial V_M} \delta V_f)^2 + (\frac{\partial A}{\partial V_M} \delta A)^2 + (\frac{\partial h}{\partial V_M} \delta h)^2 + (\frac{\partial M}{\partial V_M} \delta M)^2 \quad \ldots \quad (9.2.5.)$$

All weighings were noted to $\pm$ 0.1 m.g. and all heights of the mercury column to $\pm$ 0.002 cm. Errors in the specific volume of mercury are negligible and the maximum error in A has been assessed as $\pm$ 1 % . Since the mass of material M was obtained as a result of four weighings, the most probable error in M will be, according to the rules of combination of errors, $\pm$ 0.2 mg. The error in the calibration volume has been independently assessed, using equation 9.2.4. as $\pm$ 0.0008 ml. From equation 9.2.5. the most probable error in V_M, corresponding

to the maximum errors in h has been assessed as $\pm$ 0.1 %. With regard to the liquid and super-cooled liquid regions this appears to be a reasonable estimate since the results are reproducible to within 0.1 %.

Discrepancies in the crystalline and glass regions arise from factors which are not associated with the actual measurements. The source and explanation of these discrepancies have been discussed in the previous section.

REFERENCES

1. Husband, L.J.B., J. Sci. Instrum., 35, 30 (1958).

2. McAuley, W., M.Sc. Thesis, London (1965).

3. Catalogue of "Pyrex Industrial Glass", James A. Jobling and Co. Ltd. (1964).

4. Cleaver, B., Ph.D. Thesis, London (1963).

CHAPTER 10.

DISCUSSION

10.1. General Conclusions with Regard to the Synthesis and Stability of Tetraphenyl Allene, Triphenyl-α-Naphthyl Allene, and Triphenyl-4-biphenyl Allene.

This present research has involved the synthesis and purification of a new series of comparatively rigid, non-polar molecules based upon the allene skeleton viz: tetraphenyl allene, triphenyl-α-naphthyl allene, and triphenyl-4-biphenyl allene. These molecules were selected with a view to studying the influence of molecular shape and the tendency towards molecular interlocking upon the physical properties of melts.

The techniques of synthesis and purification which have been modified and developed for the present purpose have proved quite satisfactory, and may in principle be regarded as general techniques for the large or medium scale production of hydrocarbon allenes.

Increasing research has revealed that the allene system can be quite stable thermally. (c.f. Chapter 5, p. 141). In particular, the present research has established that the three aromatic allenes mentioned above are sufficiently stable to permit accurate studies of their physical properties in the melt. Provided that suitable precautions are taken to exclude oxygen from any apparatus used, decomposition or polymerisation

in the melts is insignificant over a period of several hours at temperatures 50° above the melting points.

10.2. Space Requirements for Rotation in the Melt.

The stereochemistry and molecular structure of allenes in general and of tetraphenyl allene, triphenyl-α-naphthyl allene, and triphenyl-4- biphenyl allene in particular are discussed in detail in chapter 6, section 6.1. Scale models of the molecules are illustrated in plate 6.

The volumes swept out by rotating each of the three molecules about the three perpendicular axes through their centres of gravity are listed in table 10.1 together with the observed molar volumes of the melts at their melting points and at 20°C above their melting points. The X, Y, and Z axes chosen in each case are indicated in Fig. 10.1.

Figure 10.1 - AXES OF ROTATION

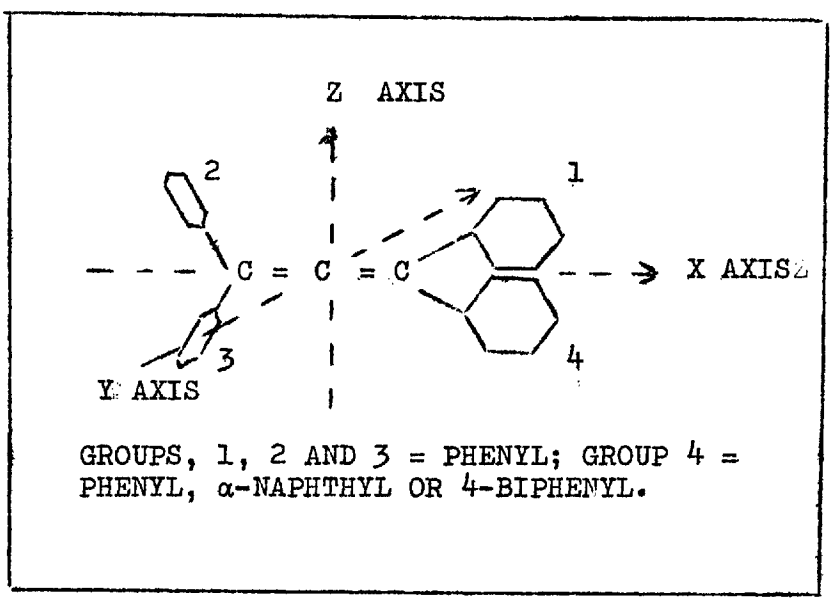

TABLE 10.1

VOLUMES REQUIRED FOR ROTATION

Compound	Molar volume at M.Pt.	Molar volume at M.Pt + 20°	Molar volume required for rotation about:		
			X Axis mls/mole	Y Axis mls/mole	Z Axis mls/mole
Tetraphenyl allene	343.3	348.7	300	741	741
Triphenyl-α-naphthyl allene	374.9	380.7	382	802	963
Triphenyl-4-biphenyl allene	404.4	413.1	676	885	1285
Pyrene	184.5	186.8	317	187	267
o-Terphenyl	216.8	219.8	295	447	310
m-Terphenyl	221.0	224.2	475	595	315
p-Terphenyl	237.4	241.3	301	695	399

The methods employed to estimate the volumes of rotation for the three allenes quoted in table 10.1 are outlined in the Appendix. The data were derived assuming the molecular conformations represented in plates 6.1, 6.3, and 6.4,* and it is felt that ± 10% is a reasonable assessment of error with regard to the volumes swept out by the molecules in these configurations. These conformations were chosen in order to reduce the complexity of the calculations, but they do not necessarily represent the most probable conformations (c.f. Chapter 6, section 6.2). The

* Facing page 170.

errors arising from this source, with regard to rotation about the Y and Z axes will, to some extent, compensate each other, and since the volumes of rotation about these axes are large compared with the observed molar volumes such errors may be safely ignored. The volumes obtaining to rotation about the X-axis, however, may tend to be an underestimate. In view of the inhibited rotation of the α-naphthyl group (see Chapter 6, section 6.2.2), the conformation of triphenyl-α-naphthyl allene represented in plate 6.3 may be considered quite realistic. Also included in table 10.1, for the purpose of comparison, are the corresponding data obtained by earlier workers for o-, m-, p-terphenyl[1] and pyrene[2].

A study of table 10.1 reveals that tetraphenyl allene and triphenyl-α-naphthyl allene may be able to rotate about their X axes in the melt at their melting points, whilst pyrene may be able to rotate about its Y axis (i.e. the axis perpendicular to the plane of the molecule. (see Fig. 10.2). Neither of the remaining molecules quoted in the table are free to rotate about any axis either at their melting points or at temperatures 20°C above their melting points. The melting points of the molecules quoted in table 10.1 are listed in table 10.2.

The influence of inhibited molecular rotation upon each of the physical properties of the melts studied in the present work will be discussed in the appropriate sections.

FIGURE 10.2.

THE PYRENE MOLECULE

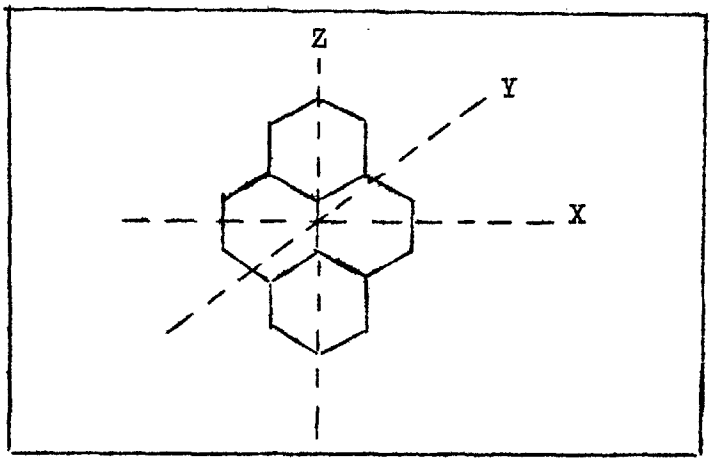

TABLE 10.2.

MELTING POINTS

Compound	Melting Point (°C)
o-Terphenyl	55.5
m-Terphenyl	87
Triphenyl-4-biphenyl allene	104
Triphenyl-α-naphthyl allene	140
Pyrene	150
Tetraphenyl allene	166

10.3 THE PURE COMPOUNDS

10.3.1. Molar Volume Data for the Pure Compounds.

10.3.1.1. Super-cooling and glass formation.

The melts of all three allenes display a marked tendency to super-cool. Under normal conditions molten tetraphenyl allene will super-cool about 10°C before it finally crystallises. If a thin film of the melt, contained between a pair of clean quartz plates, is allowed to cool slowly, the super-cooled region may be extended by some 80°C. The molar volume (V_M) vs. temperature plot for molten tetraphenyl allene, over the temperature range 168.6°C to 198.2°C, is linear within the limits of experimental error, and is illustrated in Fig. 9.1.5. (page 258).

Both molten triphenyl-α-naphthyl allene and triphenyl-4-biphenyl allene congeal to stable glasses upon cooling. It was not found possible to obtain crystalline samples of these compounds by cooling their melts.

The V_M vs. T curves for the super cooled liquids (Figs. 9.2.3.a and b, and 9.2.5 and Figs. 9.2.4. and 9.2.6., pages 287 to 294) show clear changes of slope at the glass transition temperatures which were about 35°C for triphenyl-α-naphthyl allene and about 34°C for triphenyl-4-biphenyl allene. The marked hysteresis shown in this region has been discussed in Chapter 9. part II, page 293 .

Usually, below the glass point, the slope of the V_M vs. T plot runs approximately parallel to that of the crystalline phase. With the present compounds this similarity between the slopes corresponding to the two phases is not very striking, particularly in the case of triphenyl-α-naphthyl allene for which reproducible data for the crystalline phase could not be obtained (see Chapter 9, part II, page 281). Aromalies of this type may arise from differences in molecular environment between the crystalline and glass phases, since the environment of a molecule may influence its vibrational modes. (cf. Chapter 4, section 4.3). The molecules in the comparatively discrdered glass phases are less economically packed than in the corresponding crystalline phases. Consequently the molar volumes of the glass phases are the greater.

For non-polar molecules of this type, a glass represents the ultimate condition resulting from extensive molecular interlocking and cluster formation.

The inhibited movement of the α-naphthyl group in triphenyl-α-naphthyl allene with respect to the allene skeleton results in a conformation particularly conducive to molecular interlocking (c.f. Chapter 6, section 6.2.2). Although the biphenyl group in triphenyl-4-biphenyl allene enjoys some movement (c.f. Chapter 6, section 6.2.3.) the increased asymmetry arising from this group will tend to discourage orderly packing in either

the crystalline solid or melt, and will encourage the formation of anti-crystalline clusters in which this rude appendage may be best accommodated.

It may be seen from Table 10.1 that the rotation of these molecules in the melt is strongly inhibited. Although triphenyl-α-naphthyl allene may just be able to rotate about its X axis at its melting point, rotation is denied at the glass point*.

Examples of glasses formed of non-polar hydrocarbons are quite rare. Apart from o-terphenyl[3] which may with careful cooling be congealed to a glass, the most outstanding example of a glass of this type, comparable in stability with the two allene glasses discussed above, is the "cog-wheel" shaped 1:3:5 tri-α-naphthyl benzene. The glass transition temperature of this compound is 70°C.[4]

The formation of these stable glasses provides convincing examples of the influence of molecular shape resulting in cluster formation. Inhibited molecular rotation is not <u>per se</u> the most important factor, although this will influence the predisposition of molecules to particular orientations which, provided that the molecular shape is favourable, could result in cluster formation.

For many glasses, both organic and inorganic, the viscosity

---

* The molar volume of triphenyl-α-naphthyl allene at its glass point is 348.5 ml.

at the glass points is in the order of 10^{13} poise, indicating that the activation energy and entropy both for flow and possibly for an ordering molecular re-orientation are becoming prohibitively high. (c.f. Chapter 4, section 4.3).

10.3.1.2. The crystalline phases.

The V_M vs. T plot for crystalline tetraphenyl allene was not obtained. Since this compound showed no propensity to glass formation under normal conditions, the dilatometric technique (Chapter 9, part II) was not employed. The sections of the V_M vs. T plots contained between points A and B (Figs. 9.2.3a and b, and Fig. 9.2.4) represent the crystalline regions for triphenyl-α-naphthyl allene and triphenyl-4-biphenyl allene.

The plot for triphenyl-4-biphenyl allene is quite linear, and the melting point is well defined. The corresponding section for triphenyl-α-naphthyl allene is neither linear nor reproducible. The detailed features of these plots (Figs. 9.2.3. a and b) have been discussed in Chapter 9, part II (page 281) where it was suggested that the maxima displayed at about 120°C may arise from a solid state transition.

The unusual melting characteristics of triphenyl-α-naphthyl allene have been discussed in detail in Chapter 5, page 153 and also, within the present context, in Chapter 9, part II (page 293). It seems likely that triphenyl-α-naphthyl allene exists in two polymorphic forms. That one or other of these

forms undergoes a transition involving orientational disordering (c.f. Chapter 4, section 4.1) to produce a third form is a possibility.

It was mentioned earlier (Chapter 6, section 6.2.2.) that inhibited rotation of the α-naphthyl group with respect to the allene skeleton will give rise to a pair of enantiomorphs. The onset of rotation of this group could possibly result in a change in the solid state structure. It seems unlikely that the possible solid state transition at 120°C arises from this source for two reasons.

1) A scale model of the molecule (see plate 6.3) indicates that rotation of the α-naphthyl group would be strongly opposed, even at elevated temperatures.

2) If the group were able to rotate in the solid, it would certainly rotate in the melt. This would render the molecules less conducive to interlocking; a result neither compatable with the formation of a stable glass nor with the anomalous flow properties of the melt. (see Section 10.3.2)

In the absence of adequate supporting evidence such as that supplied by calorimetry or X-ray diffraction photography, any attempt to seek an explanation for such a transition in terms of the molecular and crystal structure must inevitably be speculative.*

---

* The use of X-ray diffraction techniques over the relevant temperature range was considered, but the complexity of the molecules would render interpretation difficult and possibly misleading.

Although this question is only indirectly pertinent to the present thesis, and although no definite conclusions may be reached with regard to a possible solid-state transition in triphenyl-α-naphthyl allene, the discussion above serves to illustrate some of the complications which may arise with molecules of this type.

10.3.2. Structure of the Melts in Relation to Viscosity.

10.3.2.1. Viscous flow parameters for the pure compounds.

Plots of log η vs. 1/T often give straight lines for liquids comprising molecules with simple force fields, and for which the repulsion envelopes are figures of rotation. This indicates that the activation energy for viscous flow E_η in the equation:

$$\eta = A \exp (E_\eta / RT) \qquad (10.1)$$

is independent of temperature.

Consideration of viscosity as a rate process has led to the equation:

$$\eta = \left(\frac{\delta}{a}\right)^2 \frac{Nh}{V} \exp(-\Delta S^*/R) \exp(\Delta H^*/RT) \qquad (10.2)$$

where δ is the distance between molecular planes, a, the distance between the molecules in the same plane and the other symbols bear their usual significance[5]. ΔH^* is usually identified with E_η. Even when a plot of log η vs. 1/T is sufficiently close to a straight line to make this refinement feasible, this

probably arises only because of mutual compensation between the temperature dependence of V, ΔS^{*} and ΔH^{*} (see Chapter 2, section 2.3.4.)

For a liquid composed of spherically symmetric molecules or of anisotropic molecules which acquire this average symmetry by rotation, it is reasonable to take δ/a as unity. For anisotropic molecules like those in the present series, which cannot acquire an effective spherical shape by randomisation about all molecular axes, δ/a is not unity. However, where molecules are similar in type and the degree of approximation is roughly the same, direct application of equation (10.2), taking δ/a as unity, may be used to provide parameters, the trends in which furnish a useful means of comparison.

The plots of log η vs. 1/T for tetraphenyl allene, pyrene, and triphenyl-α-naphthyl allene are illustrated in Figs. 8.3, 8.5, and 8.8 respectively*

Values of ΔS^{*} were obtained from equation:

$$A = \left(\frac{\delta}{a}\right)^{2} \frac{Nh}{V} \exp\left(-\frac{\Delta S^{*}}{R}\right) \qquad (10.3)$$

E_{η} and A were derived from experimental data using equation (10.1).

---

* Regrettably, owing to a lack of both time and material, transport data for molten triphenyl-4-biphenyl allene is not available.

Values of these parameters are quoted in table 10.3 for tetraphenyl allene, triphenyl-α-naphthyl allene and pyrene at their melting points and at temperatures well above their melting points. Also included in table 10.3 are the corresponding values for the three terphenyls obtained by earlier workers[1] *. In all cases, except that of triphenyl-α-naphthyl allene, the values corresponding to the higher temperatures represent the linear regions of the log η vs. 1/T plots. The linear section of this plot was not reached with triphenyl-α-naphthyl allene even at 50°C above the melting point, and the high temperature values quoted correspond to 185°C. viz. 45°C above the melting point, (c.f. Fig. 8.8), and may therefore be undervalued. The trends in these parameters reflect changes in the configurational structure of the melts as the temperature is lowered. For example, in p-terphenyl there is no evidence of any marked increase in structural complexity; with pyrene a definite but not very pronounced increase may be inferred on this basis, as the temperature is lowered. Changes in E_η and ΔS^* for m-terphenyl and for tetraphenyl allene are quite closely similar, as might be expected from a resemblance

---

* The Log η vs. 1/T plots for the terphenyls are illustrated in Fig. 2.4.

in the shape of these hydrocarbons*. For o-terphenyl the changes in E_η and ΔS^* with temperature are very marked, apparently somewhat greater than for triphenyl-α-naphthyl allene. But, as stated in the preceeding paragraph, trends for this molecule are probably undervalued in table 10.3.

TABLE 10.3.

TRENDS IN VISCOMETRIC PARAMETERS

Compound	E_η (K.Cal.Mole^{-1})		ΔS^* (e.u.)		A(poise)	
	M.Pt.	Well above M.Pt.	M.Pt.	Well above M.Pt.	M.Pt.	Well above M.Pt.
p-Terphenyl	3.76	3.76	- 4.59	- 4.59	1.64×10^{-2}	1.64×10^{-2}
Pyrene	5.08	4.16	- 1.46	- 3.78	4.46×10^{-5}	1.39×10^{-4}
m-Terphenyl	7.40	5.34	4.65	- 0.84	1.73×10^{-4}	2.70×10^{-3}
Tetraphenyl allene	8.12	6.67	2.17	- 1.06	3.90×10^{-6}	1.90×10^{-5}
o-Terphenyl	16.04	7.93	29.30	5.71	7.41×10^{-17}	9.95×10^{-8}
Triphenyl-α-naphthyl allene	20.98	11.30 (185°C)	29.04	6.67 (185°C)	4.67×10^{-12}	3.55×10^{-7} (185°C)

* It may be seen from plates 6.1 and 6.2 and Fig. 2.3b, that the phenyl groups in both m-terphenyl and tetraphenyl allene enjoy about the same limited freedom of movement with respect to their basic skeletons, viz. the >C=C=C< skeleton in the case of tetraphenyl allene, and the parent phenyl group in the case of m-terphenyl.

10.3.2.2. Reduced viscosity.

Recently an attempt has been made (Magill)[6] to obtain plots of log η vs. a reduced temperature, in order to achieve a more convenient comparison between the behaviour of molecules of different types.

The reducing factor chosen was the absolute melting point of the crystalline solid T_m. Ideally, a plot of log η vs. T/T_m might be expected to reduce data for a variety of different materials to a single line, provided that the nature of the molecular interactions for each species were similar.

Plots of log η vs. T/T_m are illustrated in Fig. 10.3 for tetraphenyl allene, triphenyl-α-naphthyl allene*, pyrene and the three terphenyls. It will be seen that the curves tend to converge as the temperature is raised. For a particular value of T/T_m, the extent to which a plot has departed from the hypothetical "normal" line to which it converges may provide an indication of the degree of anomalous behaviour at that point, and furnish a means of comparison. The similarity between the behaviour of m-terphenyl and tetraphenyl allene is reflected in these plots.

---

* Melting point taken as 140°C (see Chapter 5, page 153).

FIG. 10.3.

PLOT OF $\log_{10}\eta$ VS. T_m/T.

⊠ —: P-TERPHENYL.

◇ —: PYRENE.

⊕ —: TETRAPHENYL ALLENE.

⊙ —: m-TERPHENYL.

△ —: O-TERPHENYL.

⊡ —: TRIPHENYL-α-NAPHTHYL ALLENE.

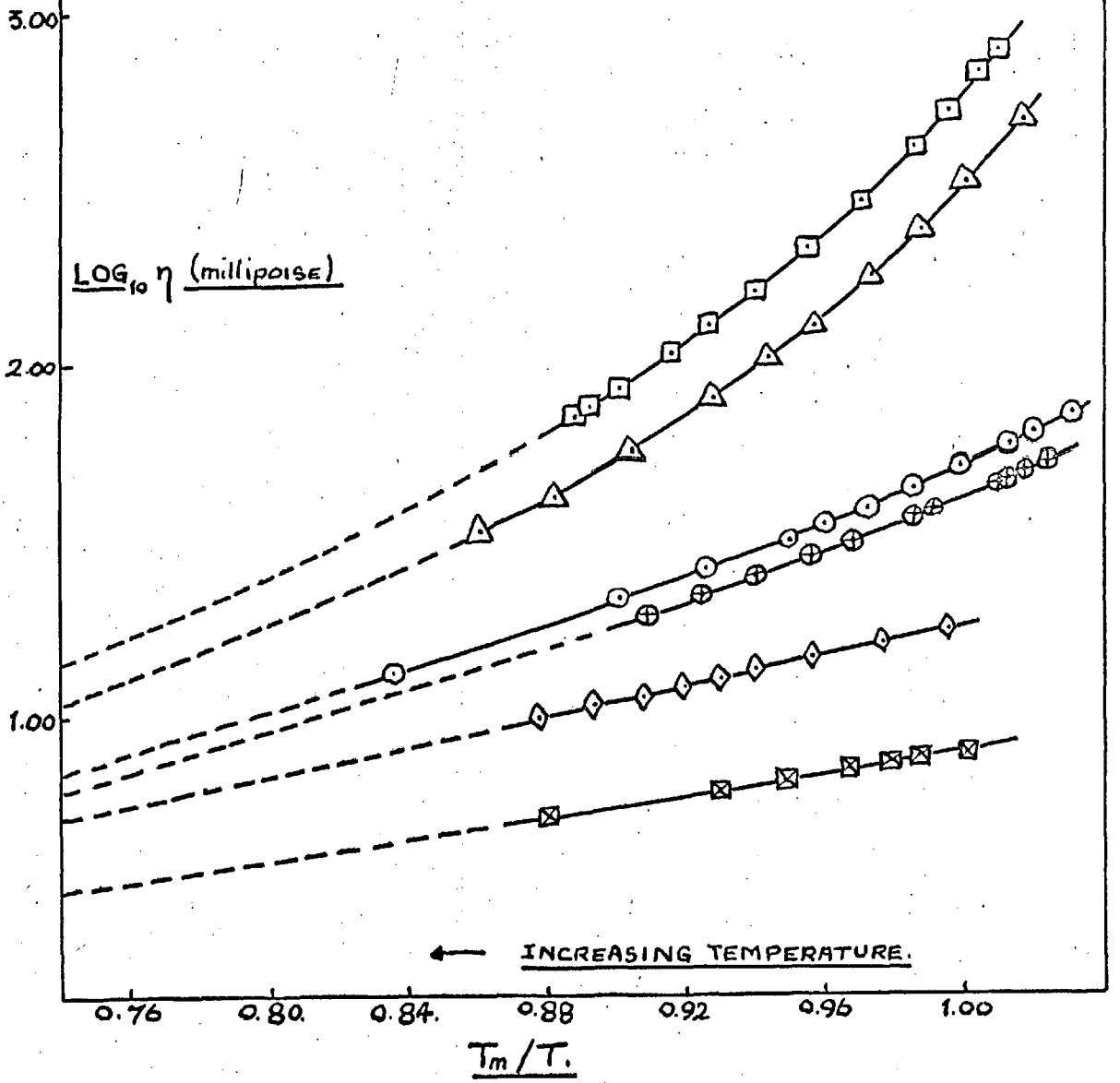

10.3.2.3. Anomalous transport behaviour and the cluster theory.

It has been suggested (Ubbelohde, et. al.[2, 4, 7]), that the marked increase in E_η and ΔS^* which arises in the case of 'cog-wheel' shaped molecules as the temperature is lowered towards their respective melting points may be interpreted in terms of the formation of anti-crystalline clusters (c.f. Chapter 4, section 4.2). These clusters arise from the collision and interlocking of the molecules. At high temperatures, when the log η vs. 1/T plots are linear, the formation and dissolution of clusters is rapid. The life-time of each cluster will be less than the relaxation time for viscous flow, and only single molecules will be effectively involved in transport. As the temperature is lowered, the decreasing free volume, thermal energy, and symmetry of packing will tend to favour the formation of such clusters and extend their life-time. The increases in E_η and ΔS^* mark the point at which the life-time of the clusters exceeds the relaxation time for viscous flow when transport will involve the movement of clusters in addition to single molecules. Further lowering of the temperature will result in an increase in both the cluster concentration and the average cluster size; marked by a corresponding increase in the values of E_η and ΔS^*. In the limit, this can lead to glass formation. (c.f. Chapter 4, section 4.3. and this chapter, section 10.3.1.1.)

Thus, the increase in E_η represents the excess activation energy required for the transport of clusters. The increase in ΔS^* is a measure of the greater local disordering of the liquid structure effected by the transport process.

It was remarked earlier that pyrene displays a small but significant anomaly at temperatures approaching its melting point. The 'disc-shaped' pyrene molecules (Fig. 10.2) will not be conducive to the formation of anti-crystalline clusters in the manner suggested for interlocking 'cog-wheel' shaped molecules. In the case of disc or plate-like molecules however, it is possible to visualise transport involving clusters comprised of repeating units of structure, viz. crystalline clusters, as the free volume is reduced. (c.f. Chapter 4, section 4.2). At low temperatures, the melt may consist of a time-averaged array of crystalline clusters and single molecules disposed at random. A physical picture of this concept is represented in Fig. 10.4.

Values of ϕ_i, the volume per ml. excluded by clusters, are quoted in table 10.4 for tetraphenyl allene, triphenyl-α-naphthyl allene, o- and p- terphenyls and pyrene at their respective melting points.

Values of ϕ_i are calculated at any temperature T using the Einstein equation:

$$\frac{\eta}{\eta_i} = 1 + 2.5\,\phi_i + 7.0\,\phi_i^2 + \ldots \qquad (10.4)$$

FIGURE 10.4.

CRYSTALLINE CLUSTERS IN MOLTEN PYRENE

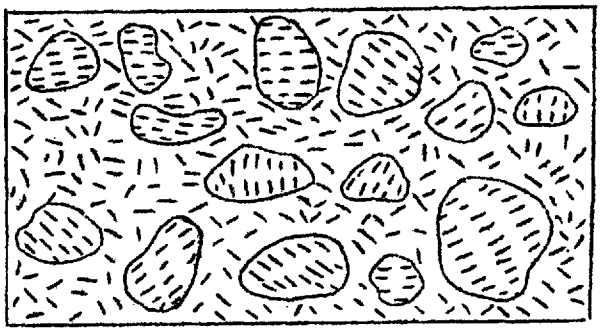

TABLE 10.4

VALUES OF ϕ_i; THE VOLUME EXCLUDED PER ML. BY CLUSTERS

Compound	M. Pt. (°C)	ϕ_i (ml) at M. Pt
p-Terphenyl	213	Nil.
Pyrene	150	0.007
Tetraphenyl allene	166	0.024
o-Terphenyl	55.5	0.58
Triphenyl-α-naphthyl allene	140	0.24*

* This value was obtained relative to the tangent to the log η vs. 1/T plot at 185°C, and will be an underestimate (See section 10.3.2.1.)

where η is the observed viscosity and η_i the ideal viscosity of the melt in question. The latter is derived by extrapolation to T from the linear portion of the log η vs. 1/T plot which prevails at higher temperatures (c.f. Chapter 2, section 2.4). Values of the blocked volume fraction ϕ_i afford a useful basis for comparison. Although equation (10.4), in its most simple form, is valid only when $\phi_i \leq 0.3$, the large values of ϕ_i for both triphenyl-α-naphthyl allene and o-terphenyl reflect the propensity of these melts to glass formation upon further cooling. In support of this correlation, the glass-forming 1:3:5 tri-α-naphthyl benzene also shows a high value for ϕ_i at its melting point viz. 0.40[4,8]. On this basis, a glass corresponds to a melt in which every part is interlocked (i.e. $\phi_i = 1$), and no changes in configurational structure may be detected within the time of observation in an experiment.

10.3.2.4. Fluidity/specific volume relationships

Amongst other methods of correlating viscosity data with molecular shape, and probable changes in the configurational structure of the melt, the Batschinski equation (equation 10.5) relating fluidity ($1/\eta$) to specific volume V_s has been most widely used (see Chapter 2, section 2.3.5.).

$$\phi \text{ or } 1/\eta = \frac{V_s - w}{c} \qquad (10.5)$$

Equation (10.5) predicts a linear relationship between fluidity

ϕ and specific volume V_s, and is obeyed by a variety of normal liquids. w and c are constants for any particular liquid.

Within the context of interlocking molecules departures from linearity, and the consequent variations in the parameters c and w, may be interpreted in terms of cluster formation. Values of these parameters at their melting points and well above their melting points are quoted in table 10.5 for the molecules under discussion including tetraphenyl allene, triphenyl-α-naphthyl allene and pyrene. The ϕ vs. V_s plots for these compounds are illustrated in Figs. 10.10g, 10.9, and 10.10 a, respectively.

Any departure from linearity displayed by these compounds is marked by a general increase in the value of c, and a decrease in the value of w. The changes in c and w as the

TABLE 10.5

BATSCHINSKI PARAMETERS

COMPOUND	Well above M.Pt		Melting point	
	c x 10^{-4}	w	c x 10^{-4}	w
p-Terphenyl	8.01	0.932	8.01	0.932
Pyrene	7.19	0.874	7.19	0.874
m-Terphenyl	7.40	0.952	12.15	0.938
Tetraphenyl allene	12.13	0.972	15.46	0.961
o-Terphenyl	10.50	0.958	37.00	0.934
Triphenyl-α-naphthyl allene	21.66 (185°C)	0.958	67.70	0.934

temperature is lowered to the melting points is of the same order for both tetraphenyl allene and m-terphenyl. The changes in c are 3.3×10^{-4} and 4.7×10^{-4}, and the changes in w are 0.011 and 0.014 respectively. This similarity reflects the conclusions reached with regard to the values of $E\eta$ and $\Delta S^{\ddagger}$ for these compounds. The anomalous behaviour of triphenyl-α-naphthyl allene is especially marked, and the changes in c and w occurring between 185°C and the melting point are 46×10^{-4} and 0.024 respectively. The corresponding values for changes in c and w for o-terphenyl are 26.5×10^{-4} and 0.024 respectively. Neither pyrene nor p-terphenyl display any measurable anomaly.

10.3.2.5. The importance of molecular shape and molecular rotation.

Matheson and Davies[9] have recently suggested that inhibited molecular rotation is largely responsible for anomalies in viscous flow (c.f. Chapter 2, section 2.4). Evidence derived from the study of polyphenyl melts has tended to refute the generality of this statement. It may be seen from table 10.1 that none of the three terphenyls is able to rotate about any of the three perpendicular axes at their melting points or at higher temperatures.

Allowing a possible error of $\pm$ 10 % in the estimates of volumes of rotation (see Appendix), tetraphenyl allene and

triphenyl-α-naphthyl allene may just rotate about their X axes, and pyrene about its Y axis at their respective melting points (see this chapter, section 10.2). It may be seen from Fig. 10.2 that since pyrene is disc-shaped, rotation about the Y axis is unlikely to influence the general orientation of the molecules to any significant extent.

It has already been mentioned that o-, and m-terphenyls show marked anomalies in transport at temperatures in the vicinity of their melting points, but that p-terphenyl shows no such anomaly. An examination of the molecular structures of the terphenyls (Fig. 2.3) reveals that whilst p-terphenyls (Fig. 2.3) reveals that whilst p-terphenyl is 'rod-shaped', o- and m-terphenyl are 'cog-wheel' shaped. Since neither molecule is able to rotate in the melt, there is a direct correlation between molecular shape and anomalous behaviour. Further evidence of this correlation is provided by the fact that whilst the 'cog-wheel' shaped tetraphenyl allene and triphenyl-α-naphthyl allene enjoy a freedom of rotation similar to that of pyrene, the allenes display marked anomalies whereas pyrene displays but a small anomaly.

Thus, it may be concluded that a comparison between molar volumes of rotation and observed molar volumes provides a general indication of molecular anisotropy. As in the case of glass formation (section 10.3.1.1.), this factor may influence the

predisposition of molecules to particular orientations which may favour cluster formation, but anomalies in the shape of departures from linearity in log η vs. 1/T and ϕ vs. V_s plots are determined, within this context of non-polar molecules, principally by the precise molecular shape.

10.4. TETRAPHENYL ALLENE/PYRENE MIXTURES

10.4.1. Introduction.

Having established that specific molecular shape may play a decisive part in the determination of a liquid's properties, it was considered that dilution of a liquid comprised of interlocking molecules with molecules of higher symmetry (e.g. discs or spheres) might produce some extraordinary changes in the liquid behaviour. Two molecules were chosen as possible diluents, viz. pyrene (disc-shaped), and the pseudo-spherical bridged hydrocarbon adamantane. Unfortunately, but as might be expected from the rigid nature of the molecule, adamantane has a very short liquid range at atmospheric pressure ($\sim 3^{\circ}C$). Adamantane could not be used therefore, without extensive adaptation of the molar volume and viscometric apparati for operation at high pressures. Pyrene was selected as a diluent.

10.4.2. Excess Volumes of Mixing and Partial Molar Volumes Re. the Tetraphenyl Allene/Pyrene System.

Changes in the liquid structure which accompany the dilution of tetraphenyl allene with pyrene are manifest in the excess

volumes of mixing and partial molar volume data for the system. In particular, features appear in the partial molar volume (actually $\bar{V}_M - V_M$ where $\bar{V}_M$ is the partial molar volume and V_M is the molar volume of the pure component) vs. composition plots for the two components may be interpreted in terms of the dissolution of tetraphenyl allene clusters effected by the addition of pyrene.

Fig. 9.1.5. illustrates the molar volume (V_M) vs. temperature plots for tetraphenyl allene/pyrene mixtures containing 0, 10, 20, 25, 40, 45, 50, 55, 60, 65, 70, 80, 90, 95, and 100 mole % tetraphenyl allene. Within the limits of experimental error ($\pm$ 0.1 %) these plots are linear. Fig. 9.1.6. represents a plot of the expansion parameter α (i.e. dV_M/dT) vs. composition.

The excess volumes of mixing per mole of mixture (ΔV_M^m) vs. composition plots at three temperatures over a range of 60°C are represented in Fig. 9.1.7. The corresponding percentage excess volumes of mixing vs. composition plots are illustrated in Fig. 9.1.7a. The molar excess volumes are positive, indicating a positive deviation from Raoult's law (c.f. Chapter 3, section 3.2), and the plots of ΔV_M^m vs. composition are unsymmetrical with respect to composition reaching a maximum of about 0.6 % at 75 mole % tetraphenyl allene. The shape of the plots and the values of ΔV_M^m vary little with temperature over a range of

$60^{\circ}C$, though there is a general tendency for ΔV_M^m to decrease with rising temperature.

Values of the partial molar volumes for each component over the full composition range were obtained from the ΔV_M^m vs. composition plot by the method of intercepts (c.f. Chapter 3, section 3.4.), tangents to the curve being constructed geometrically. Plots of $\bar{V}_M - V_M$ vs. composition for both pyrene and tetraphenyl allene at $166^{\circ}C$ are illustrated in Fig. 10.5. Since it can be seen from Fig. 9.1.7. that the nature of the ΔV_M^m vs. composition plot varies little over a range of $60^{\circ}C$, plots of $\bar{V}_M - V_M$ vs. composition at temperatures higher or lower than $166^{\circ}C$ were deemed unnecessary.

The Gibbs-Duhem equation is a necessary relation between the partial molar properties of the components in a mixture. In the present context, the Gibbs-Duhem relation may be written:

$$x_p \left(\frac{\partial \bar{V}_p}{\partial x_p} \right)_T = - x_A \left(\frac{\partial \bar{V}_A}{\partial x_A} \right)_T$$

where x_p and x_A are the mole fractions, and $\bar{V}_p$ and $\bar{V}_A$ the partial molar volumes of pyrene and tetraphenyl allene respectively. The most obvious consequence of this equation is that if

$\left(\frac{\partial \bar{V}_A}{\partial x_A} \right)_T$ is zero at a maximum of $\bar{V}_A$, then

$\left(\frac{\partial \bar{V}_p}{\partial x_p} \right)_T$ is zero at a minimum of $\bar{V}_p$ (9). It may be

FIG. 10.5.

PLOT OF $(\bar{V}_m - V_m)$ VS COMPOSITION FOR BOTH TETRAPHENYL ALLENE AND PYRENE IN THE TETRAPHENYL ALLENE / PYRENE SYSTEM. AT 166·8°C.

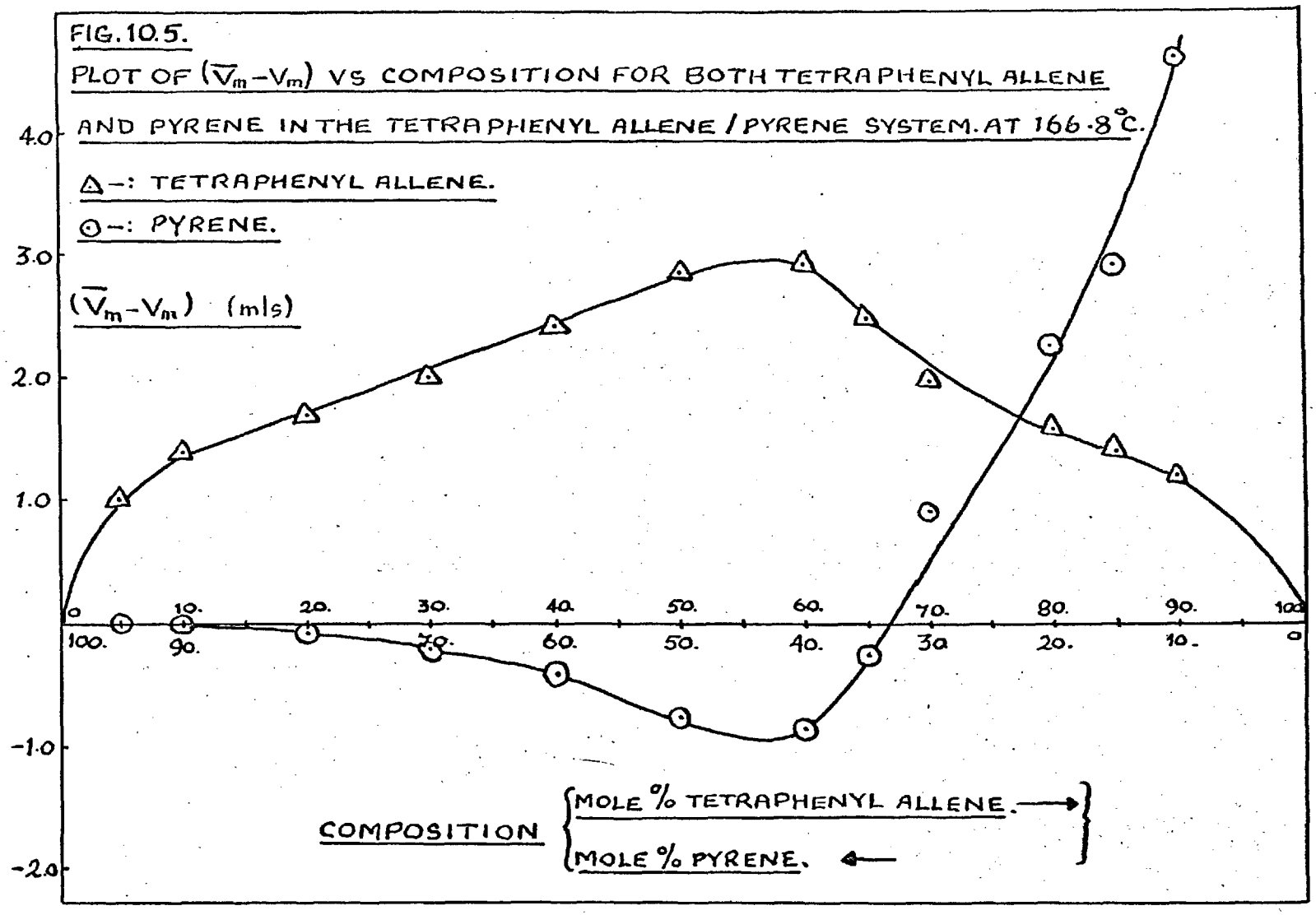

seen from Fig. 10.5 that this is in fact so. Unfortunately there is insufficient excess volume data to allow an accurate estimate to be made of the partial molar volumes of the two components for mixtures containing more than 95 mole % tetraphenyl allene. The trend in this region is however quite clear*. In this region therefore, it may be said that the pyrene component is responsible for the majority of the excess volume of mixing (Fig. 10.5). This suggests that the original structure of the tetraphenyl allene remains comparatively unchanged, and that the pyrene molecules occupy sites between each cluster of tetraphenyl allene molecules. The packing of the pyrene molecules is not economical, and a greater volume is associated with each pyrene molecule in the mixture than in pure pyrene. As progressively more pyrene is added, the partial molar volume of the pyrene decreases and the partial molar volume of the tetraphenyl allene increases. The partial molar volume of the tetraphenyl allene reaches a maximum and the partial molar volume of the pyrene reaches a minimum when the concentration of the tetraphenyl allene reaches about 57 mole %**.

---

* Although some liquid mixtures have been reported (e.g. water/dioxan) which fail to fulfill the conditions dictated by the Gibbs-Duhem equation, gross deviations therefrom normally signify a phase separation[10].

** The point of intersection of the tetraphenyl allene and pyrene curves represents the maximum excess volume of mixing, which occurs when the concentration of tetraphenyl allene reaches about 75 mole %.

It is suggested that over this region, the addition of pyrene is effecting the dissolution of tetraphenyl allene clusters. The original structure of the tetrapnenyl allene is distorted and the pyrene molecules can pack more economically in interstices between tetraphenyl allene molecules. In the vicinity of the minimum in the $\bar{V}_M - V_M$ vs. composition plot for pyrene, the average volume occupied by each molecule is slightly less than in the pure melt. As the concentration of pyrene increases towards 100 mole %, the partial molar volume of this component rapidly approaches the ideal i.e. the molar volume of pure pyrene. Under these conditions the excess volume is due primarily to tetraphenyl allene. The tetraphenyl allene molecules are probably packed at random and less economically than in the pure component, each molecule locally disturbing the basic pyrene structure.

As the shape of the ΔV_M^m vs. composition plots vary little with temperature, $\bar{V}_M - V_M$ vs. composition plots for both components of the mixture at higher temperatures ($> 185^\circ C$) will be similar to those described above for $166^\circ C$. Raising the temperature from $166^\circ C$ to $185^\circ C$ does not effect much change in the general liquid structure. The tentative interpretation of the $V_M^m - V_M$ vs. composition plot cited above should be valid at higher temperatures, the principal difference being that at higher temperatures the life-time of each cluster is less than the relaxation time for viscous flow (see Section 10.3.2.3).

10.4.3. Viscometric Parameters for the Tetraphenyl Allene/ Pyrene System.

Plots of log η vs. 1/T for tetraphenyl allene/pyrene mixtures containing 0, 20, 25, 40, 60, 80 and 100 mole % tetraphenyl allene are illustrated in Fig. 8.7. Values of E_η , A, and ΔS^* at three temperatures (> 185°C, 166°C, and 150°C) are listed in table 10.6. Figs. 10.6 and 10.7 represent plots of $E\eta$ and ΔS^* vs. composition at each temperature.

It will be noticed that the term δ/a (c.f. equation 10.2) has been estimated in the case of tetraphenyl allene/pyrene mixtures. The significance of this term has been discussed earlier, where it was defined as the ratio of the intermolecular distances in the solid lattice in the vertical and horizontal planes. In the absence of crystallographic data for tetraphenyl allene the factor has been redefined in the present context as the ratio of the shortest to the longest van de Waals' radius of the molecule* . Introduction of this factor however, does not appear to alter the general trends in the values of ΔS^* as the temperature decreases (see Table 10.6 and Fig. 10.7). Values of ϕ_i, the volume per ml. excluded by clusters, at 166°C and 150°C are quoted in table 10.7.

---

* It would seem that this approximation is reasonable. The value of δ/a for pyrene obtained by X-ray crystallography is 0.33[11]. The value for the ratio of the shortest to the longest van de Waals' radius is 0.36. Values of δ/a for the mixture are simply average values computed for each composition.

TABLE 10.6.

VISCOMETRIC PARAMETERS FOR THE TETRAPHENYL ALLENE/ PYRENE SYSTEM

Mole % tetraphenyl allene	>185°C		166°C		150°C	
	E_η K.cal. $mole^{-1}$	A poise	E_η K.cal. $mole^{-1}$	A poise	E_η K.cal. $mole^{-1}$	A poise
0.00	4.16	13.9×10^{-5}	4.31	10.9×10^{-5}	5.08	4.46×10^{-5}
20.00	4.81	7.89 "	5.45	3.94 "	5.76	2.72 "
25.00	5.08	6.26 "	5.57	3.53 "	6.08	1.97 "
40.00	5.37	5.18 "	6.27	1.91 "	6.90	0.91 "
60.00	5.73	4.04 "	6.95	1.06 "	7.83	0.38 "
80.00	6.20	2.94 "	7.60	0.62 "	8.84	0.15 "
100.00	6.67	1.90 "	8.12	0.39 "	-	-

Mole % tetraphenyl allene	200°C		166°C		150°C		$\frac{\delta}{a}$
	(i) ΔS e.u.	(ii) ΔS e.u.	(i) ΔS e.u.	(ii) ΔS e.u.	(i) ΔS e.u.	(ii) ΔS e.u.	
0.00	-3.78	-7.79	-3.26	-7.29	-1.46	-5.47	0.3642
20.00	-2.97	-5.87	-1.54	-4.44	-0.78	-3.68	0.4824
25.00	-2.58	-5.24	-1.43	-4.09	-0.21	-2.87	0.5120
40.00	-2.40	-4.43	-0.37	-2.40	1.13	-0.90	0.6006
60.00	-2.15	-3.46	0.56	-0.76	2.64	1.33	0.7188
80.00	-1.73	-2.44	1.41	-0.71	4.32	3.61	0.8370
100.00	-1.06	-1.24	2.17	1.98	-	..	0.9552

For values of $\Delta S^{(i)}$ the value of δ/a was taken as unity.
For values of $\Delta S^{(ii)}$ the values of δ/a are as indicated.

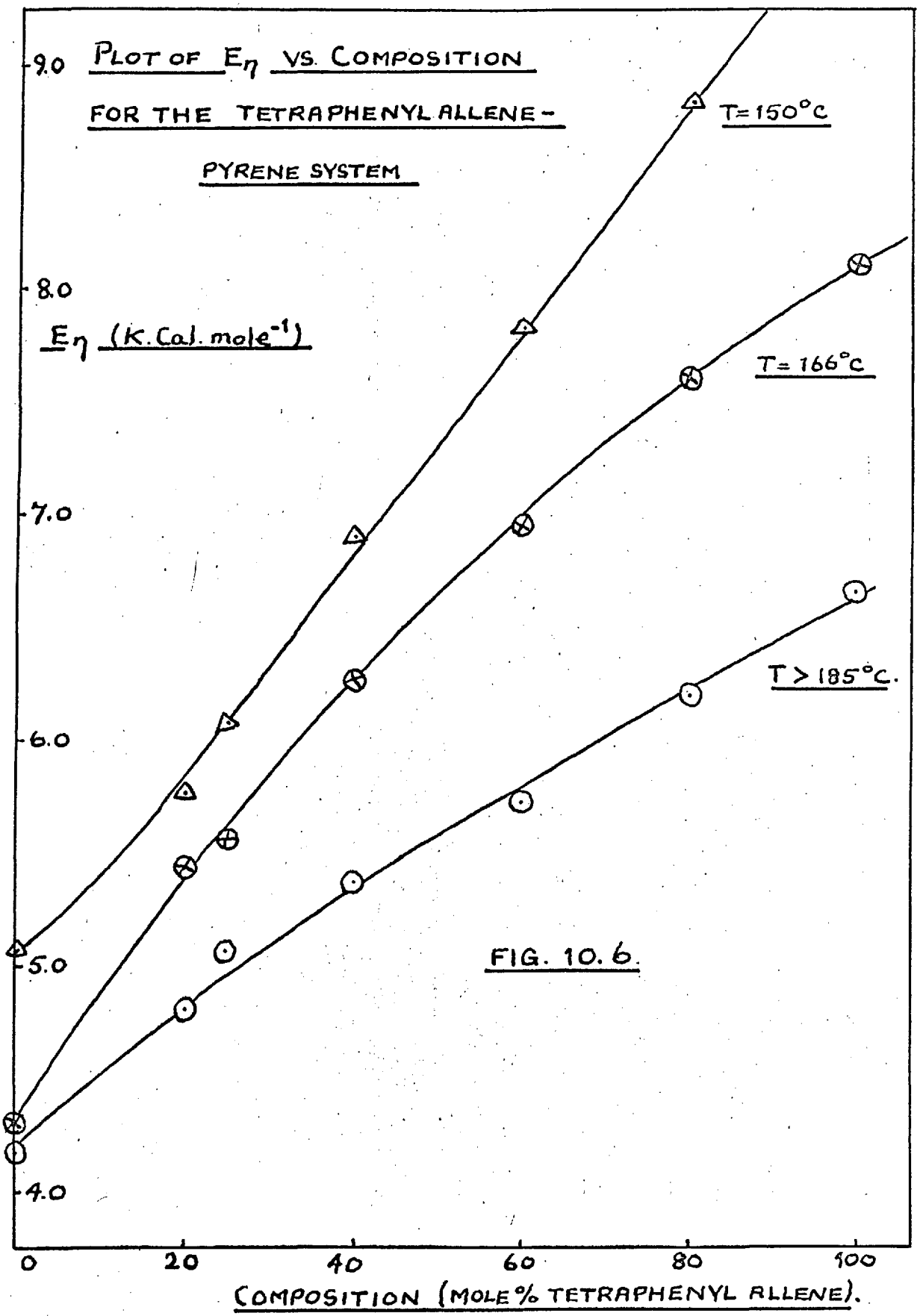
PLOT OF E_η VS. COMPOSITION
FOR THE TETRAPHENYL ALLENE-
PYRENE SYSTEM
T=150°C
T=166°C
T>185°C.
E_η (K.Cal. mole^{-1})
9.0
8.0
7.0
6.0
5.0
4.0
0
20
40
60
80
100
COMPOSITION (MOLE% TETRAPHENYL ALLENE).

FIG. 10.6.

FIG. 10.7.

PLOT OF ENTROPY OF ACTIVATION FOR VISCOUS FLOW VS. COMPOSITION.

(TETRAPHENYL ALLENE / PYRENE SYSTEM.)

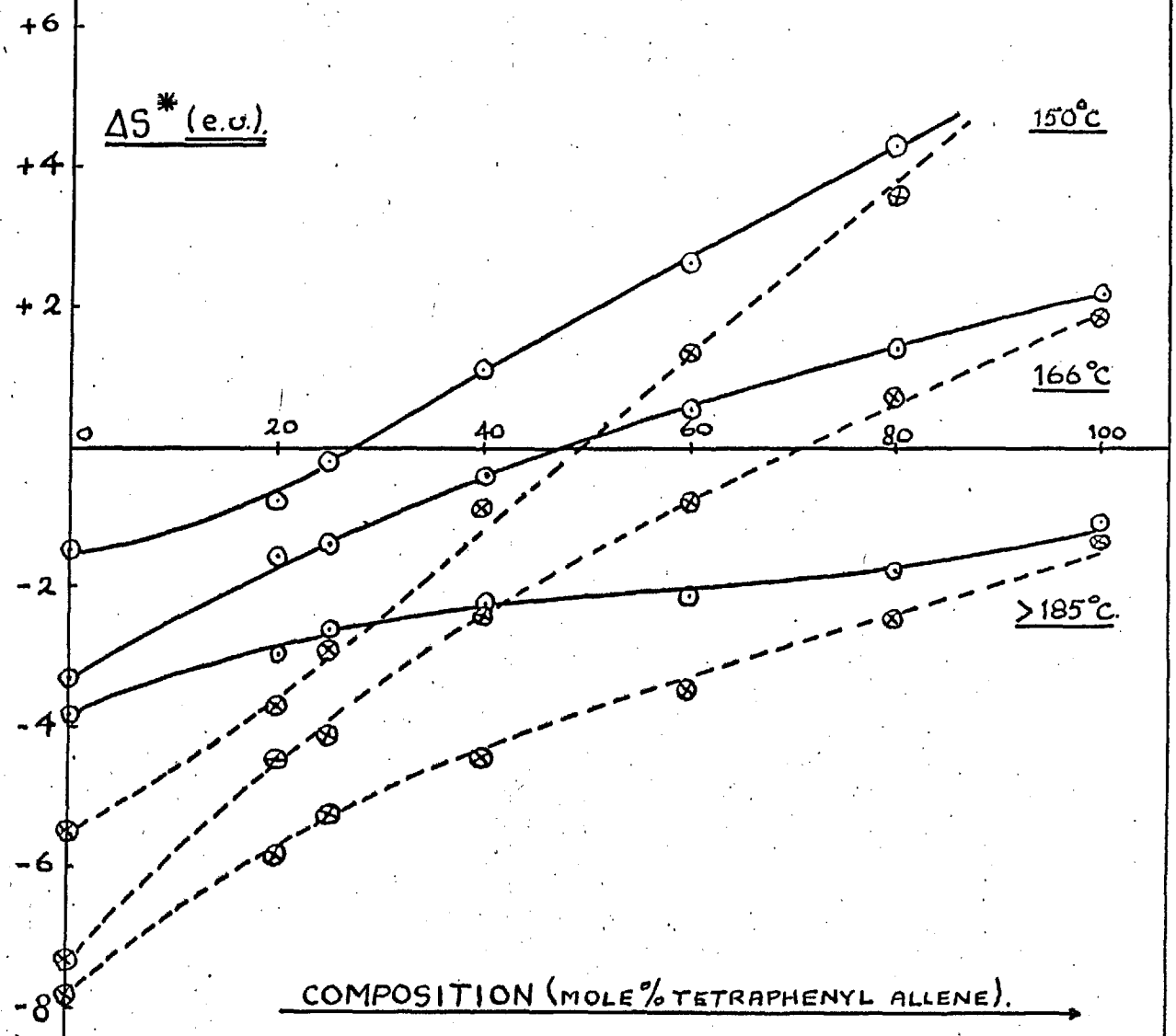

⊙ —: RATIO $\frac{\delta}{a} = 1.$

⊗ —: RATIO $\frac{\delta}{a} = 0.36\ (0\%)$ TO $0.96\ (100\%)$

The corresponding plots of fluidity vs. specific volume are illustrated in Figs. 10.10a to 10.10g :. Values of the parameters c and w arising from the Batschinski equation (equation 10.5) are listed in table 10.8 for the three temperatures mentioned above, and plots of w and c vs. composition are illustrated in Figs. 10.11 a and b, respectively.

TABLE 10.7

EXCLUDED VOLUME PARAMETER ϕ_i
(TETRAPHENYL ALLENE/PYRENE SYSTEM)

Mole % tetraphenyl allene	ϕ_i (mls) (166°C)	ϕ_i (mls) (150°C)
0.00	0.006	0.007
20.00	0.006	0.019
25.00	0.004	0.014
40.00	0.011	0.027
60.00	0.014	0.035
80.00	0.022	0.064
100.00	0.024	-

At the highest temperature quoted ($>$ 185°C) both pure tetraphenyl allene and pure pyrene behave normally, as do the mixtures over the full composition range. The values of E_η and $\Delta S^{\ddagger}$ (see table 6 and Figs. 10.6 and 10.7) represent for

each composition the average activation energy and entropy for the transport of single molecules in the mixture. The values of these parameters decrease almost linearly as the concentration of pyrene is raised since E_η and $\Delta S^{\ddagger}$ are greater for 'cog-wheel' shaped tetraphenyl allene molecules than for 'disc-shaped' pyrene molecules. At 166°C pure tetraphenyl allene displays some anomaly but pure pyrene behaves almost normally. The plots of E_η and $\Delta S^{\ddagger}$ vs. composition are not linear and indicate that the values of these parameters are decreasing more rapidly with the addition of pyrene than at the higher temperature. This implies that the progressive addition of pyrene is effecting dissolution of tetraphenyl allene clusters.

At the lowest temperature quoted (150°C), both pure tetraphenyl allene* and pure pyrene display anomalies. The cluster effects in tetraphenyl allene at this temperature will be much greater than those in pyrene, and the progressive addition of pyrene, results in a marked decrease in E_η and $\Delta S^{\ddagger}$. The plots of E_η and $\Delta S^{\ddagger}$ vs. composition are almost linear, but the decrease in slope which occurs when the concentration of pyrene exceeds 80 mole % may arise from cluster effects in pyrene alone.

---

* Values of E_η and $\Delta S^{\ddagger}$ for pure tetraphenyl allene have not been quoted at 150°C since tetraphenyl allene tended to crystallise before this temperature was reached. To estimate values of E_η and $\Delta S^{\ddagger}$ for this compound at 150°C would have involved extrapolation of the $\log \eta$ vs. $1/T$ plot over a region in which $d \log \eta / d(1/T)$ was changing rapidly. It was felt that such an extrapolation would not be meaningful.

The trends in the pre-exponential term A reflect trends in $\Delta S^{\ddagger}$ in the manner predicted by equation 10.3.

Fig. 10.8 represents a plot of $\bar{V}_M - V_M$ for both components vs. $E\eta$ for each composition over the full range at 166°C. At this temperature, the influence of clusters upon the viscosity of pure tetraphenyl allene is manifest. It will be seen that this plot is not identical but similar in form to the $\bar{V}_M - V_M$ vs. composition plot (Fig. 10.5). At higher temperatures ($>$ 185°C) when both components behave normally, $E\eta$ is an almost linear function of composition, and it might be expected at these temperatures, that the forms of the $\bar{V}_M - V_M$ vs. composition and $\bar{V}_M - V_M$ vs. $E\eta$ plots will become identical.

The dissolution of tetraphenyl allene clusters effected by dilution with pyrene is also reflected in the fluidity vs. specific volume plots. Departure from linearity decreases as the concentration of pyrene is raised (c.f. Figs. 10.10a to 10.10g). It may be seen from table 10.8 and Fig. 10.11b, that at high temperatures there is an almost linear decrease in the value of the Batschinski parameter c with the addition of pyrene. As the temperature is lowered, the rate of decrease becomes more marked. At all temperatures, the values of w decrease as the tetraphenyl allene is diluted (Fig. 10.11a and Table 10.8). If, as suggested by Batschinski the term w is associated with the effective volume of the molecules themselves (see Chapter 2,

FIG. 10.8.

PLOT OF $(\bar{V}_M - V_m)$ VS. E_η FOR BOTH TETRAPHENYL ALLENE AND PYRENE IN THE TETRAPHENYL ALLENE / PYRENE SYSTEM AT 166°C.

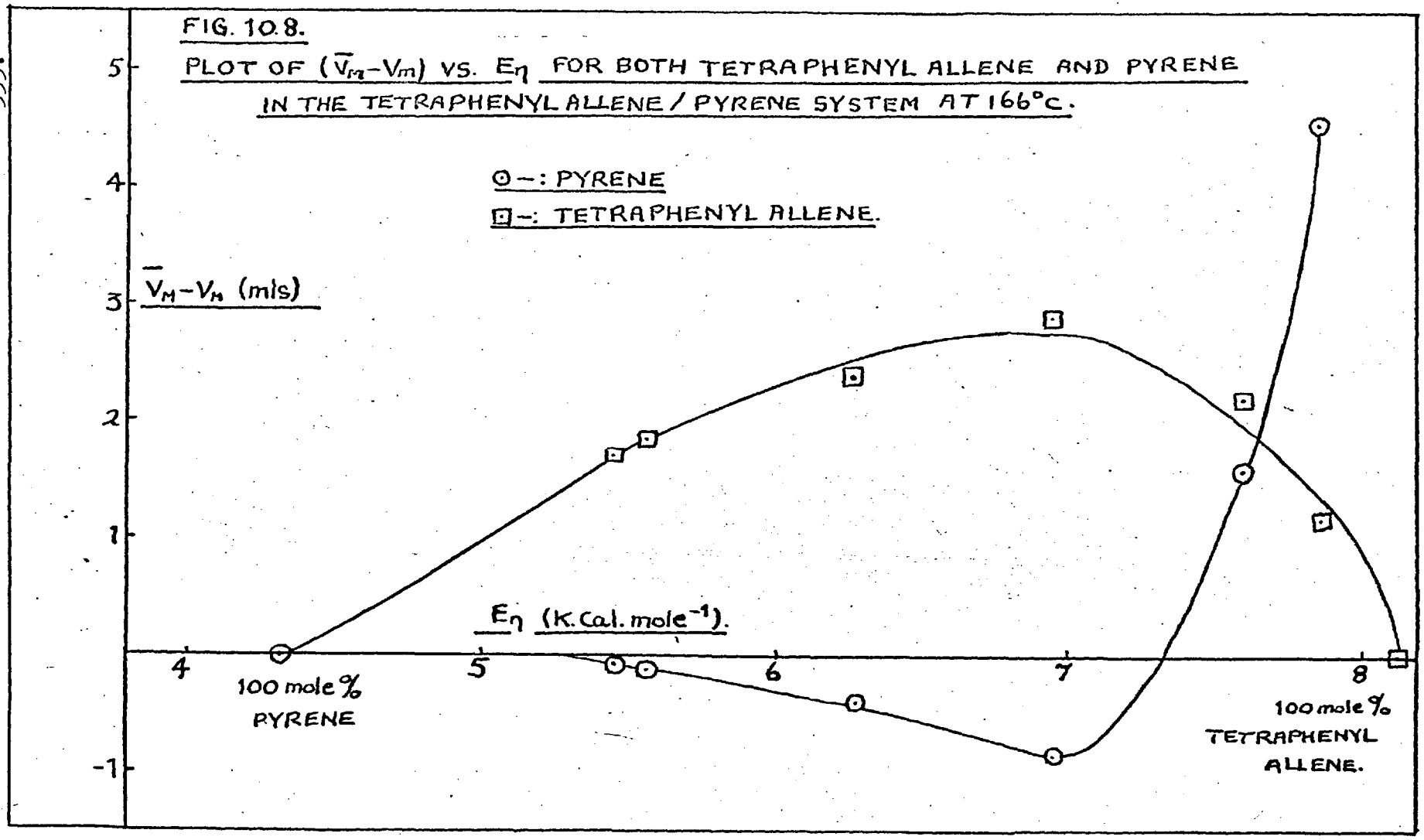

section 2.3.5), the general decrease in the values of w upon raising the concentration of pyrene may be expected. The actual volume of the tetraphenyl allene molecule (321 Å ^{3}) is greater than that of the pyrene molecule (280 Å ^{3}), (see Appendix).

TABLE 10.8

BATSCHINSKI PARAMETERS

(TETRAPHENYL ALLENE/PYRENE SYSTEM)

Mole % Tetraphenyl allene	150°C		165°C		>185°C	
	c x 10^{-4}	w	c x 10^{-4}	w	c x 10^{-4}	w
0.00	7.19	0.874	7.19	0.874	7.19	0.874
20.00	9.69	0.898	8.89	0.901	8.19	0.905
25.00	10.42	0.903	9.18	0.908	8.44	0.912
40.00	12.27	0.917	10.69	0.922	9.39	0.927
60.00	13.50	0.938	12.47	0.939	9.72	0.951
80.00	19.60	0.944	13.63	0.956	10.64	0.968
100.00	-	-	15.46	0.961	12.13	0.972

The most significant feature is the general decrease in w as the temperature is lowered which becomes less marked as the concentration of pyrene is raised.

By comparison with the data discussed earlier with regard to 'cog-wheel' shaped molecules (see this chapter, section 10.3.2.4.), this trend would seem to support the contention

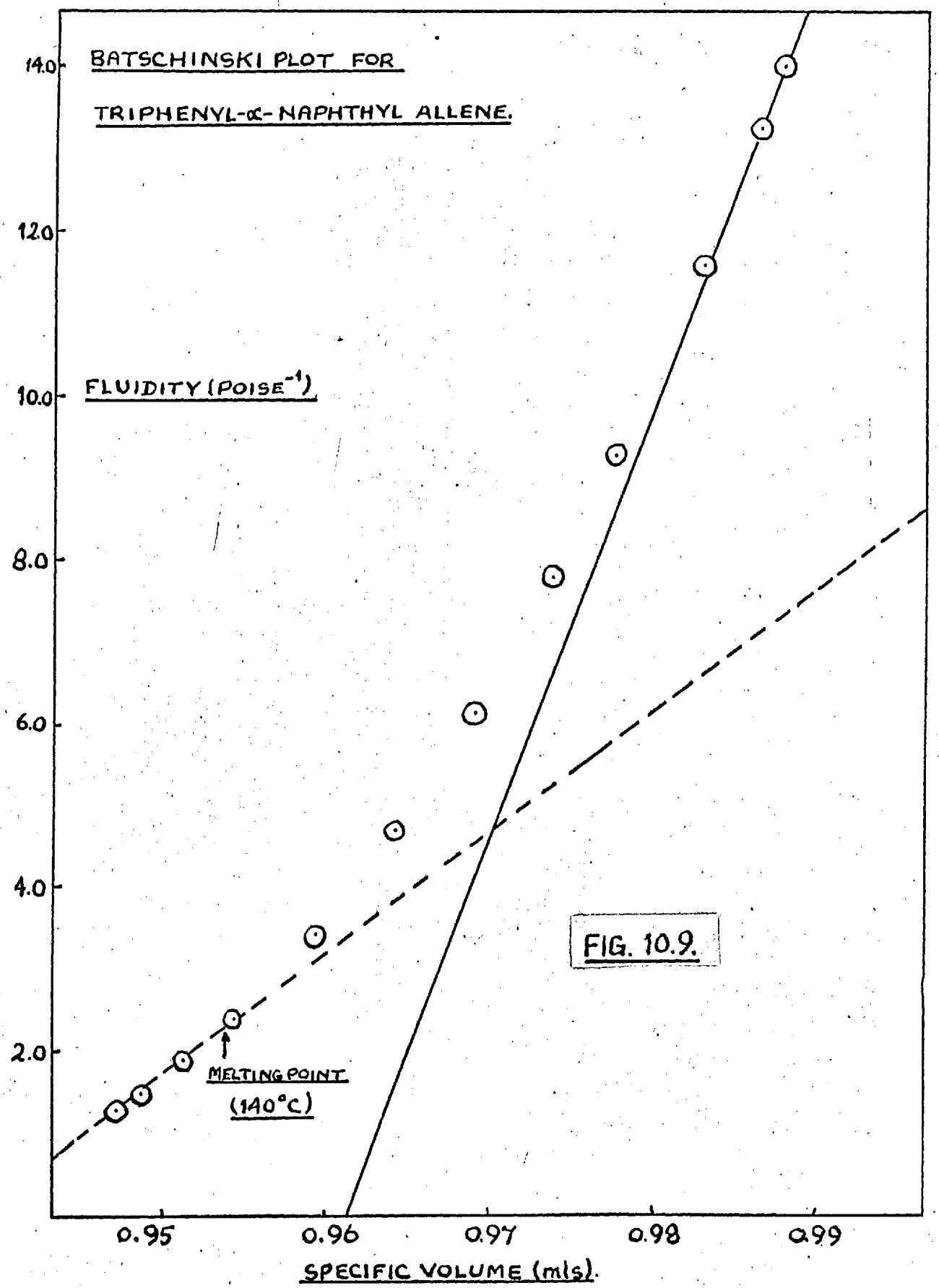
BATSCHINSKI PLOT FOR
TRIPHENYL-α-NAPHTHYL ALLENE.
FLUIDITY (POISE^{-1})
14.0
12.0
10.0
8.0
6.0
4.0
2.0
MELTING POINT
(140°C)
0.95
0.96
0.97
0.98
0.99
SPECIFIC VOLUME (ml/g).

FIG. 10.9.

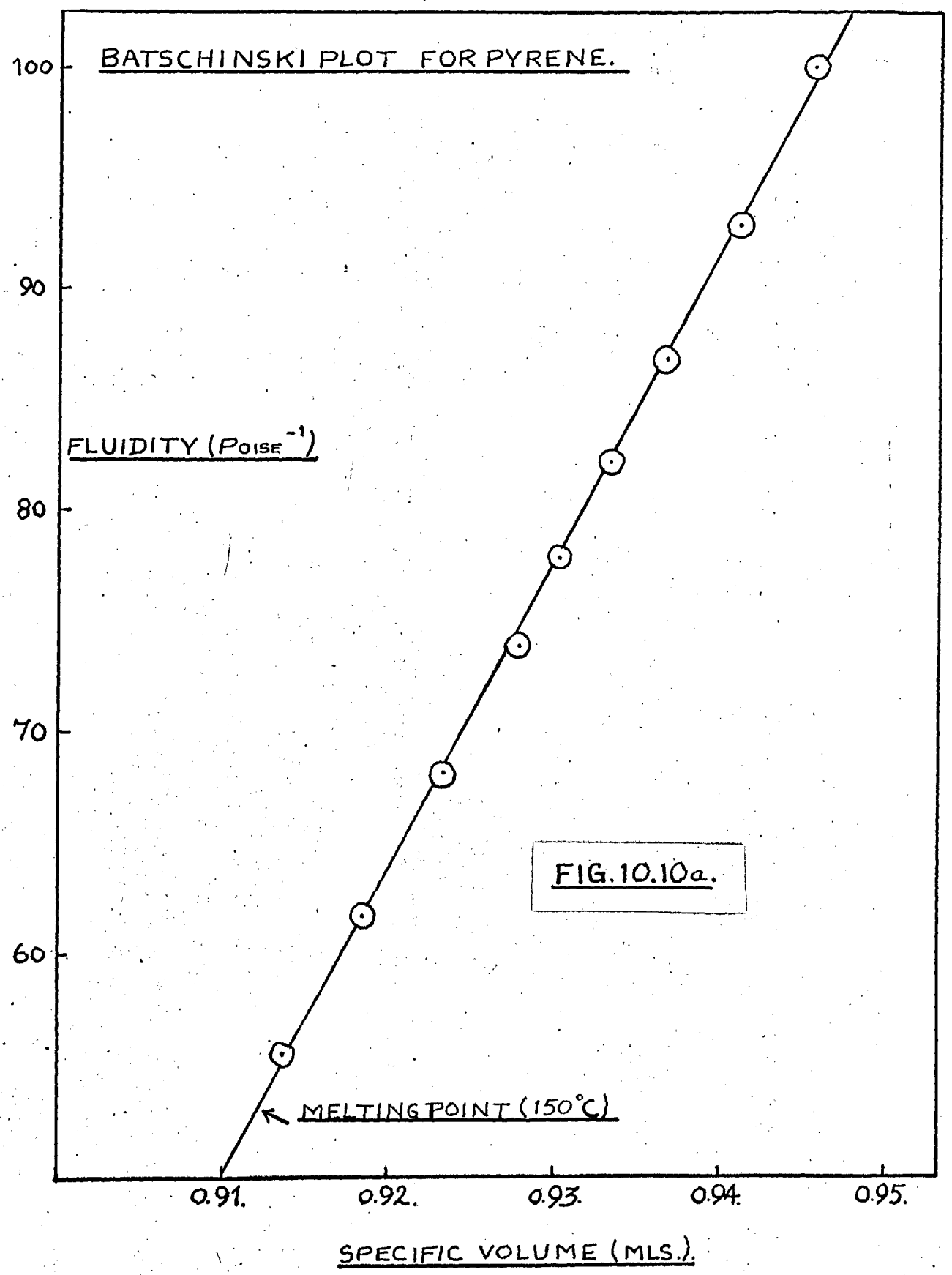
BATSCHINSKI PLOT FOR PYRENE.
100
90
80
70
60
FLUIDITY (Poise^{-1})
MELTING POINT (150°C)
0.91.
0.92.
0.93.
0.94.
0.95.
SPECIFIC VOLUME (MLS.)

FIG. 10.10a.

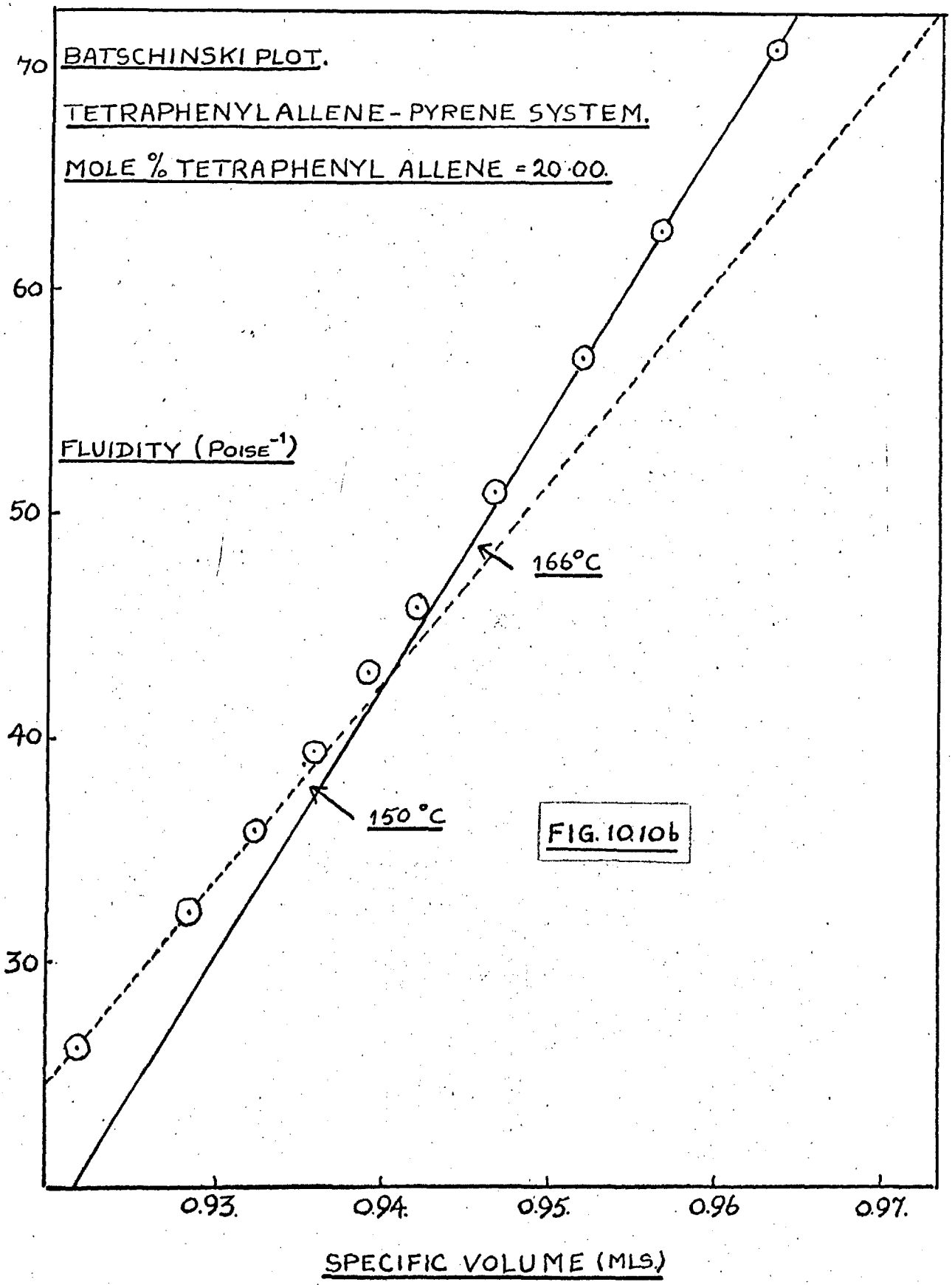
BATSCHINSKI PLOT.
TETRAPHENYLALLENE-PYRENE SYSTEM.
MOLE % TETRAPHENYL ALLENE = 20·00.
FLUIDITY (Poise^{-1})
70
60
50
40
30
166°C
150 °C
0.93.
0.94.
0.95.
0.96
0.97.
SPECIFIC VOLUME (MLS.)

FIG. 10.10b

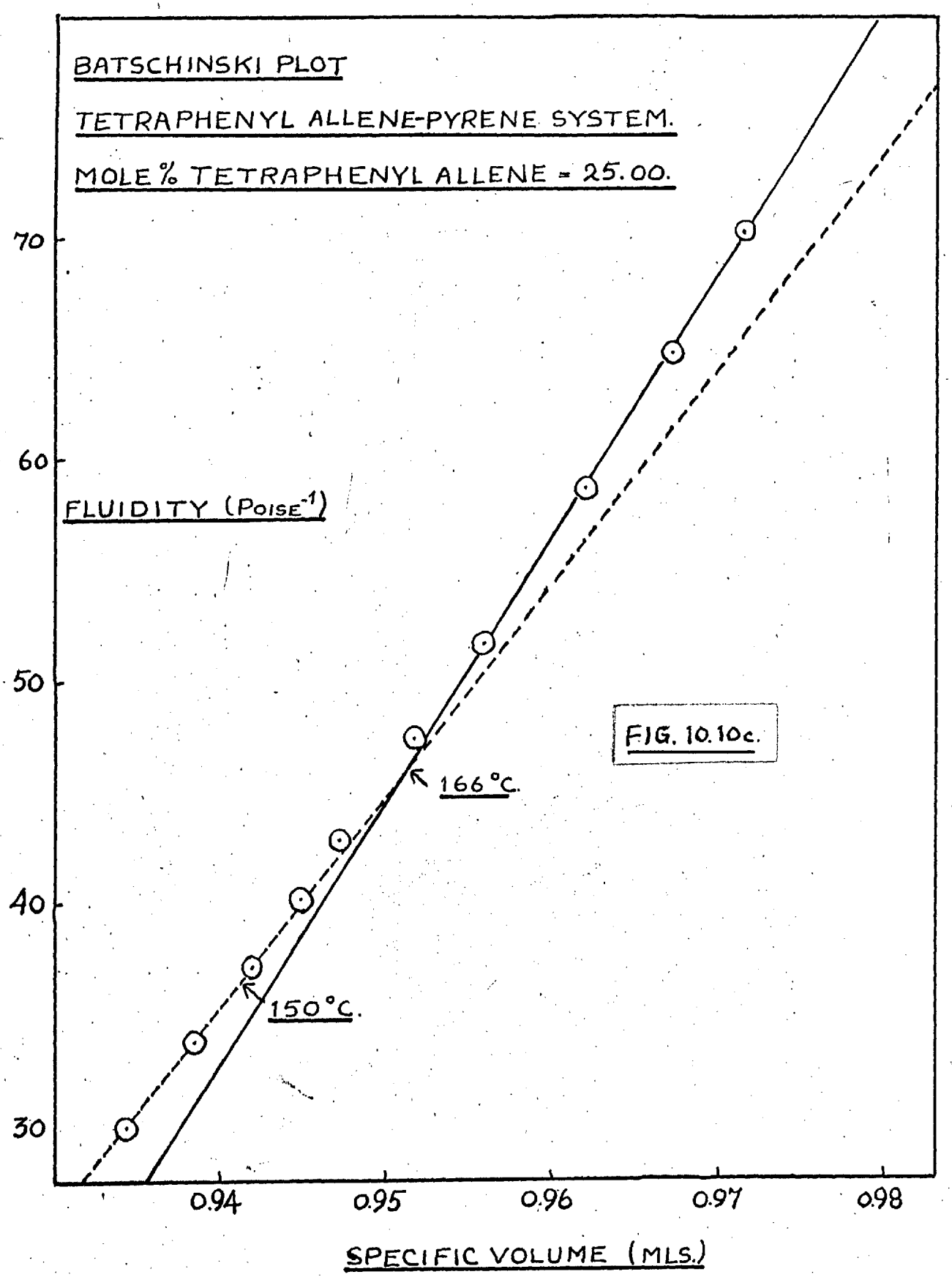
BATSCHINSKI PLOT
TETRAPHENYL ALLENE-PYRENE SYSTEM.
MOLE % TETRAPHENYL ALLENE = 25.00.
70
60
50
40
30
FLUIDITY (POISE^{-1})
166 °C.
150 °C.
0.94
0.95
0.96
0.97
0.98
SPECIFIC VOLUME (MLS.)

FIG. 10.10c.

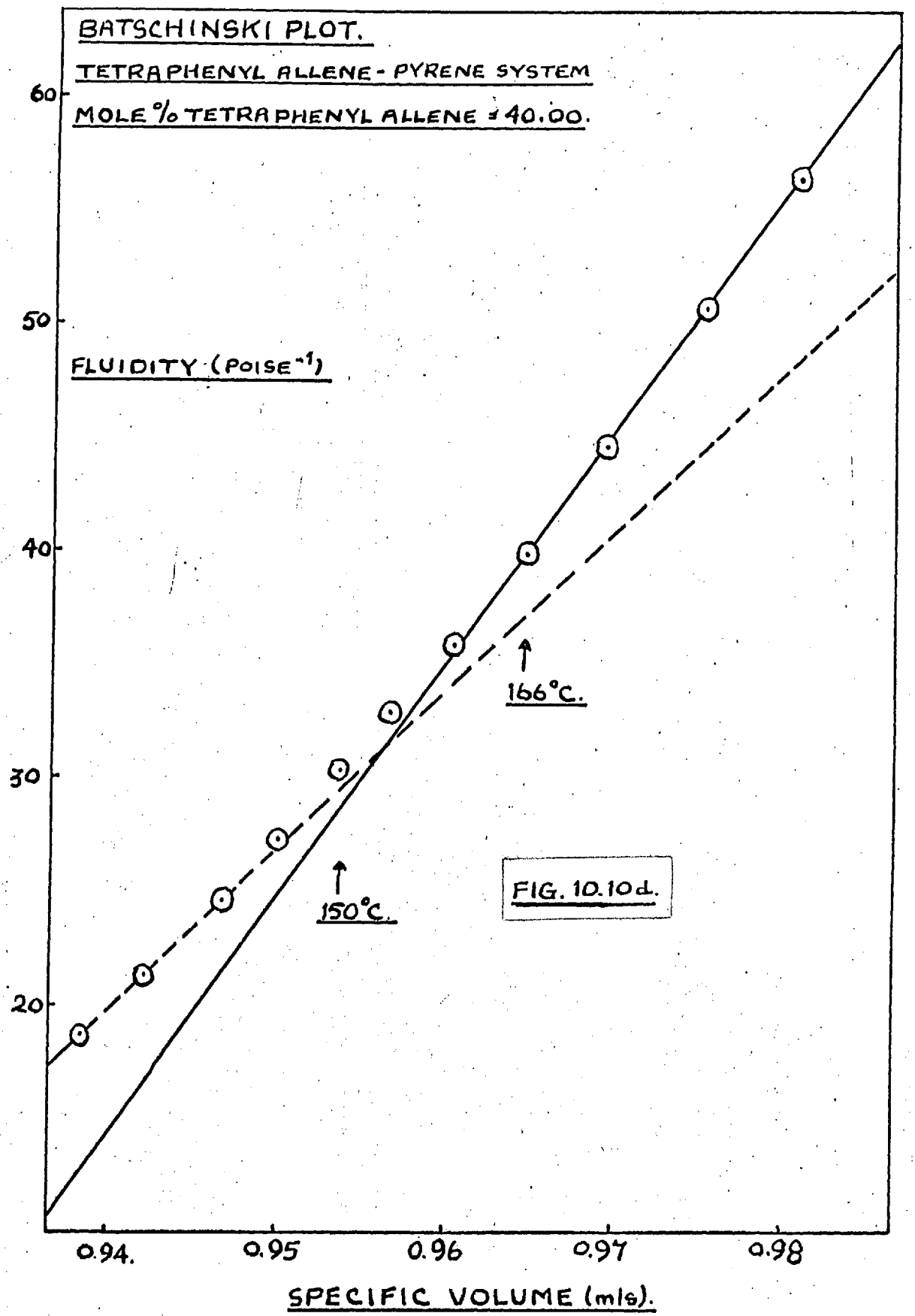
BATSCHINSKI PLOT.
TETRAPHENYL ALLENE - PYRENE SYSTEM
MOLE % TETRAPHENYL ALLENE = 40.00.
FLUIDITY (POISE^{-1})
60
50
40
30
20
166°C.
150°C.
0.94.
0.95
0.96
0.97
0.98
SPECIFIC VOLUME (ml/g).

FIG. 10.10d.

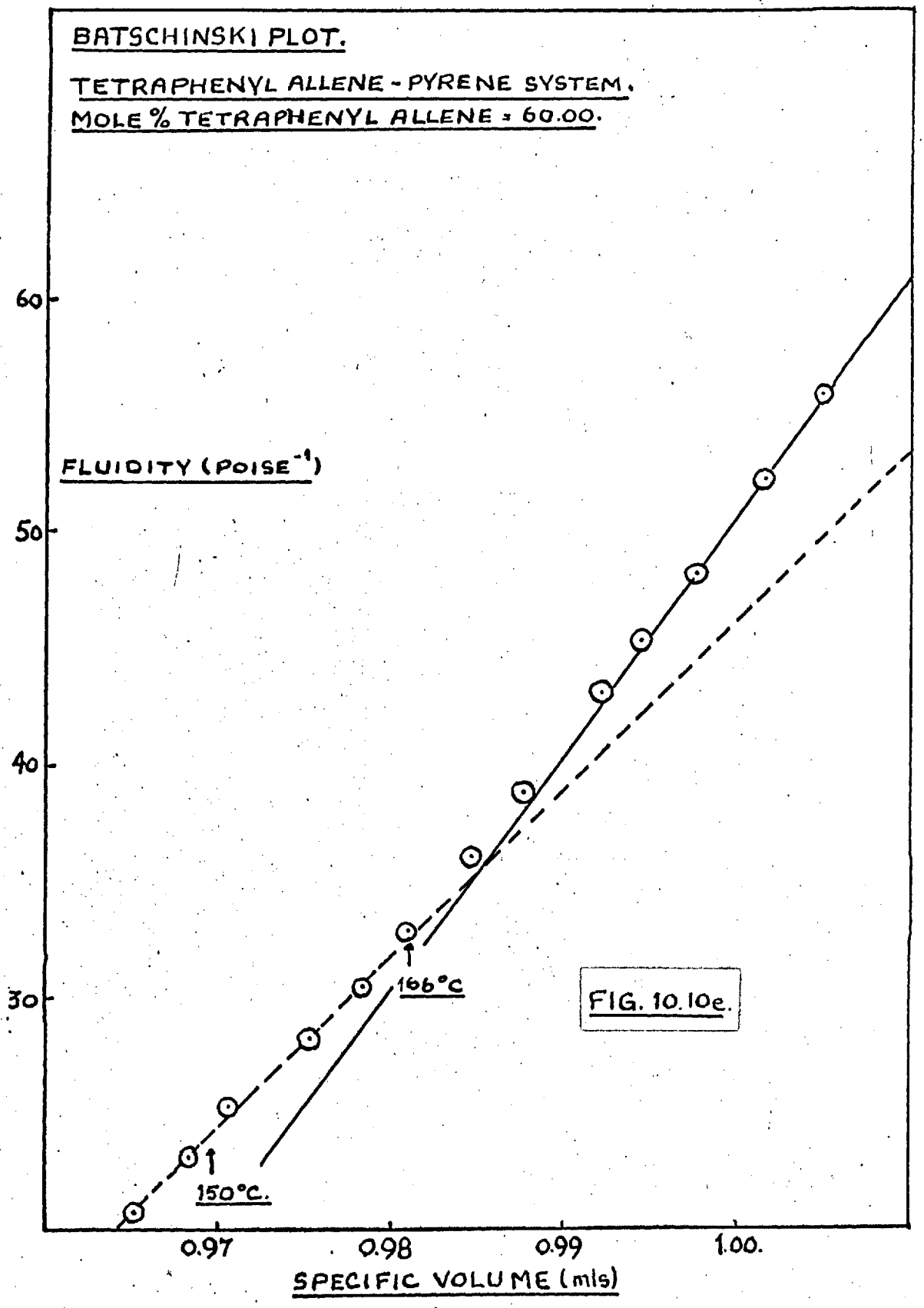
BATSCHINSKI PLOT.
TETRAPHENYL ALLENE - PYRENE SYSTEM.
MOLE % TETRAPHENYL ALLENE = 60.00.
FLUIDITY (POISE^{-1})
60
50
40
30
166°C
150°C.
0.97
0.98
0.99
1.00.
SPECIFIC VOLUME (mls)

FIG. 10.10e.

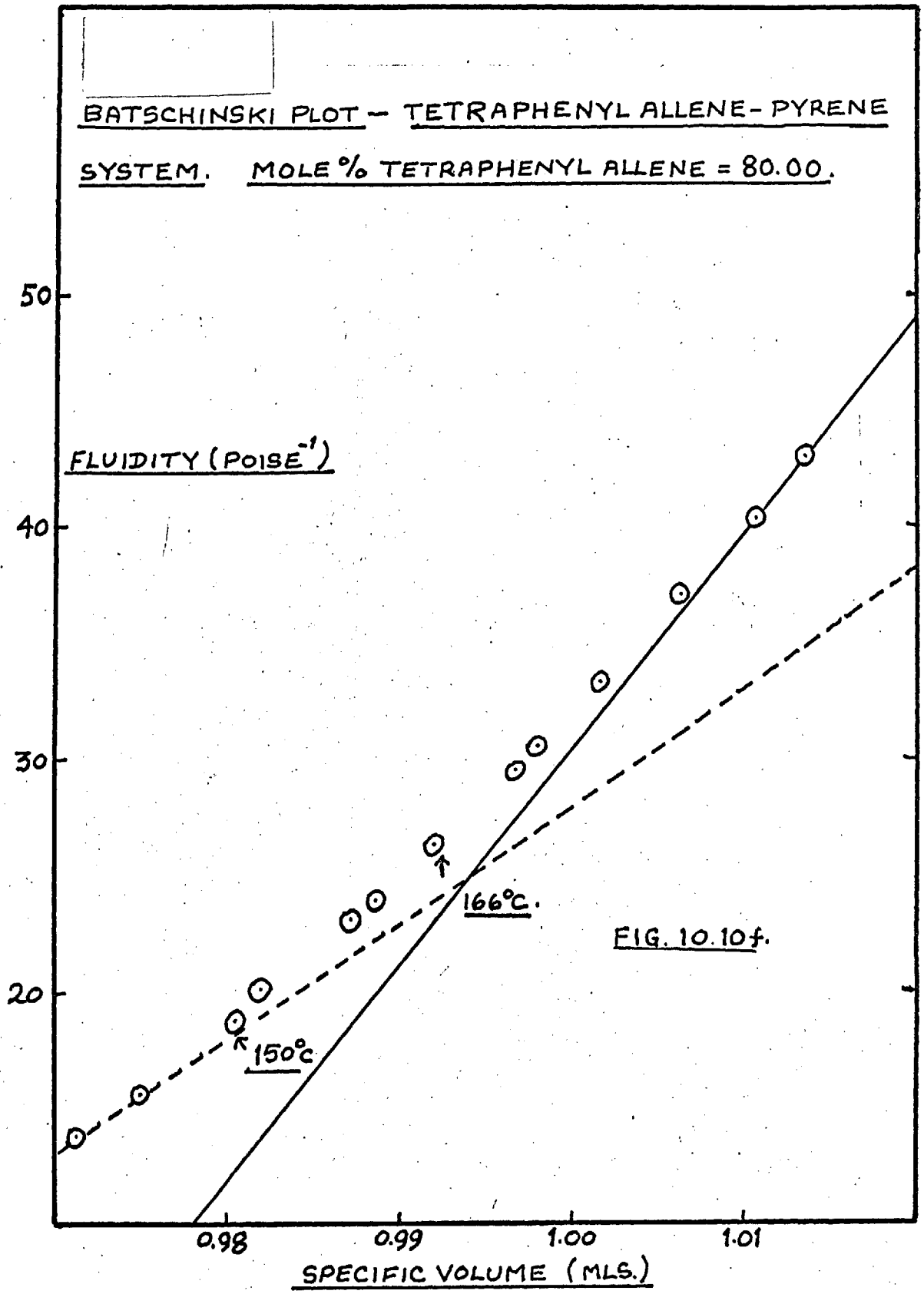
BATSCHINSKI PLOT – TETRAPHENYL ALLENE-PYRENE SYSTEM. MOLE % TETRAPHENYL ALLENE = 80.00.
FLUIDITY (POISE^{-1})
50
40
30
20
150°C
166°C.
0.98
0.99
1.00
1.01
SPECIFIC VOLUME (MLS.)

FIG. 10.10f.

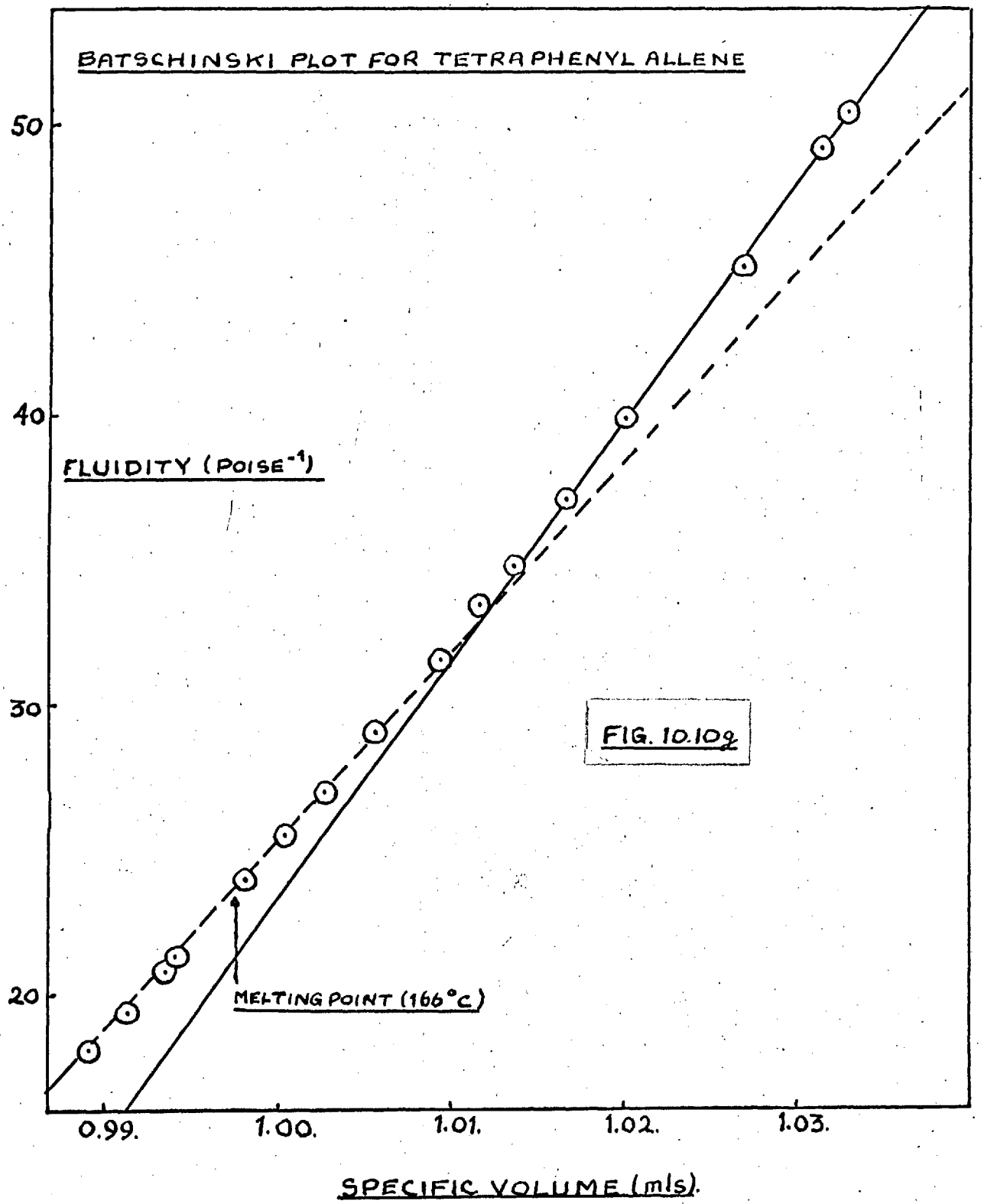
BATSCHINSKI PLOT FOR TETRAPHENYL ALLENE
50
40
30
20
FLUIDITY (POISE^{-1})
MELTING POINT (166°C)
0.99.
1.00.
1.01.
1.02.
1.03.
SPECIFIC VOLUME (mls).

FIG. 10.10g

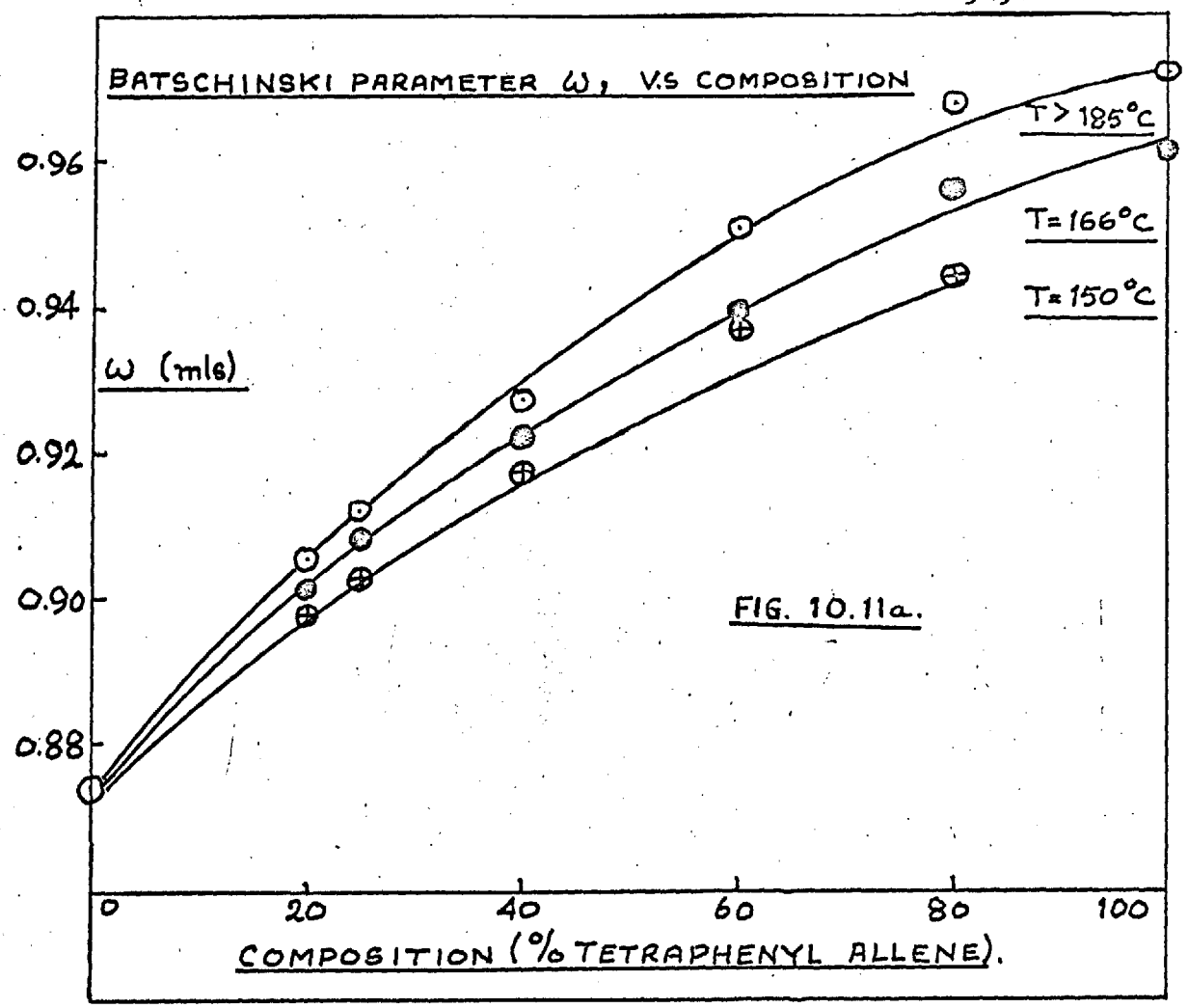

FIG. 10.11a.

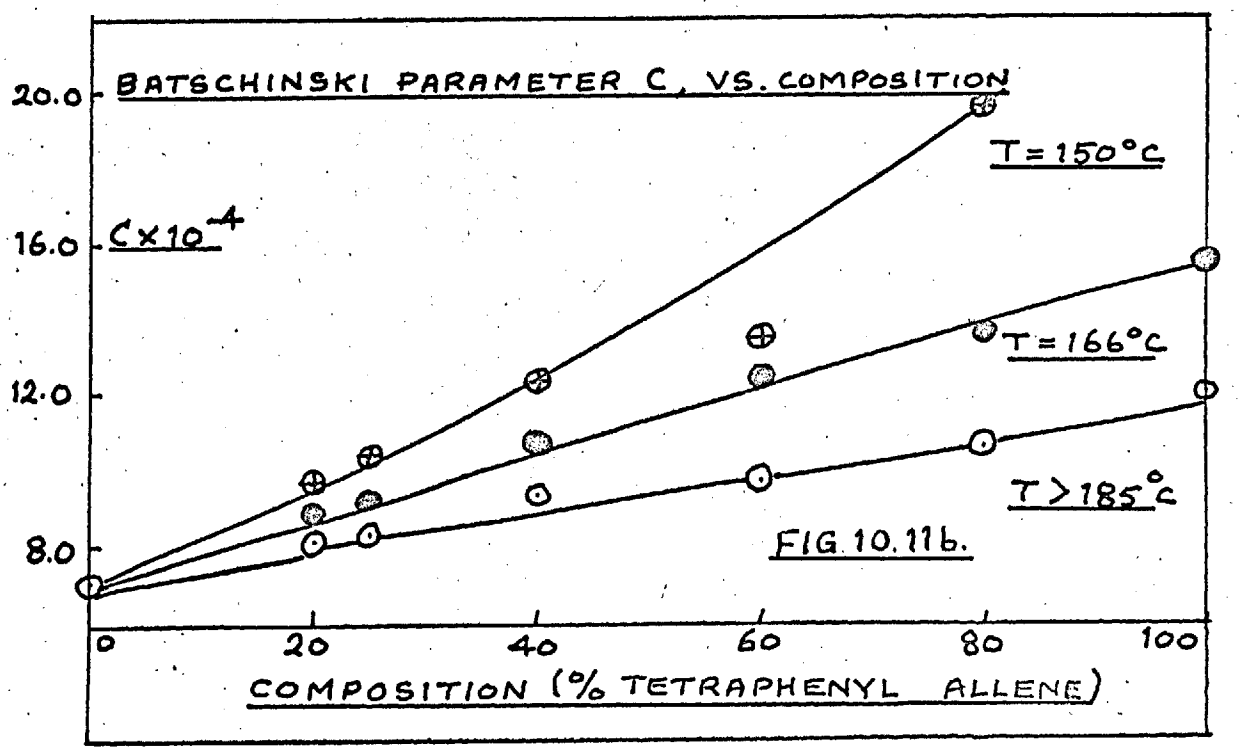

FIG. 10.11b.

that the addition of pyrene causes the break-up of tetraphenyl allene clusters.

10.4.4. Viscosity/Composition Relationships.

The problems in providing a general expression for the viscosity of a binary mixture in terms of the viscosities of the pure components and the composition are complex, and the subject is not fully understood (c.f. Chapter 2, section 2.5). Although some relationships describe specific systems quite well, none may claim general applicability.

Fig. 10.12a represents plots of viscosity vs. composition at 191.9°C, 166°C, and 150°C. The plots at both 191.9°C and 166°C are linear, although the gradient of the plot is least at the higher temperature. The plot at 150°C shows a relatively more marked decrease in viscosity as the concentration of pyrene is increased, and the plot is not linear. The increase in slope as the temperature is lowered to 166°C, and the increasing curvature at 150°C may be a further manifestation of the participation of clusters in transport. A linear viscosity vs. composition plot implies a relationship of the following form:

$$\eta_m = x_1\eta_1 + x_2\eta_2 \qquad (10.6)$$

where η_m is the viscosity of the mixture, and η_1 and η_2 and x_1 and x_2 are the viscosities and mole fractions of components 1 and 2 respectively.

FIG. 10.12a.

PLOT OF VISCOSITY (η) VS. COMPOSITION.
(TETRAPHENYL ALLENE – PYRENE SYSTEM.)

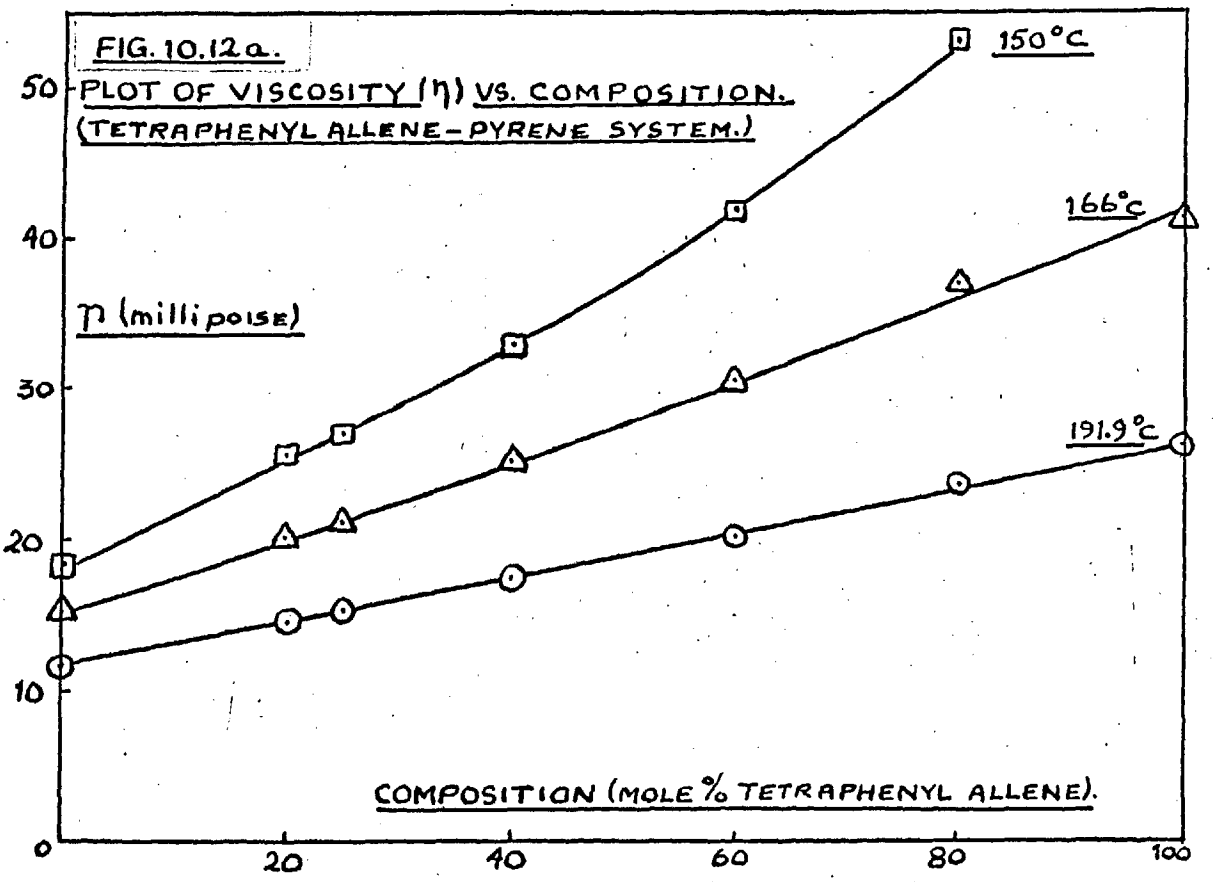

FIG. 10.12b.

PLOT OF FLUIDITY VS. COMPOSITION.
(TETRAPHENYL ALLENE – PYRENE SYSTEM)

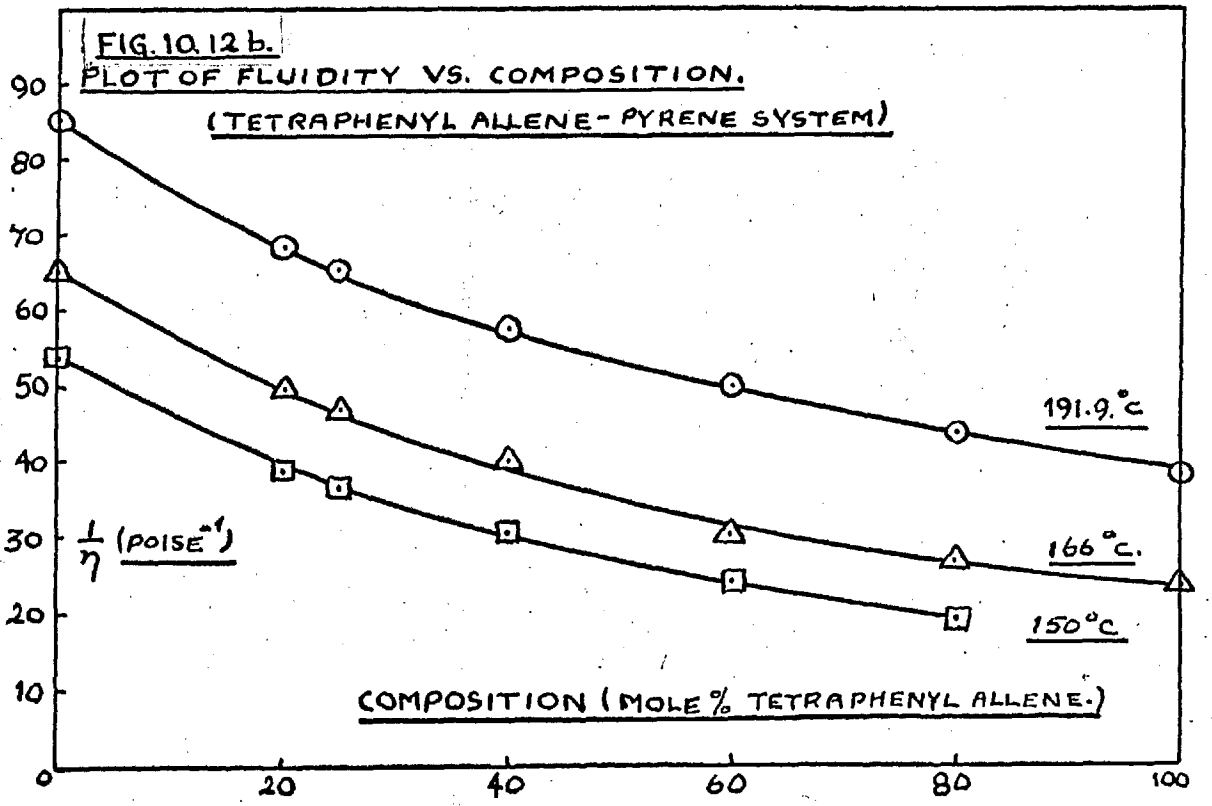

An extension of the Eyring reaction rate theory[5] leads to an expression of the following type for the viscosity of an ideal binary mixture:

$$\frac{1}{\eta_m} = \frac{x_1}{\eta_1} + \frac{x_2}{\eta_2} \qquad (10.7)$$

This relationship predicts a linear fluidity ($1/\eta$) vs. composition plot. Plots of $1/\eta$ vs. composition for the tetraphenyl allene/pyrene system at 191.9°C, 166°C, and 150°C are illustrated in Fig. 10.12 b. At all three temperatures the plots take the form of gentle curves. The fact that these plots are not linear may perhaps be expected in view of the non-ideal behaviour of the mixture and its consequent failure to fulfill the conditions dictated by the Eyring theory. (see Chapter 2, section 2.5).

The absence of any outstanding variation in the nature of the curves as the temperature is lowered suggests that an expression of the Eyring type (equation 10.7) is rather insensitive to anomalies in flow arising from cluster formation.

REFERENCES

1. Andrews, J.N. and Ubbelohde, A.R., Proc. Roy. Soc., A.228, 435 (1955)
2. McLaughlin, E. and Ubbelohde, A.R., Trans. Faraday Soc., 53, 628 (1957).
3. Greet, R.J. and Turnbull, D., J. Chem. Phys., 46, 1243 (1967)
   " " ibid 47, 2185 (1967)
4. Magill, J.H. and Ubbelohde, A.R., Trans. Faraday Soc., 54, 1811 (1958).
5. Glasstone, S., Laidler, K.J. and Eyring, H., "The Theory of Rate Processes", McGraw-Hill, New York (1941).
6. Greet, R.J. and Magill, J.H., J. Phys. Chem., 71, 1746 (1967)
7. McLaughlin, E. and Ubbelohde, A.R., Trans. Faraday Soc., 54, 1804 (1958).
8. Ubbelohde, A.R., "Melting and Crystal Structure", Clarendon Press (1965).
9. Rowlinson, J.S., "Liquids and Liquid Mixtures", Butterworths (1959).
10. Griffiths, V.S., J. Chem. Soc., 860 (1954).
11. Pierce, W.C., J. Chem. Phys., 5, 717 (1937).

APPENDIX

Volumes of Rotation for Tetraphenyl Allene, Triphenyl-α-naphthyl Allene and Triphenyl-4-biphenyl Allene About the Three Perpendicular Axes Through Their Centres of Gravity.

Owing to the complex shape of these molecules, the detailed determination of their volumes of rotation, although comparatively simple in principle, is rather involved. The following paragraphs serve to provide a general indication of the methods used and the factors which required consideration.

A.1. To locate the molecular centres of gravity.

Each molecule was divided into sections, viz. phenyl groups, allene skeleton, α-naphthyl or 4-biphenyl group. The centre of gravity of each section was located with respect to its extremities by using van de Waals' radii[1] and atomic weights, and taking moments about two perpendicular axes in the plane of each group. In neither the phenyl, α-naphthyl nor biphenyl group was the centre of gravity displaced from the centre of symmetry of benzene, naphthalene, or biphenyl respectively to a significant extent. In the worst case, the phenyl group, displacement of the centre of gravity of benzene was 0.03 Å. (i.e. < 1% of the total length of the group). For the sake of convenience these small differences were ignored, and the centres of gravity of the groups assumed coincident with the centres of symmetry of the

corresponding complete hydrocarbons. The centre of gravity of the allene skeleton is located at its centre of symmetry.

The molecules as a whole were projected onto diagrams marked with three perpendicular axes (X, Y and Z). The allene skeleton was disposed along the X-axis with its centre at the origin, and the other groups according to the molecular geometry. By way of illustration, Fig. A.1. represents the resulting diagram for triphenyl-α-naphthyl allene. It may be seen that the centre of gravity of the phenyl group adjacent to the α-naphthyl group lies in the XY plane, and the centres of gravity of the remaining pair of phenyl groups in the XZ plane. In each case the angle between each pair of geminal substituents was taken as 124°. Note that the long axis of the α-naphthyl group lies in the XZ plane, and cannot be shown in Fig. A.1. From van de Waals' radii[1], bond lengths[2], and three dimensional trigonometry, the x, y and z co-ordinates of the centres of gravity and extremities of each group were determined (c.f. Fig. A.1). Using the molecular weights of each group, and of the molecules as a whole, moments were taken about the Z, X and Y axes respectively, giving the x, y and z co-ordinates of the molecules' centre of gravity. The centre of gravity of the symmetrical tetraphenyl allene lay at the origin, but the co-ordinates for the centres of gravity of triphenyl-α-naphthyl allene and triphenyl-4-biphenyl allene were (in Angstrom units),

FIGURE A.1.

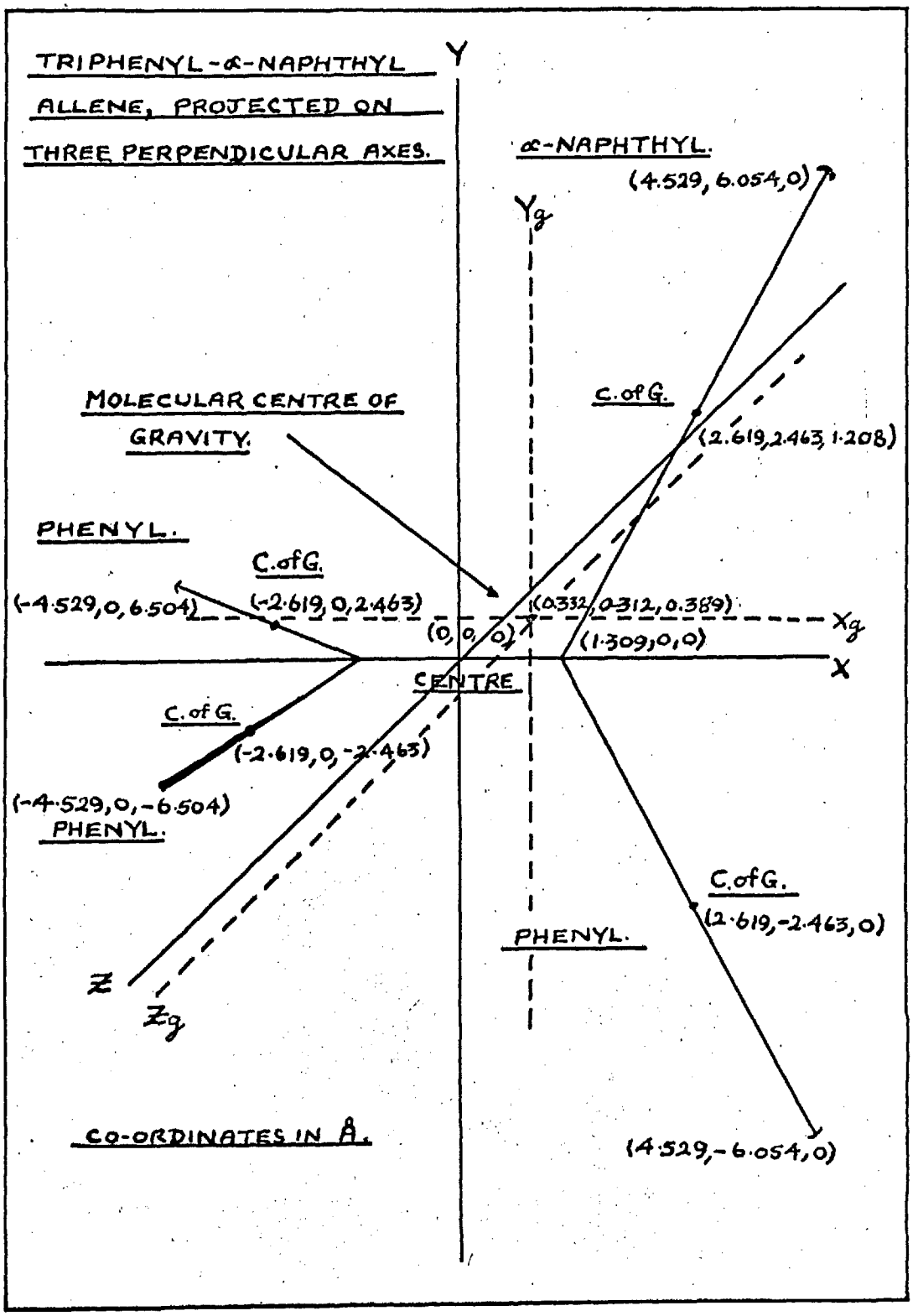
TRIPHENYL-α-NAPHTHYL ALLENE, PROJECTED ON THREE PERPENDICULAR AXES.
Y
α-NAPHTHYL.
(4.529, 6.054, 0)
Yg
MOLECULAR CENTRE OF GRAVITY.
C. of G.
(2.619, 2.463, 1.208)
PHENYL.
C. of G.
(-4.529, 0, 6.504)
(-2.619, 0, 2.463)
(0.332, 0.312, 0.389)
Xg
(0, 0, 0)
(1.309, 0, 0)
X
CENTRE
C. of G.
(-2.619, 0, -2.463)
(-4.529, 0, -6.504)
PHENYL.
C. of G.
(2.619, -2.463, 0)
PHENYL.
Z
Zg
CO-ORDINATES IN Å.
(4.529, -6.054, 0)

(0.332, 0.312, 0.389) and (0.832, 1.119, 0) respectively.

We are considering the volume swept out by rotating each molecule about three perpendicular axes through its centre of gravity, parallel to the X, Y and Z axes respectively which define the co-ordinate system used above. To avoid confusion, the actual axes of rotation will be designated X_g, Y_g, and Z_g (See Fig. A.1).

A.2. Rotation about the Y_g and Z_g axes.

For the sake of simplicity, the estimate of volumes of rotation were based upon the molecular configurations represented in plates 6.1, 6.3 and 6.4.

The difference between the perpendicular distances from the axis of rotation to the nearest and furthest point on each group represents the thickness of the ring swept out by that group on rotation through 360°. By drawing the circles of which these distances are the radii, the degree of overlap between the volumes swept out by the different groups in the plane perpendicular to the axis of rotation may be assessed. Such a diagram, corresponding to the rotation of triphenyl-α-naphthyl allene about its Z_g axis is represented by the upper portion of Fig. A.2.

To determine the degree of overlap in the same plane as the axis of rotation requires further consideration.

It may be seen from plates 6.1, 6.3 and 6.4, that when either molecule is rotated about its Y_g or Z_g axis, one pair

FIGURE A.2.

PLAN AND ELEVATION FOR THE VOLUME SWEPT OUT BY ROTATING TRIPHENYL-α-NAPHTHYL ALLENE ABOUT ITS Z_g AXIS.

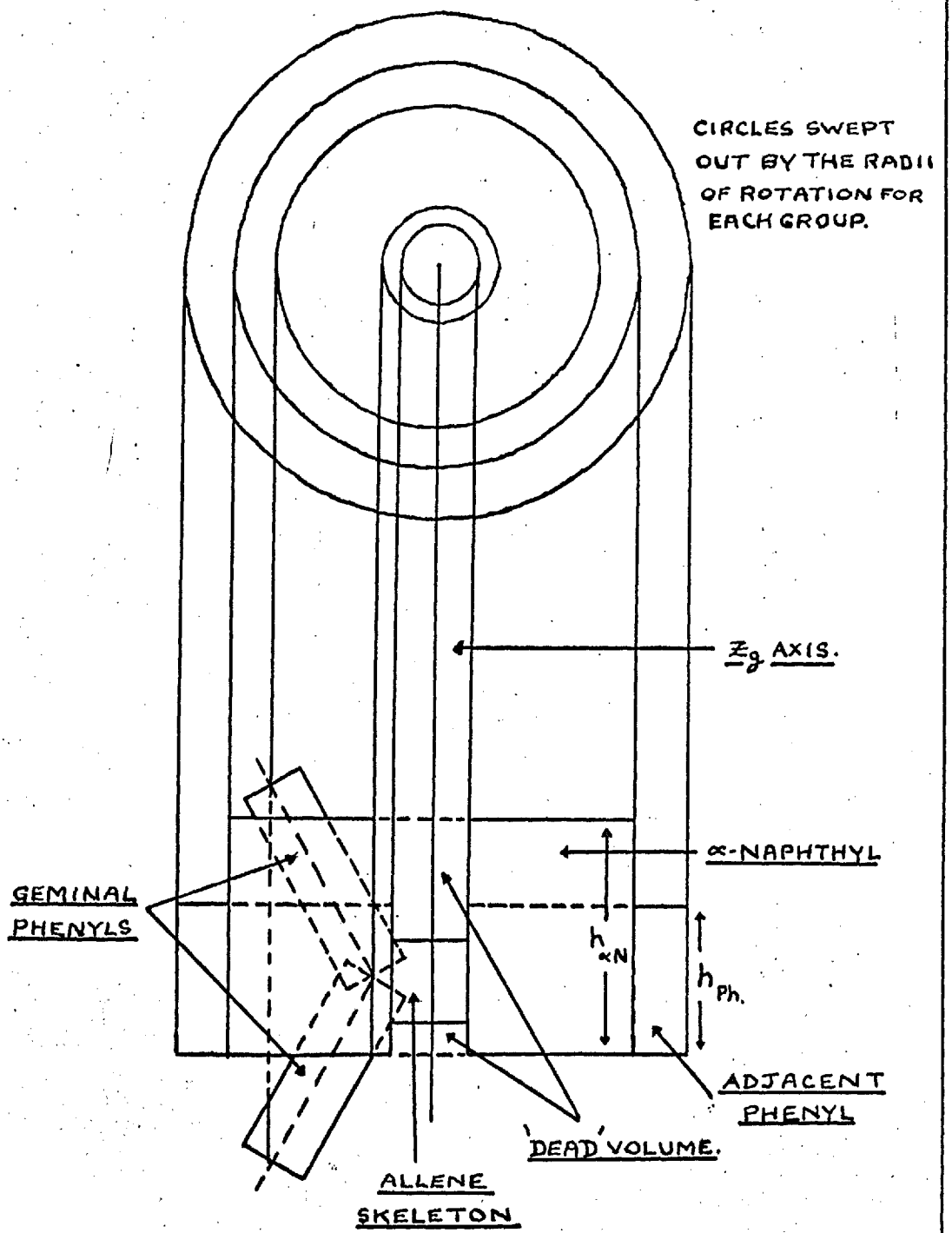

of geminal groups sweep out a volume arising from their maximum areas (i.e. broad faces), whilst the second pair, which lie in a perpendicular plane, sweep out volumes arising from the area of their edges. These latter volumes are largely overlapped by the former, but their contributions to the total volumes of rotation are significant (10-20 %). Thus, before volumes of rotation about these axes can be estimated, two pieces of information are required.

(i) The effective height of the groups which sweep out volumes with their maximum areas (broad faces).

(ii) The extent to which the volumes swept out by the edges of the second pair of geminal groups is overlapped by the cylinder formed by rotating the groups mentioned in (i).

A.2.1. To estimate the effective heights of the phenyl group, α-naphthyl group, and 4-biphenyl group.

The phenyl group is hexagonal in shape (Fig. A.3). The intersecting tangents drawn to the repulsion envelopes of the hydrogen atoms describe a hexagon, the area of which is a reasonable approximation to the maximum effective area of the group. To a first approximation the 'thickness' of the group was considered equal to the diameter of an aromatic carbon atom (2.54 Å). From bond lengths[1] and van de Waals' radii[2], a value for this area, A_{Ph} may be obtained. As a further approximation, introduced to simplify an assessment of the

FIGURE A.3.

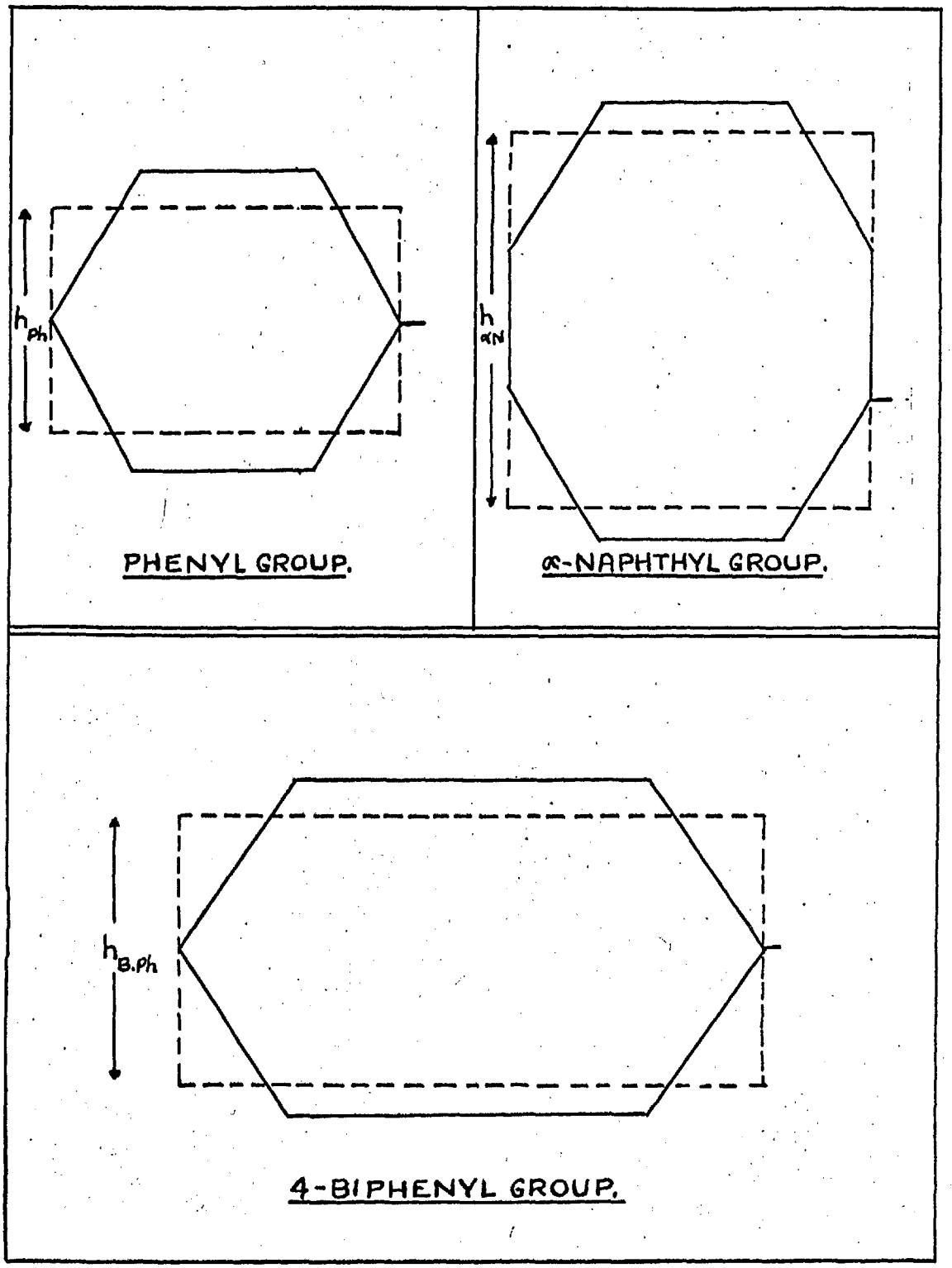
h_{Ph}
PHENYL GROUP.
$h_{\alpha N}$
α-NAPHTHYL GROUP.
$h_{B.Ph}$
4-BIPHENYL GROUP.

degree of overlap with other groups, the area A_{Ph} was represented as a rectangle of the same width as the original hexagon but of a uniform height h_{Ph}. Thus, h_{Ph} represents the mean height of the phenyl group, and the constructed rectangle is marked in Fig. A.3. with dotted lines.

Similar procedures were adopted for the α-naphthyl group (represented as a symmetrical but irregular octagon) and the biphenyl group (represented as a symmetrical but irregular hexagon). Values for the average heights, $h_{\alpha N}$ and $h_{B.Ph.}$ respectively were obtained (see Fig. A.3.). It is now possible to assess the extent of overlap between groups in the same plane as the axis of rotation, and the net volume swept out by groups presenting their maximum areas can be determined (c.f. Fig. A.2). It is evident from Fig. A.2. that the volume swept out by the allene skeleton is small and, in the cases of triphenyl-α-naphthyl allene and triphenyl-4-biphenyl allene, is largely overlapped. The space above and below this volume, reaching to the limits of the hollow cylinder swept out by the nearest group, is 'dead volume', i.e., volume which cannot be shared between molecules. It is reasonable to extend the volume swept out by the nearest group to include both the volume swept out by the allene skeleton and the dead volume, thus producing a solid cylinder (c.f. Fig. A.2.).

A.2.2. Volume arising from the second pair of geminal groups.

From the information obtained by the methods outlined above, and from a consideration of the molecules' geometry, the extent to which the second pair of groups protrude above and below the major 'cylinder of rotation' may be readily determined for the rotation of each molecule about its Y_g and Z_g axes.

As both protruding groups are treated similarly, attention will be confined to group 1, protruding above the 'cylinder of rotation'. The general situation is illustrated schematically in Fig. A.4.

Since the projecting edge of this group is sweeping out the volume, only the distances CD and CE, and the angle θ, need be known. CD is the 'thickness' of the group which, in all cases, is equal to the diameter of an aromatic carbon atom (2.54 Å). The angle θ is assigned the value of 62°, and the distance CE is forthcoming from the molecular geometry. The effective area of the group A is defined by the trapezium CDEF, and it may be seen from Fig. A.4. that:

$$A = CD \left(CE + \frac{CD}{2 \operatorname{Tan} \theta}\right) \qquad (A.1)$$

As a first approximation it is assumed that the centre of gravity of this section is located at a point G along AB such that AG = GB. Referring once again to the three dimensional co-ordinate system employed earlier, the x, y and z

FIGURE A.4.

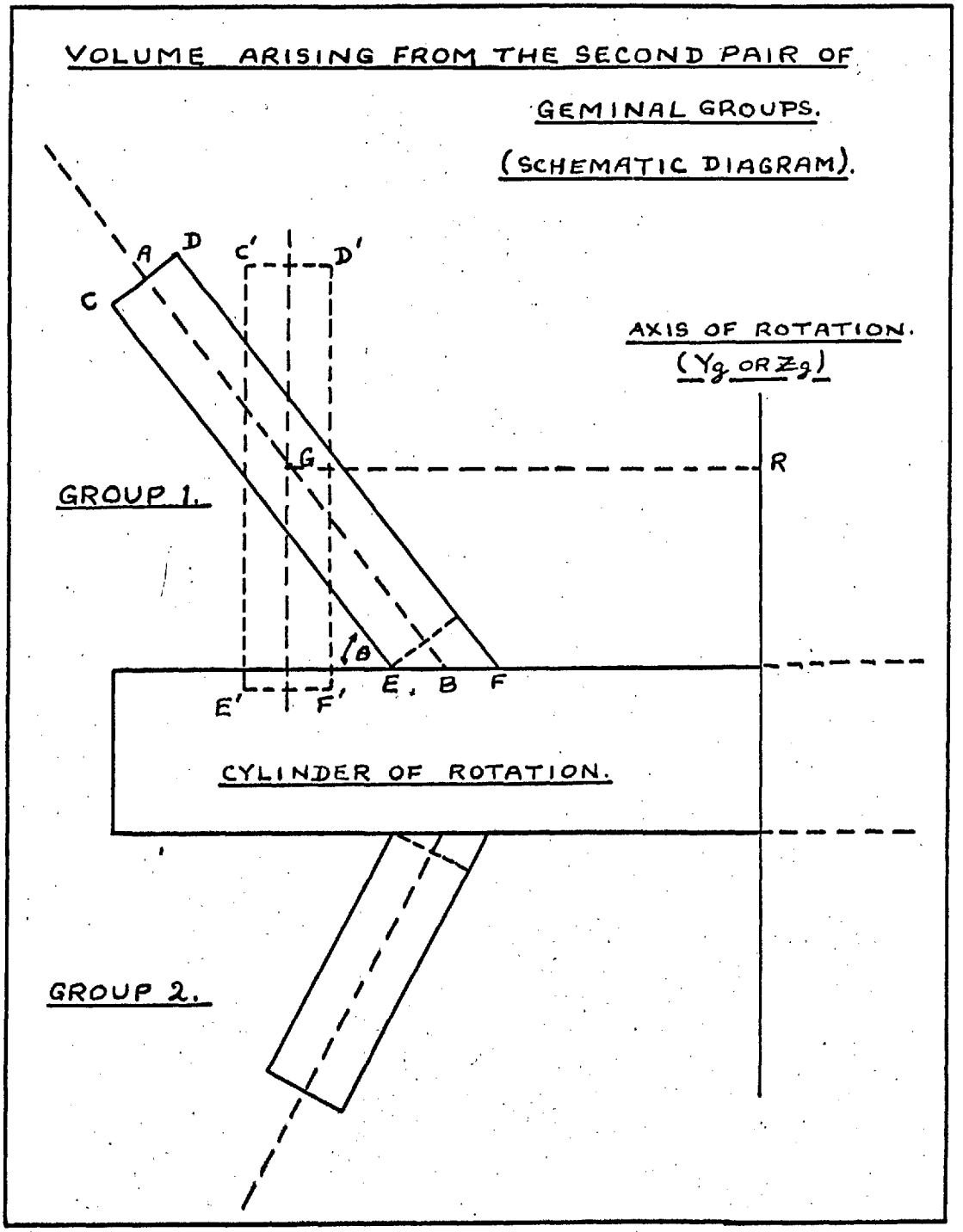
VOLUME ARISING FROM THE SECOND PAIR OF GEMINAL GROUPS.
(SCHEMATIC DIAGRAM).
A
D
C'
D'
C
AXIS OF ROTATION.
(Yg OR Zg)
G
R
GROUP 1.
θ
E'
F'
E
B
F
CYLINDER OF ROTATION.
GROUP 2.

co-ordinates of G may be obtained, and the perpendicular distance from the axis of rotation to G (i.e. GR) determined. The assumption made with respect to the position of G permits the trapezium CDEF to be replaced by the rectangle C'D'E'F' of equal area with its centre of gravity also located at G. The volume swept out by rotating this area through 360° may now be found using Pappus' theorem. This theorem states that "if a closed area be rotated through any angle not greater than 2π radians about a line in its plane that does not intersect it, the volume generated is equal to the product of the area and the path length of the centroid"(3).

Thus the volume V swept out in this case is:

$$V = 2\pi A\ GR = 2\pi\ GR.CD\ (CE + \frac{CD}{2\ Tan\ \Theta}) \qquad (A.2.)$$

In the cases of the rotation of tetraphenyl allene about both the Y_g and Z_g axes, and the rotation of triphenyl-4-biphenyl allene about the Y_g axis, the areas CDEF lie in the same plane as the axis of rotation and the procedure outlined above may be carried out without further correction. In the cases of the rotation of triphenyl-α-naphthyl allene about both the Y_g and Z_g axes, and the rotation of triphenyl-4-biphenyl allene about the Z_g axis, the areas CDEF subtend angles (ϕ) to the axes of rotation. Corrections for this may be applied by multiplying the areas CDEF as determined above by cos ϕ. The values of ϕ for the cases mentioned above are 21°43', 10°46' and 27°35', respectively.

Whilst this correction is perfectly valid for plane areas, it must be remembered that, in the present context, the areas CDEF represent portions of the maximum areas presented by the edges of polygonal blocks (i.e. the groups). The corrections applied to the areas as a result of the subtending angles ϕ will therefore be compensated in part by the leading and trailing edges of the groups. The corrections are however, very small amounting to $< 1\%$ of the total volume of rotation about the axes in question, and have been applied in the present instance.

A.3. Rotation about the X_g axes.

The general situation is illustrated in fig. A.5. Each molecule may be divided into three principal sections.

(1) The allene skeleton.

(2) The first pair of geminal groups.

(3) The second pair of geminal groups.

The treatment of each pair of geminal groups is essentially identical, and consideration will be confined to the pair of groups represented in Fig. A.5.

A.3.1. The allene skeleton.

It is assumed, as a first approximation, that the allene skeleton is a cylinder of diameter AD (= 2.54 Å) and length AB (see Fig. A.5). In the cases of triphenyl-α-naphthyl allene and triphenyl-4-biphenyl allene the axis of the cylinder does

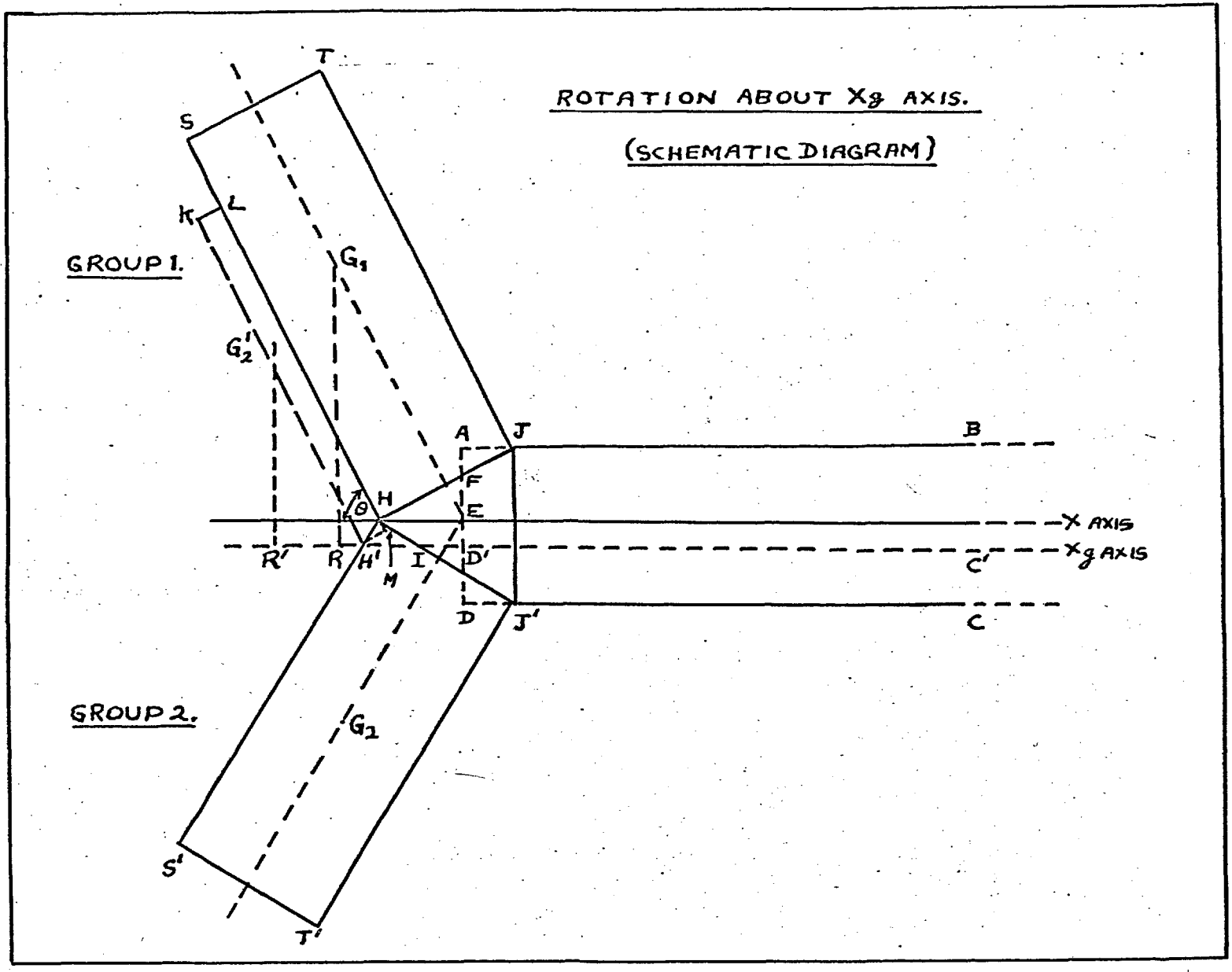
ROTATION ABOUT Xg AXIS.
(SCHEMATIC DIAGRAM)
GROUP 1.
GROUP 2.
T
S
K
L
G1
G2'
A
J
B
F
H
θ
E
X AXIS
Xg AXIS
R'
R
H'
I
M
D'
C'
D
J'
C
S'
T'

FIGURE A.5.

not coincide with the X_g axis and the effective radius of the cylinder swept out on rotation is AD'(= AE + ED'). AE is the radius of the skeleton and ED' the perpendicular distance from its centre of gravity (the origin) to the X_g axis. Thus, the volume $V_{Sk.}$ swept out by rotating this portion of the molecule through 360° is:

$$V_{Sk.} = \pi(AD')^2 . AB \qquad (A.3.)$$

A.3.2. The groups.

The volume swept out by these groups arises from their edges. That group which extends furthest from the X_g axis will contribute the largest portion of volume resulting from the rotation of each pair of geminal groups. If, as in the cases of triphenyl-α-naphthyl allene and triphenyl-4-biphenyl allene, the X_g axis is not coincident with the X axis (c.f. Fig. A.2), the overlap of one member of a geminal pair by the other will not be complete. Fig. A.5. represents a general case. It can be seen that the volume due to the edge of group 1 will largely overlap that due to group 2, and that the major portion of the volume arises from the area (rectangle) STJH. The x, y, and z co-ordinates of the centre of gravity of group 1 will have already been determined (section A.1), and the perpendicular distance from the X_g axis to this point (G, R) is readily obtained. Since the area of group 1 is STJH, the volume swept out by this group will be according to Pappus' theorem:

$$V_{G_1} = ST.JH.\ 2\pi.\ G_1R \qquad (A.4)$$

The small area AJF is duplicated with that swept out by the allene skeleton but this compensates in part the small area HFD'I which is otherwise ignored. The distances ST and SH etc. will have already been estimated from van de Waals' radii and bond lengths (section A.1).

There now remains the uneclipsed volume arising from group 2. The effective area of this group is represented, as a first approximation, by the rectangle KLH'M.

A consideration of the geometry reveals that the distance KL is related to the perpendicular distance between the X and X_g axes (i.e. ED') as follows:

$$KL = 2ED' \cos \theta \qquad (A.5)$$

(N.B. $\theta = 62^{\circ}$).

Having determined the length KL, and assuming that the centre of gravity G'_2 of the element lies at the centre of symmetry of the rectangle KLH'M, the perpendicular distance from the X_g axis to G'_2 (G'_2 R') may be obtained by either plane geometry or reference to a three-dimensional co-ordinate diagram of the type illustrated in Fig. A.2.

The area of this element is KL.KH', and by Pappus' theorem the volume swept out on rotation will be:

$$V_{G_2} = 2\pi.G'_2R'.\ KL.KH \qquad (A.6)$$

In the case of triphenyl-α-naphthyl allene, group 1 may

be identified with phenyl, and group 2 with α-naphthyl. Since the centre of gravity of this molecule does not lie in the XY plane (see Fig. A.2), the planes of the areas ST.JH and KL.H'M subtend small angles (ϕ) to the axis of rotation. The values of ϕ are 7° and 18° respectively. To correct for this the areas may be multiplied by Cos 7° and Cos 18° respectively. (See section A.2.2.). This correction is small, amounting to about 1% of the total volume of rotation.

Thus, the total volume of rotation about the X_g axis will be the sum of the volumes due to each geminal pair of groups and the allene skeleton.

If the values of the van de Waals' radii and bond lengths used are accepted as correct, $\pm$ 10% is a reasonable estimate for the maximum error in the values for the volumes of rotation obtained by the methods outlined above.

Table A.1 contains the values obtained for the three allenes together with the volumes of the molecules themselves (see also table 10.1).

TABLE A.1.

VOLUMES OF ROTATION

Compound	Volume of molecule	Rotation about X_g axis	Rotation about Y_g axis	Rotation about Z_g axis
Tetraphenyl allene	321 Å^3	490 Å^3	1230 Å^3	1230 Å^3
Triphenyl-α-naphthyl allene	363 Å^3	620 Å^3	1332 Å^3	1599 Å^3
Triphenyl-4-biphenyl allene	384 Å^3	1122 Å^3	1469 Å^3	2134 Å^3

It should be mentioned that to resolve the rotation of an unsymmetrical molecule along three perpendicular axes is not truly realistic if the molecule is allowed to rotate freely. The molecule will tend to precess. Since in the present instance, the molecules are strongly confined by their neighbours, such a resolution is a reasonable approximation.

REFERENCES

1. van de Waals' radii obtained from 'Catalin' Ltd., London (Manufacturers of scale molecular models).

2. International Tables for X-ray Crystallography, Vol. III Kynoch Press, London (1962).

3. Blakey, J., "University Mathematics", 2nd edition, Blakie & Son Ltd., London (1958).